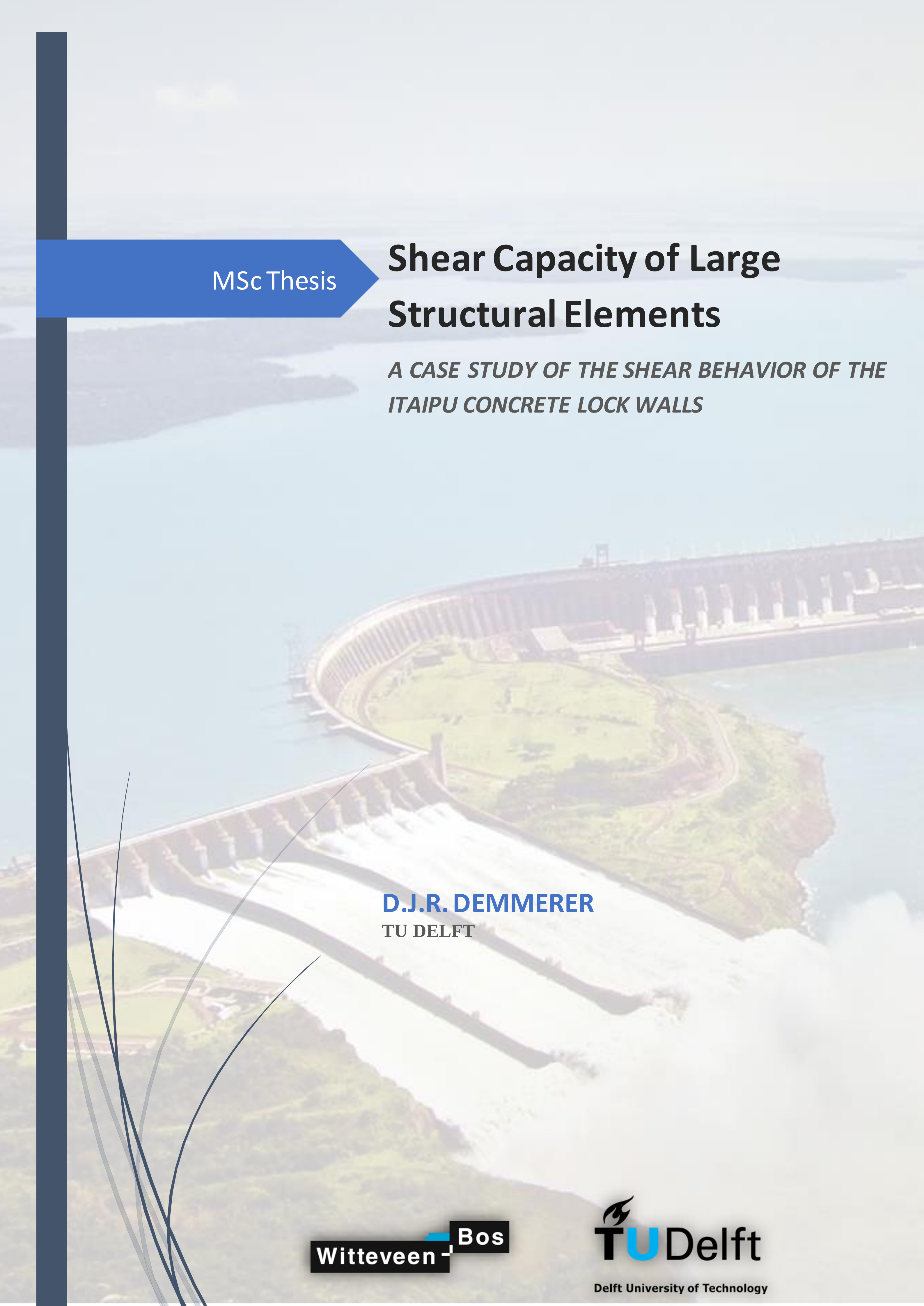

MSc Thesis

Shear Capacity of Large Structural Elements

A CASE STUDY OF THE SHEAR BEHAVIOR OF THE ITAIPU CONCRETE LOCK WALLS

D.J.R. DEMMERER
TU DELFT

Witteveen + Bos

TU Delft
Delft University of Technology

(This page is left blank intentionally)

Shear Capacity of Large Structural Elements

A CASE STUDY OF THE SHEAR BEHAVIOR OF THE ITAIPU CONCRETE LOCK WALLS

BY

D'TASHA DEMMERER

STUDENT NUMBER: 4298748

in partial fulfilment of the requirements for the degree of

Master of Science
in civil engineering

at the Delft University of Technology,
to be defended publicly on Tuesday December 15, 2020

Thesis committee:

Prof. Ir. S.N. Jonkman	TU Delft (Chairman)
Ir. W. Molenaar	TU Delft (Daily Supervisor)
Prof. Ir. M. Hendriks	TU Delft
Ir. H. de Waardt	Witteveen+Bos (Daily Supervisor)

An electronic version of this thesis is available at http://repository.tudelft.nl/.

(This page is left blank intentionally)

Abstract

The concept of shear loading and the shear resistance is well known for 'regular' sized beams, meaning beams that can be characterized as a slender beam. However, once the beam increases in size such that it is characterized as a deep beam or even falls outside the range of the typical deep beam, less knowledge is available. A case study of the Itaipu lock walls is used to compare three different calculation methods for shear loading (sectional method, strut & tie method and a linear and nonlinear finite element model) to each other. The calculation methods are applied to the large concrete lock walls in order to determine which of these methods can best be used for shear calculations on structural elements that fall out of the range of these so called 'regular' sized beams.

The effect of increasing thickness is studied and it can be concluded that the combination of a certain crack width and the aggregate interlock mechanism, and thus the grain size of the concrete mixture, play an important role in the shear capacity of beams.

The existing norms and guidelines, such as the Eurocode and the American Concrete Institute codes, have been proven to be inadequate for shear calculations on structural elements that surpass the definition of a deep beam in size, such as the Itaipu lock walls. The sectional calculation, which is based on these norms and guidelines is however still used as a rough reference calculation in this research. The first calculation, which is the sectional calculation, resulted in two alternative designs next to the original lock wall design by Witteveen+Bos: total wall thickness original design: 33m, total wall thickness alternative design 1 (i): 17m and total wall thickness alternative design 2 (ii): 29m. The Strut & Tie calculation is then performed for the original Witteveen+Bos design, resulting in a reinforcement plan based on the normal forces in the ties. The third calculation type consisted of three linear models (of the original design and the two alternative designs) and one nonlinear model of the original Witteveen+Bos design. The stress trajectories of the linear models illustrated that the wall is predominantly stressed in compression, as a result of the large self-weight of the wall. Only the lower part of the wall and the lock floor connected to this wall are stressed in tension. The nonlinear model was therefore reinforced only in the lock floor and the lower part of the wall connected to the lock floor.

Because the linear finite element approach does not include material behavior beyond the elastic stage, this approach is not sufficient and does not provide the necessary required insight for a shear resistance calculation. The nonlinear finite element model has proven to be the most accurate and adequate calculation method. The downside is that this method will take longer and requires more background information about the materials used, the connection between structural elements and the type of subsoil. The Strut & Tie approach, is a good first design step. However, for a thorough tradeoff between wall thickness, the complex connection between the floor and the wall, and amount of reinforcement necessary to prevent cracking, the nonlinear finite element method gives the most accurate estimate.

From the calculation results, the conclusion is drawn that the current wall design by Witteveen+Bos is an overly conservative design. Decreasing the current total wall thickness and increasing the amount of reinforcement in the lock floor and the lower part of the wall connected to the lock floor, will also result in a design that is able to resist the shear loading.

Preface

This thesis is my final work for the master Hydraulic Engineering, specialization: hydraulic structures, at the faculty of civil engineering and geosciences of the Delft University of Technology. This research is partially commissioned by Witteveen+Bos with the purpose to gain a better understanding of the shear behavior of large structural elements. In order to achieve this goal, the yet to be built Itaipu bypass is used as a case study.

I could not have done this without a few people who I would like to thank first. I would like to start by expressing my gratitude towards my thesis committee for their guidance during this period and for sharing their valuable knowledge with me. Thank you Bas Jonkman, chair of my committee, for your extensive comments on my report and Max Hendriks for sharing your experience with finite element modeling. A special thanks to my daily supervisors Wilfred Molenaar and Huig de Waardt for being more than just a supervisor but also caring for my personal wellbeing and health. Thank you!

I would also want to like to thank Witteveen+Bos for providing me with an environment full of knowledge. A special thanks to my Witteveen+Bos team and colleagues for the time being and especially Apostolos Bougioukos from Witteveen+Bos who has shared his experience with DIANA with me and provided me with valuable feedback on my model.

My warmest gratitude also goes out to my parents, Mama (Karin) and Papa (Eric), my siblings, Shelby and Jyoti, my grandparents Opa (Robbi) and Oma (Hilde), and my brother in law, Sharvano, for the unlimited amount of support.

And last but certainly not least, I want to thank my boyfriend, Vinay, for the continuous support and motivation throughout my entire study period and for always being my rock whenever it got overwhelming.

D. J. R. Demmerer
Delft, December 2020

Table of Contents

1 Introduction

Hydraulic structures keep increasing in size. Earth's population increased from 1.5 billion to 6.1 billion in only the last century (Roser, 2013). This strong growth in population demands more and bigger civil engineering structures such as hydroelectric dams to provide for enough electricity and locks to allow ship navigation for commercial use. The growing demand is not the only thing that has to be considered. The effect of climate change on sea level rise and the intensity of storms, floods and draughts also puts a bigger demand on the design and strength of structures. With increasing size and increasing amount of structures, technical challenges arise.

Reinforced concrete is the most common composite material used for construction around the world. The combined material characteristics of concrete and steel have proven to be particularly suitable for various construction applications for not only buildings but also hydraulic structures.

1.1 Application of Reinforced Concrete in Hydraulic Structures

Reinforced concrete structure elements can be found all around us and occur in many shapes and formats. The combination of concrete and steel is a common solution in construction. The concrete bears the pressure while the steel takes over when the element is loaded in tension. Reinforced structure elements can be bought as prefab elements or casted in-situ; they are pre-tensioned or post-tensioned, found in various applications such as bridges, buildings, hydraulic structures etc.
Reinforced concrete, with or without prestressed reinforcement, is mostly found as a construction material of beams and plates in buildings. Its application in hydraulic structures is also common due to its watertight characteristics, high strength, stiffness and the possibility to apply the material in structures of large dimensions such as locks and dams.

A well-known large concrete hydraulic structure is World's biggest hydroelectric dam, the Three Gorges Dam (see Photograph 1), located in the Yangtze river in China. This dam has over 28 million cubic meters of concrete and 463000 cubic meters of steel.

Photograph 1 Three Gorges Dam (The Editors of Encyclopaedia Britannica, 2020)

Just like the Three Gorges, many more hydropower dams around the world have been constructed with mainly reinforced concrete, such as the Itaipu dam (also partially a buttress dam) and the Hoover dam on the Arizona-Nevada border (see Photograph 2). Another common type of dam is a fill dam. However, concrete dams are preferred due to the fact that this type of dam allows gates and outer outlet structures to be built into the dam so that discharge outflow can be controlled.

Photograph 2 Hoover Dam left (History.com,2020) and Itaipu Dam right (Dutchwatersector, 2018).

Closer to home, we can also find reinforced concrete in large hydraulic structures such as the concrete pillars of the Eastern Scheldt (see Photograph 3) storm surge barrier and the locks of the North Sea Canal in Ijmuiden.

Photograph 3 Eastern Scheldt left (TU Delft. (n.d.)) and Ijmuiden right (Port of Amsterdam, 2020)

1.2 Uncertainty for increasing wall thickness (member depth)

Because of the common use of reinforced concrete, it is important to have enough knowledge about the failure mechanisms that occur when structural elements are subjected to loading. Reinforced concrete members can be subjected to a combination of shear, flexure, axial load and in some cases also torsion. This thesis focusses mainly on the shear loading, especially in beams with a non-constant depth, referred to as thickness in the remainder of this report. As this thickness, dimension parallel to the shear loading, increases, the available general methods cannot always be applied anymore.

Important note:

The beam/wall thickness which is referred to often in this research, can be compared to the direction commonly indicated as the height of a beam. The terms thickness and height are used interchangeably. Figure 1-1 below can be used for clarification.

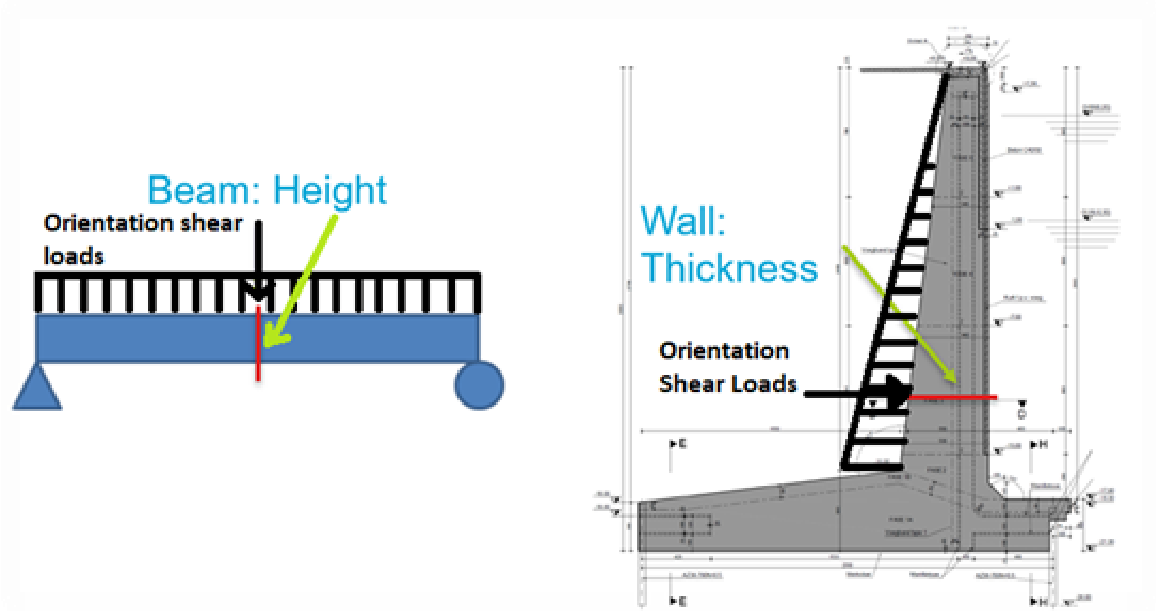

Figure 1-1 Beam height and wall thickness

The available amount of research conducted for these type of structure elements with increasing heights is limited. A study published in the ACI Structural Journal (Sherwood, E., Bentz, E. (2008)), which studied the results of 1849 physical tests on the shear capacity of beams mentioned that only 144 of these 1849, which accounts for a little less than 8%, considered beams with a depth larger than 560 mm. This 560 mm is still much smaller than the depths that will be analyzed in this report. Figure 1-2 below illustrates the amount of shear research performed in the 60 years before 2008 and also the type of tests that have been performed. The part of the histogram that is hatched indicates the tests done on beams with a depth larger than 560 mm.

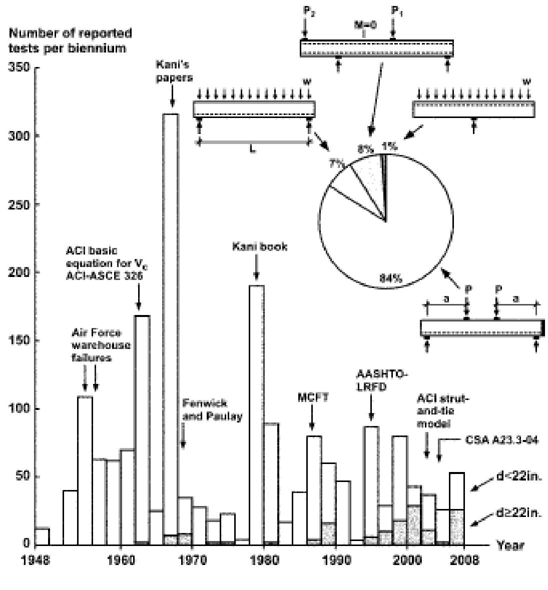

Figure 1-2 Shear tests performed over 60 years

1.3 Problem definition

The concept of shear loading and the shear resistance is well known for 'regular' sized beams, meaning beams that can be characterized as a slender beam and beams characterized as a deep beam. However, once the beam increases in size, such that it falls outside the range of the typical deep beam, less knowledge about its shear behaviour is available. Larger beams are much more expensive to construct making it therefore simply not feasible to make enough large beams available for testing.

Most of the tests, on which the different national codes such as the Eurocode (EC), American Concrete Institute building code (ACI), British Standard building code (BS) and even methods for shear dimensioning are based, have been performed on beams with a thickness up to 1,0 m. Data for larger thicknesses is mostly extrapolated from these test results and therefore inaccurate. A study by Shioya (1989) focused on the shear capacity of beams with a thickness up to 3,0 m. These results showed that the shear capacity as predicted by the Eurocode is overestimated for beams with a thickness between the studied range (1,0 m and 3,0 m). The question arises whether this is also the case for beams with a thickness larger than 3,0 m and if the values calculated by the norms are even more inaccurate than for the range studied by Shioya (1989).

1.3.1 Objective

The main objective of this research is the following:
To gain a better understanding of the available methods for shear calculation of large lock walls and the effect of the increasing thickness of such a wall on its shear capacity.

In order to successfully achieve this objective, a case study of the Itaipu locks will be used. For reference projects with lock walls of the same order of size as the current design of the Itaipu locks by W+B, such as the Panama locks, Tucuruí Lock and Deurganckdok lock, not one uniform approach was used. For most of the cases, a combination of different methods was used. In early design stages it would be valuable if a general easy approach exists in the form of a quick hand calculation without having to perform the expensive time consuming task of doing a thorough analysis of the flow paths of forces and stresses inside the wall.

Main question
The main research question is the following:

Based on existing different methods of calculation, which method can best be used for concrete structure elements with increasing/large thickness?

Sub-questions
The sub-questions that will ultimately also lead to an answer of the main question are the following:
- What are the similarities and differences between the different methods used to determine the shear capacity of walls in the same order of size as the Itaipu lock walls?
- Do the different norms provide adequate methods for shear calculation of walls in the same order of size as the Itaipu lock walls?
- How does the size of aggregates in the concrete mixture influence the shear resistance of a concrete element?

1.4 Thesis Structure

The thesis consists of 8 chapters, each having multiple subchapters and a set of appendices. The first chapter gives a general introduction to the topic and describes the main objective of the thesis.

In the second chapter, that includes the first part of the literature study, the focus is mainly placed on the different types of beams and the common failure methods for beams. This chapter is especially necessary in order to understand what is already well known and how that differs from what is not yet. The main part of the literature research is summarized in this chapter: the concept of Shear. This chapter will also describe the take of the different norms and guidelines on shear and how they differ with respect to each other.

From chapter 3 onward, a case study will be used of the, yet to be built, Itaipu locks. This chapter gives an introduction to this case study.

In chapter 4, the first of the three calculation methods is performed. The shear resistance of the lock walls of the Itaipu locks is calculated using the approach as described in the Eurocode 2 for ‘normal’ non-deep beams.

In chapter 5, the wall is considered to be a deep beam and a strut and tie calculation is performed as the basis of a reinforcement design plan. This method is the second calculation method performed for shear calculations of the Itaipu lock wall.

The third calculation is performed in chapter 6. In this chapter, the same wall is analyzed, however this time with the FEM software DIANA FEA as a both a 2D linear and nonlinear model. The model characteristics and assumptions are described in this paragraph.

The results from the literature study and the different calculation methods are discussed in section 7 and a general conclusion is given.

Finally the limitations and recommendations for future research are given in section 8.

Figure 1-3 also gives an illustrative overview of the outline of the report and the thesis approach.

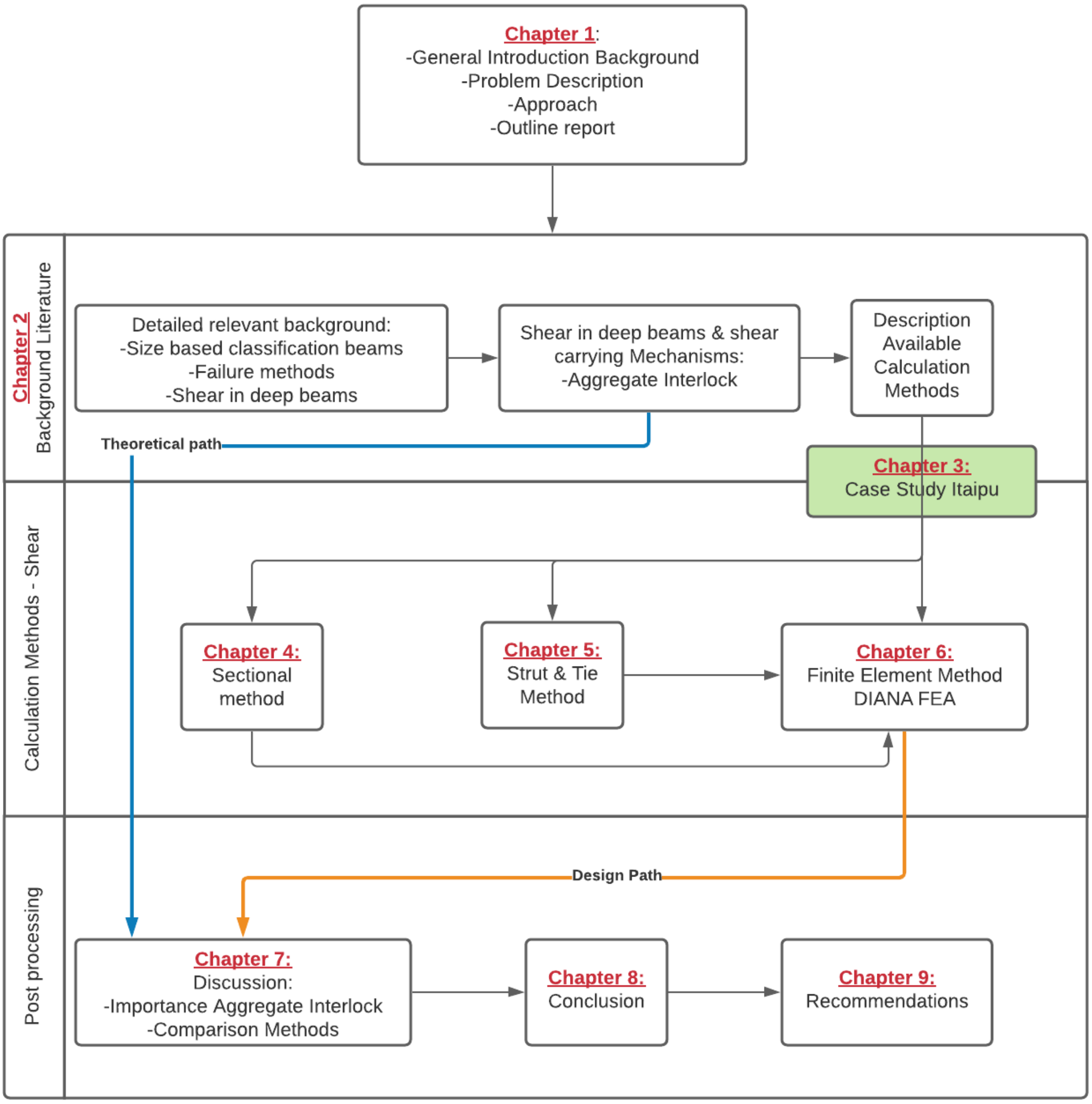

Figure 1-3 Flow chart outline report

1.5 Research Approach

Larger beams are much more expensive to construct making it therefore simply not feasible to make enough large beams available for testing. In order to still be able to understand how these large beams react to shear loading, this research will use three existing methods to perform calculations for a lock wall of the Itaipu locks. The Itaipu locks are designed as a solution to create a bypass next to the Itaipu dam on the border of Brazil and Paraguay. The lock wall that is used for the calculations has a thickness that increases from 6m to 33m and a height of 47m. This lock wall is chosen because this research is commissioned by Witteveen+Bos and the purpose of this assignment for Witteveen+Bos is to obtain a complete analysis of the behaviour of the wall as a result of shear loading.

The approach consists of four main steps: an extensive literature search, a sectional calculation (as used for 'normal' Bernoulli sections), a strut & tie calculation (as used for 'deep beams') and a finite element calculation (linear and nonlinear calculations with DIANA FEM software). The results of these methods are then compared to determine the thickness of the wall of the Itaipu lock, after which general advice is given for calculating this type of wall.

Calculation 1: Sectional Method
This method will be used to determine the required wall thickness for the wall to be able to resist the shear loading and the maximum crack widths that occur as a result of this shear loading, based on the Eurocode 2. The results from this calculation will be the most inaccurate. Beforehand, based on the literature research, see chapter 2, it can be determined that this method is not suitable to determine the shear resistance and required wall thickness. However, this calculation is still performed as a reference calculation.

Calculation 2: Strut & Tie method
This calculation method will also be used to determine the required wall thickness in order to resist the shear loading. This method is also used to design a reinforcement plan for the wall. These results can then be used as an input for the third method.

Calculation 3: Nonlinear finite element method
The third calculation type consisted of three linear models (of the original design and two alternative designs derived from the results of calculation 1) and one nonlinear model of the original Witteveen+Bos design. In the last step, a nonlinear model is used.

The three calculation methods will be compared in order to decide which method can best be used for concrete structure elements with increasing/large thickness.

2 Shear in large structural elements

Structural elements are loaded in different ways, most commonly by normal force, shear force, bending, torsion and combinations between these types of loading. This report will focus on the shear loading and shear behaviour of concrete elements.

Shear capacity increases for deep beams (beams with a large height compared to the distance between the supports) or in case a force acts close to the supports. This is due to the fact that a big part of the loads is directly transferred to the supports (Braam, C. R., Lagendijk, P., Dees, W.C., 2010). This chapter will start with a general introduction into beams, their size classification and the types of failure that can occur. After that, the focus will shift to the shear behavior of deep beams.

2.1 Size-based classification of beams

The most common type of beam is described with the Bernoulli theory: 'plain sections remain plain'. The Euler-Bernoulli beam theory (see Figure 2-1) is the basis of most structural handbooks. Slender beams and plates are described with the Euler-Bernoulli beam-theory. A typical Bernoulli beam has a length to height ratio of $\frac{l}{h} = 20$ (Molenaar, W. F., Voorendt, M. Z., 2016). This approach is based on the assumption that the fibers of the beam that are perpendicular to the normal axis, stay perpendicular to this axis when the beam is bent; in other words: plane sections remain plane. A linear strain distribution is assumed. Individual cross sections are used to derive the internal state of stress from the equilibrium of stresses: the sectional method.

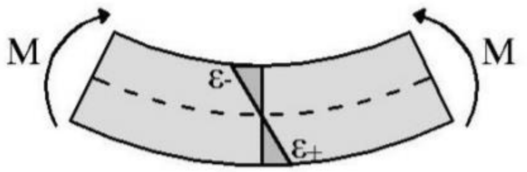

Figure 2-1 Euler-Bernoulli Theory

The Timoshenko beam is an extension of the Euler Bernoulli beam by adding an extra degree of freedom to the beam, a rotation. Addition of this degree of freedom means that plane sections no longer remain plane. The Timoshenko beam theory allows a rotation of the individual sections around the neutral axis which will cause shear stresses in the beam (see Figure 2-2).

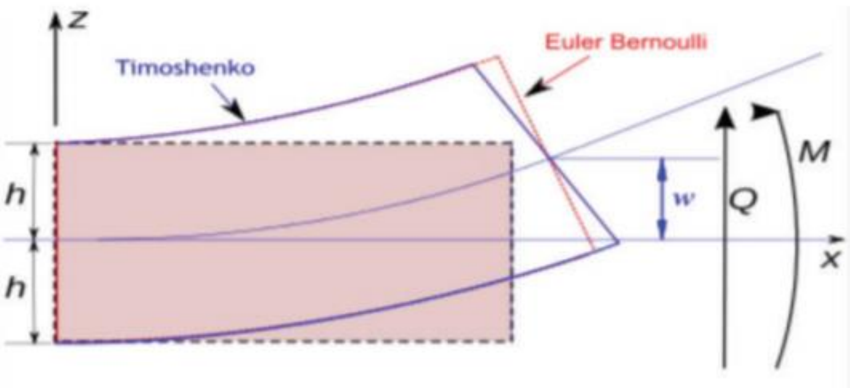

Figure 2-2 Difference Euler & Timoshenko Beam

The theories of Euler-Bernoulli and Timoshenko both describe the so called slender beams. However, as the length to height ratio of a beam increases and beams become less slender, the beams are characterized as deep beams.

Deep beams are described as beams with a length to height ratio of $\frac{l}{h} = 3$. This type of beam has a non-linearity of the strain distribution (Molenaar, W. F., Voorendt, M. Z., 2016).

However, for (hydraulic) structures of a certain size, neither the Euler-Bernoulli theory, the Timoshenko theory nor the deep beam theory apply anymore. As the thickness of a beam increases, it becomes a deep beam and specific deep beam conditions are applied. The characteristics of deep beams are well understood. However, as the depth of a beam is increased even more and a beam is not considered a deep beam anymore, the use of one approach is often not sufficient anymore and methods are combined in this case. Furthermore, the mechanics of these types of beams are still not fully understood.

2.2 Failure methods

There are 5 known failure methods for a reinforced concrete beam (Braam, C.R., Langendijk, P., 2011):

- Flexural failure (Zuivere Buigbreuk)
- Anchorage failure (Verankeringsbreuk)
- Flexural Shear failure (Afschuifbuigbreuk)
- Shear tension failure (Afschuiftrekbreuk)
- Shear compression failure (Afschuifdrukbreuk)

This flexural analysis is based mainly on the Bernoulli theory, describing that plain sections remain plain.

2.2.1 Flexural failure

If two point loads act on a beam symmetrical with respect to each other, neglecting the self-weight of the beam, the part of the beam between the two point loads is loaded in pure bending and flexural cracks will occur at the locations where the cracking moment M_{cr} is exceeded. These cracks form in the same direction as the point loads. The cracks will develop upwards in the beam, reducing this compressive zone of the concrete (see Figure 2-3). If the tensile strength of the reinforcement is high enough, the beam will fail due to compressive strain (stuik).

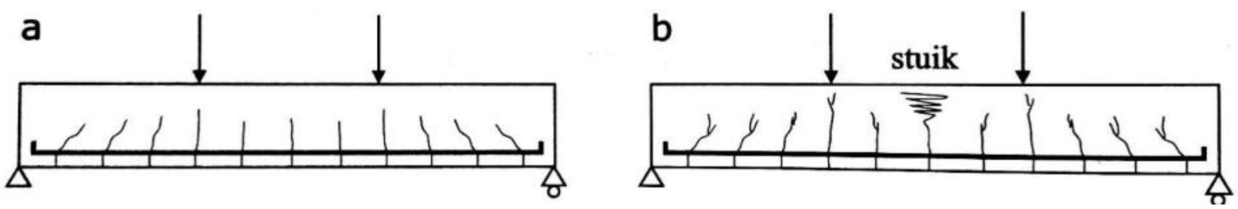

Figure 2-3 (Braam, C.R., Langendijk, P., 2011) Flexural Failure: (a) Crack Pattern in SLS, (b) Crack Pattern in ULS

2.2.2 Anchorage Failure

The crack closest to the support will develop from the inner face of the support in an angle of 45° with the horizontal tie. The distance from the start of this crack to the end of the beam is called the anchorage length. This length has to be large enough to prevent the reinforcement from slipping through the concrete. The support reaction R_d, the compressive strut $R_d\sqrt{2}$ and the tensile tie R_d, need to be in equilibrium to prevent this type of failure (see Figure 2-4).

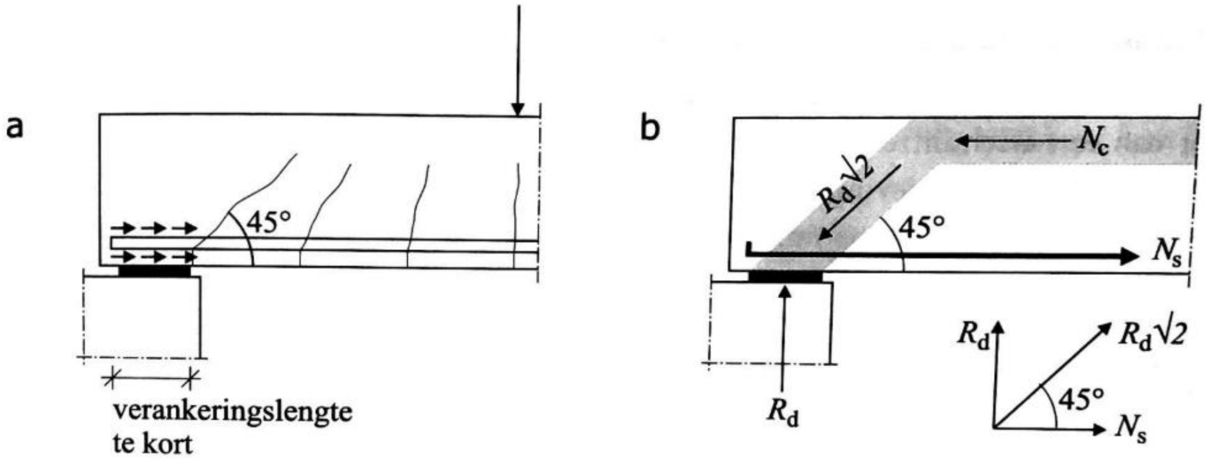

Figure 2-4 (Braam, C.R., Langendijk, P., 2011) Anchorage Failure: (a) Anchorage Length too short, (b) Force distribution at support

2.2.3 Flexural Shear Failure

This type of failure is the most common for reinforced concrete structures loaded by shear force. This type of failure occurs from a combination of bending moment and shear force. The bending moment will first cause flexural cracks that are oriented parallel to the direction of the shear force. However, this is not how the beam will fail. The increasing shear force will result in the development of the flexural cracks into diagonal shear cracks, over a large distance. The internal equilibrium of the beam is not reached anymore and failure will occur (see Figure 2-5).

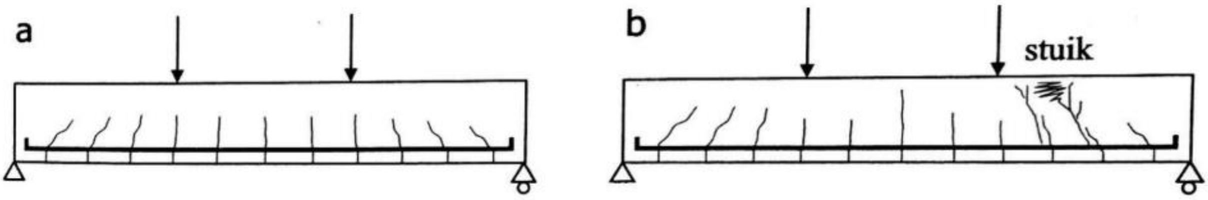

Figure 2-5 (Braam, C.R., Langendijk, P., 2011) Flexural Shear Failure: (a) Crack Pattern in SLS, (b) Crack Pattern in ULS

2.2.4 Shear Tension Failure

If the bending moment Med is smaller than the cracking moment Mcr the cracks will not occur from the bottom of the beam, as they do in the other three cases. The cracks will develop in the centre of the web and make an angle of 30° to 45° with the horizontal tie. Shear reinforcement can be used to prevent failure as a result of these cracks. Failure will mostly occur for cases where the load acts close to the support, the bending moment is small and not enough shear reinforcement is applied. The bursting effect will cause failure of the beam (see Figure 2-6).

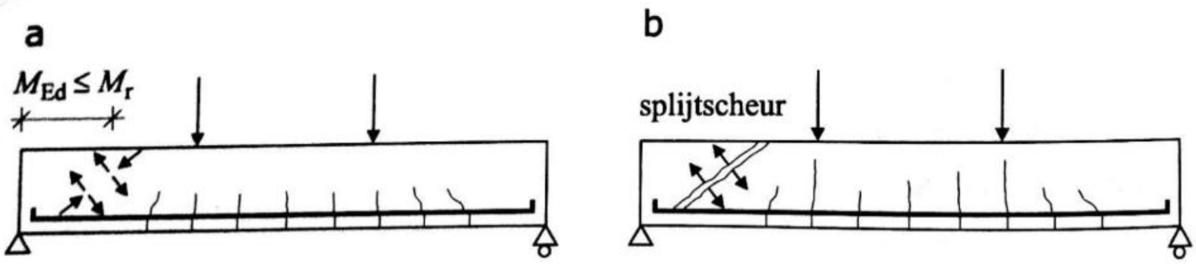

Figure 2-6 (Braam, C.R., Langendijk, P., 2011) Shear Tension Failure: (a) Crack Pattern in SLS, (b) Crack Pattern in ULS

2.2.5 Shear Compression Failure

As mentioned before, to prevent shear tension failure and flexural shear failure, shear reinforcement can be applied in the form of vertical stirrups. The forces from the point loads will be transferred between the cracks to the supports of the beam. This flow of forces can be schematized as a truss (see Figure 2-7).

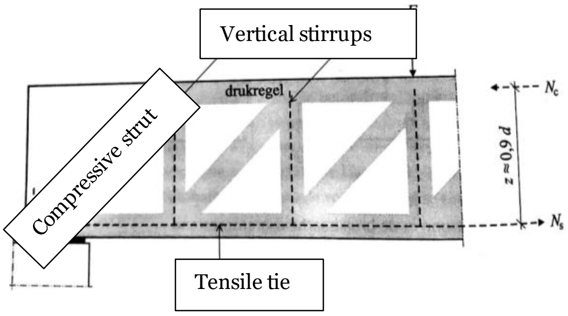

Figure 2-7 Truss

Failure can occur when the loads keep increasing and the beam contains an abundance of shear reinforcement. The result is that the concrete compressive struts will fail before the tensile ties can yield (see Figure 2-8). This type of failure is sudden and the result of too much compression.

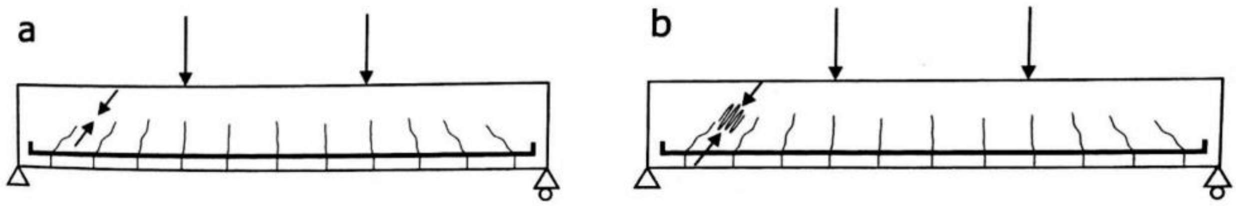

Figure 2-8 (Braam, C.R., Langendijk, P., 2011)Shear Compression Failure: (a) Crack Pattern in SLS, (b) Crack Pattern in ULS

2.2.6 Other Failure Modes

Different papers mention different failure methods. In most cases, the principle of these failure methods is similar to the failure methods mentioned in the research of Braam, C.R. and Langendijk, P. (2011). The naming however differs.

The shear compression failure and shear tension failure are also listed. As can be seen in Figure 2-9 below, three additional failure methods have been listed: (a) diagonal tension failure, (d) web crushing failure and (e) arch rib failure.

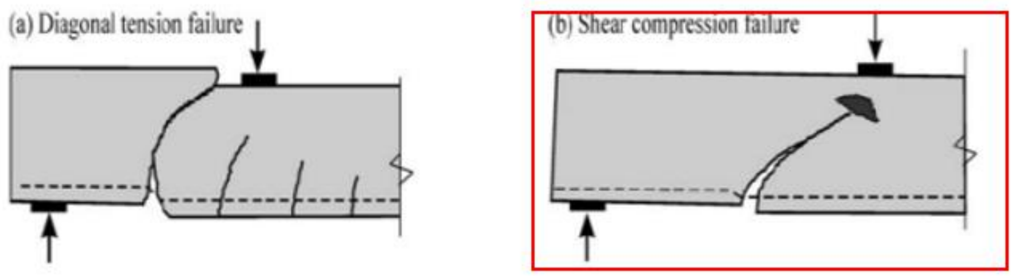

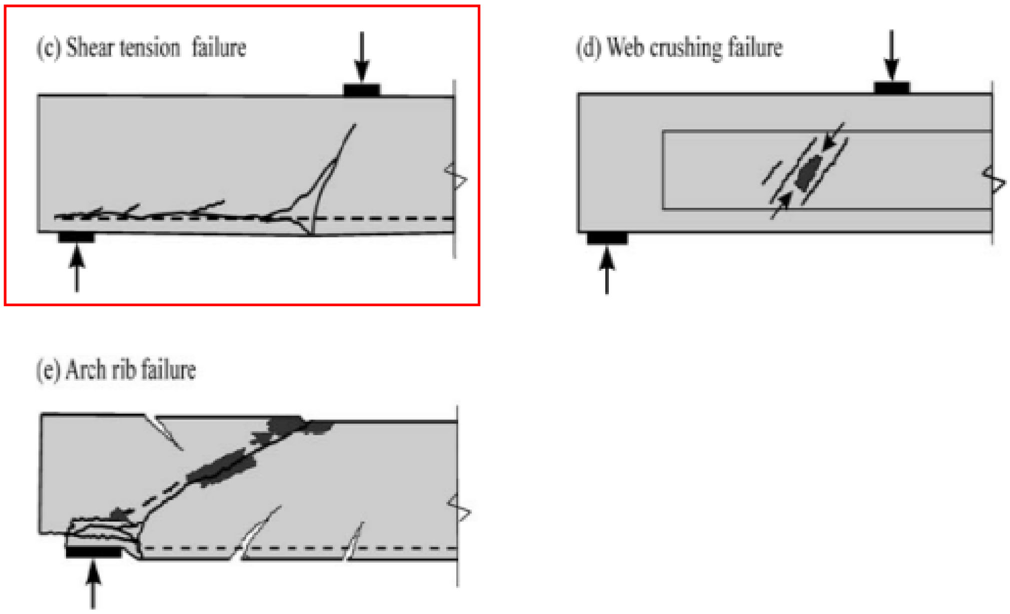

Figure 2-9 Failure methods (Raju,2014).

The diagonal tension failure is similar to the previously mentioned flexural shear failure. This type of failure occurs when the amount of shear reinforcement is not enough and flexural cracks develop to diagonal cracks. The cracks propagate upward in the beam until the beam collapses.

Web crushing failure occurs mostly in beams with a small web, such as beams with an I-profile. The amount of concrete is not enough to bear the compression forces in the beam. This failure method occurs suddenly without warning (Sengupta, 2005).

Arch rib failure occurs mostly in deep beams. This type of failure is similar to anchorage failure.

2.3 Shear Stress

The shear stress is directly dependent on the amount of shear loading of a structural element. It's an important value for the design of structures. Deformation of a structural element by loading will lead to internal stresses: normal stresses and shear stresses. These stresses are visually represented for a three dimensional element inside a larger structural element in Figure 2-10 below. The out of plane stresses are called the normal stresses, indicated with the symbol σ, and the in plane stresses are called the shear stresses, indicated with the symbol τ. A more detailed explanation of stresses and the use of a graphical approach to determine the stress state of an element, Mohr's circle, can be found in the appendix.

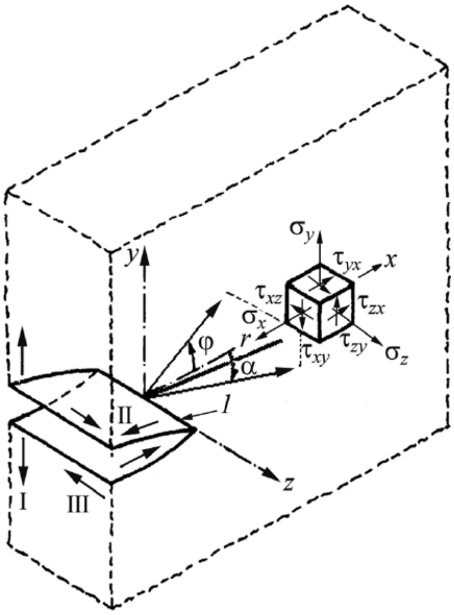

Figure 2-10 Stresses inside an element (Rozumek, D., Macha, E., 2009).

2.3.1 Shear Behaviour of a flexural member

An element loaded in shear is, at a certain point, either uncracked or cracked. The term cracked refers to all the different crack stages. Eventually, when a crack gets large enough, it will lead to failure of a structural element. Idealistically, a structural element gives a warning before failure. This is not the case for brittle failure, where failure occurs suddenly and without warning. Shear failure is in most of the cases characterized as a brittle type of failure and should therefore be avoided (Sherwood, E. G., Bentz, E. C., Collins, M. P., 2005). This brittle failure especially occurs in the case where the reinforced concrete element is not equipped with shear reinforcement. Instead, flexural failure is preferred.

Shear failure can be prevented by, among other measures, adding shear reinforcement: the so called stirrups. As can be seen in Figure 2-11 below, the shear reinforcement also affects the crack spacing in a reinforced concrete member, which in turn affects the aggregate interlock.

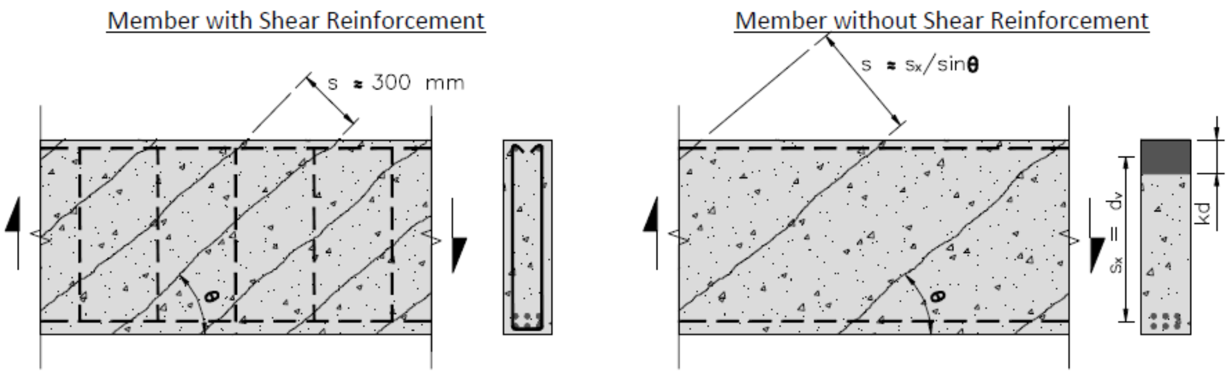

Figure 2-11 Effect of shear reinforcement on crack spacing

The function of shear reinforcement is to connect the flexural compressive part of a structural element to the flexural tensile part. Shear failure can occur when both sides don't act as a unit (anymore).

2.4 Shear capacity

An element loaded by shear has three main shear transfer mechanisms being: direct shear transfer, aggregate interlock and dowel action (see Figure 2-12).

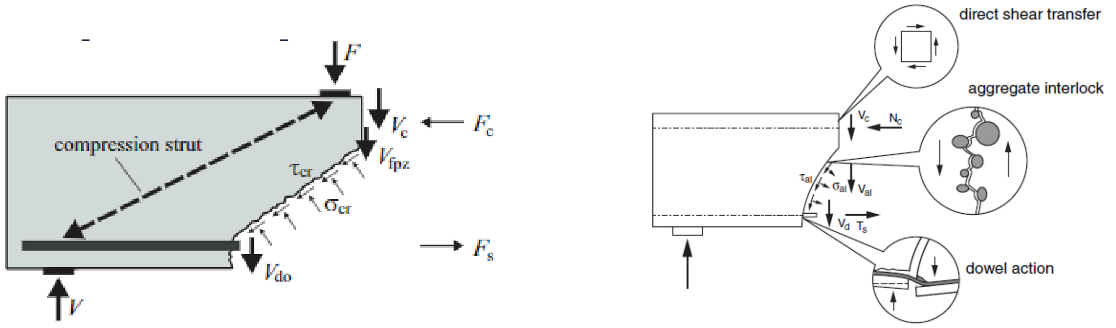

Figure 2-12 Shear transfer mechanisms (Yang, Y., Walraven, J., Uijl, J., 2017)

V_c shear-load bearing of the uncracked compression zone
V_{do} dowel-action of the longitudinal reinforcement
V_{fpz} tensile stresses over cracks in the fracture process zone
τ_{cr} crack friction
arche action or direct compression struts (near supports)

Because the shear capacity is based on the combination of the different shear carrying mechanisms (dowel action, the contribution of the concrete compression force, aggregate interlock), the contribution of each of these mechanisms can be calculated and summed to determine the shear capacity. The downside of this approach is that these components are related to each other as well. In the case where shear reinforcement is added to the structural element, the transfer of shear by this reinforcement is a fourth shear transfer mechanism.

2.5 Aggregate Interlock

Cracks develop through the path with the least resistance, the weakest link. For concrete this is the bond zone between two particles in the hardened cement paste, given that the concrete strength is 'sufficiently low'. The properties of the hardened cement paste therefore play an important role in the shear capacity of a beam. Because the crack develops along the edges of particles, particles will extend from one crack face and interlock in the other crack face. This mechanism is called aggregate interlock (see Figure 2-13) and results in the resistance of shear displacements.

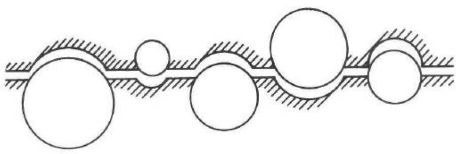

Figure 2-13 Aggregate Interlock (Walraven, J. C., 1980).

The shear capacity gained by aggregate interlock depends on the surface roughness of cracks, the type of aggregate used for the concrete mixture and the displacements across the cracks (Taylor, H. P. J., 1974). Aggregate interlock can contribute from 33% – 90% to the shear capacity. This percentage depends on the strength of the aggregates. Weaker aggregates will contribute less to the shear capacity (Hamadi, Y. D., Regan, P. E., 1980). In the literature a broad range of dependency of aggregate interlock on the shear capacity is found, see Figure 2-14 below. The largest contribution on the shear capacity from aggregate interlock comes from stronger particles and larger particle sizes.

Reference	Percentage	Comments
Fenwick and Paulay (1968)	60	Measured
Taylor (1972)	33–50	Measured
Sherwood et al. (2007)	<70	
Kani et al. (1979)	50–60	
Hamadi and Regan (1980)	44	Natural gravel aggregates
	26	Expanded clay aggregates
Swamy and Andriopoulos (1973)	50–90	

Figure 2-14 Contribution of Aggregate Interlock as Percentage of Total Shear-Carrying Capacity at Failure. (Lantsoght, E., Veen, C., Walraven, J., Boer, A., 2016).

The effect of aggregate interlock on the shear capacity can be calculated for the case with a through crack, a crack through the entire height of the wall. If the crack has developed all the way to the section, the contribution of aggregate interlock is smaller than for a flexural crack (see Figure 2-15).

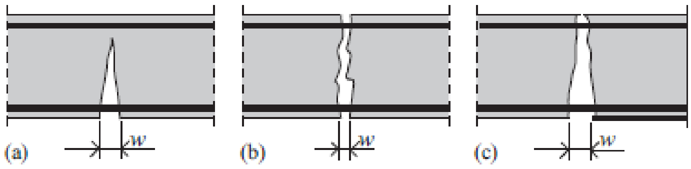

Figure 2-15 Types of cracks: (a) flexural crack; (b) through crack for equal bottom and top reinforcement; (c) through crack for uneven bottom and top reinforcement. (Lantsoght, E., Veen, C., Walraven, J., Boer, A., 2016).

The contribution of aggregate interlock in the case of a through crack is governing due to the fact that a larger crack leads to less contact area between the two sides. This contribution on the shear capacity depends on the shear stress and the concrete strength and yield strength of the steel and can be calculated as follows:

$$V_{agg} = \tau_u * d * b$$

With the shear Stress:

$$\tau_u = C_1 * (\rho * f_y)^{C_2}$$
$$C_1 = (f_{\acute{c}})^{0,36}$$
$$C_2 = 0,09 * (f_{\acute{c}})^{0,46}$$

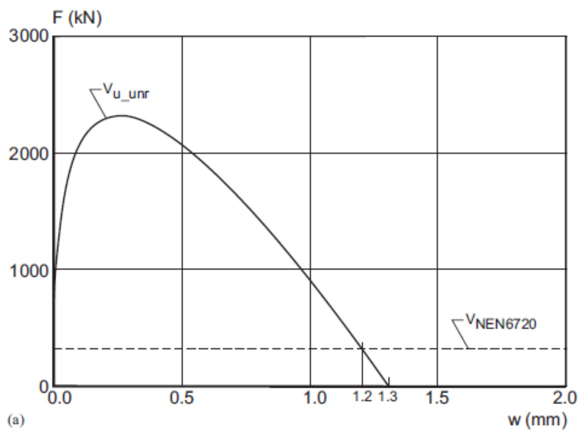

Figure 2-16 Contribution Aggregate Interlock based on unreinforced section. (NEN Committee 351001 1995)

The contribution of the aggregate interlock on the shear capacity increases for crack widths between 0 and 0.3mm. Once a crack width of 0.3mm has been reached, the contribution of aggregate interlock decreases again. For crack widths larger than 1.3mm, there is no contribution of aggregate interlock left. Figure 2-16 is based on normal strength concrete with a maximum aggregate size of 32mm.

Figure 2-17 illustrates the amount of calculated shear that is carried by the above mentioned transfer mechanisms for different concrete profiles.

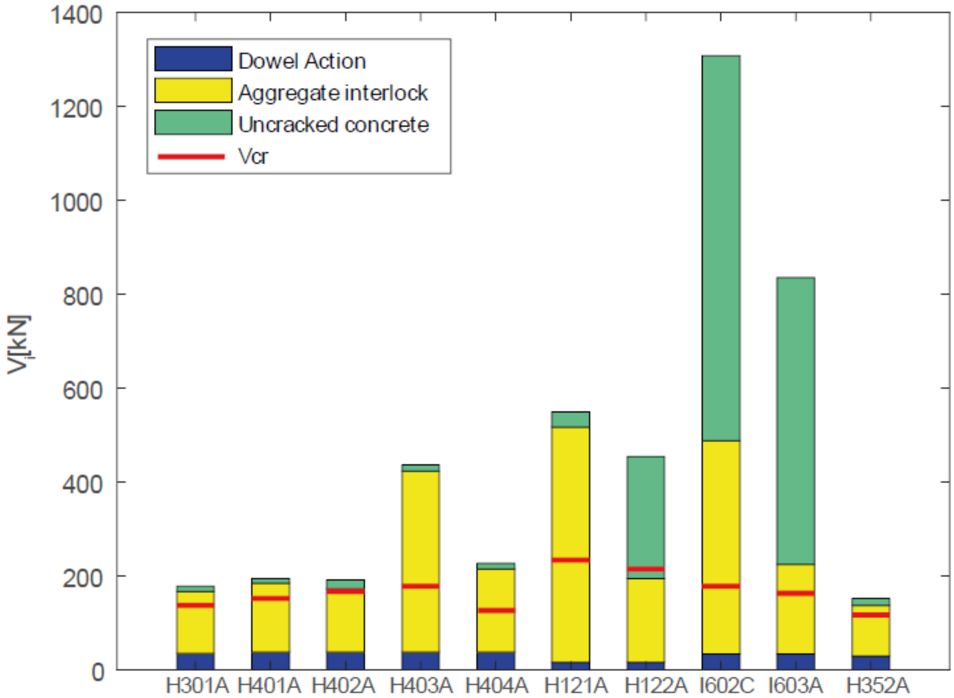

Figure 2-17 calculated shear of different transfer mechanisms (Zárate Garnica, G. I., 2018)

2.5.1 Effect of aggregate size on aggregate interlock

The aggregate interlock is mostly affected by the roughness of a crack; the rougher a crack, the better shear is transferred by the aggregate interlock mechanism. The aggregate size also plays a role in the roughness of a crack (Quach, P., 2016). Another study (Sherwood, E., Bentz, E., Collins, M.P., 2007) however states that the outcomes of tests performed with grain sizes larger than 25mm are not predictable anymore. It is therefore concluded that grain sizes larger than 25 mm should be taken as effectively 25 mm in size. This is confirmed by other experimental research (Sherwood, E., Bentz, E., Collins, M.P., 2006). Two graphs from this research have been presented below. As can be seen in Figure 2-18, the shear strength of a beam does not increase anymore after a maximum aggregate size of 25 mm, given that the aggregate size is the only variable parameter.

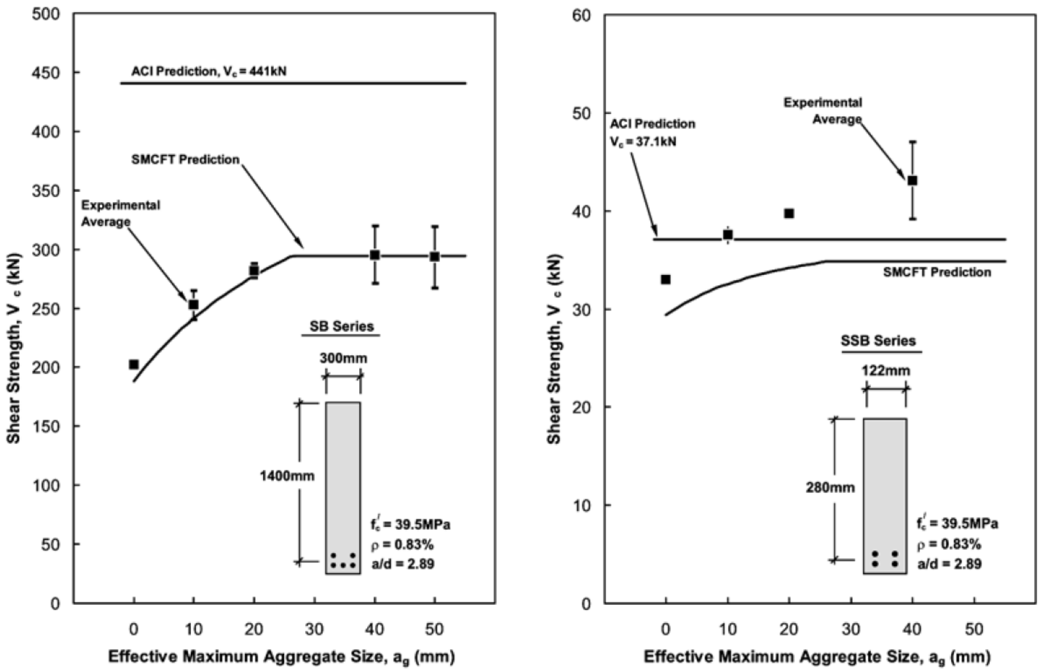

Figure 2-18 Comparison ACI, SMCFT and experimental results for different aggregate sizes (Sherwood, E., Bentz, E., Collins, M.P., 2006).

This result is obtained with experiments that used limestone aggregates.

2.5.2 Effect of concrete strength on aggregate interlock

The quality of concrete keeps on improving over the years. Environmental issues request for more durable concrete. Also, the use of lightweight concrete becomes more popular. Concrete technology keeps on improving which also means that concrete is not the same as a few years ago. This difference in concrete composition also affects the aggregate interlock mechanism of the concrete, mainly because the smoothness of the crack is directly dependable of the quality of the cement paste and the type of aggregate that is being used. The higher the concrete strength, the smoother the crack and therefore also the lower the shear transfer effect of aggregate interlock.

2.5.3 Aggregate interlock in design codes

Previous research proves that the aggregate interlock is an important mechanism to include when predicting the shear behaviour of a structural element. However, in the design codes (fib Model Code 2010, Canadian code (CSA), Eurocode 2 and the ACI-318), the effect of aggregate interlock and with that the aggregate fracture, is not included in the shear capacity predictions (Presvyri, S. 2019). To include this effect in the calculation, the equation should require input regarding the aggregate size, aggregate type and concrete composition.

2.6 Calculation methods for shear capacity

Different methods are used to cope with the shear force inside a wall. These methods are sometimes also used in combination with each other. The available methods will be subdivided into three main calculation methods, the first two being an analytical method and the third one a numerical method:

- Sectional Methods: Codes & Guidelines
- Strut and tie models
- Linear and non-linear finite element method

Truss analogy and strut & tie models

The non-linearity in deep beams is caused by concentrations of loading or an abrupt change in geometry. Due to the concentration of loading, there will be a disturbance in the Bernoulli region of the beam. This disturbance has a length of the largest width over which the force has to be spread (St.Venant's Principle) (Braam, C. R., Ing, H. C., Walraven, J. C., 2019). The area where a local disturbance occurs, is called a D-region (D of disturbed) and the area where the beam is undisturbed by the concentration of loading is called a B area (B from Bernoulli or beam). This part of the beam behaves like a slender beam and sectional methods be used to determine this part of the beam. As can be seen on the right side of Figure 2-19, the B region has a linear strain distribution while the strain distribution for the D region is non-linear.

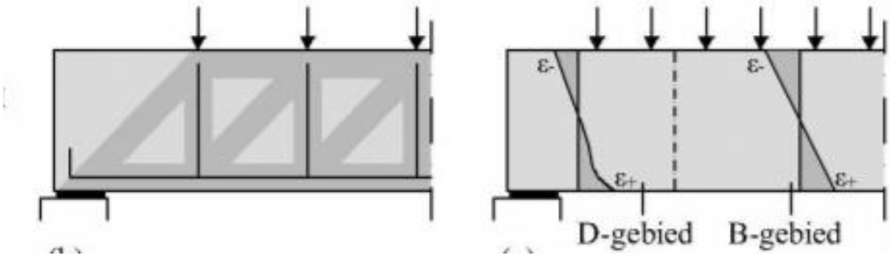

Figure 2-19 Left: Strut and tie method. Right: D-region and B-region of the beam. (Alfrink, 2015)

To determine the reinforcement based on the flow of forces in de D-region, the strut and tie method can be used (see left side of the image above). This method is also described in the Eurocode 2. The use of shear reinforcement changes the flow of forces within a beam. The flow of forces can be modelled as a truss with compression struts and tension ties (see Figure 2-20). This method is referred to as the 'strut and tie model'.

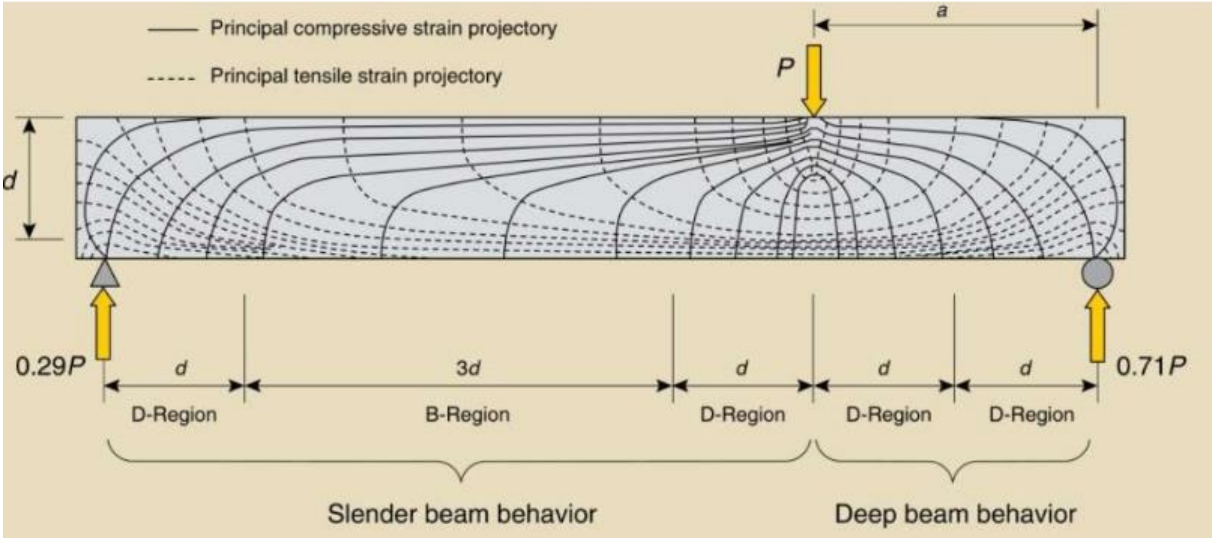

Figure 2-20 D- and B-regions of a beam (Sarkhosh, R., den Uijl , J. A., Braam, C. R., & Walraven, J. C., 2010).

The method is based on the lower limit theorem of the plasticity theory in which it is stated that a support system, from which the failure stress is not exceeded, forms a lower limit for the actual load bearing capacity of the structure (Walraven, J. C., 1988).

The Strut and tie method has the following approach (Walraven, J, Lehwalter, N., 1989):

- Distinguish B and D regions.
- Forces have to be in equilibrium in D region
- Make Strut and Tie Model
- Calculate forces in struts and ties
- Check struts and ties for failure

M. Voorendt & W.Molenaar (2019) give a similar approach but also emphasize the calculations for crack control reinforcement and the anchorage for the ties.

Critical shear displacement theory

One method to calculate the shear capacity is the critical shear displacement theory (Yang, Y., Walraven, J., Uijl, J., 2017). This theory of calculating shear capacity sums the contribution of the three mechanisms, taking into account their relation to each other.

In his paper on the critical shear displacement theory, Yuguang Yan combines the shear-carrying capacity of the concrete under compression, aggregate interlock (with an improvement as compared to the original Walraven expressions so that it better represents structural elements), and dowel action.

This theory takes into account the shear force at which the critical inclined crack opens and marks this as the lower bound for the shear capacity of a structural member. When the shear displacement in an existing flexural crack reaches a critical value, Δcr, this affects the unstable opening of the critical inclined crack and therefore also the shear capacity of the structural member.

Compression field theory (CFT), the modified compression field theory (MCFT) and the simplified modified compression field theory (SMCFT)

This theory is modified, later on referred to as the *Modified Compression Field Theory*, by Vecchio and Collins. This model makes use of three sets of equations/conditions: (i) equilibrium, (ii) geometric conditions and (iii) the stress strain relationships. The effect of aggregate interlock is included in this approach to calculate the maximum shear stress on a crack that can be transmitted by aggregate interlock (equation 15 in Figure 2-21). Therefore, this equation requires the user to be aware of the used aggregate size and the crack width. Applying this theory also illustrates the decrease of member shear strength for increasing crack widths and an increase of member shear strength for increasing aggregate sizes.

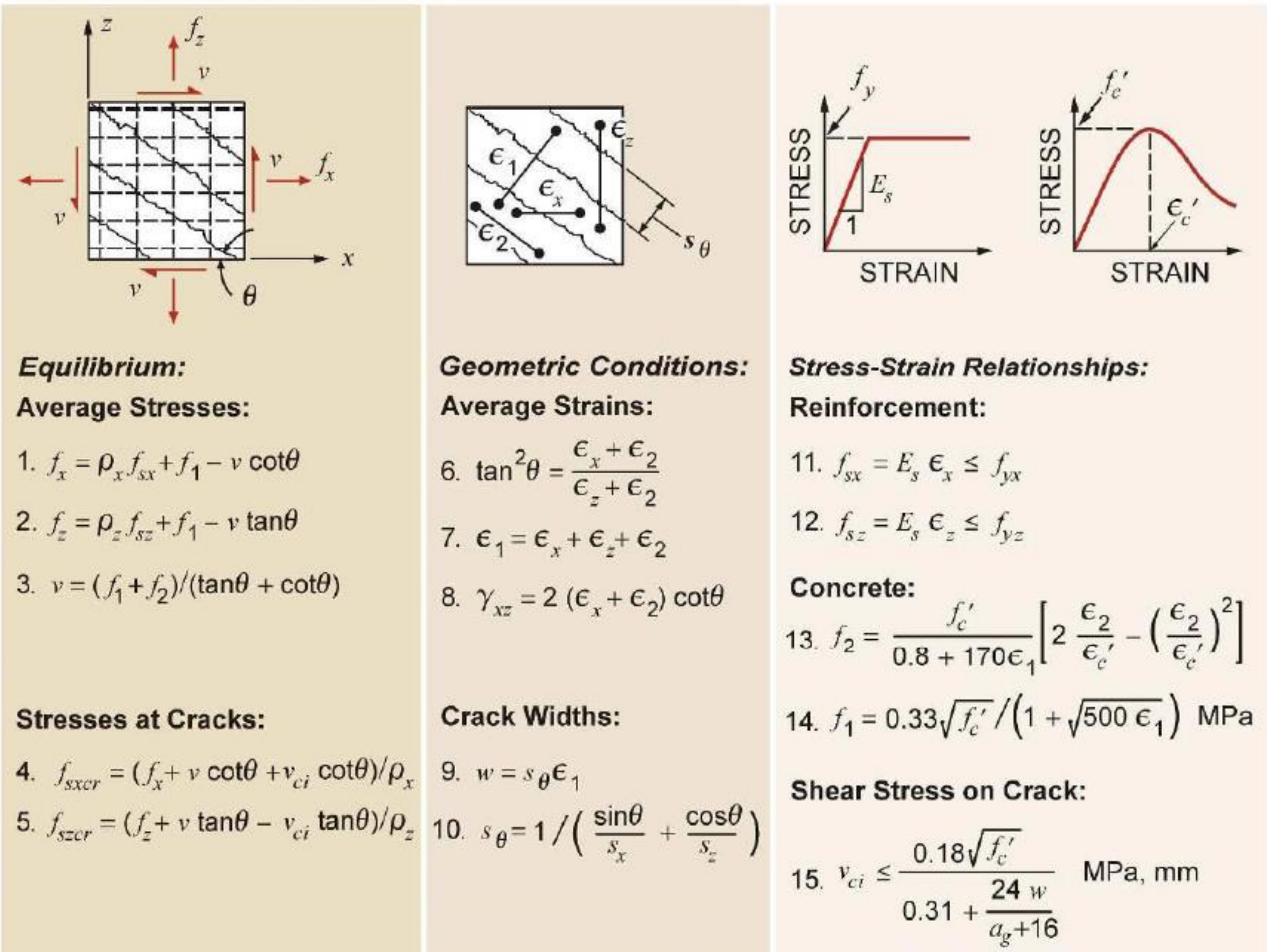

Figure 2-21 Conditions Modified Compression Field theory

Later on, a simplified version of the MCFT method was developed: the Simplified Modified Compression Field Theory (SMCFT) by Bentz and his research team (Bentz et al. 2005). This method was not only more simple than the previous MCFT but in most cases the prediction of shear strength of reinforced concrete members even improved (Sherwood et al., 2005). The SMCFT is illustrated in Equation 1 below:

$$V = V_c + V_s = \beta\sqrt{f_c^{'}} b_w d_v + \frac{A_v f_y}{s} d_v \cot\theta$$

Equation 1 Equation SMCFT (source: Sherwood et al., 2015)

Equation 1 has a contribution of the concrete as well as the reinforcement on the shear resistance of a reinforced concrete structural element.

The biggest advantage of these methods (CFT, MCFT and SMCFT) is that they are based on theoretical knowledge of shear behavior of reinforced concrete elements, in contrast to other methods such as design codes that are based on empirical knowledge with a lack of tests for larger structural elements.

2.7 Strain Effect and Size effect

Another article (El-Sayed, A.K., Shuraim, A. B., 2015) describes the result of a study of the size effect in high strength concrete deep beams without web reinforcement. Experimental research concluded that the shear stresses at failure decreased with increasing beam depth. This corresponds with the size effect as first described by Bazant (1984). The research by El-Sayed and Shuraim also proved that an increase of the concrete strength will also lead to an increase of the size effect. This size effect occurs especially for reinforced members without web reinforcement (Sherwood, E., Bentz, E., Collins, M.P., 2006).

This size effect is directly related to the spacing of the cracks and the crack width. An increase in crack spacing or reinforcement strain will lead to an almost linear increase in crack width. If the thickness of a beam is doubled, without changing the reinforcement strain, the crack width mid beam will also double. A larger crack width has a negative effect on the aggregate interlock mechanism, and thus by increasing the beam thickness, the shear stress for which failure will occur will also decrease.

The variation of nominal shear stress for increasing beam sizes can be described with the size effect, first mentioned by Bazant (1984). For small beams, the nominal shear stress at failure is nearly constant. This is the result that is mostly obtained for laboratory tests due to the fact that the majority of beams that have been tested fall within the category of 'small beams'. However, as beams increase in size, the nominal shear stress at failure decreases. This effect can be seen for beams categorized as 'deep beams'.

In conclusion, the size effect describes that the nominal shear strength of a concrete element decreases as the characteristic dimension of the member such as the effective depth increases.

2.8 Sectional Method: Codes, guidelines and other literature

The different region codes and guidelines have a similar directive to estimate the shear capacity of reinforced concrete beams. This subchapter will briefly list

TU Delft literature and Eurocode 2 (NEN-EN 1992-1-2)

The 5% lower limit of shear capacity of beams without shear reinforcement (J.C.Walraven & C.R.Braam (2018)):

$$V_{Rk,c} = 0{,}15(3\frac{d}{a})^{\frac{1}{3}}\xi(100\rho_l f_{ck})^{\frac{1}{3}} b_w d$$

and for the mean value:

$$V_{Rm} = 0{,}18(3\frac{d}{a})^{\frac{1}{3}}\xi(100\rho_l f_{cm})^{\frac{1}{3}} b_w d$$

which lead to the design value:

$$V_{rd} = \frac{V_{Rm}}{\gamma_c}$$

where:

$$\xi = 1 + \sqrt{\frac{200}{d}} \leq 2{,}0 \text{ where d is mm}$$

$$\rho_l = \frac{A_{sl}}{b_w d}$$

$$\gamma_c = 1{,}5$$

The expression that is found in Eurocode 2 is similar to the equation above. Eurocode 2 gives the following expression for design value of the shear force capacity:

$$V_{Rd,c} = \left[C_{Rd,c} k (100\rho_l f_{ck})^{\frac{1}{3}} + k_1 \sigma_{cp}\right] b_w d$$

$$V_{Rd,c} \geq \left[\vartheta_{min} + k_1 \sigma_{cp}\right] b_w d$$

where:

$$k = 1 + \sqrt{\frac{200}{d}} \leq 2{,}0 \text{ where d is mm}$$

$$\sigma_{cp} = \frac{N_{Ed}}{A_c} \leq 0{,}2 f_{cd}$$

$$\vartheta_{min} = 0{,}035 k^{\frac{3}{2}} f_{ck}^{\frac{1}{2}}$$

The Dutch Annex of Eurocode 2 uses the recommended values:

$C_{Rd.c}$=0,12

k_1=0,15

The former Dutch Concrete code, VBC (NEN6720)

The precursor of the Eurocode 2 is the NEN6720. In this former Dutch code, the shear capacity is tested by setting an lower limit for the shear stress such that:

$$\tau_d \leq \tau_u$$

The shear capacity by new regulations such as the Eurocode2 gives a smaller value than the previously used VBC code. As a result, stirrups are more frequently needed compared to the recommended amount of shear reinforcement by the VBC code.

American Code (ACI 318)

Calculations from Dutch engineering firms for previous projects outside the EU, are often based on the Eurocode norms. However, in South America, the American construction code ACI318 is mainly used as a guideline by, in the case of the Itaipu case that will be focused on for the calculations in this report, Latin American engineers. The ACI (American Concrete Institution) provided the guideline ACI318 for Structural Concrete.

The basic equation for shear capacity (without torsion and for non-prestressed members) in the ACI318-11 (Section 11.2.1.1) is the following:

$$V_c = 2\lambda\sqrt{f'_c} b_w d$$

where λ depends on the weight of the concrete used; for normalweight concrete λ equals 1 and $\sqrt{f'_c}$ (expressed in psi) shall not exceed 100psi, so the concrete compressive strength shall not exceed 68 MPa.

In the presence of a compressive Normal force and a Shear force, according to the ACI318-11 (equation 11-4), this equation can be extended to:

$$V_c = 2(1 + \frac{N_u}{2000A_g})\lambda\sqrt{f_c'}b_w d$$

where the factor N_u/A_g is expressed in psi.

2.8.1 Code Comparisons

Rombach, Kohl, & Nghiep, 2011 describes the differences between the different region codes based on the case of a simple rectangular 200mm by 300mm beam. This research compares the ACI 318 code, EC2 and the British Standard code (see Figure 2-22).

ACI 318 $\phi_c = 0{,}75$	$V_{Rd} = 0.17 \cdot \phi_c \cdot \sqrt{f_c'} \cdot b_w d$	$V_{Rd} = 38 / 54$ kN
BS 8110-1 $\gamma_m = 1.25$	$V_{Rd} = \frac{0.79}{\gamma_m}(100 \cdot \rho_l)^{1/3}\left(\frac{400}{d}\right)^{1/4}\left(\frac{f_{ck}}{25}\right)^{1}$	$V_{Rd} = 47 / 60$ kN
EC2 γ_c=1.5, k=1.8	$V_{Rd} = \frac{0.18}{\gamma_c} \cdot k \cdot (100 \cdot \rho_l \cdot f_{ck})^{1/3} \cdot b_w d$	$V_{Rd} = 45 / 56$ kN

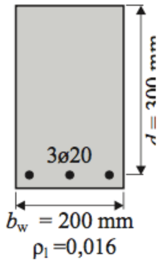

Figure 2-22 Comparison Shear Capacity for ACI318, BS 8110-1 and EC2. (Rombach, Kohl, & Nghiep, 2011)

The results of this comparison are that the EC2 has the highest estimation of the shear capacity. The ACI has the most conservative estimation (84%-96% of the EC2 value) and is therefore the most safe.

Shioya (1989) states that the in the expressions of the scaling effect on the shear force resistance of concrete beams included in the norms have been derived from experiments on beams with a useful height, d, op to 1,0 m. The results of research into the shear force resistance beams with a useful height up to a d of 3,0 m are described by Shioya. An analysis of the test results shows that the scaling effect in the shear force resistance can be described as:

$$k = \frac{1}{d^{0,25}}$$

with d in m. Here d=1,0 m is chosen as the basic value, so that the scaling effect is 1,0 for a d of 1,0 m. This means that for beams with a useful height larger than 1,0 m, the shear capacity is smaller than predicted in the EC2.

A more recent study (Þórhallsson, E., Runar Birgisson, S., 2014) has a similar result. This study compared the shear capacity as estimated by three different norms, EC2, ACI and Model Code 2010, to the measured shear capacity during tests of concrete beams without shear reinforcement. The results of this comparison where that the Model Code 2010 and the EC2 estimated a shear capacity that was lower than the real shear capacity of the test beams, with EC2 being the least safe approach. The ACI code, in contrast, estimated a conservative value for the shear capacity.

With 4 bars Asl with a diameter of 32mm, b_w of 1000mm, C30/37 and no compressive force, Table 2-1 gives a comparison between the shear capacity as calculated with the equation of k from the Eurocode and the shear capacity with the k as given by Shioya. The final column shows how much smaller the shear capacity calculated with Shioya is when compared to that of the Eurocode 2.

d (m)	k EC2	k Shioya	Vrd,c EC2 (N)	Vrd,c Shioya (N)	%
1	1.45	1	370	255	30
2	1.32	0.84	534	341	36
3	1.26	0.76	669	404	39
4	1.22	0.71	788	455	42
5	1.20	0.67	896	500	44
6	1.18	0.64	998	539	45
7	1.17	0.61	1093	575	47

Table 2-1 Comparison results Eurocode 2 and Shioya

2.9 Concluding Remarks

The most important shear transfer mechanisms are: aggregate interlocking, residual tensile strength of concrete, dowelling action and the inclination of the compression chord. In deep beams, the aggregate interlock is the most important shear parameter. This is due to the fact that structure elements with increased size and strain have a larger crack width, resulting in a decrease of aggregate interlock and residual tensile strength from the concrete. The shear transfer capacity for these types of larger beams depends mainly on the amount of shear that is transferred across cracks. The effect where shear stress at failure decreases with increasing beam depth is called the 'Size Effect'. A higher concrete strength will lead to an increase in the size effect. In other words: shear resistance is lower for structure elements consisting of high strength concrete and larger effective depths. The shear capacity of a concrete mixture increases if the cracks go around the aggregate instead of through the aggregates. Marine aggregates are therefore assumed to be a better type of aggregate to use than limestone due to their higher strength.

3 Case Study Itaipu Bypass

This chapter gives an introduction to the case study that will be used for the shear calculations.

In January 1971, construction of the Itaipu Dam began and on 5th May 1984 the dam was officially opened. The Itiapu Dam, see Figure 3-1, is located on the border between Paraguay and Brazil in the Parana river. At the time of construction, the Dam was designed to be the World's biggest hydroelectric Dam. Currently, this title belongs to the Three Gorges Dam in the Yangtze river in China, but the Itaipu dam still holds the record for most amount of Energy produced in one year. The Dam was designed to provide households in Brazil, namely the biggest part of Rio de Janeiro and São Paulo, and almost every household in Paraguay with Energy.

Figure 3-1 Itiapu dam (Itaipu Binacional)

After a thorough site investigation, the current Dam location was chosen mainly because of the hard basalt subsoil which would be able to carry the loads of the big structure and the large water head difference that can be achieved at the dam. Thus, due to the topographic conditions and the water flow, this location was therefore the most suitable for efficient energy production. Closing off the Parana river at the location of the Dam, results in a reservoir behind the Dam. The level in the reservoir is controlled by the discharge through the turbines and a spillway. The discharge through the turbines induces the production of Energy while the spillway is created to release water from the reservoir to prevent overflow over the Dam. This discharge is therefore activated in case of a high water level in the reservoir.

Two of the most important features that determine the capacity of a hydroelectric dam are the size of the reservoir and the water level difference in front of the dam and behind the dam. Before the dam was built, the Parana river fell into a 60m deep canyon after which it had turbulent flow conditions for 60m. A total water head difference of 100m was then achieved. From this canyon to the location of the dam, another 20m of water level difference is achieved. The delta of the Parana river around the Itaipu dam and the location of the dam can be seen in Figure 3-2 below.

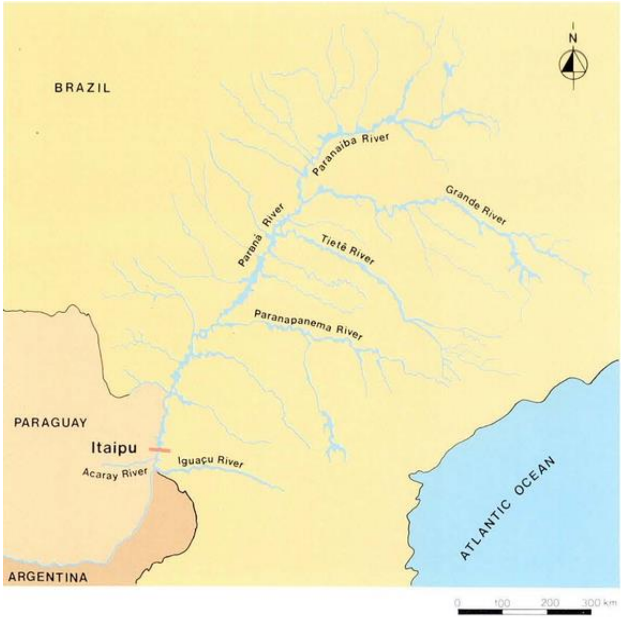

Figure 3-2 Parana Delta (Itaipu Binacional, 1994)

Currently, navigation through the Paraná river is blocked by the Dam and therefore not possible at that location. In a feasibility study done by Witteveen+Bos in the Netherlands (referred to as W+B in the following parts of this document), a bypass with locks to allow navigation is designed.

The channel trajectory of the bypass has a subsoil of mostly volcanic basalt layers topped by a layer of clay with a thickness ranging from approximately 5 to 10m. This top clay layer can easily be excavated. The soil characteristics provide a challenge to the project due to the fact that the soil consists of Basalt. These hard rock layers are difficult and expensive to excavate. The amount to be excavated has therefore been minimized in the case study done by W+B (see Figure 3-3), for example by optimizing the design of the wall. However, this subsoil also provides the opportunity for new and improved designs that implement the existing basalt into the design requiring less concrete and therefore less cement. However, the combination of concrete and basalt falls outside the scope of this thesis.

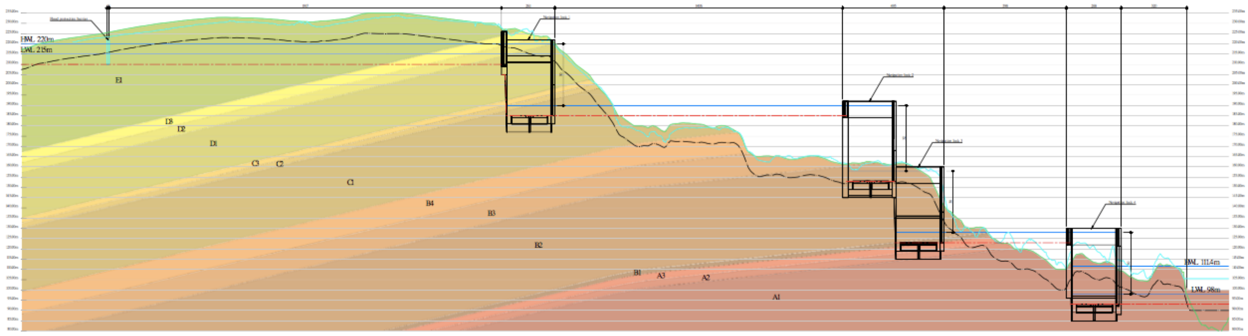

Figure 3-3 Channel Trajectory with the 4 locks in black. Design: Witteveen+Bos

The current design of the Itaipu bypass and lock complex by W+B consists of 4 navigation locks with a head difference of 30+ m for each lock and 41+ m high solid concrete walls with a variable thickness from 6 up to 30+ m under a 1:0.7 slope. The lock design is based on the design which was already performed in an initial feasibility study by the Itaipu Binacional Committee. Figure 3-4 and Figure 3-5 below show a cross section of the four locks with the black dashed line being the top of a basalt layer and the green line the top of a clay layer. As can be seen, the design of the locks differ from each other due to a difference in the level of the layers in the subsoil.

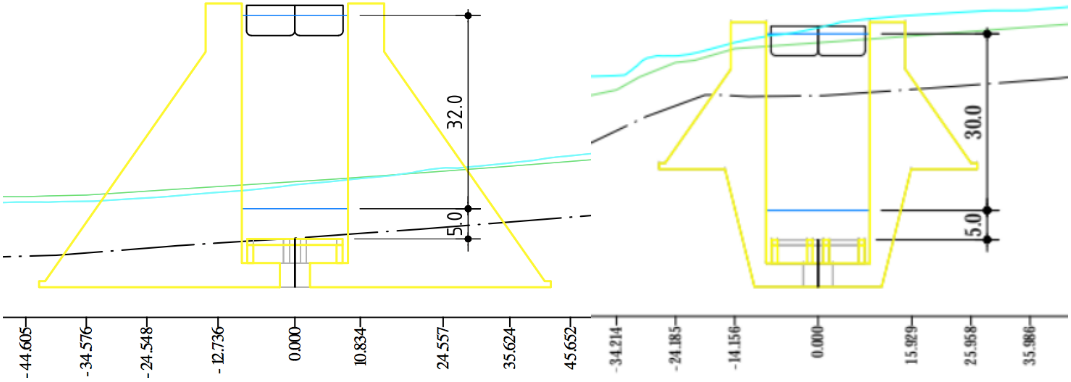

Figure 3-4 Left: Lock 2. Right: Lock 3 Design: Witteveen+Bos

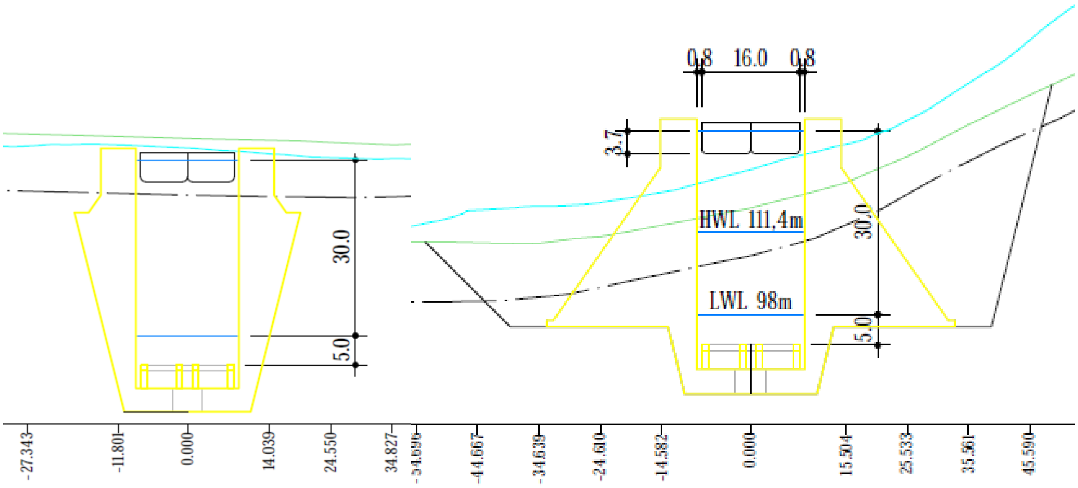

Figure 3-5 Left: Lock 1. Right: Lock4 Design: Witteveen+Bos

The current solid concrete design requires the use of 1,653,624 m^3 of concrete for the lock walls of the 4 locks combined.

3.1 Geometry

For this thesis, only lock 2 will be analysed because this is a more basic and generic design that will also be applied in other projects. It will therefore be more valuable to gain insight of the effect of the external loading on the behaviour of the wall. But most importantly, this design is used because, compared to the design of the other locks, lock 2 is the most interesting in terms of shear force, the main aim of this graduation project. It has by far the thickest lock walls compared to the other three locks. The cross section of lock 2 is given in Figure 3-6 below.

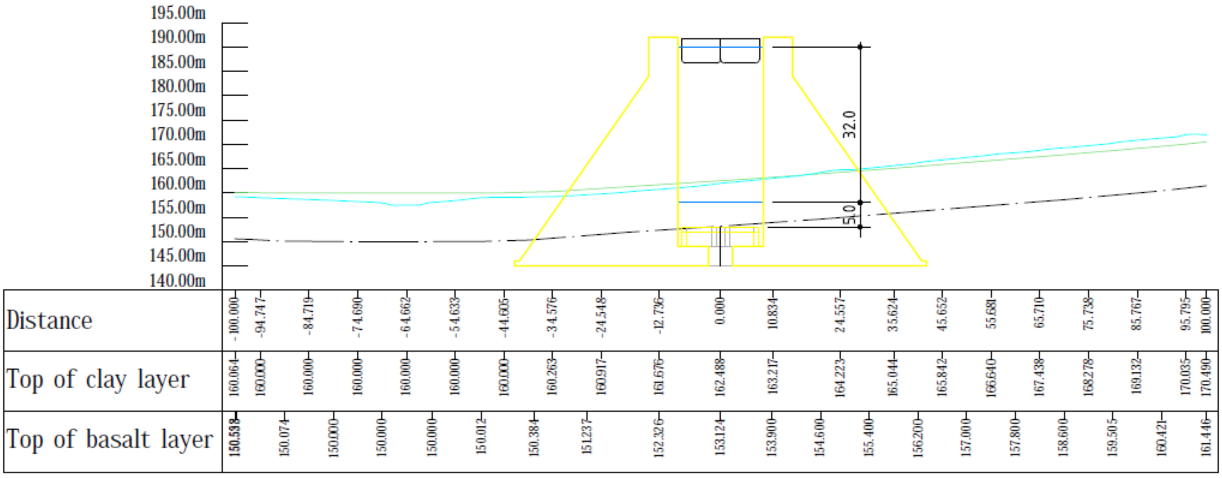

Figure 3-6 Geometry Itaipu Lock wall

For further calculations, the original design from Witteveen+Bos is simplified to the design in orange (see Figure 3-7).

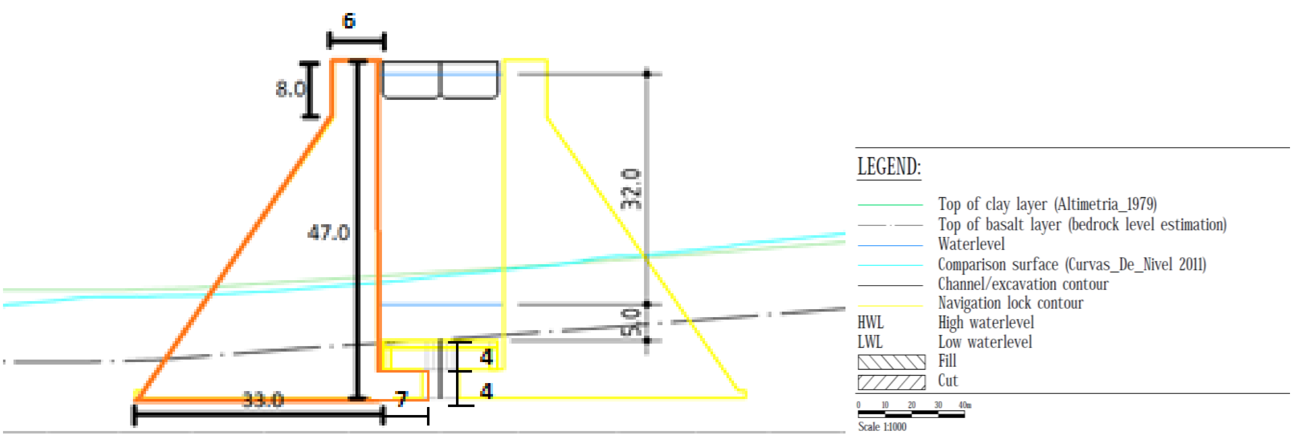

Figure 3-7 Simplified design

3.2 Construction Method

The construction method of the lock is divided in three main steps: excavation of the clay layer, blasting of the basalt layer and construction of the lock. For the following calculations, the assumption is made that the lock will be constructed on top of the basalt layer. After excavation of the soil layers and construction of the lock, the soil will not be backfilled. An cross section of the site for the initial situation and the three main excavation steps is given in Figure 3-8, Figure 3-9, Figure 3-10 and Figure 3-11. The green colour indicates the top clay layer and the grey colour indicates the basalt layer.

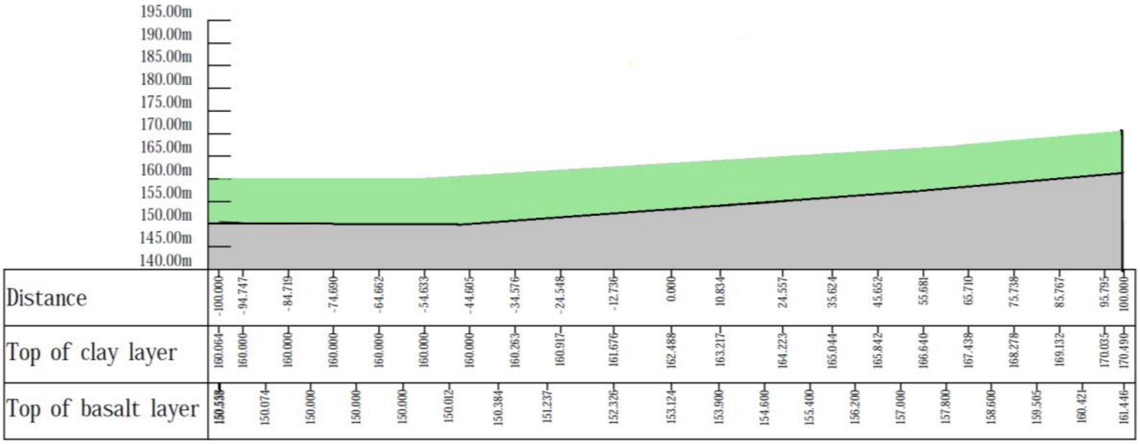

Figure 3-8 Cross section site

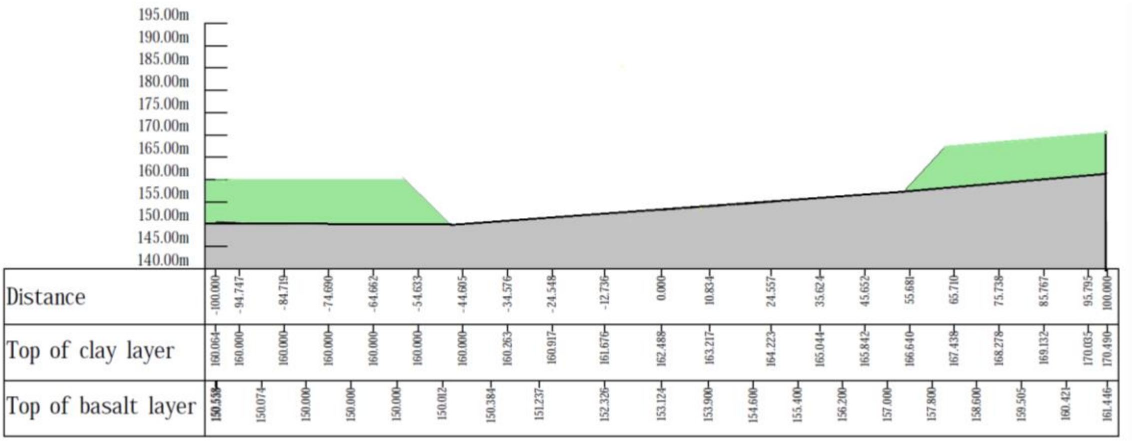

Figure 3-9 Step 1: Excavation of the clay layer.

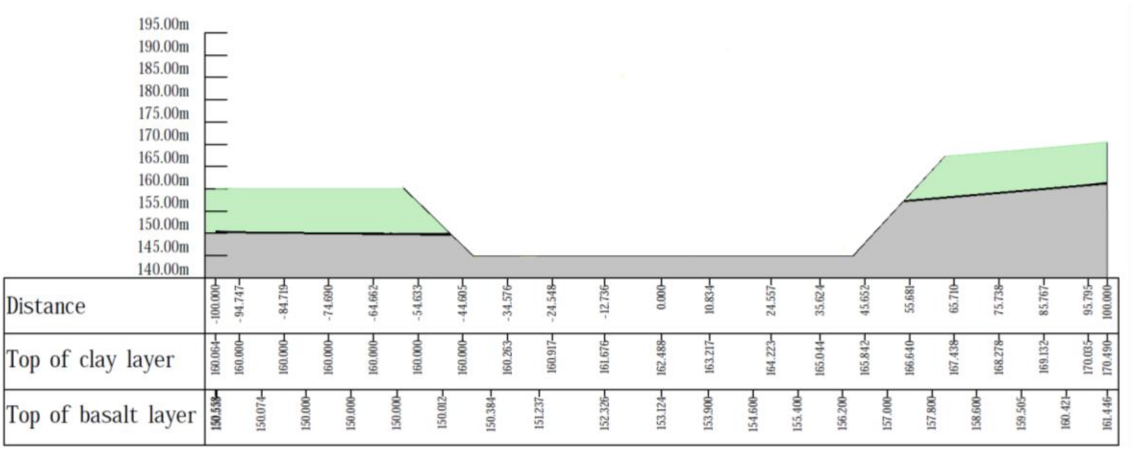

Figure 3-10 Step 2: Blasting of the Basalt layer

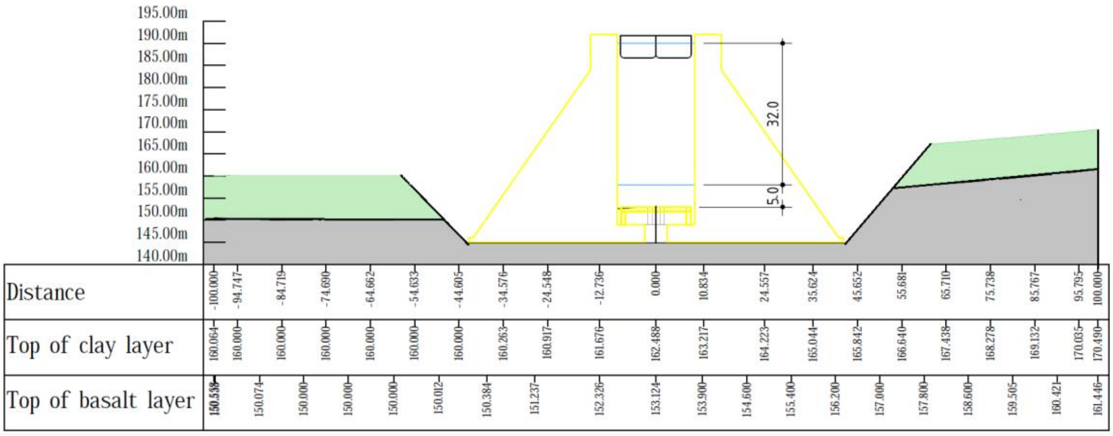

Figure 3-11 Step 3: Construction of the lock

3.3 Boundary Conditions

Figure 3-12 below shows the different levels in the cross section. The maximum design water level inside the lock is at 190m. However, for the calculations, 192m is used as the maximum water level so that incidental exceedance of the design water level does not lead to failure of the lock. The bottom of the lock is at 149m. The top of the levelling system is at level 153m.

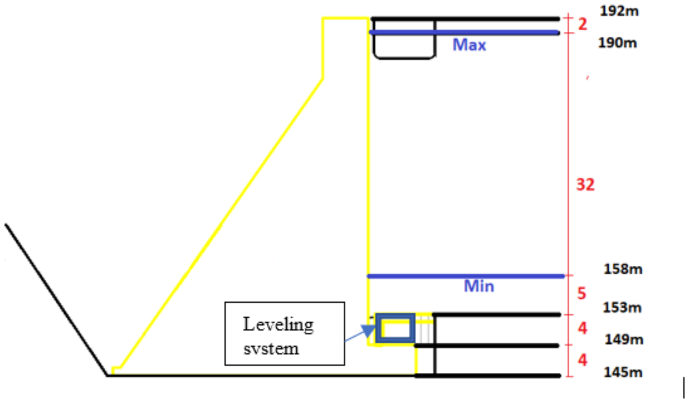

Figure 3-12 Boundary Conditions

Ground level

For the construction of the lock walls, the existing soil is excavated at the location of the walls. Before excavation, the soil was at level 160m. After completion of the lock walls, the soil will not be filled back up, resulting in zero horizonal soil stress on the wall.

Ground water table

The ground water table is assumed to be 1m below the ground level at 159m.

3.4 Loads

3.4.1 Permanent Loads

Self-weight concrete structure

The self-weight is calculated with the volume of the concrete structure and a specific weight of reinforced concrete. The calculations are executed per meter length (b_w = 1m).

Characteristics reinforced concrete:

- Specific weight: 25 kN/m³
- Strength class: C30/37
- f_{ck}: 30 MPa
- f_{cd}: 20 MPa
- Reinforcement: B500B

Upward water pressure

Due to the fact that the lock is constructed on top of the basalt layer, it's likely that there will not be an upward groundwater pressure.

Variable loads

When the lock is in use, the water level fluctuates between 158m and 190m. The loads are therefore calculated for two load cases for the lock in use and one load case for the lock during maintenance.

<u>Water level inside lock</u>

Case 1: Minimum water level inside lock

When the lock is in use, the minimum water level is at 158m. The bottom of the lock is at 149m.
At level 158m, the water pressure equals:

$$P_{hydr}=h*\rho*g=9*1000*9{,}81= 88290 \text{ N/m}^2 \approx 88 \text{ kN/m}^2$$

Case 2: Maximum water level inside lock

At level 192m, the water pressure equals:

$$P_{hydr}=h*\rho*g=43*1000*9{,}81= 421830 \text{ N/m}^2 \approx 422 \text{ kN/m}^2$$

Case 3: empty lock

During maintenance, situations can occur when there is no water in the lock at al. In this case there will be no force from the right side of the wall.

The governing load situation occurs for the maximum water level in the lock. Load case 2 will be the governing load case.

3.4.2 Load Combinations

The effect of the different loads is taken into account with the following equation:

$$E_d = E\left\{\sum_{j\geq 1}^{n}\gamma_{G,j}\,.\,G_{k,j} + \gamma_{Q,1}.Q_{k,1} + \sum_{i\geq 1}^{n}\gamma_{Q,1*}\psi_{0,i}.Q_{k,1}\right\}$$

The lock is considered a CC3 consequence class as described in Eurocode 1: NEN-EN-1990 due to the fact that failure of the lock will lead to flooding of the area around and as a result loss of flora and fauna, large economical damage and in the worst case even devastating social damage such as loss of

human life. For the unfavourable load case, the partial factor for the permanent load therefore equals 1,2 and for the favourable load case, this factor equals 0,9.
The partial factor for the main variable load equals 1,5 in case this load is favourable and 0 for the case where unfavourable.
The partial factor for other variable loads also equals 1,5 where favourable and 0 where unfavourable.
Due to the lack of information for this type of structure, the combination reduction factor for the accompanying variable loads, $\psi_{0,i}$, equals 1,0.

The loads are combined in Figure 3-13 below.

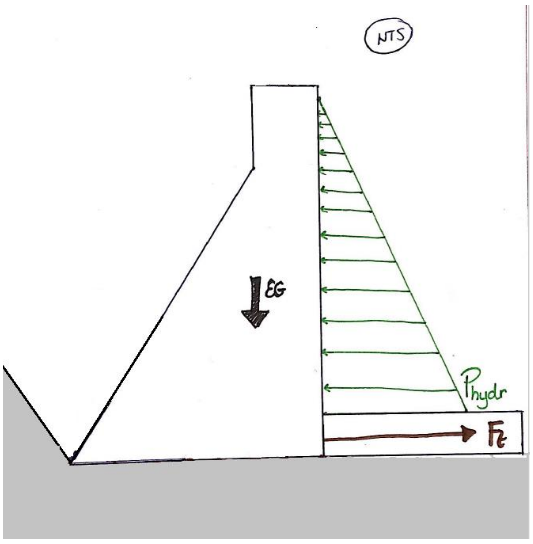

Figure 3-13 Loading wall

The partial factors for the different load cases are shown in Table 3-1.

	Unfavourable	Favourable
Self Weight Concrete (EG)	1,2	0,9
Horizontal Water Pressure (P_{hydr})	1,2	0,9

*Table 3-1 Partial factors *Used partial factors are highlighted*

The loading conditions as mentioned in this chapter are used in the three calculations (sectional calculation, Strut & Tie calculation and finite element calculation) that are performed in the following chapters (respectively chapter 4,5,6).

4 Verification Shear Resistance using cross-sectional method

The first calculation method that will be used to determine the shear resistance is the method as described by section 6.2.2. of Eurocode 2. The results of the shear resistance verification performed with this method will be compared to the results of a shear resistance verification performed with both the Strut & Tie method and a finite element analysis with the DIANA FEM software.

Due to the fact that the lock wall has a varying thickness over the height of the wall, the shear resistance is different for the various cross sections along the height of the wall. The Eurocode states that the calculation of the shear resistance is not required for shear sections that are positioned closer to the support than the point forming the intersection between the axis of the elastic center of gravity and a line drawn at an angle of 45° from the inner edge of the support. Theoretically this can be explained by the angle in which a shear crack will develop.

This method as stated by the Eurocode is applied to the Itaipu lock wall. Figure 4-1 illustrates this approach.

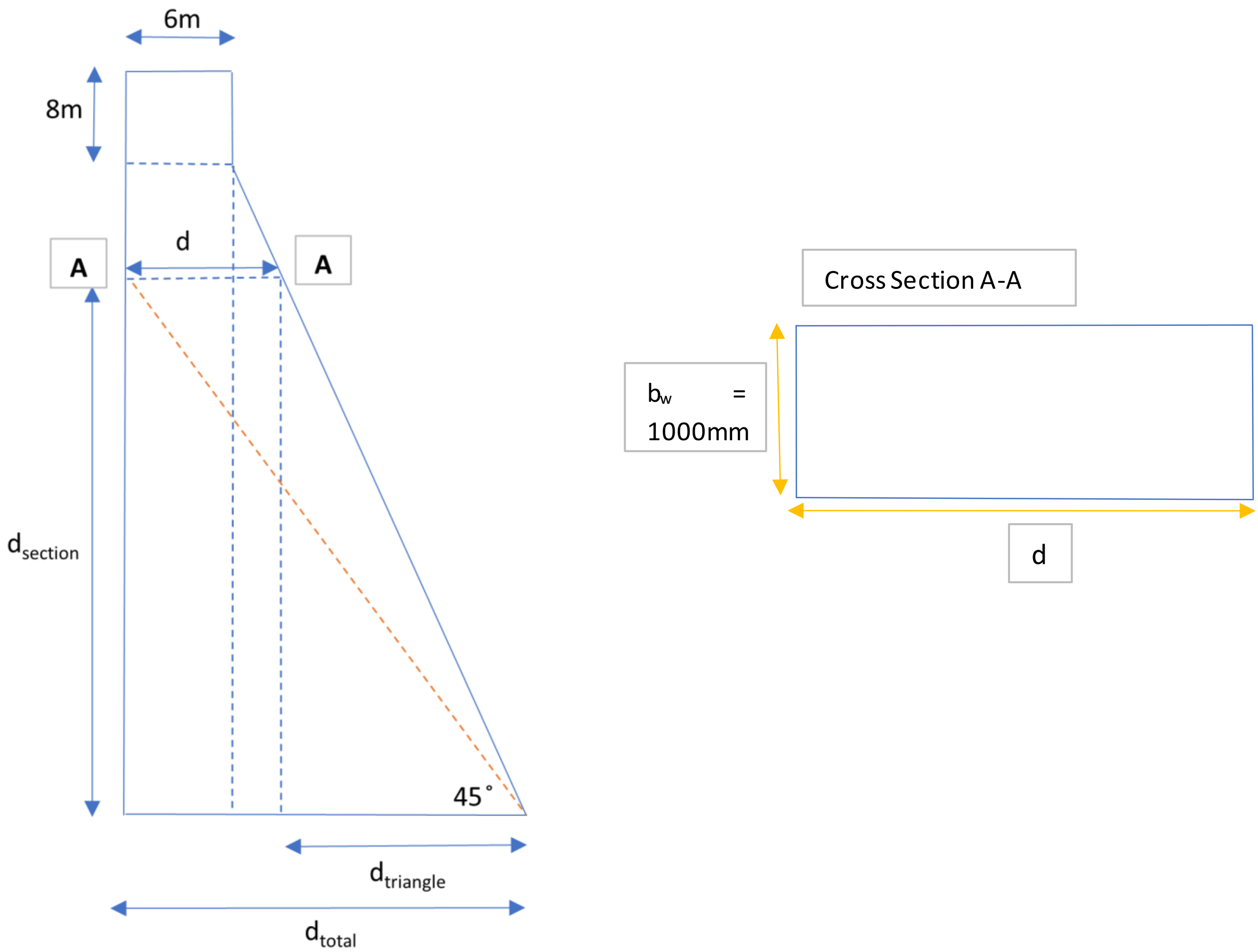

Figure 4-1 Itaipu Wall with cross section A-A

The method can iteratively be used by varying the d_{total}. As a result also $d_{section}$ will vary and the optimal thickness of the section can be reached for the case that $V_{ed} < V_{Rd,c}$ so that no shear reinforcement is necessary.

For the verification of shear resistance, the Eurocode2 equations are used (6.2(a) and 6.2(b) from NEN-EN 1992-1-1+C2 2011).

The design value of the shear resistance as given by the Eurocode is expressed with the following equations:

$$V_{Rd,c} = \left[C_{Rd,c}k(100\rho_l f_{ck})^{\frac{1}{3}} + k_1\sigma_{cp}\right]b_w d$$

The shear resistance should be taken no smaller than:

$$V_{Rd,c} \geq [\vartheta_{min} + k_1\sigma_{cp}]b_w d$$

where:

$$k = 1 + \sqrt{\frac{200}{d}} \leq 2{,}0 \text{ where d is mm}$$

$$\sigma_{cp} = \frac{N_{Ed}}{A_c} \leq 0{,}2f_{cd}$$

$$\vartheta_{min} = 0{,}035k^{\frac{3}{2}}f_{ck}^{\frac{1}{2}}$$

The Dutch Annex of Eurocode 2 uses the recommended values:

$C_{Rd.c}$=0.12

k_1=0.15

The material parameters as well as the values and limits of the constant parameters in the equations as recommended by the Eurocode are listed in Table 4-1 below.

Parameter	**Value**	**Unit**	**Limits**
f_{cd}	20	N/mm²	
f_{ck}	30	N/mm²	
k			≤ 2
b_w	1000	mm	
σ_{cp}			< 4
$C_{rd,c}$	0.12		
k_1	0.15		

Table 4-1 Parameters Sectional Calculation

4.1 Calculation results

From the results of the calculation it could be concluded that the longitudinal reinforcement does not result in an increase of the shear capacity of a certain cross section. For the given cross sections, the shear resistance will be fully determined by the minimum shear resistance as described by the Eurocode. This value is the shear resistance as a result of the high axial force originating from the self-weight of the concrete. However, longitudinal reinforcement might still be necessary for other usability and/or durability requirements. Because the addition of longitudinal reinforcement will lead to a more favourable situation for the shear resistance, the longitudinal reinforcement will be omitted from this calculation.

Main result: Unity check for Shear resistance

As can be seen in Figure 4-2, a unity check of just below 1.0 is achieved for a total wall thickness of 17 m. Thus, in order for the wall to be able to resist the shear loading, the total wall thickness has to be a minimum of 17m. This corresponds to a sectional thickness of 12,2m at a level of 17m (due to the 45° angle) above the floor.

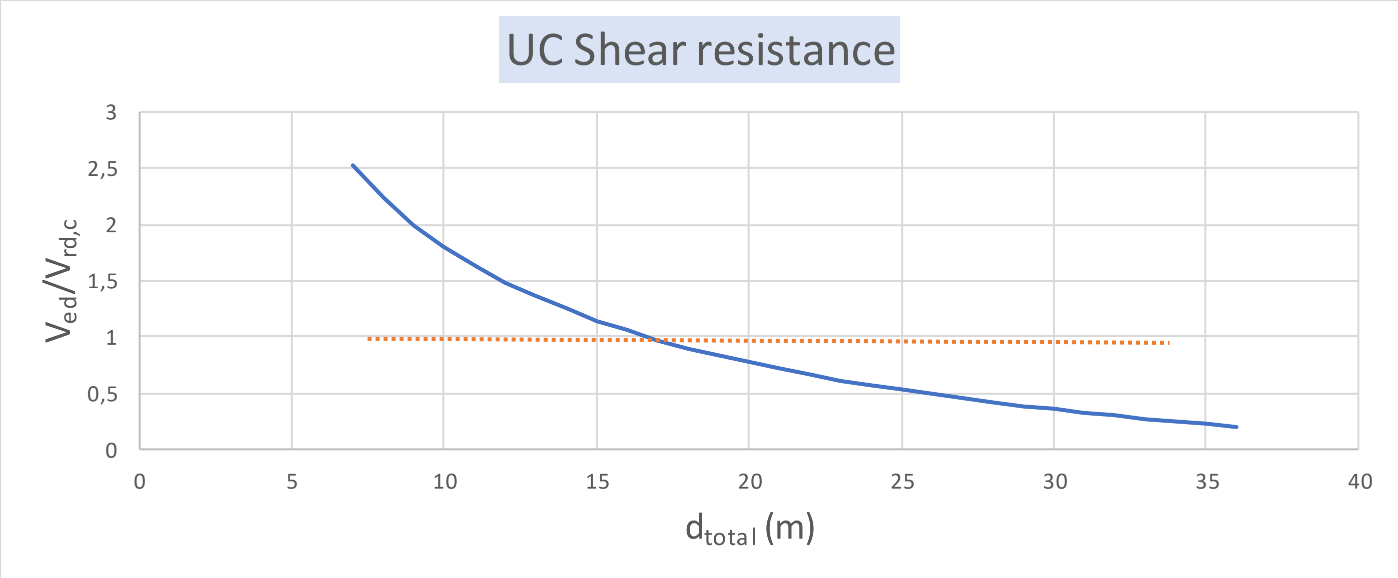

Figure 4-2 Unity check shear resistance

Shear resistance and total wall thickness
Figure 4-5 shows the relation between the shear resistance of the wall and the total wall thickness that corresponds with this shear resistance.

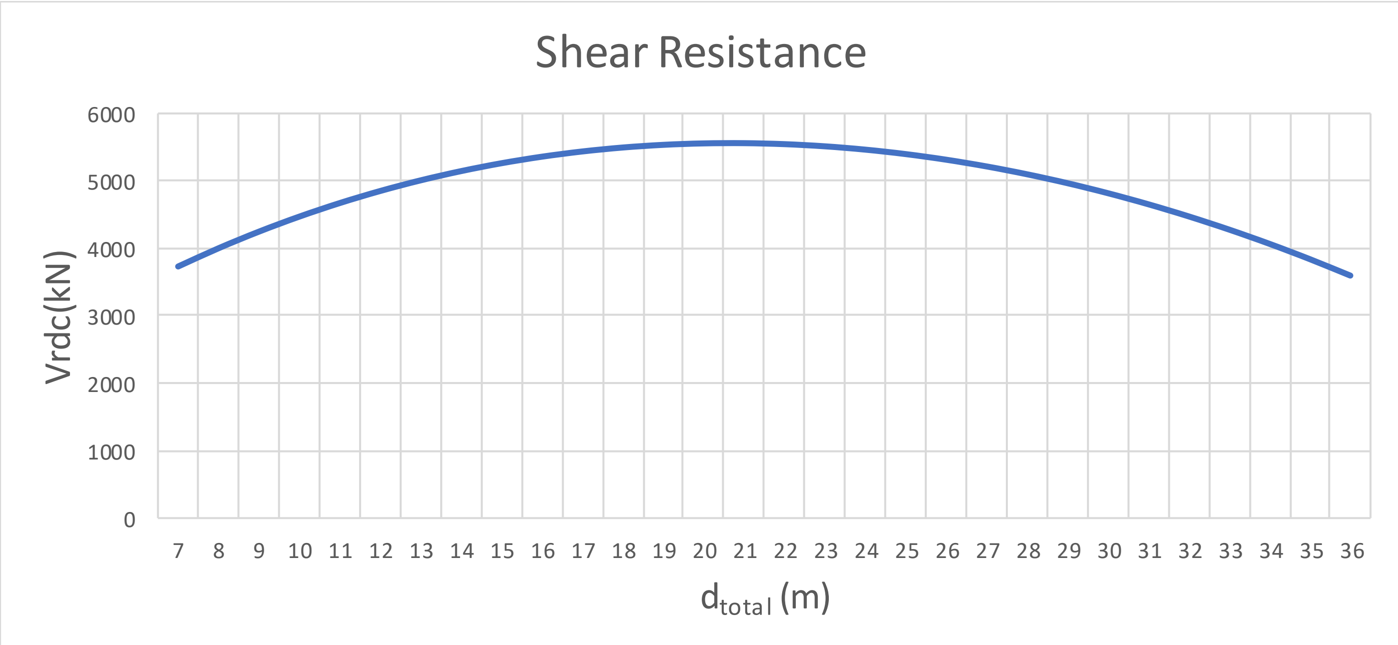

Figure 4-3 Relation between shear resistance and total wall thickness

Shear stress
Figure 4-4 shows the shear stress at the different sections of the wall. The shear stress is calculated by dividing the design value of the shear force by the total cross sectional area:

$$\tau_{ed} = \frac{V_{ed}}{A_c}$$

Where:

$$A_c = d * b_w$$

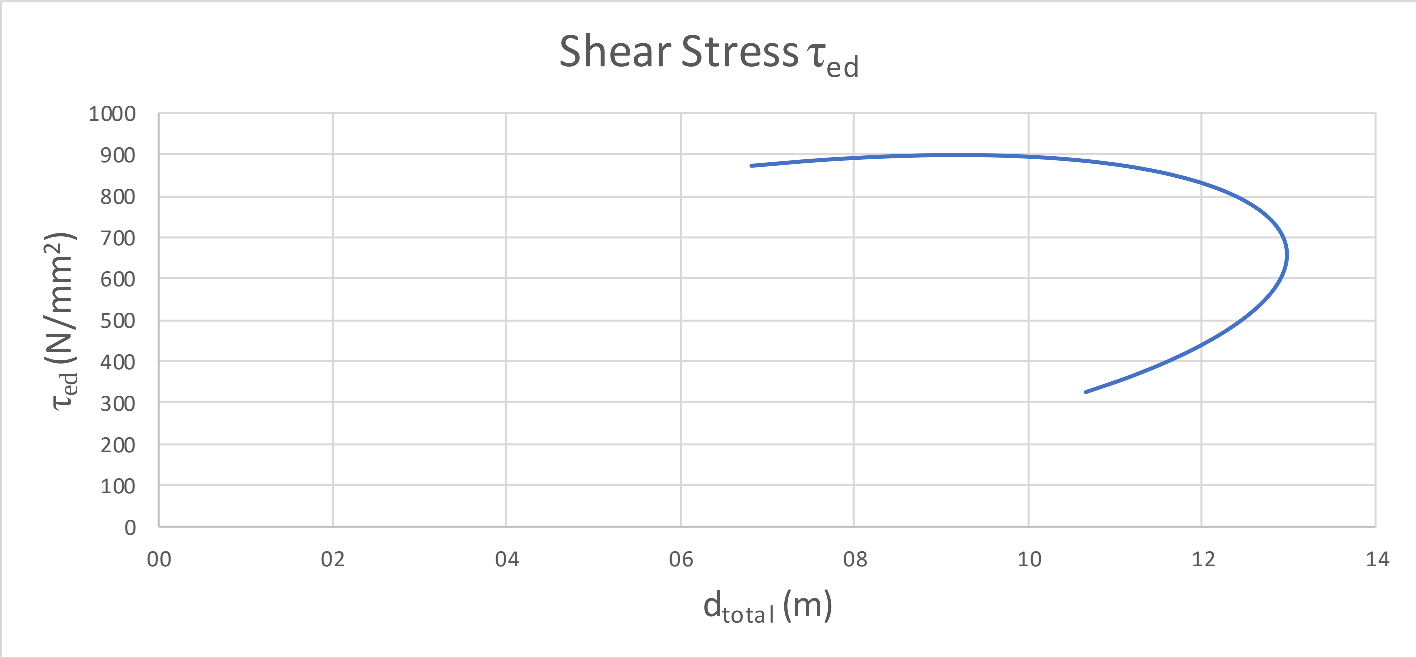

Figure 4-4 Relation shear stress and total wall thickness

Table results

Table 4-2 below shows the exact values from the shear resistance calculation using the sectional method. The graphs in the chapter above have been derived from the values in this table. The green row highlights the values for which the unity check of the shear resistance is just below one.

d(m)	d section = d total (m)	k (-)	α (degrees)	Total Concrete Volume (m^3)	Self Weight (kN)	d triangle (m)	Ned (kN)	Ac [mm^2]	σcp [N/mm^2]	vmin (-)	Min Vrdc (kN)	Vrdc (kN)	Max [(Min Vrdc); (Vrdc)] (kN)	Ved (kN)	Shear Stress τ [N/mm^2]	UC Shear
6.82	7	1.17	88.5	301.5	7537.5	0.18	5695	6820513	0.84	0.42	3731	854	3731	9418	1.38	**2.52**
7.59	8	1.16	87.1	321	8025	0.41	5819	7589744	0.77	0.41	4001	873	4001	8953	1.18	**2.24**
8.31	9	1.16	85.6	340.5	8512.5	0.69	5909	8307692	0.71	0.40	4248	886	4248	8499	1.02	**2.00**
8.97	10	1.15	84.1	360	9000	1.03	5965	8974359	0.66	0.40	4471	895	4471	8058	0.90	**1.80**
9.59	11	1.14	82.7	379.5	9487.5	1.41	5991	9589744	0.62	0.39	4672	899	4672	7628	0.80	**1.63**
10.15	12	1.14	81.3	399	9975	1.85	5987	10153846	0.59	0.39	4850	898	4850	7210	0.71	**1.49**
10.67	13	1.14	79.8	418.5	10462.5	2.33	5955	10666667	0.56	0.39	5008	893	5008	6804	0.64	**1.36**
11.13	14	1.13	78.4	438	10950	2.87	5897	11128205	0.53	0.38	5145	885	5145	6410	0.58	**1.25**
11.54	15	1.13	77.0	457.5	11437.5	3.46	5815	11538462	0.50	0.38	5262	872	5262	6027	0.52	**1.15**
11.90	16	1.13	75.6	477	11925	4.10	5711	11897436	0.48	0.38	5359	857	5359	5656	0.48	**1.06**
12.21	17	1.13	74.2	496.5	12412.5	4.79	5586	12205128	0.46	0.38	5436	838	5436	5297	0.43	**0.97**
12.46	18	1.13	72.9	516	12900	5.54	5442	12461538	0.44	0.38	5495	816	5495	4950	0.40	**0.90**
12.67	19	1.13	71.6	535.5	13387.5	6.33	5280	12666667	0.42	0.37	5535	792	5535	4615	0.36	**0.83**
12.82	20	1.12	70.3	555	13875	7.18	5103	12820513	0.40	0.37	5556	765	5556	4291	0.33	**0.77**
12.92	21	1.12	69.0	574.5	14362.5	8.08	4912	12923077	0.38	0.37	5559	737	5559	3979	0.31	**0.72**
12.97	22	1.12	67.7	594	14850	9.03	4709	12974359	0.36	0.37	5545	706	5545	3679	0.28	**0.66**
12.97	23	1.12	66.4	613.5	15337.5	10.03	4495	12974359	0.35	0.37	5513	674	5513	3390	0.26	**0.62**
12.92	24	1.12	65.2	633	15825	11.08	4273	12923077	0.33	0.37	5463	641	5463	3114	0.24	**0.57**
12.82	25	1.12	64.0	652.5	16312.5	12.18	4044	12820513	0.32	0.37	5397	607	5397	2849	0.22	**0.53**
12.67	26	1.13	62.9	672	16800	13.33	3810	12666667	0.30	0.37	5314	572	5314	2596	0.20	**0.49**
12.46	27	1.13	61.7	691.5	17287.5	14.54	3572	12461538	0.29	0.38	5214	536	5214	2354	0.19	**0.45**
12.21	28	1.13	60.6	711	17775	15.79	3333	12205128	0.27	0.38	5098	500	5098	2125	0.17	**0.42**
11.90	29	1.13	59.5	730.5	18262.5	17.10	3093	11897436	0.26	0.38	4966	464	4966	1907	0.16	**0.38**
11.54	30	1.13	58.4	750	18750	18.46	2856	11538462	0.25	0.38	4818	428	4818	1701	0.15	**0.35**
11.13	31	1.13	57.3	769.5	19237.5	19.87	2622	11128205	0.24	0.38	4654	393	4654	1507	0.14	**0.32**
10.67	32	1.14	56.3	789	19725	21.33	2393	10666667	0.22	0.39	4474	359	4474	1324	0.12	**0.30**
10.15	33	1.14	55.3	808.5	20212.5	22.85	2170	10153846	0.21	0.39	4278	326	4278	1154	0.11	**0.27**
9.59	34	1.14	54.3	828	20700	24.41	1957	9589744	0.20	0.39	4067	294	4067	995	0.10	**0.24**
8.97	35	1.15	53.4	847.5	21187.5	26.03	1754	8974359	0.20	0.40	3839	263	3839	848	0.09	**0.22**
8.31	36	1.16	52.4	867	21675	27.69	1563	8307692	0.19	0.40	3596	234	3596	712	0.09	**0.20**

Table 4-2 Shear resistance calculation results

4.2 Resistance Check lower section

The shear resistance will also be checked for the section at the level that also indicates the top of the lock floor, section B-B, as shown in Figure 4-5. This is the section where the largest shear force will occur. In this calculation, the d_{total} is also increased to obtain these results for the same range of total thicknesses as the previous calculation.

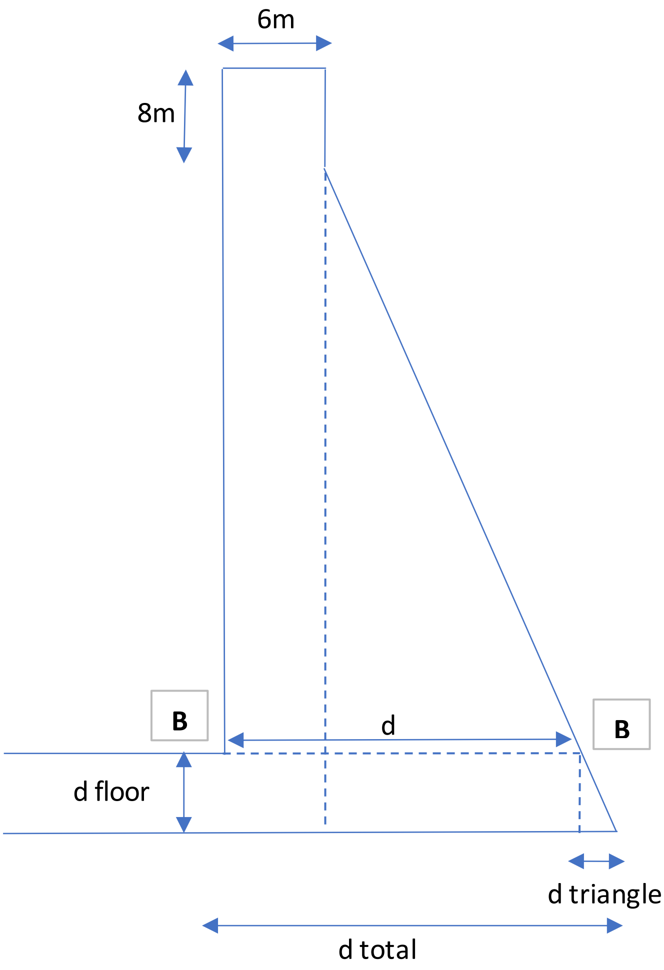

Figure 4-5 Itaipu Wall with cross section B-B

Main result: Unity check for Shear resistance

As can be seen in Figure 4-6, a unity check of just below 1.0 is achieved for a total wall thickness of 29m. Thus, in order for the wall to be able to resist the shear loading, the total wall thickness has to be a minimum of 29 m. This corresponds to a sectional thickness of 26.64m at a level of 4m above the floor.

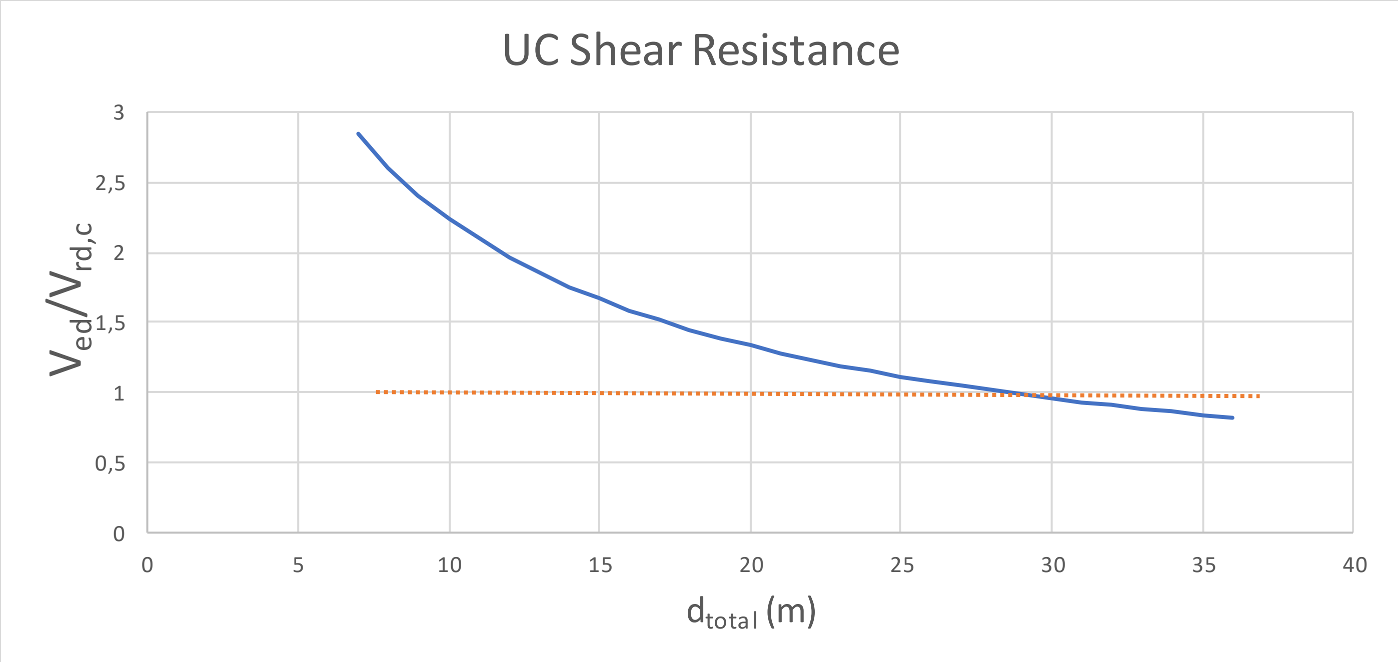

Figure 4-6 Unity Check Shear Transfer

Shear resistance and total wall thickness

Figure 4-7 shows the relation between the shear resistance of the wall and the total wall thickness that corresponds with this shear resistance.

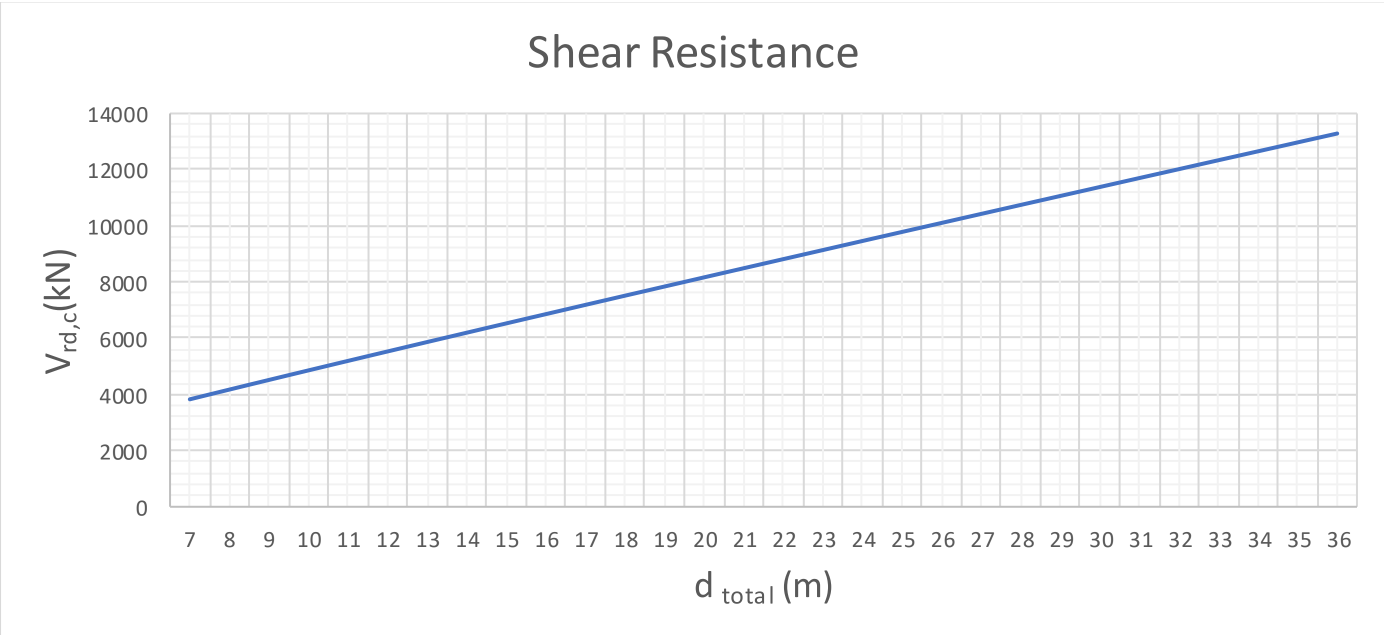

Figure 4-7 Relation Shear Resistance and total wall thickness

Shear stress

Figure 4-8 shows the shear stress at the different sections of the wall. The shear stress is calculated by dividing the design value of the shear force by the total cross sectional area:

$$\tau_{ed} = \frac{V_{ed}}{A_c}$$

Where:

$$A_c = d * b_w$$

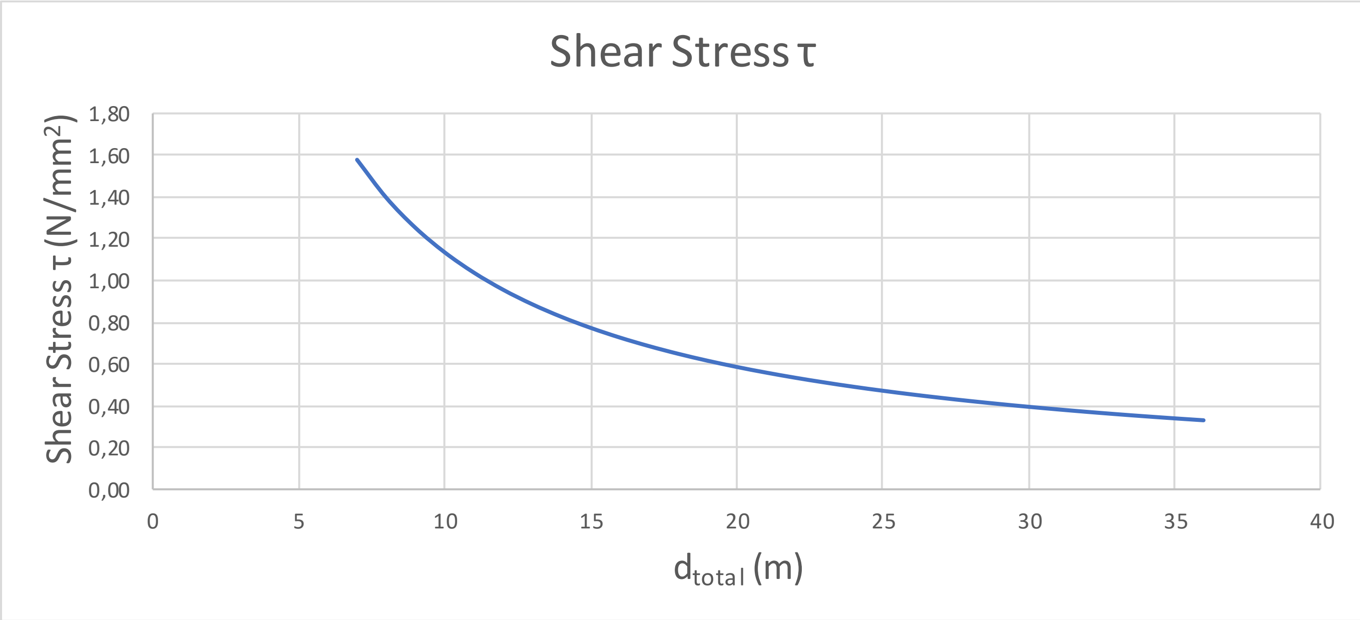

Figure 4-8 Relation Shear Stress and total wall thickness

Table results

Table 4-3 below shows the exact values from the shear resistance calculation using the sectional method in the governing section. The graphs in the chapter above have been derived from the values in this table. The green row highlights the values for which the unity check of the shear resistance is just below one.

d(m)	k (-)	α (degrees)	d total (mm)	Total Concrete Volume	Self Weight (kN)	d triangle (m)	Ned (kN)	Ac [mm^2]	σcp [N/mm^2]	vmin (-)	Min Vrdc (kN)	Vrdc (kN)	Max [(Min Vrdc); (Vrdc)] (kN)	Shear Stress τ [N/mm^2]	UC
6.90	1.17	88.5	7	301.5	7537.5	0.10	6158	6897436	0.89	0.42	3826	924	3826	1.58	**2.84**
7.79	1.16	87.1	8	321	8025	0.21	6512	7794872	0.84	0.41	4172	977	4172	1.40	**2.61**
8.69	1.15	85.6	9	340.5	8512.5	0.31	6865	8692308	0.79	0.40	4515	1030	4515	1.25	**2.41**
9.59	1.14	84.1	10	360	9000	0.41	7218	9589744	0.75	0.39	4856	1083	4856	1.13	**2.24**
10.49	1.14	82.7	11	379.5	9487.5	0.51	7572	10487179	0.72	0.39	5194	1136	5194	1.04	**2.10**
11.38	1.13	81.3	12	399	9975	0.62	7925	11384615	0.70	0.38	5530	1189	5530	0.96	**1.97**
12.28	1.13	79.8	13	418.5	10462.5	0.72	8279	12282051	0.67	0.38	5864	1242	5864	0.89	**1.86**
13.18	1.12	78.4	14	438	10950	0.82	8632	13179487	0.65	0.37	6197	1295	6197	0.83	**1.76**
14.08	1.12	77.0	15	457.5	11437.5	0.92	8985	14076923	0.64	0.37	6528	1348	6528	0.77	**1.67**
14.97	1.12	75.6	16	477	11925	1.03	9339	14974359	0.62	0.36	6858	1401	6858	0.73	**1.59**
15.87	1.11	74.2	17	496.5	12412.5	1.13	9692	15871795	0.61	0.36	7187	1454	7187	0.69	**1.51**
16.77	1.11	72.9	18	516	12900	1.23	10045	16769231	0.60	0.36	7514	1507	7514	0.65	**1.45**
17.67	1.11	71.6	19	535.5	13387.5	1.33	10399	17666667	0.59	0.36	7841	1560	7841	0.62	**1.39**
18.56	1.10	70.3	20	555	13875	1.44	10752	18564103	0.58	0.35	8166	1613	8166	0.59	**1.33**
19.46	1.10	69.0	21	574.5	14362.5	1.54	11105	19461538	0.57	0.35	8491	1666	8491	0.56	**1.28**
20.36	1.10	67.7	22	594	14850	1.64	11459	20358974	0.56	0.35	8815	1719	8815	0.53	**1.23**
21.26	1.10	66.4	23	613.5	15337.5	1.74	11812	21256410	0.56	0.35	9138	1772	9138	0.51	**1.19**
22.15	1.10	65.2	24	633	15825	1.85	12166	22153846	0.55	0.34	9460	1825	9460	0.49	**1.15**
23.05	1.09	64.0	25	652.5	16312.5	1.95	12519	23051282	0.54	0.34	9782	1878	9782	0.47	**1.11**
23.95	1.09	62.9	26	672	16800	2.05	12872	23948718	0.54	0.34	10103	1931	10103	0.45	**1.08**
24.85	1.09	61.7	27	691.5	17287.5	2.15	13226	24846154	0.53	0.34	10424	1984	10424	0.44	**1.04**
25.74	1.09	60.6	28	711	17775	2.26	13579	25743590	0.53	0.34	10744	2037	10744	0.42	**1.01**
26.64	1.09	59.5	29	730.5	18262.5	2.36	13932	26641026	0.52	0.34	11063	2090	11063	0.41	**0.98**
27.54	1.09	58.4	30	750	18750	2.46	14286	27538462	0.52	0.34	11382	2143	11382	0.40	**0.96**
28.44	1.08	57.3	31	769.5	19237.5	2.56	14639	28435897	0.51	0.33	11700	2196	11700	0.38	**0.93**
29.33	1.08	56.3	32	789	19725	2.67	14993	29333333	0.51	0.33	12018	2249	12018	0.37	**0.91**
30.23	1.08	55.3	33	808.5	20212.5	2.77	15346	30230769	0.51	0.33	12336	2302	12336	0.36	**0.88**
31.13	1.08	54.3	34	828	20700	2.87	15699	31128205	0.50	0.33	12653	2355	12653	0.35	**0.86**
32.03	1.08	53.4	35	847.5	21187.5	2.97	16053	32025641	0.50	0.33	12969	2408	12969	0.34	**0.84**
32.92	1.08	52.4	36	867	21675	3.08	16406	32923077	0.50	0.33	13286	2461	13286	0.33	**0.82**

Table 4-3 Shear resistance calculation results lower section

4.3 Crack Control

The calculations for crack control are based on chapter 9 of the CIE3150 / 4160 'Prestressed Concrete' reader from the Delft University of Technology (Walraven, J.C & Braam, C.R. February 2019), Eurocode 2 (NEN-EN 1992-1-1) and the national Annex of Eurocode 2 (NEN-EN 1992-1-1 NB).

First, the shear force diagram and the bending moment diagram are drawn for the given load load situation. Figure 4-9 shows a cross section of the lock wall in which the distance from the top wall to the lock floor is indicated. Based on this distance, the shear force and the bending moments are given for the different wall sections, see Figure 4-10 and Figure 4-11.

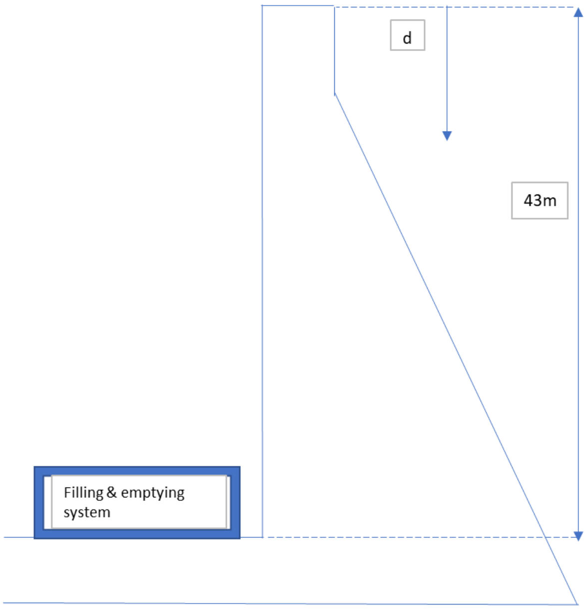

Figure 4-9 Cross section lock wall

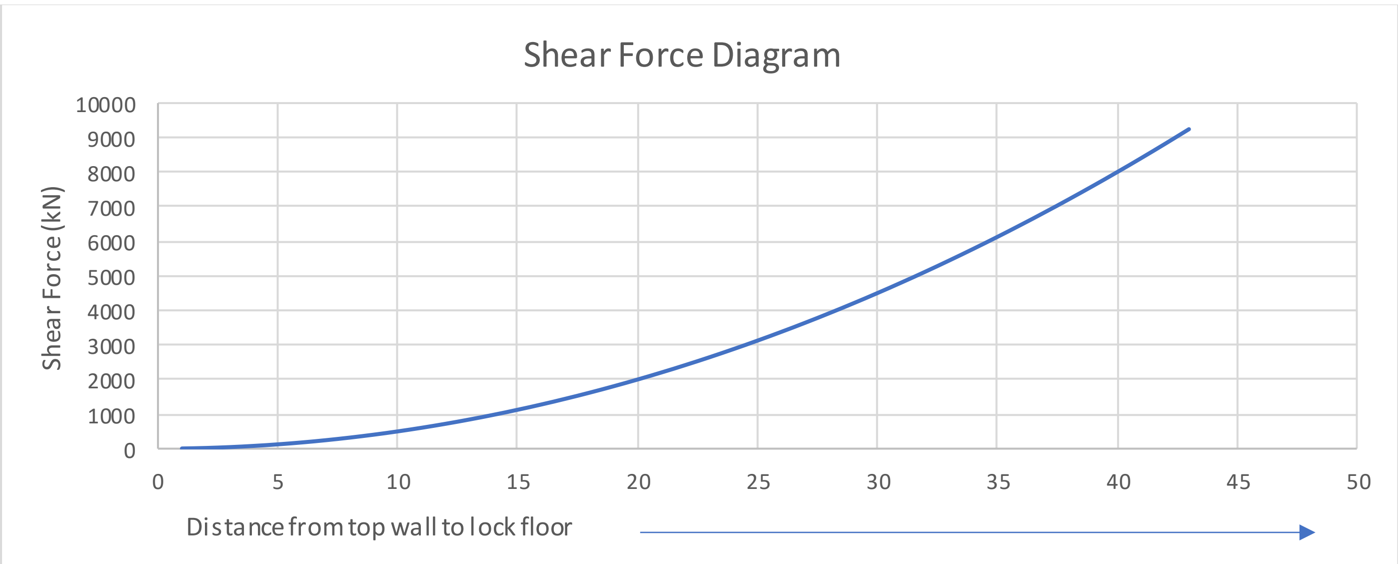

Figure 4-10 Shear force diagram

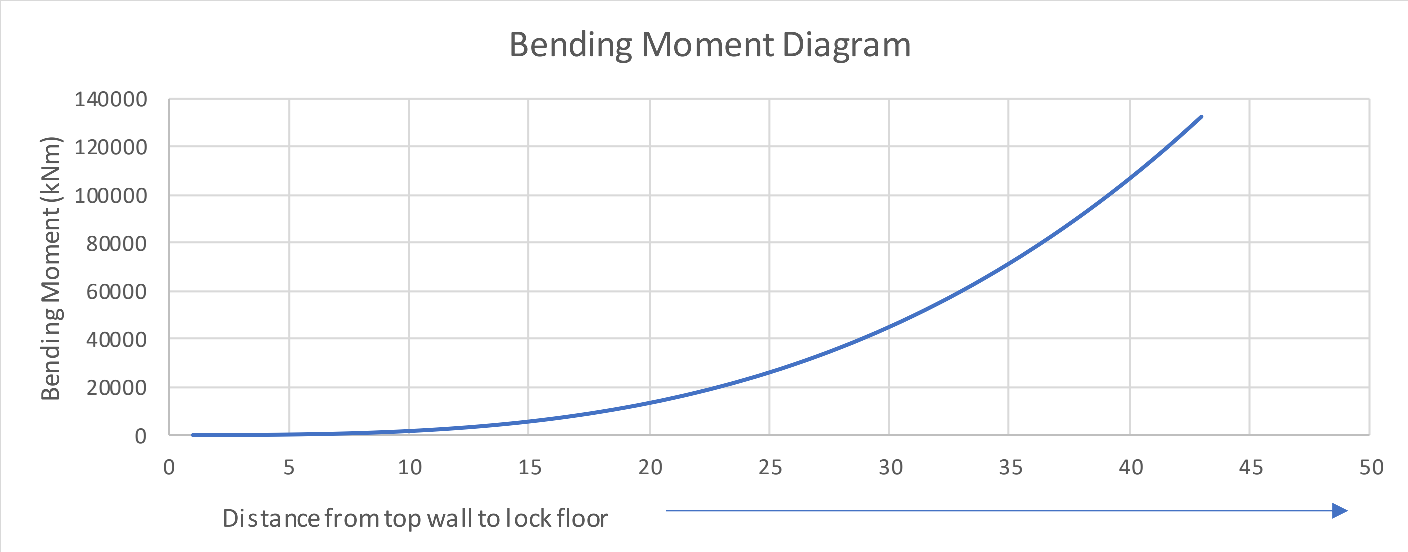

Figure 4-11 Bending moment diagram

The general equation to calculate the maximum crack width in SLS conditions is:

$$w_{max} = \frac{1}{2}\frac{f_{ctm}}{\tau_{bm}}\frac{\emptyset}{\rho_{eff}}\frac{1}{E_s}(\sigma_s - \alpha\sigma_{sr} + \beta\varepsilon_{cs}E_{cs})$$

The concrete properties of the applied strength class are given in Table 4-4:

Strength Class	Loading	E_c [GPa]	f_{ctm}/τ_{bm} [-]	$\alpha_e=E_s/E_c$ (E_s=210GPa)
C30/37	Short term	33	1/2	6
	Long term	11*	1/1,6	19

Table 4-4 Concrete properties applied strenght class

*For the long term loading, creep is taken into account by reducing the Young's modulus of the concrete with a factor 3,0.

The concrete strength class used is C30/37 and the reinforcement at the tension side consists of 8∅12, resulting in A_{sl} = 905 mm². The concrete cover is 40mm (see next paragraph for the calculation).

$$\rho_{sl} = \frac{A_{sl}}{b.d}$$

where:
b = 1000mm

$$d = d_{total} - c - \frac{\emptyset}{2}$$

The tensile strength in practical situations might be lower than what is given based on laboratorial results due to different environmental effects. Walraven & Braam (2019) therefore advise a factor of 0,75 to account for this difference in strength. In practice the strength of concrete is actually higher than the characteristic cube compressive strength of the mixture. However, calculating with a higher concrete strength will result in a larger maximum crack width. To be on the safe side, the characteristic concrete strength is increased by 10N/mm². Table 3.1 of Eurocode 2 gives the following expression for the mean concrete tensile strength in the actual structure for concrete strength categories ≤C50/60:

$$f_{ctm} = 0{,}30.f_{ck}^{(2/3)}$$

Substitution of the corrections listed above, this equation can be modified to:

$$f_{ctm} = 0{,}75.0{,}30(f_{ck} + 10)^{(2/3)}$$

The maximum cracking stress is calculated with the following equation:

$$f_{ctm,fl} = \sigma_{cr} = max\{(1{,}6 - h).f_{ctm};\ f_{ctm}\}$$

where the variable h is equal to the thickness of the concrete wall in the case of the Itaipu lock wall.

The cracking moment can then be calculated with the help of the following equation"

$$M_{cr} = f_{ctm,fl}.W = f_{ctm,fl}.\frac{1}{6}.b.h^2$$

The cracking moment can be compared to the maximum bending moment at SLS. If the cracking moment is smaller than the maximum SLS bending moment, the structure will crack in bending and it can be concluded that the structure is in the stabilized cracking stage.

The type of loading is characterized by long term, so the variables used have been indicated with a red square in Table 4-5 below:

	crack formation stage	stabilised cracking stage
short term loading	$\alpha = 0{,}5$ $\beta = 0$ $\tau_{bm} = 2{,}0\, f_{ctm}$	$\alpha = 0{,}5$ $\beta = 0$ $\tau_{bm} = 2{,}0\, f_{ctm}$
long term or dynamic loading	$\alpha = 0{,}5$ $\beta = 0$ $\tau_{bm} = 1{,}6\, f_{ctm}$	$\alpha = 0{,}3$ $\beta = 1$ $\tau_{bm} = 2{,}0\, f_{ctm}$

Table 4-5 Variables depending on loading type

With the following equation, the concrete compression zone is calculated:

$$\frac{x}{d} = -\alpha_e \rho_{sl} + \sqrt{(\alpha_e \rho_{sl})^2 + 2\alpha_e \rho_{sl}}$$

The internal lever arm after cracking is then:

$$z = d - \frac{x}{3}$$

The maximum steel stress depends on the maximum bending moment and can be calculated by:

$$\sigma_s = \frac{M_{max}}{A_s.z}$$

To calculate the maximum crack width, the value for the height of the effective tensile area is needed, which for which the minimum of the following two equations is chosen:

$$h_{eff} = min\begin{cases} 2{,}5(c+\frac{\emptyset}{2}) \\ (h-x)/3 \end{cases}$$

The effective reinforcement ratio of the hidden tensile member can then be calculated by:

$$\rho_{eff} = \frac{A_{sl}}{h_{eff}.b}$$

The steel stress in the crack in the crack formation stage is calculated as follows:

$$\sigma_{sr} = \frac{f_{ctm}}{\rho_{p.eff}}(1+\alpha_e.\rho_{p.eff})$$

With the equations given above, the maximum crack width can be calculated for both the section right above the floor and the section that is governing for the calculation of shear capacity.

The concrete cover is determined by using Eurocode2.
$C_{nom}=C_{min}+\Delta C_{dev}$ (EC2 4.4.1.1)

$C_{min}=$ max{$c_{min.b}$; $c_{min.dur}+\Delta c_{dur.\gamma}-\Delta c_{dur,st}-\Delta c_{dur,add}$; 10mm)

The minimum value of $c_{min,b}$ has to be greater than the diameter of the reinforcing bars used. If the nominal grain size is larger than 32 mm, 5 mm is added to the minimum value. Since it is not yet known what the maximum grain diameter for the concrete will be at this point, the safe value of the diameter of the reinforcement bars will be used for the minimum coverage $c_{min,b}$. In the case of the lock wall, reinforcement with a diameter of 12mm is used, so $c_{min,b}$ > 12mm.

The national annex of Eurocode 2 states that the values of the safety margins $\Delta c_{dur.\gamma}$, $\Delta c_{dur,st}$ en $\Delta c_{dur,add}$ must be taken to be 0 mm.

Based on table 4.1 of Eurocode 2, a class designation of XC4 is used for the lock wall. The environment in which the wall is located falls into the category characterized by "corrosion induced by carbonation" and is described as "alternating wet and dry". Table 4.3N is used for the structural classification. For the lock wall of Itaipu, a design life of 100 years is maintained. The used concrete strength class is C30/37. For an environmental class of XC4, these assumptions require a construction class of S6 according to the Eurocode. From table 4.4N it can then be deduced that for the coverage requirements with regard to durability a value of 40 mm must be chosen, so $c_{min.dur}$ = 40 mm.

The execution tolerance ΔC_{dev} is equal to 5mm as described in the national annex of Eurocode 2.

A value of 40mm must therefore be used for the nominal value of the cover, thus C_{nom} = 45 mm.

The results of these calculations are found in Table 4-6 below.

Parameter	Value	Unit/ Description
Number of bars	8	-
Asl	1231,50	mm^2
fck	30	Mpa
fctm	2,6	Mpa
b	1000	mm
c	45	mm
fctm/tbm	0,625	long term loading
diam	14	mm
αe	19	-
Es	210000	Mpa
α	0,5	-

Table 4-6 Parameters crack width

Table results

Table 4-7 shows the exact results of the crack width calculation for the different wall sections. The maximum allowable crack width as described by the Eurocode is given in Table 0-1 in Appendix B: Cracks in Concrete.

Thickness section [m]	Ved (kN)	Med [kNm]	d eff [m]	Ac [m^2]	rho (As/Ac)	ρsl [-]	fctm,fl equation	fctm,fl ≥ fctm	W [m^3]	Mcr [kNm]	x [m]	z [mm]	σs [N/mm^2]	σs corrected [N/mm^2]	heff [mm]	ρpeff [-]	σsr [N/mm^2]	σs-ασsr [-]	Wmax [mm]	Wmax corrected
1	5	2	0,95	1	0,0012	1299,06	1,58	2,63	0,17	439	0,9	0,6	2,14	2,14	17,3	0,0710	87,05	-41,39	-0,012	**0,000**
2	20	13	1,95	2	0,0006	632,19	-1,05	2,63	0,67	1754	1,9	1,3	8,34	8,34	17,4	0,0709	87,10	-35,21	-0,010	**0,000**
3	45	45	2,95	3	0,0004	417,74	-3,68	2,63	1,50	3947	2,9	2,0	18,59	18,59	17,4	0,0708	87,17	-24,99	-0,007	**0,000**
4	80	107	3,95	4	0,0003	311,93	-6,32	2,63	2,67	7018	3,9	2,6	32,91	32,91	17,4	0,0706	87,28	-10,73	-0,003	**0,000**
5	125	208	4,95	5	0,0002	248,89	-8,95	2,63	4,17	10965	4,9	3,3	51,28	51,28	17,5	0,0703	87,41	7,58	0,002	**0,002**
6	180	360	5,95	6	0,0002	207,05	-11,58	2,63	6,00	15790	5,9	4,0	73,72	73,72	17,6	0,0700	87,58	29,93	0,009	**0,009**
7	245	572	6,95	7	0,0002	177,25	-14,21	2,63	8,17	21492	6,9	4,6	100,21	100,21	17,7	0,0697	87,78	56,32	0,017	**0,017**
8	320	853	7,95	8	0,0002	154,95	-16,84	2,63	10,67	28071	7,9	5,3	130,76	130,76	17,8	0,0693	88,00	86,76	0,026	**0,026**
9	405	1215	8,95	9	0,0001	137,63	-19,47	2,63	13,50	35527	8,9	6,0	165,37	165,37	17,9	0,0688	88,26	121,24	0,037	**0,037**
10	500	1667	9,95	10	0,0001	123,79	-22,11	2,63	16,67	43860	9,9	6,6	204,04	204,04	18,0	0,0683	88,55	159,77	0,049	**0,049**
11	605	2218	10,95	11	0,0001	112,49	-24,74	2,63	20,17	53071	10,9	7,3	246,77	246,77	18,2	0,0677	88,86	202,34	0,062	**0,062**
12	720	2880	11,95	12	0,0001	103,07	-27,37	2,63	24,00	63159	11,9	8,0	293,56	293,56	18,3	0,0671	89,21	248,95	0,077	**0,077**
13	845	3662	12,95	13	0,0001	95,11	-30,00	2,63	28,17	74124	12,9	8,6	344,41	344,41	18,5	0,0665	89,59	299,61	0,094	**0,094**
14	980	4573	13,95	14	0,0001	88,29	-32,63	2,63	32,67	85966	13,9	9,3	399,31	399,31	18,7	0,0658	90,00	354,31	0,112	**0,112**
15	1125	5625	14,95	15	0,0001	82,39	-35,26	2,63	37,50	98686	14,9	10,0	458,27	435,00	18,9	0,0651	90,44	389,78	0,125	**0,125**
16	1280	6827	15,95	16	0,0001	77,22	-37,90	2,63	42,67	112282	15,9	10,6	521,30	435,00	19,1	0,0643	90,91	389,55	0,126	**0,126**
17	1445	8188	16,95	17	0,0001	72,66	-40,53	2,63	48,17	126756	16,9	11,3	588,37	435,00	19,4	0,0636	91,41	389,30	0,128	**0,128**
18	1620	9720	17,95	18	0,0001	68,62	-43,16	2,63	54,00	142107	17,9	12,0	659,51	435,00	19,6	0,0627	91,94	389,03	0,129	**0,129**
19	1805	11432	18,95	19	0,0001	64,99	-45,79	2,63	60,17	158336	18,9	12,6	734,71	435,00	19,9	0,0619	92,50	388,75	0,131	**0,131**
20	2000	13333	19,95	20	0,0001	61,74	-48,42	2,63	66,67	175441	19,9	13,3	813,96	435,00	20,2	0,0611	93,09	388,45	0,133	**0,133**
21	2205	15435	20,95	21	0,0001	58,79	-51,05	2,63	73,50	193424	20,9	14,0	897,27	435,00	20,5	0,0602	93,71	388,14	0,134	**0,134**
22	2420	17747	21,95	22	0,0001	56,11	-53,68	2,63	80,67	212284	21,9	14,6	984,64	435,00	20,8	0,0593	94,37	387,82	0,136	**0,136**
23	2645	20278	22,95	23	0,0001	53,66	-56,32	2,63	88,17	232021	22,9	15,3	1076,06	435,00	21,1	0,0584	95,05	387,48	0,138	**0,138**
24	2880	23040	23,95	24	0,0001	51,42	-58,95	2,63	96,00	252635	23,9	16,0	1171,54	435,00	21,4	0,0575	95,76	387,12	0,140	**0,140**
25	3125	26042	24,95	25	0,0000	49,36	-61,58	2,63	104,17	274127	24,9	16,6	1271,08	435,00	21,8	0,0566	96,50	386,75	0,142	**0,142**
26	3380	29293	25,95	26	0,0000	47,46	-64,21	2,63	112,67	296495	25,9	17,3	1374,67	435,00	22,1	0,0557	97,28	386,36	0,145	**0,145**
27	3645	32805	26,95	27	0,0000	45,70	-66,84	2,63	121,50	319741	26,9	18,0	1482,33	435,00	22,5	0,0547	98,08	385,96	0,147	**0,147**
28	3920	36587	27,95	28	0,0000	44,06	-69,47	2,63	130,67	343864	27,9	18,6	1594,04	435,00	22,9	0,0538	98,92	385,54	0,149	**0,149**
29	4205	40648	28,95	29	0,0000	42,54	-72,11	2,63	140,17	368865	28,9	19,3	1709,80	435,00	23,3	0,0529	99,78	385,11	0,152	**0,152**
30	4500	45000	29,95	30	0,0000	41,12	-74,74	2,63	150,00	394742	29,9	20,0	1829,62	435,00	23,7	0,0519	100,67	384,66	0,154	**0,154**
31	4805	49652	30,95	31	0,0000	39,79	-77,37	2,63	160,17	421497	30,9	20,6	1953,50	435,00	24,1	0,0510	101,60	384,20	0,157	**0,157**
32	5120	54613	31,95	32	0,0000	38,55	-80,00	2,63	170,67	449129	31,9	21,3	2081,43	435,00	24,6	0,0501	102,56	383,72	0,160	**0,160**
33	5445	59895	32,95	33	0,0000	37,38	-82,63	2,63	181,50	477638	32,9	22,0	2213,42	435,00	25,1	0,0492	103,54	383,23	0,162	**0,162**
34	5780	65507	33,95	34	0,0000	36,28	-85,26	2,63	192,67	507025	33,9	22,6	2349,47	435,00	25,5	0,0482	104,56	382,72	0,165	**0,165**
35	6125	71458	34,95	35	0,0000	35,24	-87,90	2,63	204,17	537288	34,9	23,3	2489,57	435,00	26,0	0,0473	105,60	382,20	0,168	**0,168**
36	6480	77760	35,95	36	0,0000	34,26	-90,53	2,63	216,00	568429	35,9	24,0	2633,72	435,00	26,5	0,0464	106,68	381,66	0,171	**0,171**
37	6845	84422	36,95	37	0,0000	33,33	-93,16	2,63	228,17	600447	36,9	24,6	2781,94	435,00	27,0	0,0455	107,79	381,11	0,174	**0,174**
38	7220	91453	37,95	38	0,0000	32,45	-95,79	2,63	240,67	633342	37,9	25,3	2934,20	435,00	27,6	0,0447	108,92	380,54	0,178	**0,178**
39	7605	98865	38,95	39	0,0000	31,62	-98,42	2,63	253,50	667115	38,9	26,0	3090,53	435,00	28,1	0,0438	110,09	379,95	0,181	**0,181**
40	8000	106667	39,95	40	0,0000	30,83	-101,05	2,63	266,67	701764	39,9	26,6	3250,90	435,00	28,7	0,0429	111,29	379,36	0,184	**0,184**
41	8405	114868	40,95	41	0,0000	30,07	-103,69	2,63	280,17	737291	40,9	27,3	3415,34	435,00	29,3	0,0421	112,52	378,74	0,187	**0,187**
42	8820	123480	41,95	42	0,0000	29,36	-106,32	2,63	294,00	773695	41,9	28,0	3583,82	435,00	29,8	0,0413	113,78	378,11	0,191	**0,191**
43	9245	132512	42,95	43	0,0000	28,67	-108,95	2,63	308,17	810976	42,9	28,6	3756,36	435,00	30,4	0,0404	115,06	377,47	0,194	**0,194**

Table 4-7 Results crack width calculation

4.4 Summary of main results

The first finding is that the shear resistance from the wall is sufficient without the addition of longitudinal reinforcement due to the large self-weight of the concrete lock wall.

This first calculation, the sectional calculation, resulted in two alternative designs next to the original lock wall design by Witteveen+Bos: total wall thickness original design: 33m, total wall thickness alternative design 1 (i): 17m and total wall thickness alternative design 2 (ii): 29m. A linear finite element model is used to study the behavior of the two alternative thicknesses in chapter 5.

Also, the calculated crack widths in this calculation method are lower than the maximum allowable crack width as described by Eurocode 2.

5 Verification Shear Resistance using Strut & Tie Method

The STM approach provides a solution to analyse the flow path of forces within concrete structures/sections in elements that cannot be described with Bernoulli's theorem and are therefore characterized as D-regions (disturbed/discontinuous regions) instead of B-regions (Bernoulli regions) and therefore cannot be described with Bernoulli's theorem. The essence of this theorem is that plain sections remain plain which is not the case for deep beams and beams with increasing thickness

The use of STM requires the user to be able to visualize the stress field of structural elements. This approach will likely result in different models, based on the engineer who performs it, given that some models may be better or more efficient than other models. This approach is not only widely used because it provides a solution for the load transfer of construction elements that fall beyond the scope of the Bernoulli theory but also because this model is based on the lower bound theorem of plasticity, guaranteeing its safety.

5.1 The S&T design

The S&T design is based on the direction of the governing load situation: a full lock and no loading from the soil side.

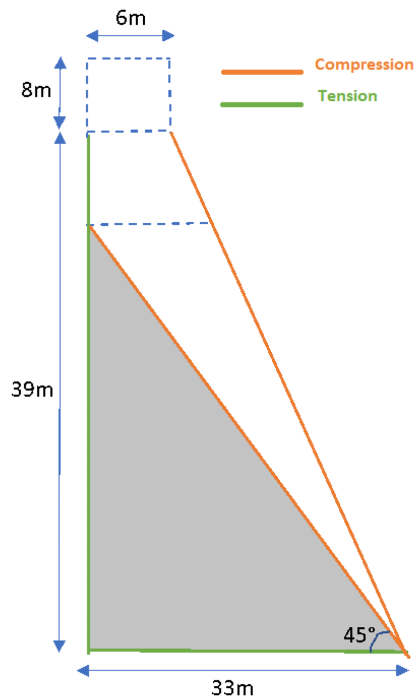

Figure 5-1 Diagonal direction

With basic structural mechanics it is possible to determine on which side tension will mainly occur and on which side compression will occur based on the orientation of the loads on the structure. This first indication of compression and tension is showed in Figure 5-1 on the left. Note that the figure is not to scale. To stimulate compression in the diagonal direction, it is desirable to start from the strut at an angle of 45° with the normal (parallel to the subsurface). The struts symbolize the concrete and the ties the reinforcement. With constructability in mind, it is desirable to avoid diagonally oriented ties, and thus reinforcement in the diagonals.

To determine the layout of the truss, nodes are first indicated in the structure. These nodes are determined in such a way as to indicate at which places the load acts. For the lock wall, a distributed load acts over the entire height of the wall. However, both distributed loads and bending moments cannot be applied to the truss and the distributed load will therefore be divided into point loads.

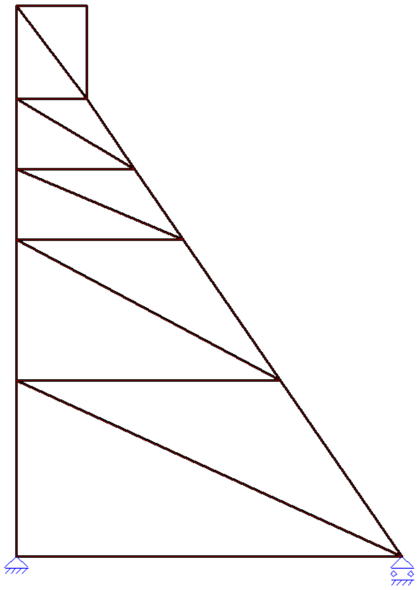

Figure 5-2 Strut and tie design

Below the 45° strut, a significant large part of the surface of the wall is shaded in Figure 5-1. Since the resultant of the distributed load acts in this shaded area, it is necessary, according to the S&T theory, to add nodes in this specific area. However, these nodes would then lead to truss elements oriented in the direction of the opposite diagonal, which would lead to tension. Therefore, a strut at an angle of less than 45° is chosen.

As a guideline, the angle between a strut and a tie should not exceed 25°. This is needed to avoid tension and compression at the same point in the node as much as possible. Therefore, a tradeoff is made between the position of the nodes, the angles between the struts and ties and the avoidance of tension in the diagonal bars. These considerations result in the design in Figure 5-2.

5.2 B & D regions

For the design of a strut & tie model it is also necessary to analyze which parts of the structure element are categorized as B-region and which parts as D-region. This is the most important principle on which this method is based. The truss is only drawn in the D regions of the construction element. The process of drawing the truss and determining B- & D regions is partly iterative. The truss design is needed to determine where the forces act and therefore determine the distance between these points of engagement to the supports.

The following rule applies to the D regions:

$$a < 2{,}5.d$$

where:

- a [mm] = distance between applied load and support
- d [mm] = effective depth
  - $d = d_{total} - c - \frac{\emptyset}{2}$

Using this definition for B and D regions leads to the results in Table 5-1.

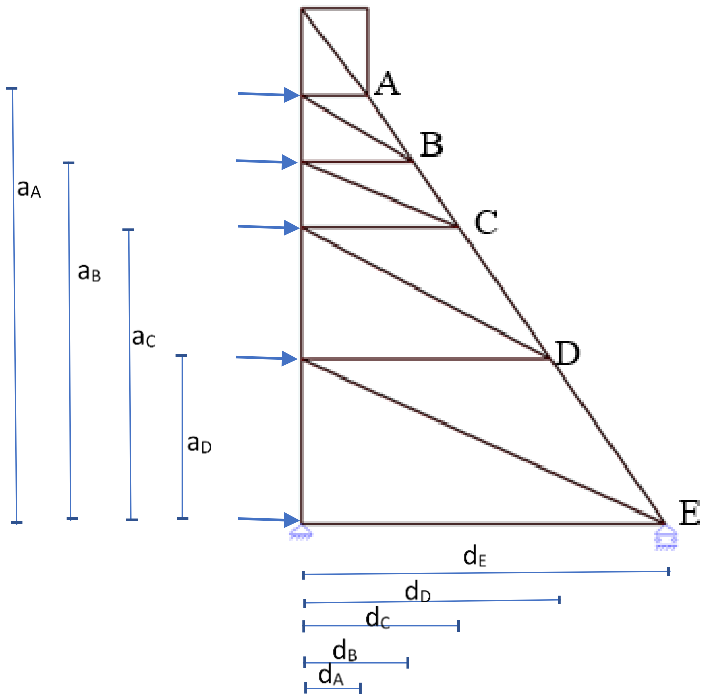

Figure 5-3 Levels as indicated in Table 5-1

level	a	dtotal	d	2,5.d	a<2,5.d	Region
A	39000	6000	5948	14870	-24130	B
B	33000	10154	10139	25348	-7652	B
C	27000	14308	14291	35728	8728	D
D	15000	22615	22085	55213	40213	D
E	0	33000	32000	80000	80000	D

Table 5-1 B&D Regions

5.3 Loads on truss

5.3.1 Horizontal loads (Shear Loading)

Since the horizontal load only acts on the straight side of the wall, it will also be applied in the truss only to the nodes on the straight side of the wall. Figure 5-4 below shows which part of the shear force is transferred to which node.

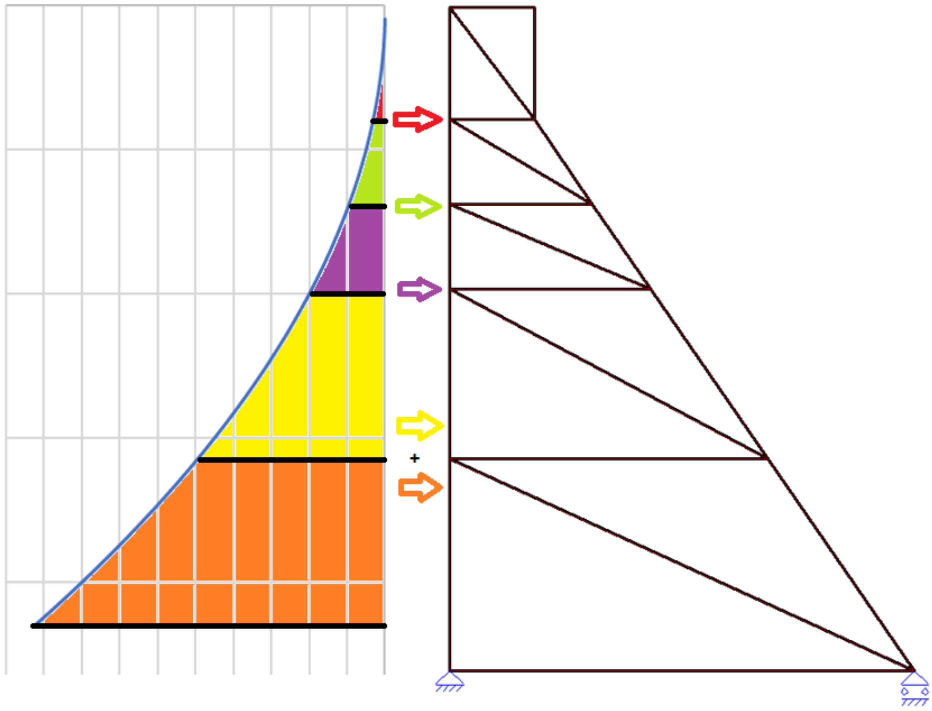

Figure 5-4 Loads on truss

The nodes that are on the top of the orange layer also bear the load that is applied under that node. Because the minimum angle between struts and ties and the orientation of the struts and ties makes it undesirable to add an additional node below the yellow layer, the load of the bottom orange layer is transferred one node higher. This was method is chosen because the transfer to the bottom layer would mean that the highest load on the wall is transferred directly to the subsoil, while in actuality this load will still be transported through the wall before it is transferred to the subsoil. This would therefore lead to an underestimation of the forces and stresses in the wall, compared to what would actually happen.

5.3.2 Vertical Loads (Self weight & Upward pressure)

The vertical load originates from the self-weight of the wall.

In contrast to the position of nodes on which the horizontal load originating from the lower part of the wall acts, the vertical load originating from the self-weight of the lower part of the wall (refer to the blue layer in Figure 5-5 below), will be transferred directly to the subsoil because the self-weight is considered a favorable load.

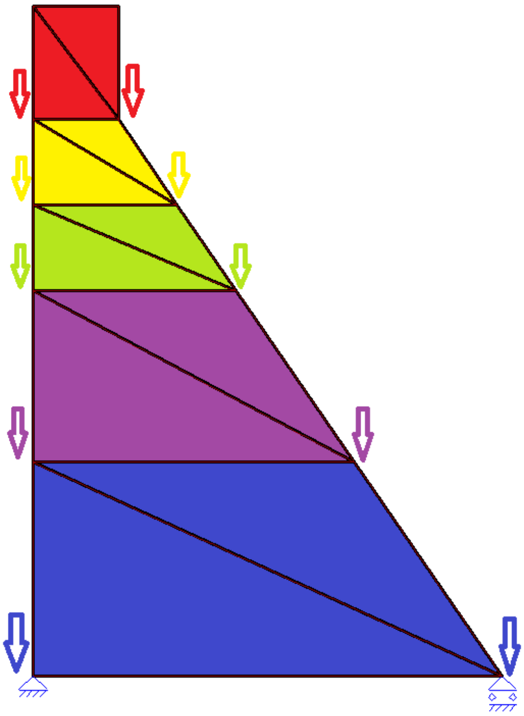

Figure 5-5 Vertical loads on truss

5.3.3 Magnitude acting loads

The Matrixframe software program is used to calculate the normal forces in the truss (see Figure 5-6). During the modeling of the truss, two supports were chosen to symbolize the subsoil. The support at the toe of the dike is a hinged support with no restrictions parallel to the subsoil to indicate that small displacements of the wall in this direction are possible and that the bending moment at this location is equal to zero. On the other side of the lock there is also a hinged support, this time with a restriction in the direction parallel to the subsoil. In actuality, the type of support depends on the connection of the wall to the floor. A fixed connection will result in large bending moments in this connection and thus also in the floor, which should as a result be heavily reinforced. A hinged connection, however, means that no bending moment occurs in this connection, which is desirable for the floor. Because this choice is not fixed in the W+B report, a hinged connection will be chosen, but with the restriction of vertical and horizontal displacements.

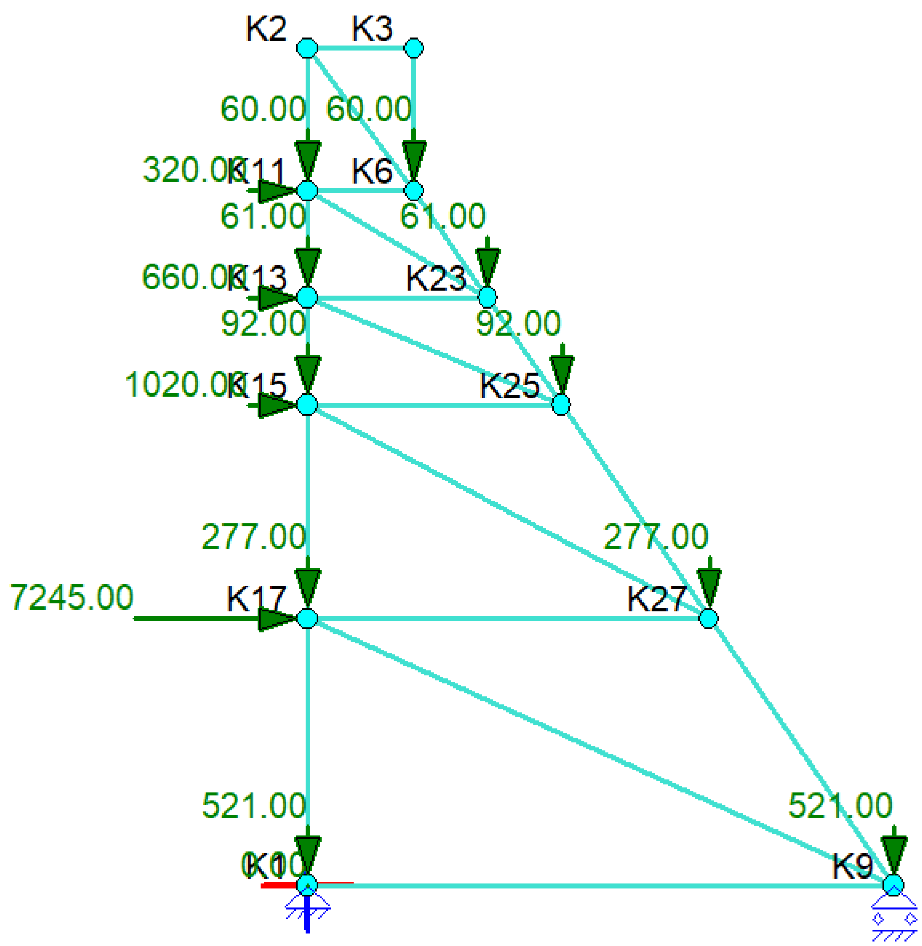

Figure 5-6 Loading Matrixframe

5.4 Shear Check initial geometry

The geometry of the initial wall design is checked to determine whether the wall will crack in the D-region as a result of shear loading. Because the thickness of the wall is not constant along the height, this check will be done at each level of nodes. As described in Voorendt & Molenaar (2018), the following equation is used:

$$V_{actual} < V_{cr} = \left[6{,}5 - 3\frac{a}{d}\right].\sqrt{f'}.b_w.d$$

where:

- V_{actual} [N] = actual shear force (in this case the loading inside the lock)
- V_{cr} [N] = critical shear force
- f' [N/mm²] = compressive strength concrete (30MPa in this case)
- b_w [mm] = width of structural web (1000mm)

The results of this check performed on the different sections is given in Table 5-2.

level	a	d_{total}	d	2,5.d	a<2,5.d	V_{actual} (N)	V_{cr}
A	39000	6000	5948	14870	-24130	320000	-429074897
B	33000	10154	10139	25348	-7652	660000	-181272584
C	27000	14308	14291	35728	8728	1020000	65141252

D	15000	22615	22085	55213	40213	3120000	539807967
E	0	33000	32000	80000	80000	4125000	1139262920

Table 5-2 Shear Check

5.5 Forces in Struts & Ties

The internal forces in the strut and ties are shown in the table below, which is computed in Matrixframe. The design has been placed next to the table for clarification. The ties in the wall are marked in red. In accordance with the Strut & Tie approach, reinforcement must be applied at these locations.

Staafkrachten

Staaf	B.G.	T/D	Nxmax
S2	B.G.1	-	0.00
S8		-	0.00
S14		-	-0.00
S16		T	104.55
S18		T	371.61
S20		T	1081.63
S26		D	-72.98
S28		D	-347.30
S30		D	-858.21
S39		D	-41.54
S40		T	122.31
S41		T	491.50
S45		-	0.00
S46		D	-323.44
S47		D	-848.32
S78		T	9245.00
S86		T	764.49
S87		D	-1711.10
S88		T	4445.31
S89		D	-2170.58
S90		D	-8798.09

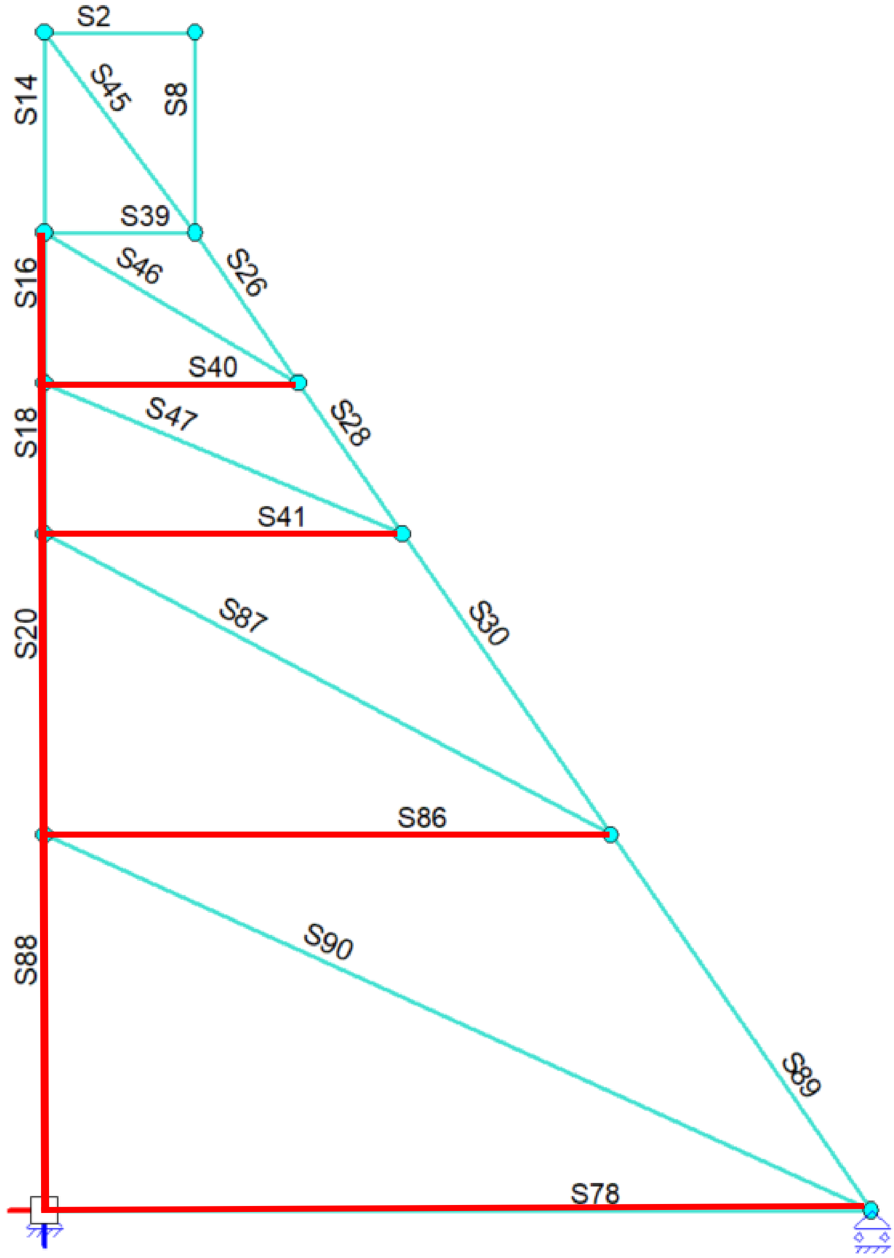

Figure 5-7 Internal forces

5.6 Proportion of the ties

The amount of reinforcement and the diameter of the reinforcement bars is determined at the locations where the normal force in the truss elements is a tensile force instead of a compression force, indicated by D in the Table in the previous chapter. The following equation is used to determine the required area of reinforcement:

$$A_{tie} = \frac{F_{tie}}{f_y}$$

where:

- f_y [N/mm²] =design yield strength of the reinforcement.
- For B500B this value is equal to 435 N/mm²
- F_{tie} [N] =tensile force of the tie

With the required A_{tie} the reinforcement can be proportioned as follows:

$$A_{tie} = \#.\frac{1}{4}.\pi.\emptyset^2$$

where:

- # = number of reinforcement bars
- ∅ [mm] =diameter of reinforcement bars. A diameter of 32 mm is chosen.

Tie	Nmax (kN)	Atie (mm²)	# ties
S16	105	241	1
S18	372	855	2
S20	1082	2487	4
S40	122	280	1
S41	492	1131	2
S78	9245	21253	27
S86	765	1759	3
S88	4445	10218	13

Table 5-3 Proportion Ties

5.7 Summary of main results

The strut and tie approach resulted in a reinforcement plan as shown in Table 5-3. As can be seen in Figure 5-7, the largest tensile forces occur at the bottom of the wall. The upper part of the wall is only slightly reinforced.

The disadvantage of this method is that it's not easy to determine the required thickness of a structural element with this method. This calculation method is a more robust design approach.

6 Verification Shear Resistance using a Finite Element Calculation

The third method that is used to perform calculations regarding shear loading in the Itaipu lock walls is a finite element calculation using the software: 'DIANA FEA'. Both a linear and a non-linear model have been used in order to achieve the desired output. Both models are plane stress models instead of plane strain models. In the case of this lock wall, with a large length (out of plane direction), it would be more suitable to make use of a plane strain model. However, this raised some issues with the correct modelling of the reinforcement of the nonlinear model. Therefore, the choice has been made to use a plane stress model instead for both the linear and nonlinear models. The results of this decision is that the model will give zero stresses in the out of plane z-direction while in real life this is not the case. However, for the 2D analysis in the x-y plane, this tradeoff does not affect the results.

First, the linear 2D model of the wall and the part of the floor that is attached to the wall is set up. The symmetry of the other half of the wall and floor is included in the model. The two geometry components of this model are the concrete part and an interface part. The interface represents the basalt subsoil and has a stiffness in vertical y direction (direction parallel to the self-weight/gravity) equal to the bedding constant of the basalt (50 MN/m^3). The bedding constant is a parameter which is determined by the Young's modulus of the material. In addition, the interface also has a shear stiffness in the horizontal x direction for which 1/100 of the stiffness in the y direction is taken as a rule of thumb, so 0.5 MN/m^3. The actual value of the shear stiffness is hard to precisely determine. The decision has therefore been made to model the stiffness in such a way that the stiffness is relatively low and it is assumed that the wall can shear off. This means that the friction is negligible compared to the large normal force originating from the self-weight of the wall.

Using a structural linear static analysis, the displacements and stresses in the wall & floor are calculated. Subsequently, the thickness of the wall is varied in this model and the results (displacements and stresses) will be displayed for different wall thicknesses. Based on the linear model, it can be concluded where the stresses are exceeded above a certain "failure" level.

In the nonlinear model, both concrete and reinforcement are modelled with non-linear material properties. The interface is the same as in the linear model. The first is the model of the current geometry of the wall and floor as designed / conceived by Witteveen+Bos. And the second model is includes the geometry with the thickness that is proposed as the optimal thickness where the wall still has sufficient shear capacity, derived from the results of the linear model. The added value of the non-linear model is to focus on the locations where it can be seen in the linear model that a certain limit value of stresses is exceeded. In the non-linear model, the structure can also be reinforced in such a way to assure a certain stress path.

The out of plane z direction is modelled to be 1m for both models. This means that the wall, floor and interface have a DIANA thickness[1] of 1m.

6.1 Linear Model

The current design of the Itaipu locks is translated into a 2D linear model.

---

1 This thickness differs from the use of the term thickness in this report. The thickness mentioned here is the dimension as defined by DIANA FEA, corresponding to the dimension 'width' (dimension out of plane; perpendicular to the thickness dimension used in this report). Note that this dimension will be referred to as DIANA thickness in the remainder of this report.

6.1.1 Geometry

The model consists of one regular plane stress concrete element for the wall and the floor with the following material characteristics:

- Young's modulus: 30 MPa (C30/37)
- Poisson's ratio: 0.2
- Mass density: 2400 kg/m^3

The subsoil is modeled as a boundary interface with the following characteristics:

- Type: 2D line interface
- Normal stiffness modulus-y: 50 MN/m^3
- Normal stiffness modulus-x: 0.5 MN/m^3

The thickness for the wall+floor geometry and the interface is 1m.

6.1.2 Supports

The interface of the wall and floor are supported in both the x- and y-direction. And the floor is supported in only the x-direction to indicate the symmetry of the wall+floor.

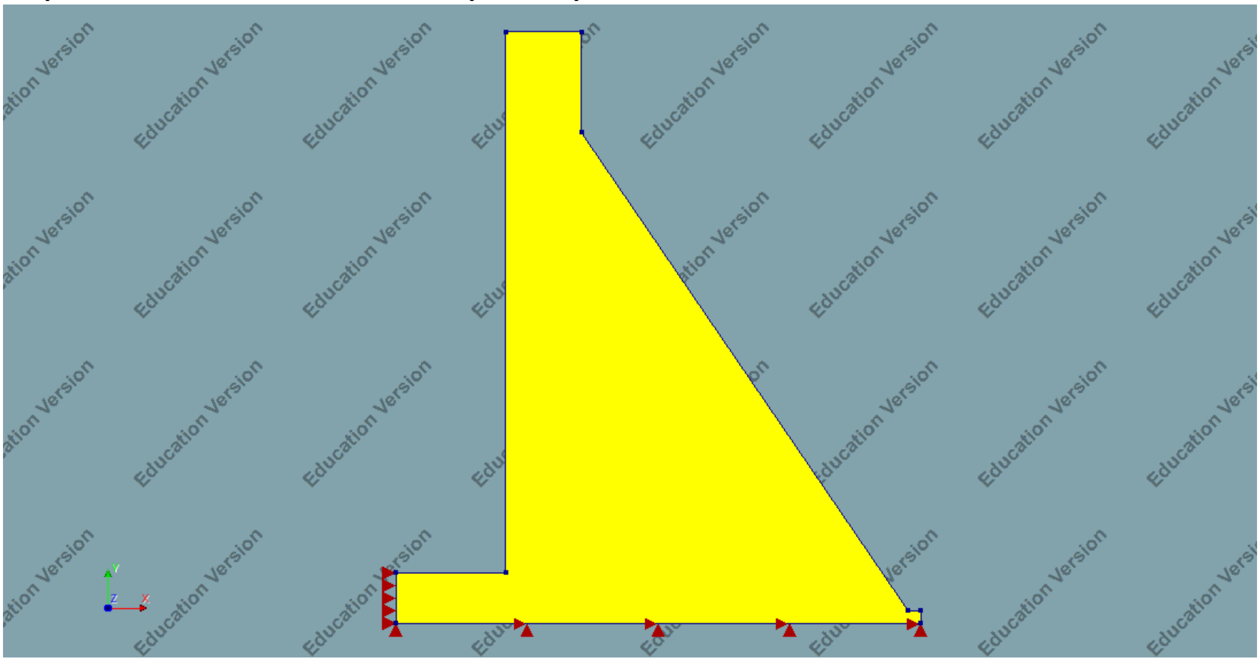

Figure 6-1 Supports

6.1.3 Loading

The loads consist of:

- Self-weight of the concrete
- Horizontal hydrostatic pressure on the wall (43m) and the vertical component of the hydrostatic pressure on the floor.

The analysis is performed with only 1 load combination where both loads act with a load factor of 1.0 simultaneously.

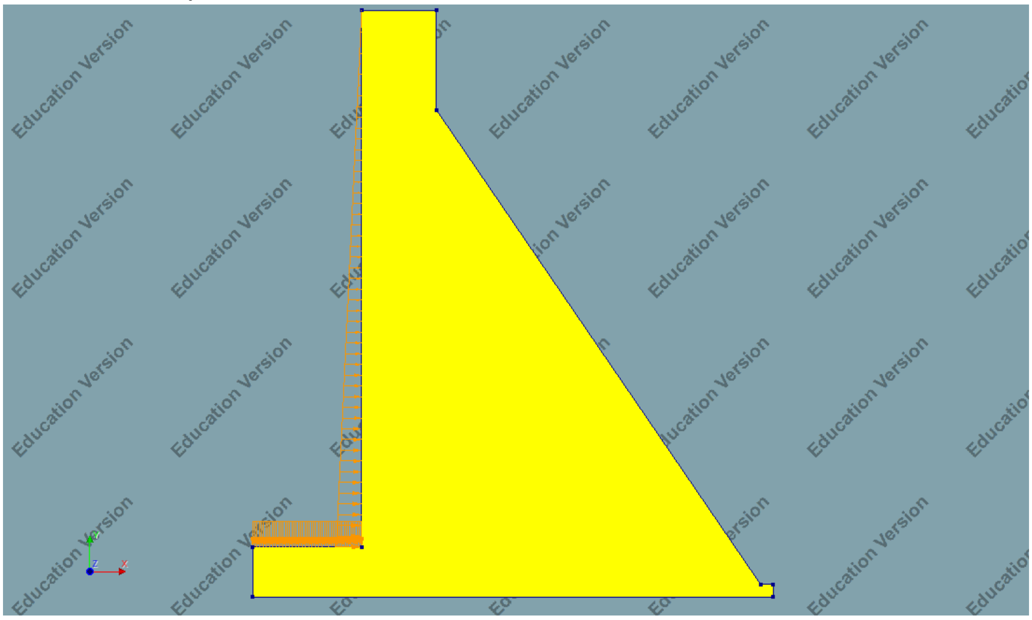

Figure 6-2 Loading

6.1.4 Mesh

A mesh is applied with an element size of 200mm over the entire shape of the wall+floor.

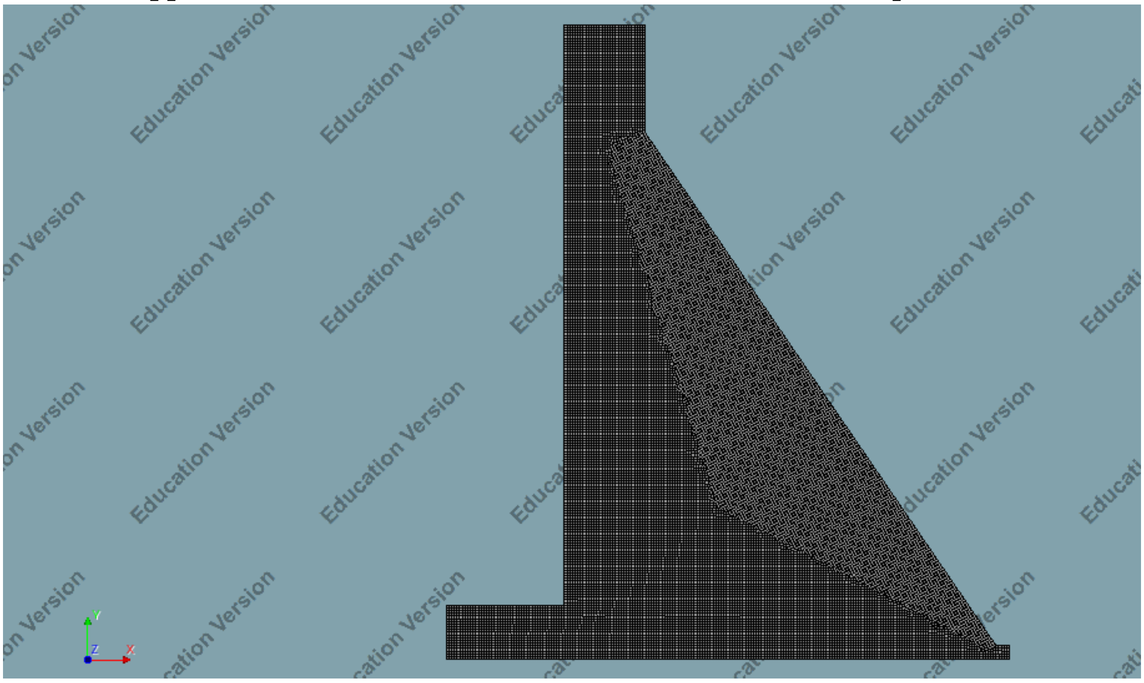

Figure 6-3 Mesh

6.1.5 Analysis

The type of analysis performed is a structural linear static analysis.

6.1.6 Results

The results of the linear analysis of the original design by W+B are shown in contour plots and vector plots. Note that for some of the contour plots, the maximum and minimum values are adjusted in order to prevent the plot being highly influenced by peak values. The actual maximum and minimum values can be seen in the description box in the top of each plot.

Results Stresses

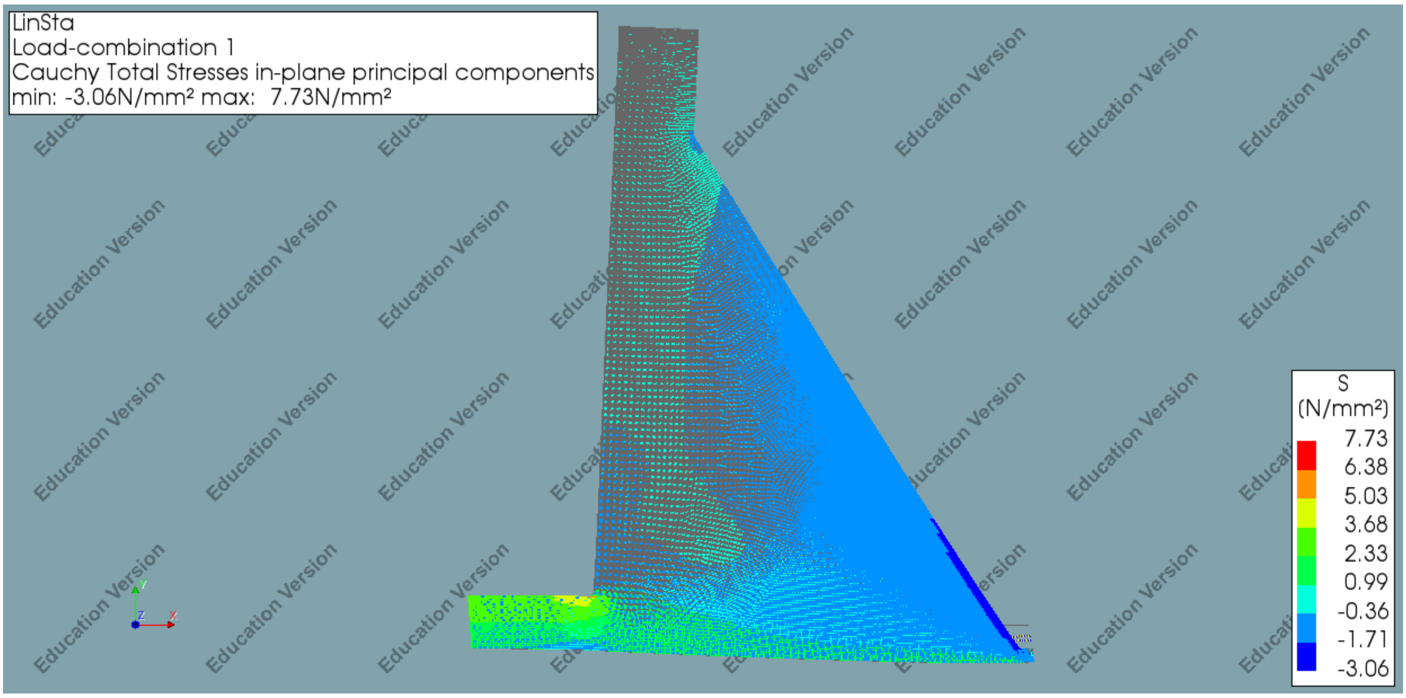

Figure 6-4 Principal Stresses linear model original design

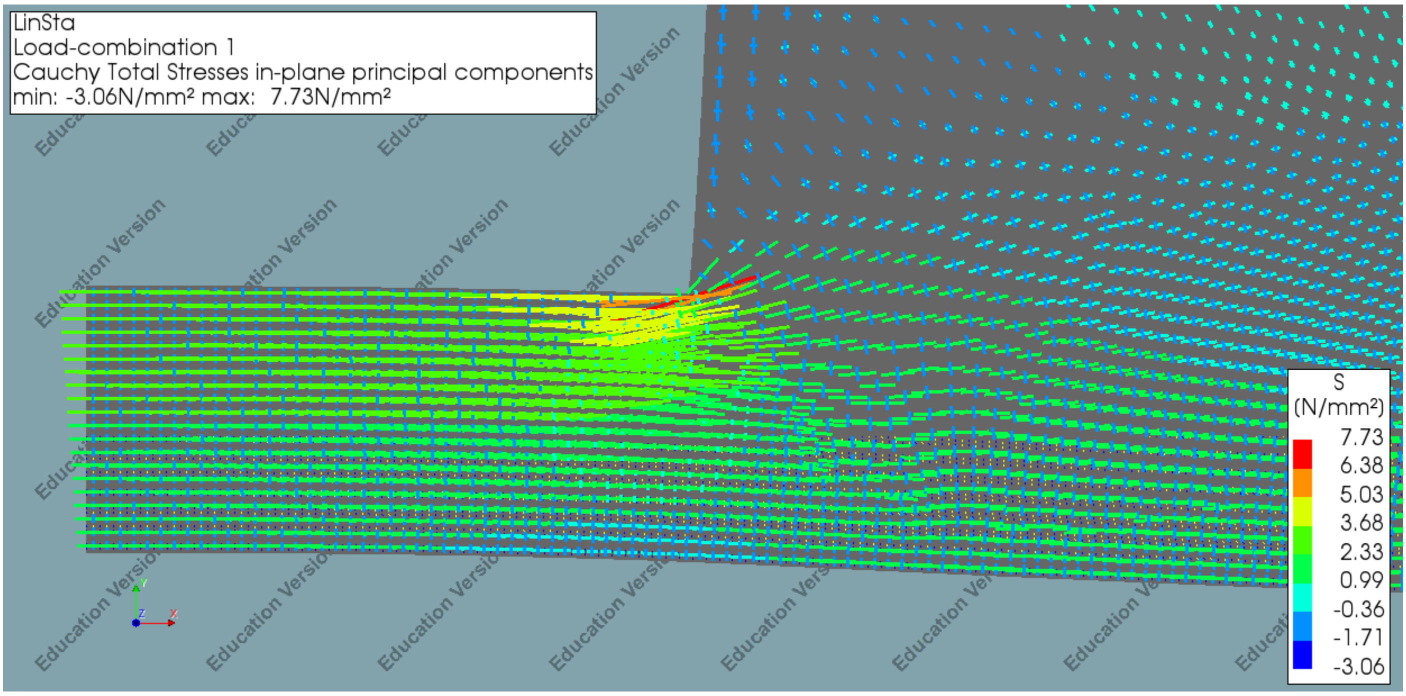

Figure 6-5 Zoom in on principal Stresses linear model original design

6.2 Decreasing wall thickness Linear Model

The same analysis has also been performed for the two alternative designs. The second alternative design is analyzed before the first alternative design so that the results can be checked for a gradually decreasing wall thickness.

6.2.1 Results second alternative design: total wall thickness of 29 m.

The results of the linear analysis of the second alternative design are shown in contour plots and vector plots.

Stresses

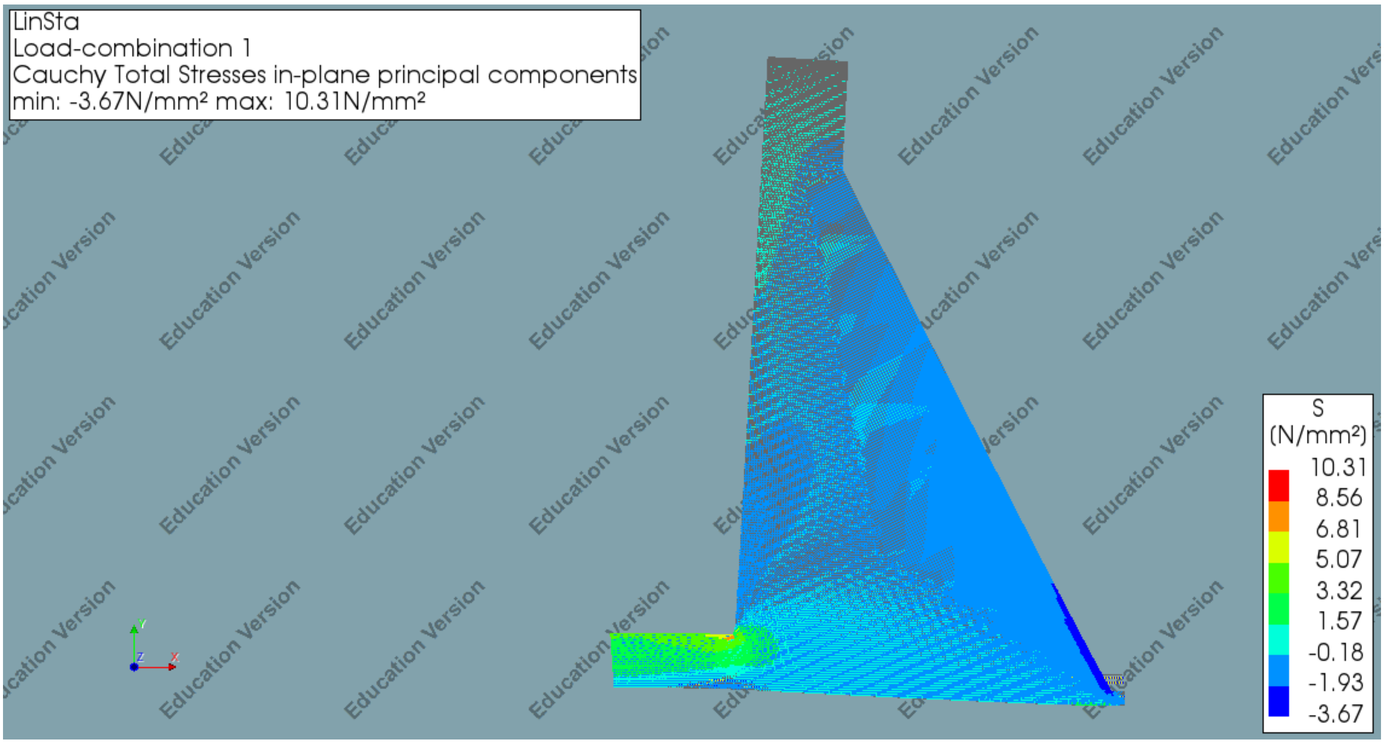

Figure 6-6 Principal stresses second alternative design

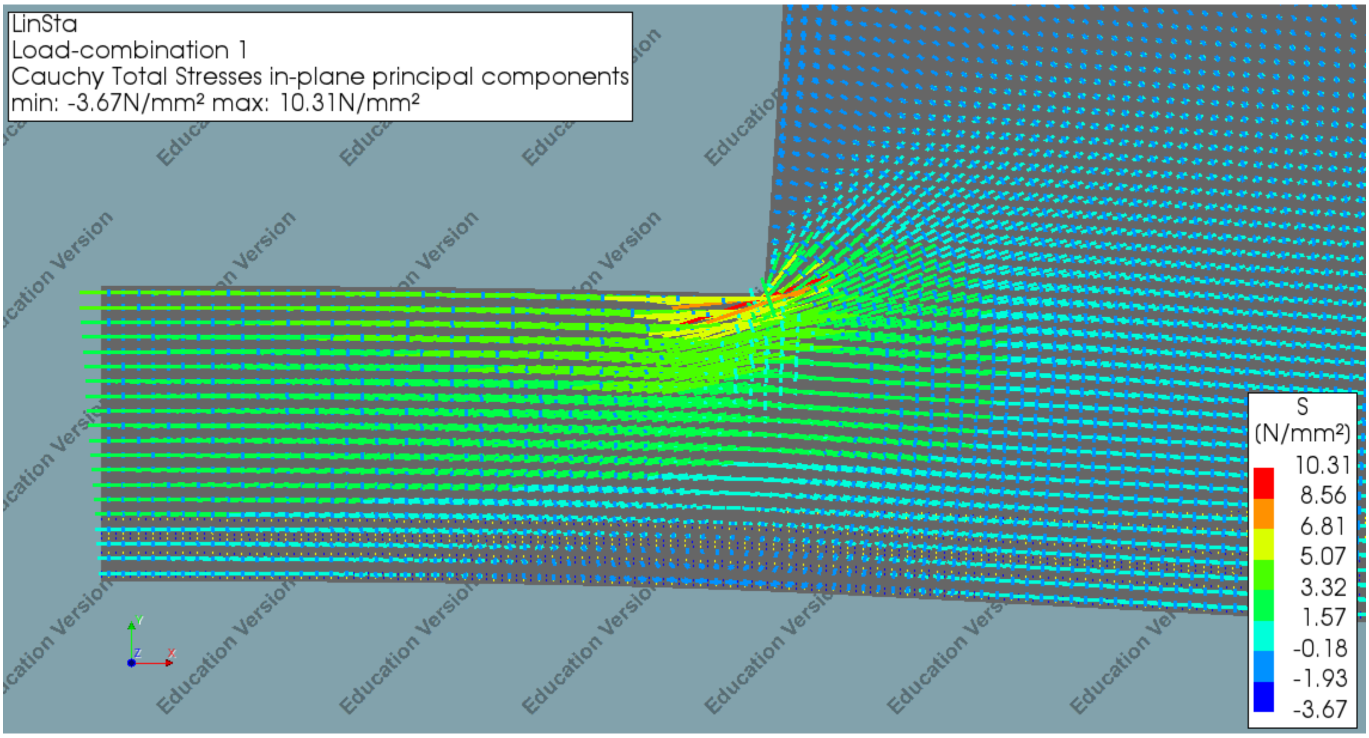

Figure 6-7 Zoom in on principal stresses second alternative design

6.2.2 Results first alternative design: total wall thickness = 17 mm.

The results of the linear analysis of the second alternative design are shown in contour plots and vector plots.

Stresses

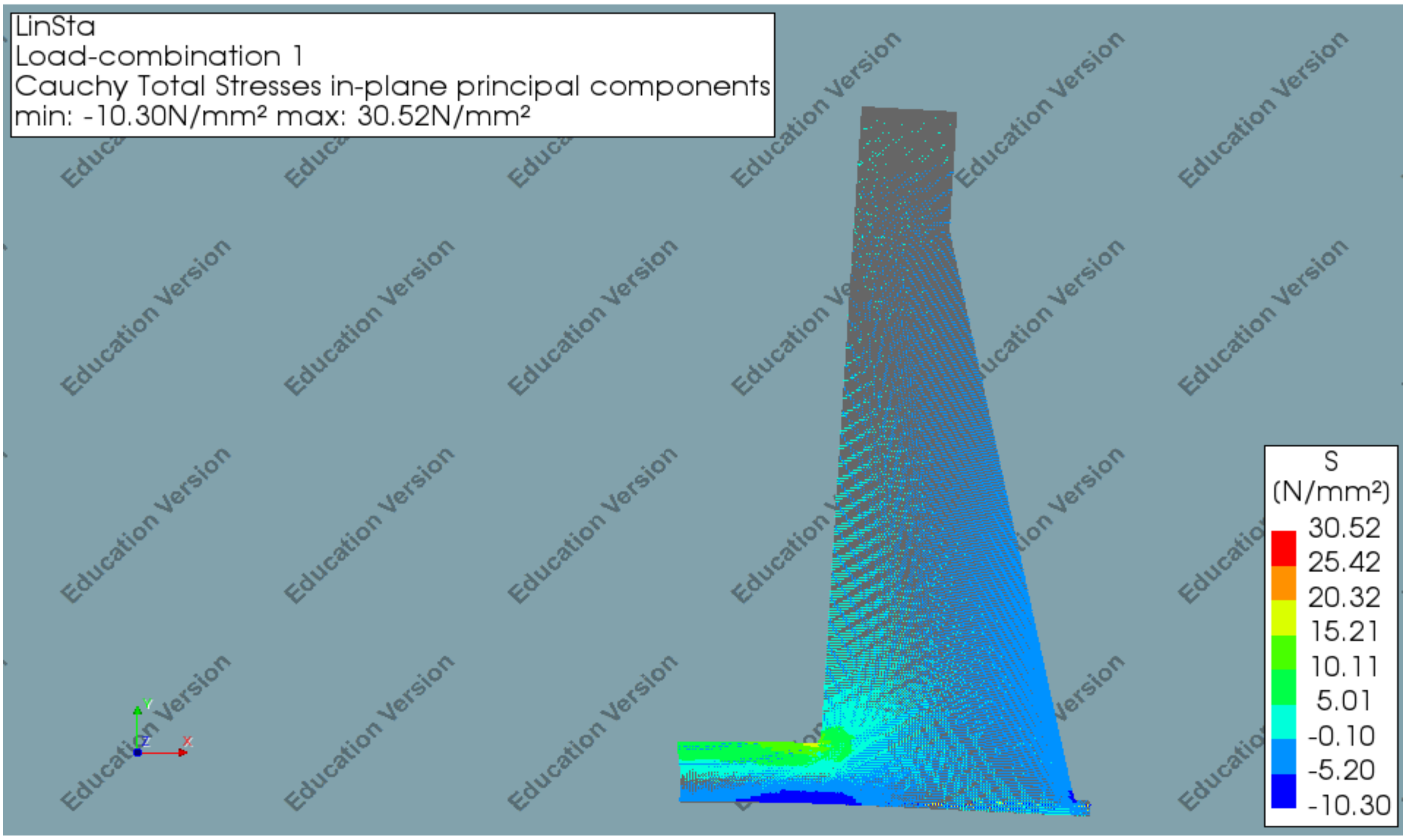

Figure 6-8 Principal stresses first alternative design

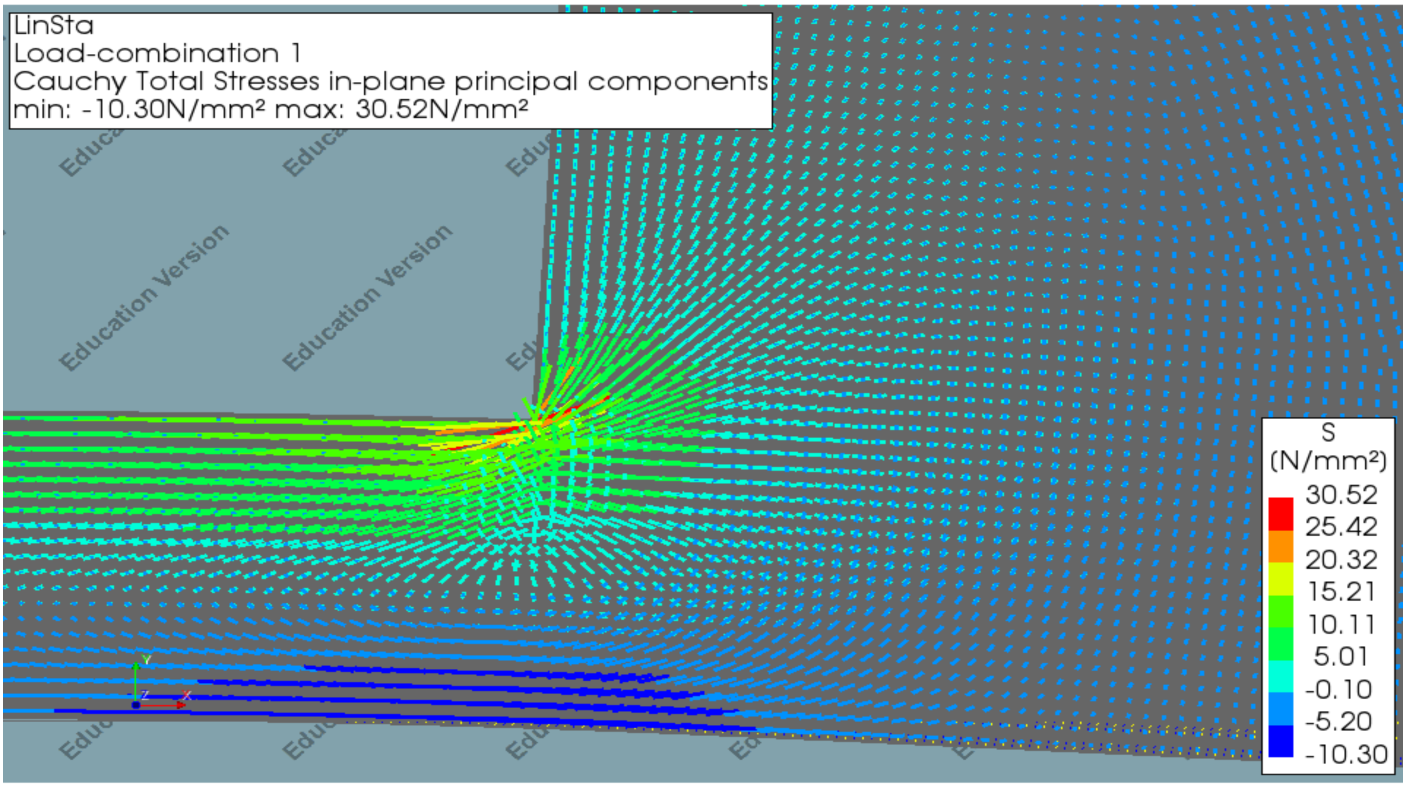

Figure 6-9 Zoom in on principal stresses first alternative design

6.3 Nonlinear Model

The original W+B design of the Itaipu locks is also translated studied with a 2D nonlinear model.

6.3.1 Geometry

The model consists of one **regular plane stress concrete element** for the wall and the floor with the following material characteristics:

Linear material properties:

- Young's modulus: 30000 N/mm^2
- Poisson's ratio: 0.2
- Mass density: 2400 kg/m^3

Total Strain based crack model:

- Crack orientation: Fixed

Tensile behaviour:

- Tensile curve: Hordijk
- Tensile strength: 2.7 N/mm^2
- Mode-I tensile fracture energy: 0.144 N/mm
- Crack bandwidth specification: Govindjee
- Poisson's ratio reduction model: Damage based

Compressive beahviour:

- Compressive curve: Parabolic
- Compressive strength: 37 N/mm^2
- Compressive fracture energy: 35.975 N/mm
- No reduction due to lateral cracking
- Stress confinement model: Selby & Vecchio

Shear behaviour:

- Shear retention function: aggregate size based
- Mean aggregate size: 25mm

The model also includes the reinforcement of the floor. Resulting from the lack of high tensile stresses in the wall, as can be seen in the results of the linear analysis, the choice has been made not to reinforce the wall. In terms of project costs, minimal reinforcement is ideal. However, this decision is based purely on the results of the shear analysis. For other usability and/or durability requirements, the outer layer of the wall might still be reinforced. This specific reinforcement is not included in this calculation.

The **material properties** of all the **reinforcement bars** are the same and are modelled as follows:

Linear elasticity:

- Young's modulus: 200000 N/mm^2

Eurocode 2 EN1992-1-2:

- Yield stress: 435 N/mm^2
- Peak stress: 500 N/mm^2
- Strain at peak stress: 0.015
- Strain at start decay: 0.045
- Ultimate strain: 0.05
- Reinforcement class: hot rolled class N – Table 3.2a

The position of the reinforcement bars is indicated with the red color in the image below:

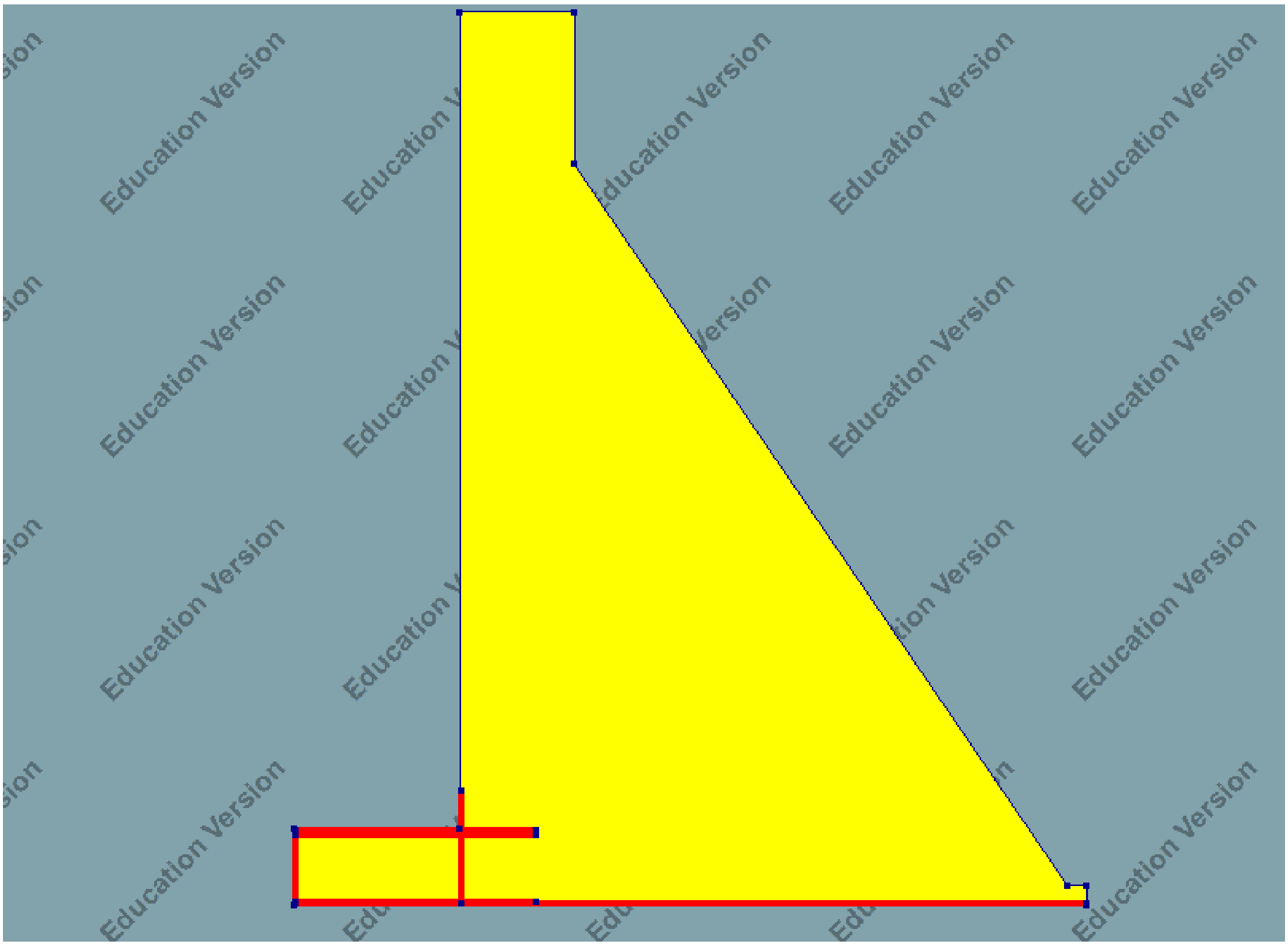

Figure 6-10 Reinforcement

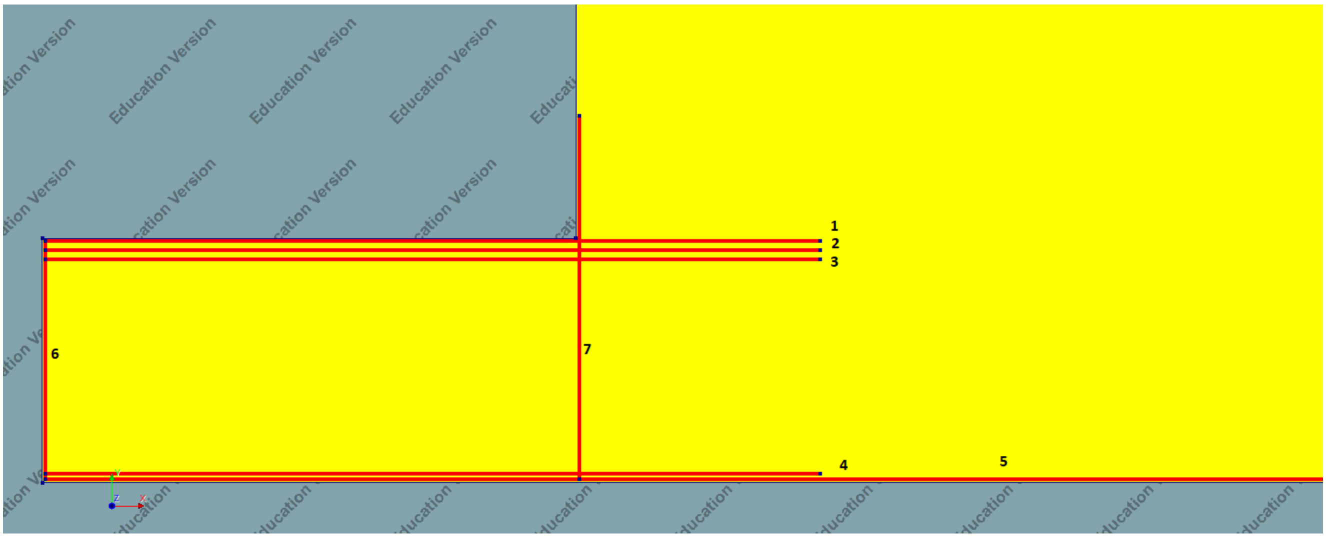

Figure 6-11 Reinforcement zoomed in

The reinforcement is modelled as imbedded bars and the total area per reinforcement is given. This means that the model doesn't include information about the amount of bars. The initial total area per reinforcement position is derived from the Strut and Tie model. Afterwards, this area was adjusted to meet the minimal crack width requirements as described by the Eurocode based on the results from the nonlinear model.

Reinforcement position	Total area (mm^2)
1	31253
2	31253
3	31253
4	31253
5	31253
6	31253
7	31253

Table 6-1 Total area of reinforcement

6.3.2 Supports

The supports, and mesh are similar to that of the linear model.

6.3.3 Loading and Analysis

The loads consist of:

- Self-weight of the concrete
- Horizontal hydrostatic pressure on the wall (43m) and the vertical component of the hydrostatic pressure on the floor.

The analysis performed is a structural nonlinear phased analysis with start steps. The first start step has a specified size of 1 and includes the load of only the self-weight. Afterwards, the load of both the vertical and horizontal water pressure is added to the structure with steps of 0.1 until the load factor of 1.0 is reached.

6.3.4 Results

The results of the final load step (load factor of 1.0 for both the water pressure and the self-weight) of the nonlinear analysis performed with DIANA FEA are included in this subchapter.

Stresses

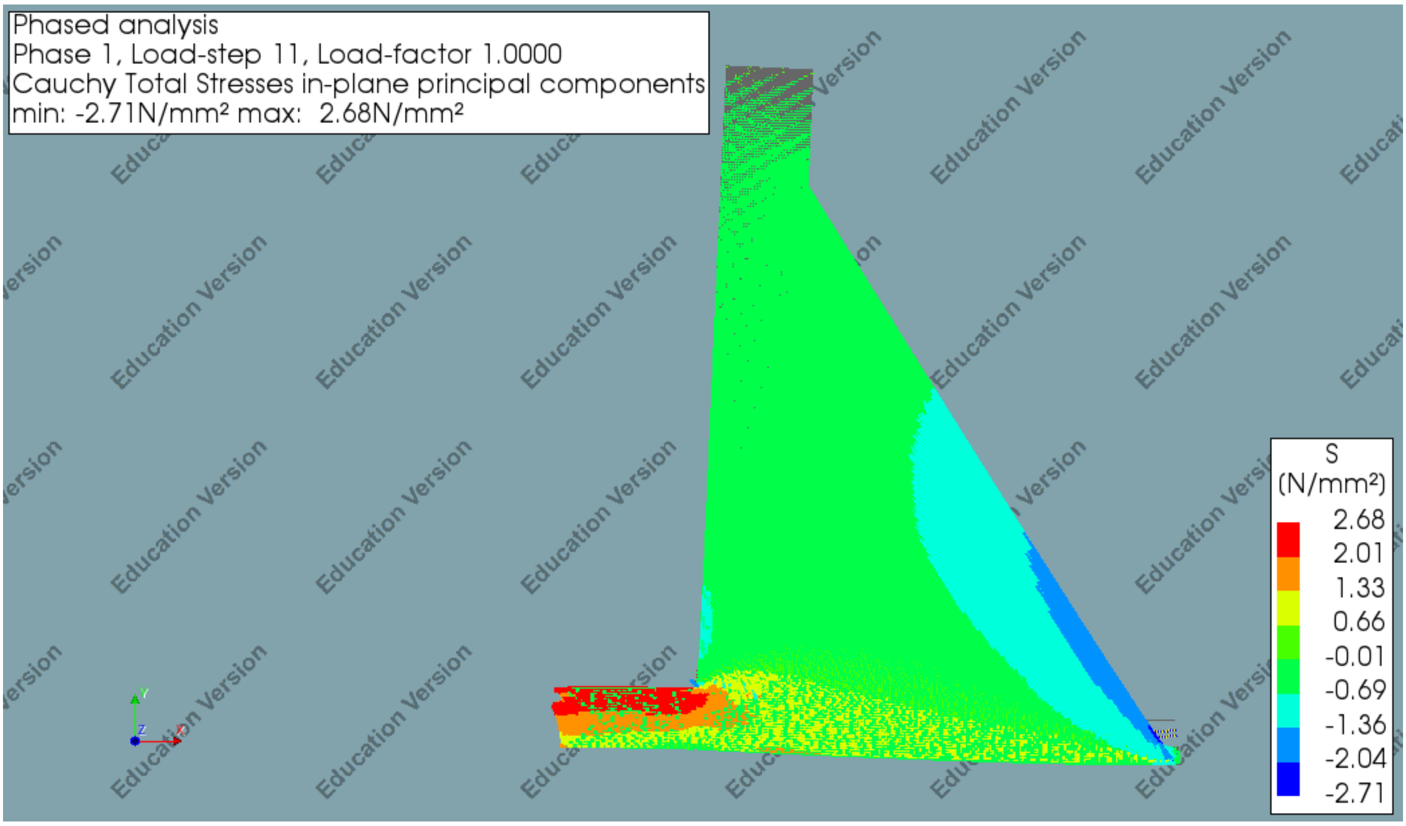

Figure 6-12 Principal stresses nonlinear model original design

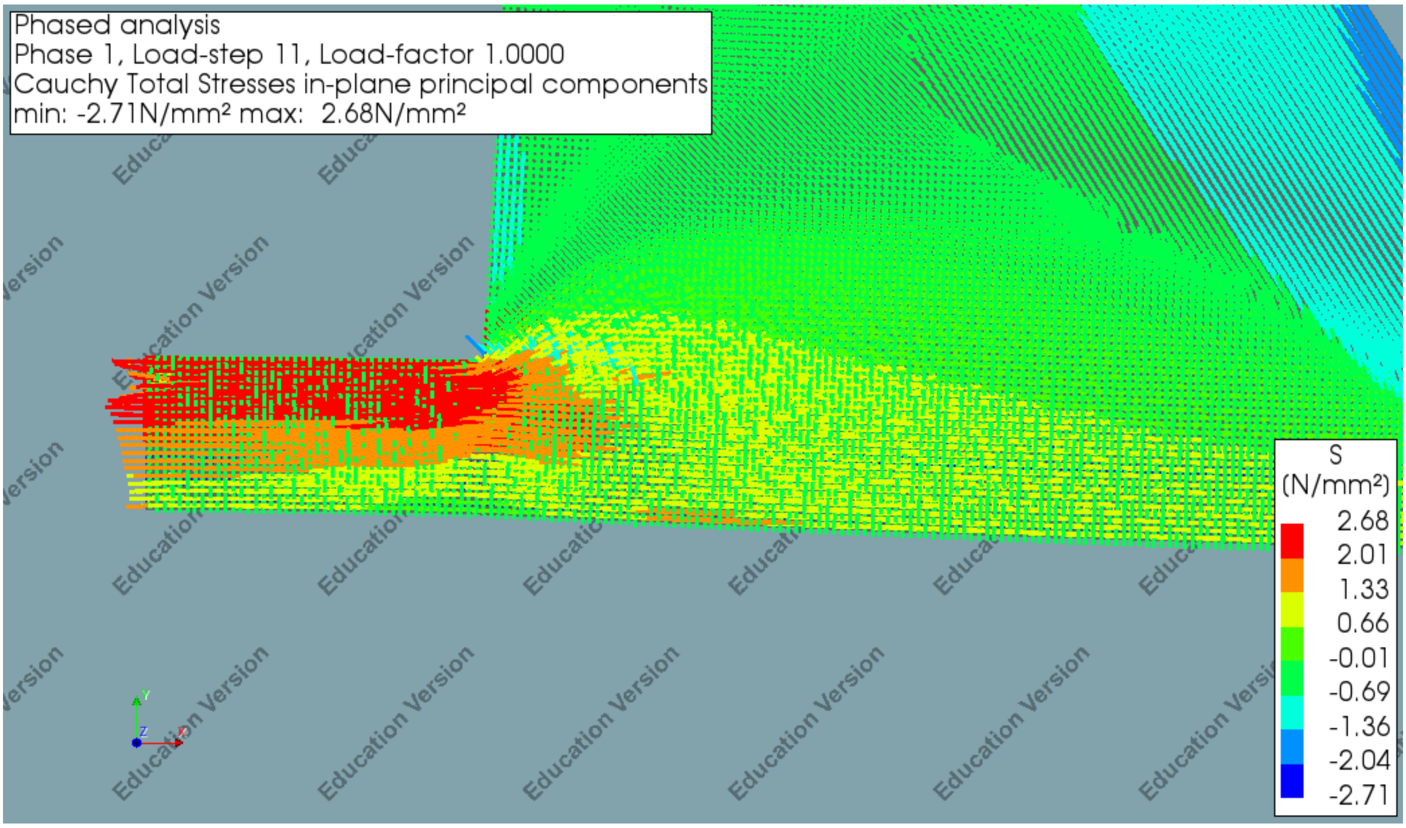

Figure 6-13 Zoom in on Figure 6 12 Principal stresses nonlinear model original design

Crack Widths

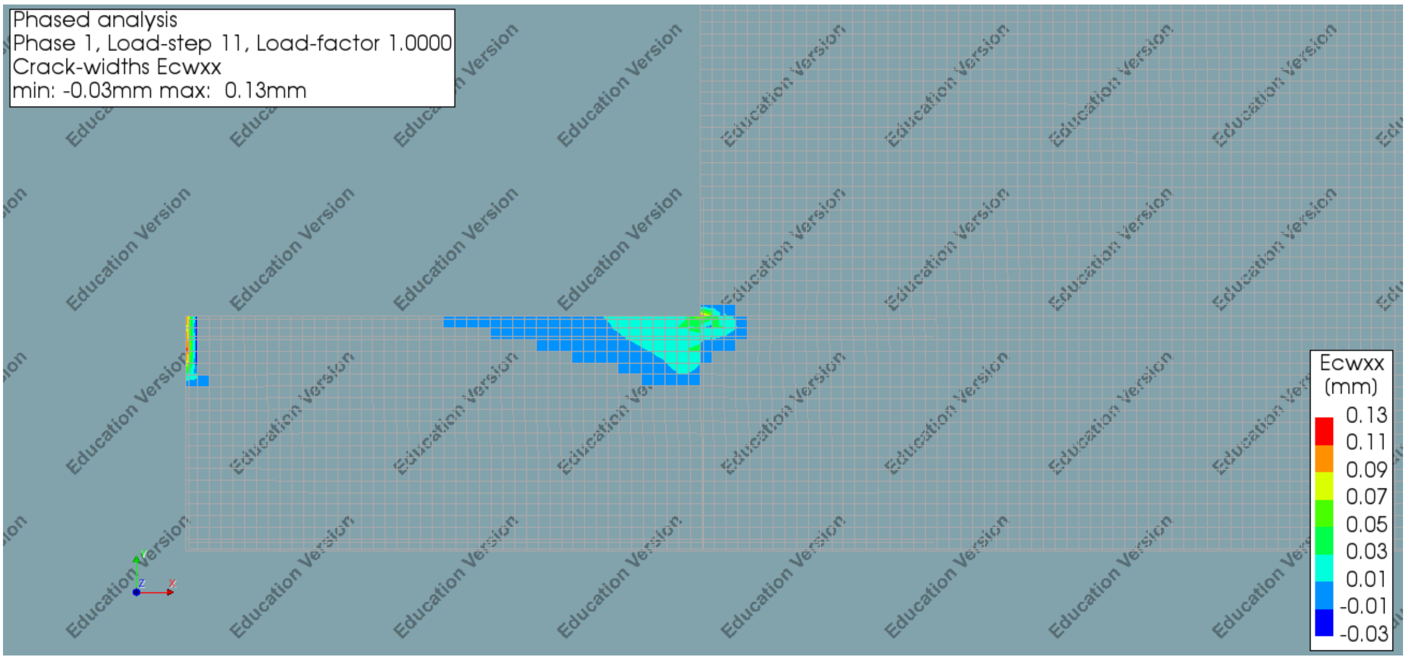

Figure 6-14 Crack widths nonlinear model original W+B design

Cross-Section Forces

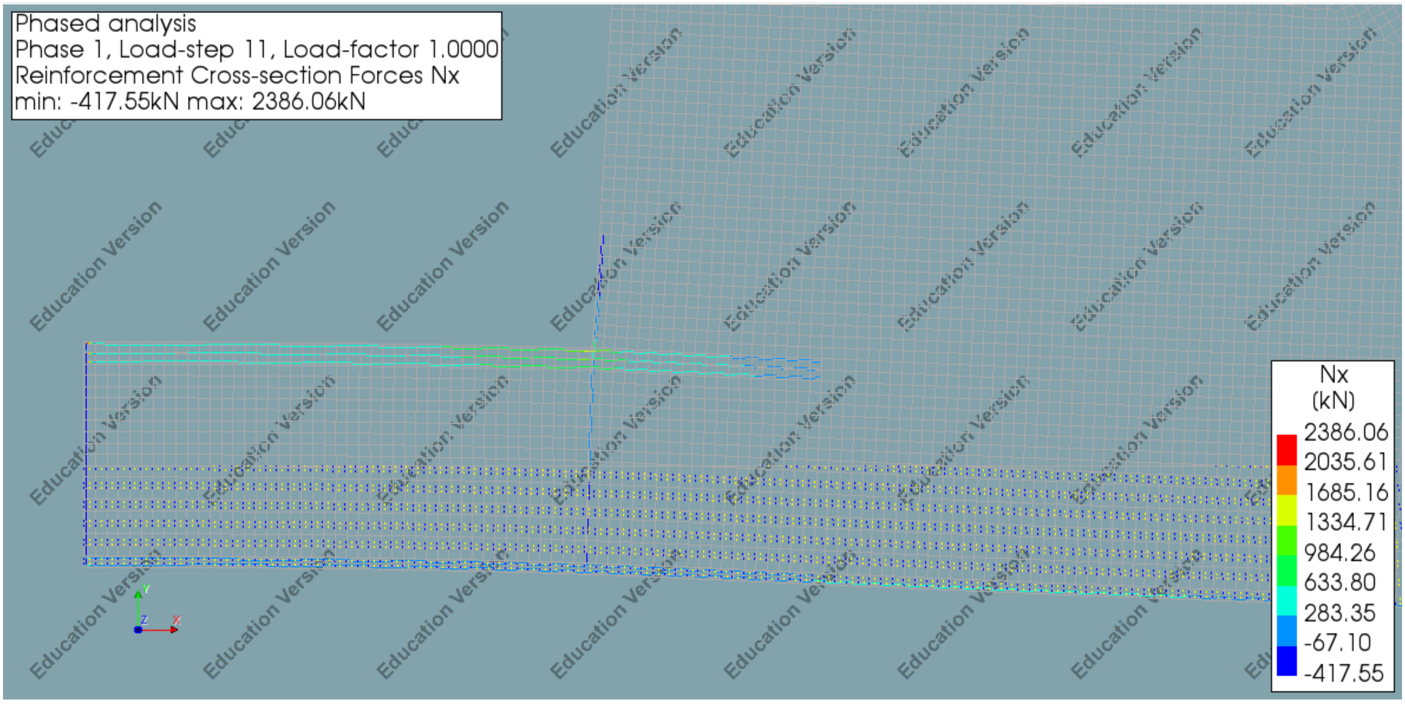

Figure 6-15 Reinforcement cross-section forces nonlinear model original W+B design

6.4 Check Modified Compression Field Theory using Mohr's circle

As stated in paragraph 7.4, the sectional method is not the right approach for deep beams and structural elements in the same order of size as the Itaipu lock walls. The (simplified) modified compression field theory gives a much better approximation of the allowable shear stresses in deep beams. Ideally, the sectional calculation could have been replaced or complemented by the (simplified) modified compression field theory.

Due to time constraints the decision has been made not to add this extra calculation step. However, a part of this calculation method can still be used as a quick shear assessment method to check whether the shear stress exceeds the allowable shear stress on a crack. This is done by using equation 15 from Figure 2-21:

$$v_{ci} \leq \frac{0.18\sqrt{f'_c}}{0.31 + \frac{24w}{a_g + 16}} \quad MPa, mm$$

Where:

- v_{ci} is the shear stress on a crack (MPa)
- f'_c is the concrete compressive strength (MPa)
- w is the crack width
- a_g is the maximum aggregate size (mm)

The shear stress on a crack is derived from Mohr's method by using the principal stresses at the location of the biggest crack from the nonlinear DIANA model.

- f'_c = 30 MPa
- w = 0.13 mm (the maximum crack width is taken from Figure 6-14)
- a_g = 32 mm (the maximum aggregate sized used in the Netherlands)

The principal stresses in the element with the largest crack width are shown in Figure 6-16. These principal stresses are used to draw Mohr's circle to find the maximum shear stress in that element. A more detailed explanation of stresses and Mohr's circle is given in Appendix A: Normal and shear stresses.

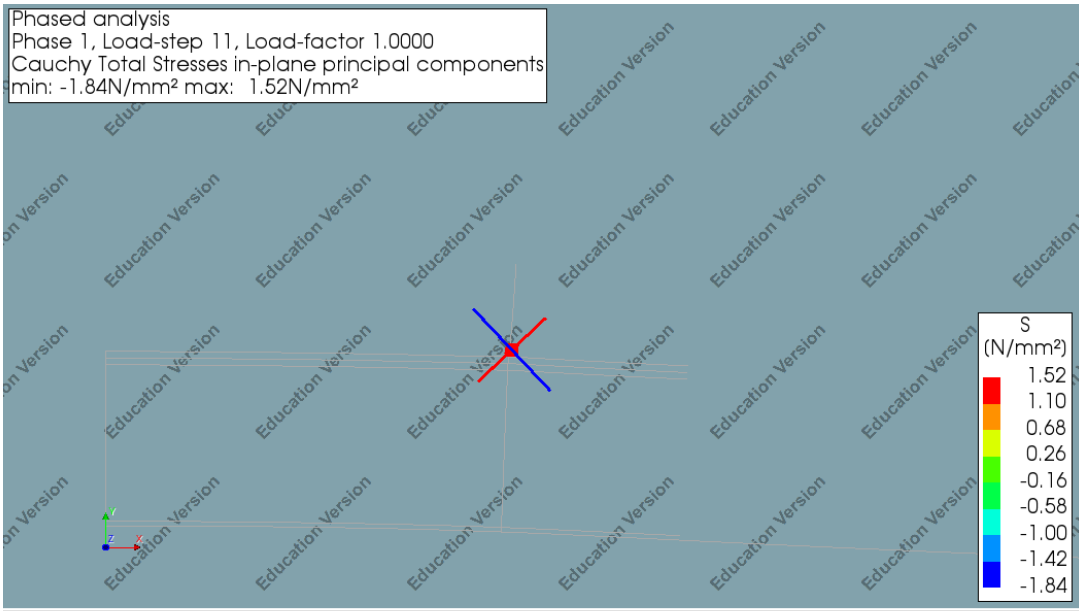

Figure 6-16 Principal stresses critical element

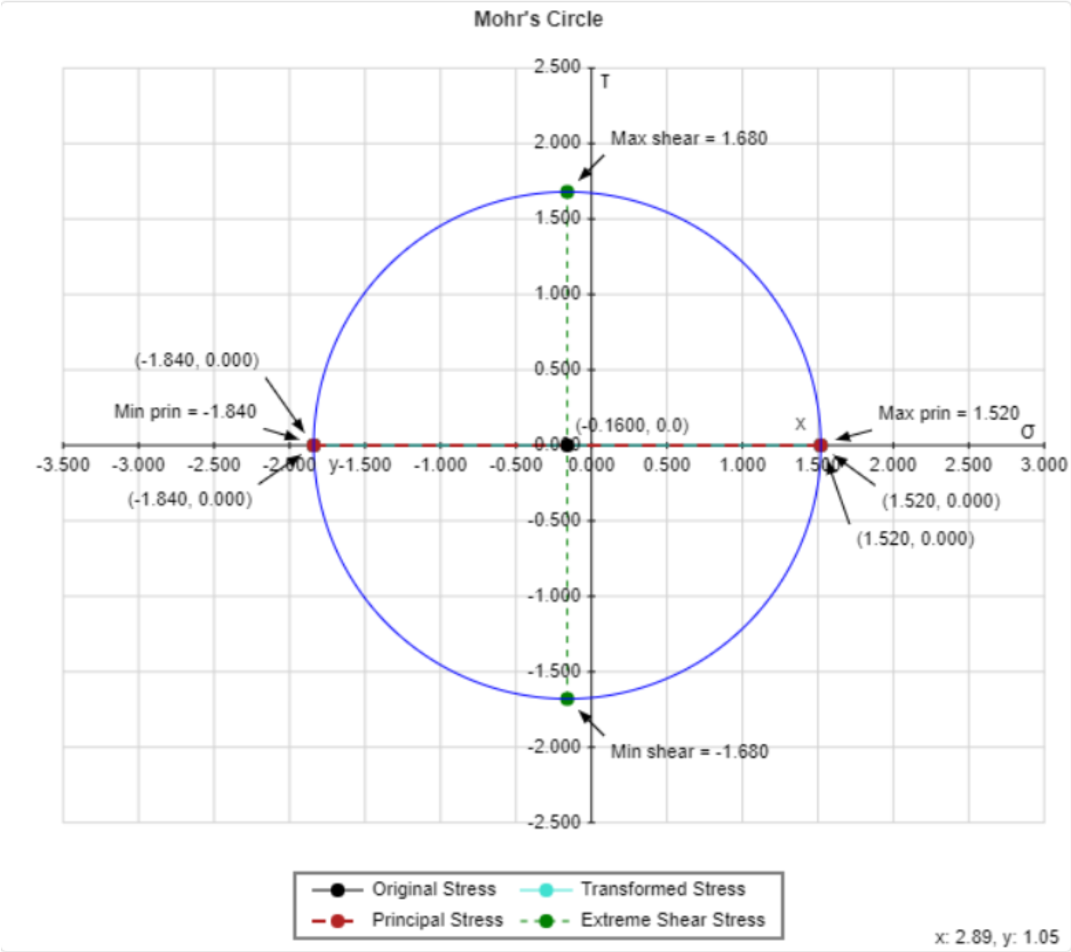

Figure 6-17 Mohr's circle critical element

The maximum shear stress in the element is derived form Mohr's circle:

- v_{ci} = 1.680 MPa

Substituting the values in equation 15 from Figure 2-21:

$$v_{ci} \leq \frac{0.18\sqrt{30}}{0.31 + \frac{24 * 0.13}{32 + 16}} = 2.63\ Mpa$$

$$1.680\ MPa\ \leq 2.63\ Mpa$$

A quick check with the modified compression field theory shows that including the aggregate interlock aspect results in the conclusion that the occurring shear stress in the most critical governing element is below the allowed shear stress.

7 Discussion

The shear capacity of the wall is studied with three main calculation methods. The results of these methods will be discussed in this chapter, also highlighting the conditions for which the methods can be used and the limitations of each method. At last, the use of these methods on the Itaipu lock wall is discussed.

7.1 Sectional Analysis

The first calculation is the sectional calculation based on the norms and guidelines. This analytical approach is too limiting to correctly calculate the shear behavior of the lock wall as well as the floor. Also, this method is based on empirical results for smaller regular sized beams making it inaccurate for application on deeper beams and larger structural elements.
For this method, the floor is modeled as a support with restrictions in horizontal x-direction and vertical y-direction, ignoring the spring-like behavior of the subsoil and the behavior of the floor itself. Multiple sections in the wall are tested to see if the shear capacity is sufficient in order to resist the loading by the self-weight and hydrostatic pressure. This approach resulted in two proposed wall thicknesses: (i) a design with a total thickness that is 4m smaller than the original W+B design and (ii) a design with a total thickness that is 16m smaller than the original W+B design. The first proposed thickness is based on a check with the assumption that the shear crack will be diagonal with an angle of 45° and the second proposed thickness is based on a check in the most heavily loaded section of the lock. The proposed thicknesses are:

- Total wall thickness original design: 33m
- Total wall thickness alternative design 1 (i): 17m
- Total wall thickness alternative design 2 (ii): 29m

As can be seen, the alternative thicknesses differ quite a lot. This is a result of the large wall thickness, indicating the inaccuracy of this model for this type of use.

The self-weight of the wall is much larger compared to the hydrostatic pressure of the water inside the lock and the shear capacity of the wall, as calculated with this method, therefore depends solely on the concrete part of the wall. Longitudinal reinforcement is thus not necessary to increase the shear capacity. The shear capacity as a result of the large normal force in the wall is sufficient to resist the loading of the water inside the lock. A check for crack width is also performed for the original design and the allowable maximum crack width as a result of shear loading is not exceeded. However, to keep the crack width to a minimum as a result of bending, some reinforcement had to be added: 8ø14.

7.2 Strut & Tie Method

The Strut & Tie method resulted in a reinforcement plan based on the predicted stress trajectories within the wall. In the Strut & Tie approach, the forces are assumed to be transferred into the subsoil via two supports while in reality the subsoil will act more as a continuous spring over the entire area of lock wall and lock floor that is located upon the subsoil. This results in more concentrated stresses in the wall in the Strut & Tie approach than will occur in reality, making this calculation method more conservative.

The Strut & Tie method has proven not to be the ideal method to determine the required thickness of the lock wall. Instead, the method resulted in a reinforcement layout for the original wall design of W+B with horizontal and vertical ties. According to this method, the largest tensile force will be found in the horizontal tie that is located in the bottom of the lock wall with small tensile forces in the ties higher up in the wall. This corresponds to what is expected beforehand.

However, because the lock floor was not included in this model, the results are not as accurate. A better approach would be to include the lock floor in the S&T design. This would have resulted in a better approximation of the behavior of the lock floor.

7.3 Finite Element Method

The third calculation is the most accurate because it not only includes the floor, which is ignored in the previous two calculations, but it also includes the effect of the subsoil. A finite element calculation is performed with the use of the DIANA FEA software. At first, the original W+B design is modelled linearly. Then, the same linear approach is also applied to the two alternative designs that are derived from the sectional analysis. At last, a nonlinear model is made for the original W+B design. For a more extensive explanation regarding the use of a finite element approach and the differences between a linear and nonlinear approach, see Appendix C: Finite Element Approach.

From the results of the linear model of the original design, it can be observed that the wall is predominantly stressed in compression. Tensile stresses occur only at the lower part of the wall and the floor. The tensile stresses can be compared to the tensile strength of the concrete with quality B30/37. This tensile strength is only exceeded in the lower part of the wall and floor. This is thus the part of the structure that has to be reinforced.

The results of the original W+B design and the second alternative design (the design with a total thickness of 29m), see the first two images in Figure 7-1, illustrate that the wall itself will be stressed in tension only at the bottom and in the floor.

In the case of a thinner version of the wall such as the first alternative design, see the last image on the right in Figure 7-1, some tension will also occur also in the upper part of the wall. However, these tensile stresses will still not exceed the tensile strength of the concrete. So, if the total thickness of the wall exceeds a certain thickness, the extra amount of concrete is not required in order to resist the shear loading of the wall. Due to spreading of the forces as a result of the extra volume of concrete, the stresses in the different elements within the wall will decrease.

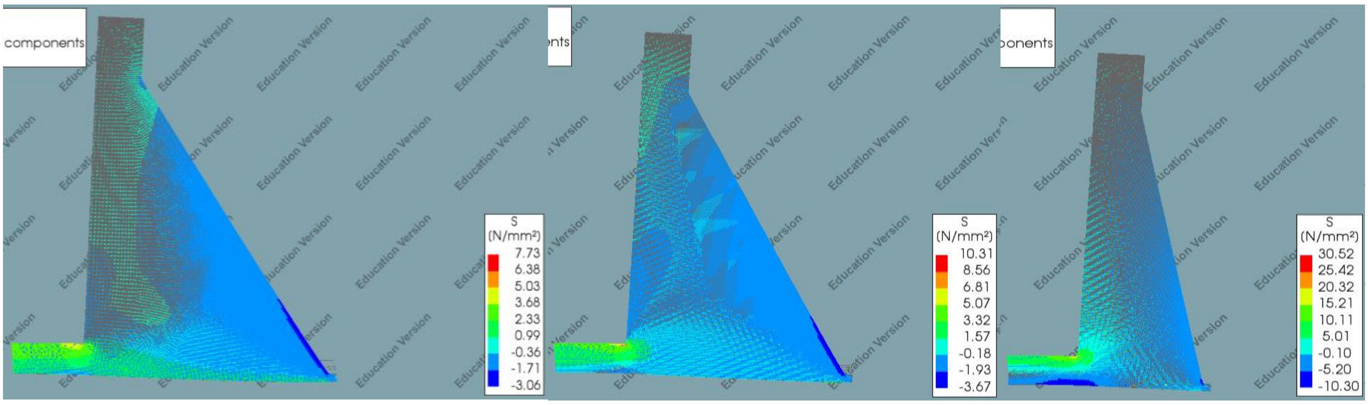

Figure 7-1 Principal stresses. From left to right: original design, alternative design 2 (d_{total}=29m), alternative design 1 (d_{total}=17m).

For all three designs, the 90° inner-angle between the wall and the floor is the most critical part when looking at the stresses (see Figure 7-2). The results also show that for all three models, the stresses in the floor exceed the tensile strength of the concrete which means that without reinforcement, this will lead to severe cracking of the floor, especially in the inner L-shaped angle.

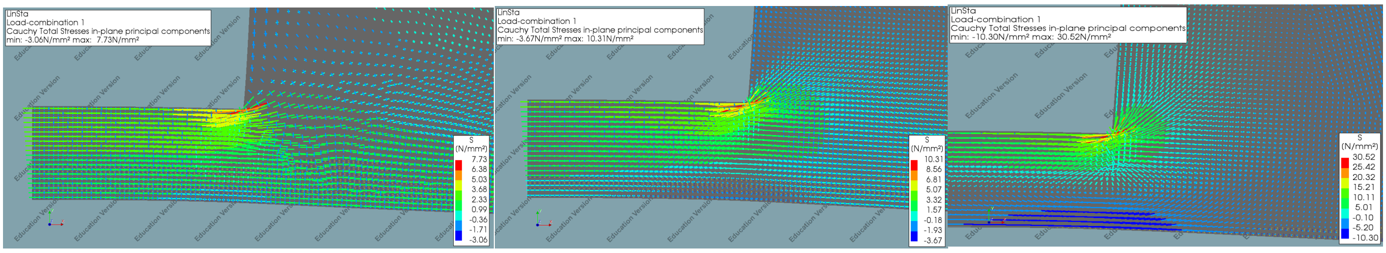

Figure 7-2 Zoom in on principal stresses in L-shaped corner. From left to right: original design, alternative design 2 (d_{total}=29m), alternative design 1 (d_{total}=17m).

Based on these results, a nonlinear model is used for the original design of the wall, where the bottom part of the wall and floor are reinforced in order to keep the maximum crack width below a value of 0.2mm as described by the norms. The results of this model also illustrate that the upper part of the wall is governed by compression and does not need to be reinforced to resist the shear loading, see Figure 7-3.

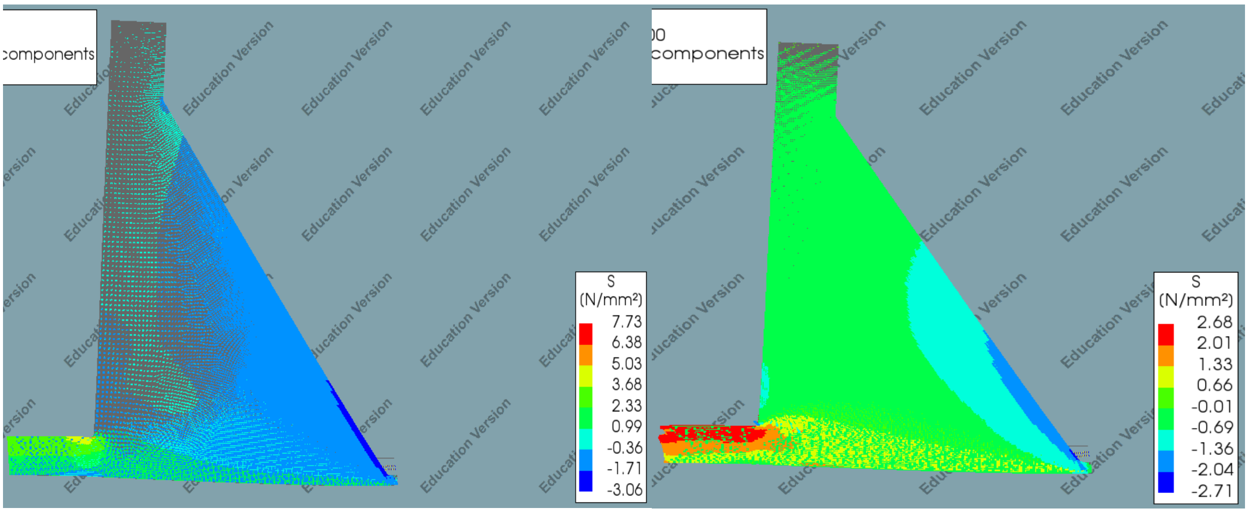

Figure 7-3 Principal stress original design W+B. Left: linear model. Right: nonlinear model.

An important notice is that in the linear models, the cracking of the concrete is not included. This means that the stresses will keep increasing which will not be the case in reality, because the exceedance of the tensile strength of the concrete would also lead to a reduction in concrete compressive strength in the cracking zone. This would especially be the case when large tensile strains occur in the direction perpendicular to the principal compressive direction.

7.4 Comparison Methods

As a result of the literature study, it was concluded that the first calculation method, the sectional method, is not applicable for the use in cases with larger structural elements. A one on one comparison between this method and the other two methods can therefore not be justified. This method is thus mainly used as a rough reference method.

Because both the Strut & Tie method and the finite element method are methods that can better be applied in cases of deep beams and other larger structural elements, the comparison between the results of these methods will be made for the Itaipu lock walls.

The first observation is that for the Strut & Tie approach on the original W+B design, the normal forces of the ties that are located higher up in the wall, are negligibly small. The orientation of the stresses from the linear DIANA model correspond to the orientation of the ties in the Strut & Tie model, as can be seen in Figure 7-4.

The principal stresses for the first alternative design (total thickness equal to 17m) have been compared to the orientation of the ties from the S&T approach. Even though the S&T method is performed for the original W+B design only and not for the other two alternative designs, the comparison will be made between the S&T results and the DIANA finite element results of the first alternative design. This first alternative design has the smallest wall thickness, and is therefore the design with the governing stresses when compared to the other two designs. The pattern and direction of the struts and ties for this first alternative wall design would be the same for the original W+B design, hence this comparison.

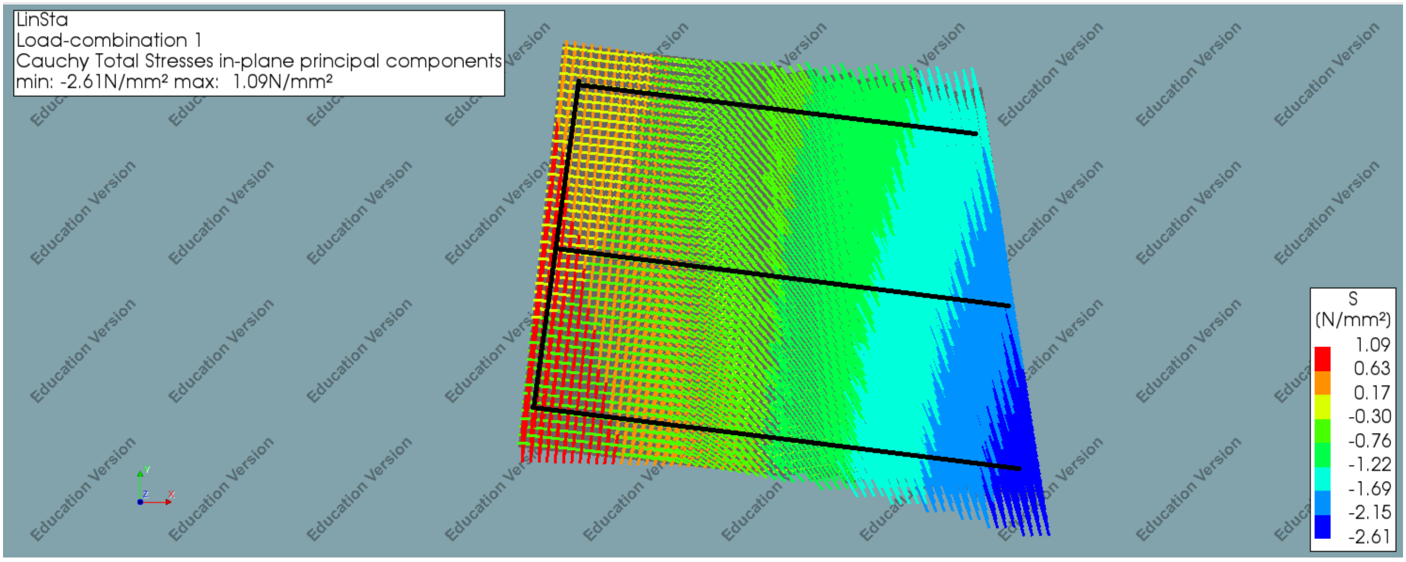

Figure 7-4 Comparison results linear DIANA model first alternative design with ties S&T approach original design

The principal stresses of the first alternative design show that the maximum stress is a vertical tensile stress parallel to the left edge of the wall and that perpendicular to these stresses, small horizontal stresses occur. In the more upper part of the wall, these horizontal stresses are tensile stresses and more downward these stresses are compressive stresses. So, the orientation of the ties are sufficient to transfer the tensile stresses in the concrete, given that these stresses would be larger than the tensile stress of the concrete, this being not the case in this situation.

The orientation of the struts form the Strut & Tie approach also corresponds to the compressive stresses in the DIANA model.

A comparison between the cross-sectional reinforcement forces (normal force reinforcement) of both the Strut & Tie results and the DIANA nonlinear results of the original W+B design, shows that the cross section forces in the ties from the Strut & Tie results are larger (see Figure 7-5).

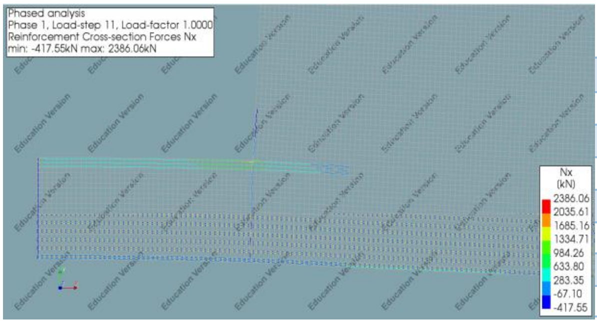

Tie	T/D	Nmax (kN)	Atie (mm²)	# ties
S16	T	105	241	1
S18	T	372	855	2
S20	T	1082	2487	4
S40	T	122	280	1
S41	T	492	1131	2
S78	T	9245	21253	27
S86	T	765	1759	3
S88	T	4445	10218	13

Figure 7-5 Reinforcement Cross-section Forces (Left DIANA and right Strut & Tie)

The reinforcement of the DIANA model is located mainly in the lock floor and in the connection area between the wall and floor, precisely the part that was not included in the Strut & Tie approach. Another limiting aspect of the Strut & Tie approach is that it does not allow for a thorough crack width calculation.

7.5 Aggregate interlock and the (Simplified) Modified Compression Field theory

The most important outcome of the literature study for this research is that the aggregate interlock plays an important role in the shear transfer and shear resistance in deep beams. In the case of the Itaipu lock walls, the aggregates will consist of much bigger aggregates than normally used for construction in the Netherlands. This is expected to have a significant effect on the aggregate interlock in the wall. The role of the aggregate interlock however, is not included in the three calculation methods: sectional method, S&T method and the finite element method. The first two methods normally do not include the composition of the concrete mixture and therefore also not the aggregate interlock as well. The input of the third method however, can be much more detailed than the other two methods. The wall can be modelled as extensive as is required but this requires the user to be more skilled in DIANA or a similar FEA software. Due to the time available for this research and the lack of experience with DIANA, the aggregate interlock mechanism is also not included in the finite element calculation performed in this research.

A quick check is performed in paragraph 6.4 with an equation from the modified compression field theory. This equation is used as a rough check whether the shear stress in a cracked element is allowable. This approach includes the aggregate size and is a small first step into including the effect of aggregate interlock in the calculations.

8 Conclusion

8.1 Research Sub-Questions

"Do the different norms provide adequate methods for shear calculation of walls in the same order of size as the Itaipu lock walls?"

A comparison between the different norms (EC2, ACI, etc.) highlights the difference between these methods and concludes that the EC2 has the highest estimation of the shear capacity. The ACI has the most conservative estimation (84%-96% of the EC2 value) and is therefore the 'most safe' of the considered norms. However, applied to beams that surpass the definition of a deep beam, the available norms do not provide an adequate estimation of the shear capacity anymore. The norms are based on empirical results that do not include large size members and more recent literature has proved that interpolation of these results do not fit the behavior of larger elements. A better analytical approach is the use of the (Simplified) Modified Compression Field Theory that approaches the shear resistance of larger beams more accurately.

"How does the size of aggregates in the concrete mixture influence the shear resistance of a concrete element?"

Aggregate interlock plays an important role in the shear capacity of deep beams and structure elements that surpass the definition of a deep beam in the order of element thickness. This aggregate interlock is related directly to the types of aggregates and the aggregate size. Previous research states that after an aggregate size of 25 mm, the added shear resistance as a result of this aggregate size cannot be predicted accurately anymore. The main limitation of previous research however is the use of only one aggregate type: limestone aggregates. Therefore, one question that needs to be asked is whether other stronger types of aggregates would lead to a different conclusion. As concluded by previous research (Sherwood, 2007), the effect of the aggregate size can also be ignored for a concrete compressive strength larger than 70 MPa. However, for larger strength aggregates, this is not expected to be the case. One way to check whether this conclusion is indeed correct would be to have a more detailed DIANA model in which the aggregate gradation and strength is included.

"What are the similarities and differences between the different methods used to determine the shear capacity of walls in the same order of size as the Itaipu lock walls?"

The sectional method falls into a different calculation category and is not applicable for calculations for deep beams. The main difference between the Strut & Tie method and the finite element method is that in the strut and tie approach, the loads are attached to specified nodes and these loads are also transferred to the subsoil to a set of specified nodes. However, the finite element model makes use of the entire cross sectional area of the wall to eventually transfer the loads to the subsoil. The strut and tie approach by definition will therefore lead to a more conservative design in theory. This is confirmed by the DIANA results. The Strut & Tie calculation resulted in a reinforcement layout over the entire area of the wall while the DIANA results proved that the reinforcement is only necessary at the bottom part of the wall.

8.2 Research Main Question

"Based on existing different methods of calculation, which method can best be used for concrete structure elements with increasing/large thickness?"

The Strut & Tie approach is a safe approach to be used as a quick first calculation. However, the disadvantage of this method is that it's not easy to determine the required thickness of a structural element with this method.

Because the linear finite element approach does not provide any insight in material behavior beyond the elastic stage, this approach is not sufficient and does not provide the necessary required insight for a shear resistance calculation. The nonlinear finite element model has proven to be the most accurate and adequate calculation method. The downside is that this method will take longer and requires more background information about the materials used, the connection between structural elements and the type of subsoil. The Strut & Tie approach, is therefore a good first design step when the designer does not have a lot of information of the material properties and the construction site yet. However, for a thorough tradeoff between wall thickness, the complex connection between the floor and the wall, and amount of reinforcement necessary to prevent cracking, the nonlinear finite element method gives the most accurate estimate.

From the calculation results, the conclusion is drawn that the current wall design by Witteveen+Bos is an overly conservative design. Decreasing the current total wall thickness and increasing the amount of reinforcement in the lock floor and the lower part of the wall connected to the lock floor, will also result in a safe design when studied in shear.

9 Recommendations

Based on the approach and results of this research, a few recommendations can be listed. These recommendations have to be taken into account considering that mostly due to time constrain, some simplifications had to be made. In future research, this can be more thoroughly analysed.

The recommendations are described per section in this chapter.

As concluded, the aggregate interlock plays an important role in the shear capacity of deep beams. It will be valuable to also model the composition of the concrete, and especially the aggregate gradation, in DIANA to reveal detailed results about the effect of increasing grain size on the shear capacity of structural elements in the same size range as the Itaipu lock walls.

The current Eurocode 2 will soon be renewed. Chapter 4 of this report focusses mainly on a approach as described by the current code. The literature part of this report also makes an comparison between the current Eurocode and other building norms. Part of the conclusion is that this norm does not predict the behaviour of deep beams well enough and aggregate interlock is not taken into account. It is therefore recommended to check whether the renewed version of the Eurocode does include this approach.

This research focusses mainly on shear force, neglecting other structural design checks such as stability, shrinkage of the concrete, the effect of environmental parameters and characteristics on the quality of the materials used, construction method, heath development in the concrete, etc. For the final design of the wall, the effect of these elements on the behaviour of a large structural element will also need to be further analysed.

For this research, the Strut & Tie approach was one of the methods used to determine the shear capacity in the original W+B design of the wall. A better approach would be to use the Strut & Tie model to also determine the required wall thickness in order to resist shear loading. This might be done by decreasing the wall thickness to a certain level, while maintaining the maximum allowable reinforcement ratio. Also, the Strut & Tie approach was only performed on the wall itself, ignoring the lock floor. A more accurate approach would be to include the lock floor. This would also mean that the comparison between the Strut & Tie approach and the finite element approach can be made more thoroughly.

The main result of this research is a better understanding of the stress trajectories within the wall. The next step would be to use this approach for a larger series of wall thicknesses so that the exact thicknesses for which the shear capacity is just sufficient can be found. This should preferably be done with the nonlinear approach instead of the linear one, so that the effect of reinforcement is also included in the analysis. A tradeoff can then be made between the amount of reinforcement and the total wall thickness, with a larger thickness resulting in a larger concrete volume and a smaller thickness in a smaller concrete volume.

The interface between the wall and the subsoil influences the results of the calculation considerably. It is therefore important that the correct characteristics are chosen for the interface. In this research, the characteristics chosen have been derived from previous projects. For a more detailed and accurate approach of the behavior of the wall, additional site research will have to be done to obtain the accurate interface characteristics.

Abbreviation List

- $V_{Rk,c}$ characteristic shear force capacity
- a distance from concentrated load to support
- ξ size effect coefficient
- ρ_l reinforcement ratio
- b_w web width
- d effective depth
- f_{ck} characteristic cylinder compressive strength of concrete
- V_{rm} mean shear force capacity
- f_{cm} mean cylinder compressive strength of concrete
- $V_{Rd,c}$ design value of shear force capacity
- k size effect coefficient
- σ_{cp} axial stress caused by loading or prestressing
- N_{Ed} axial force ($N_{Ed}>0$ for compression)
- A_c cross sectional area of concrete
- f_{cd} design cylinder compressive strength of concrete
- EC2 Eurocode 2
- ACI American Concrete Institution (Building Code Requirements for Structural Concrete)
- $\sqrt{f'_c}$ Square root of specified compressive strength of concrete (in psi)
- τ_{cr} Crack friction

Appendix A: Normal and shear stresses

The nominal shear force at failure can be converted into a nominal shear stress, the stress as a result of the force on a specific area. Two stresses can be defined on a cross section: a normal and a shear stress. Stresses are indicated with a double index, the first one referring to the cross section in which the stresses act and the second one referring to the direction of the stress.

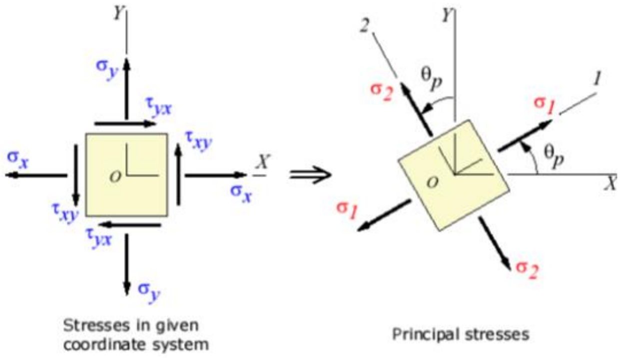

Figure 0-1 Principal Stresses for the case of Plane Stress (Miedema, S., 2001)

<u>Mohr's Circle</u>

With the rules of transformation, an analytical solution exists to determine how the components of the second order tensor in the x-y coordinate system change when this coordinate system is rotated over an angle α. The principal stresses are related to each other as follows:

$$k_{1,2} = \frac{1}{2}(k_{xx} + k_{yy}) \pm \sqrt{\left[\frac{1}{2}(k_{xx} - k_{yy})\right]^2 + k_{xy}^2}$$

$$(k = \sigma)$$

This transformation can be performed graphically with Mohr's circle.

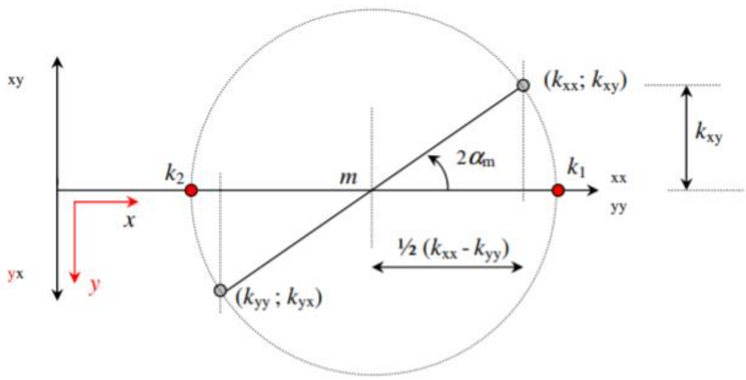

Figure 0-2 Mohr's Circle

<u>Failure</u>

With the knowledge of the definition of stress and strain and the relations between these characteristics, the kinematic relations, the failure mechanisms for linear elastic materials can be considered. Two common material based models are the failure model of von Mises and the failure model of Tresca. Both of these models require the stresses to be transferred to the principal stress situation, as explained above, using for example Mohr's method.

<u>Von Mises Failure Model</u>

The von Mises Model describes that the difference between the maximum and minimum principal stress, referred to as the deviator stress, is bounded. Failure will occur when this bounded value is exceeded. The failure criterium is the following:

$$\frac{1}{3}[(\sigma_1-\sigma_2)^2+(\sigma_2-\sigma_3)^2+(\sigma_3-\sigma_1)^2]\leq S_{max}^2$$

The constant S_{max} depends on the yield strength of the material and is based on an uniaxial tension test. The result of this test is the following equation for the maximum length of the deviator stress:

$$S_{max}^2=\frac{2}{3}f_y^2$$

Combining the two equations leads to:

$$\frac{1}{6}[(\sigma_1-\sigma_2)^2+(\sigma_2-\sigma_3)^2+(\sigma_3-\sigma_1)^2]\leq\frac{1}{3}f_y^2$$ **<u>Von Mises Criterion</u>**

This leads to the following illustrative representation of the von Mises criterion in the principal stress area.

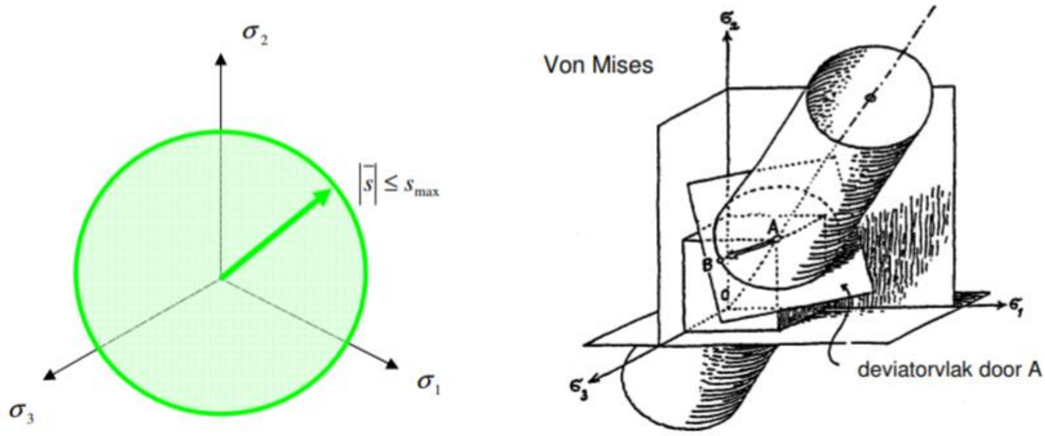

Figure 0-3 Von Mises Criterion

<u>Tresca Failure Model</u>

Tresca's model indicates that failure occurs when a maximum shear stress, c, in a material is exceeded. This maximum shear stress depends on the yield strength of the material as follows:

$$c=\frac{1}{2}f_y$$

In relation to the principal stresses, the following equations hold in the 3D coordinate system:

$$|\sigma_1-\sigma_2|\leq 2c$$

$$|\sigma_2-\sigma_3|\leq 2c$$

<u>Tresca's Criterion</u>

$$|\sigma_3-\sigma_1|\leq 2c$$

The principal stresses are not equal to zero and the largest circle, see figure below, is governing and will lead to the larges shear stress. This leads to the following illustrative representation of the von Mises criterion in the principal stress area.

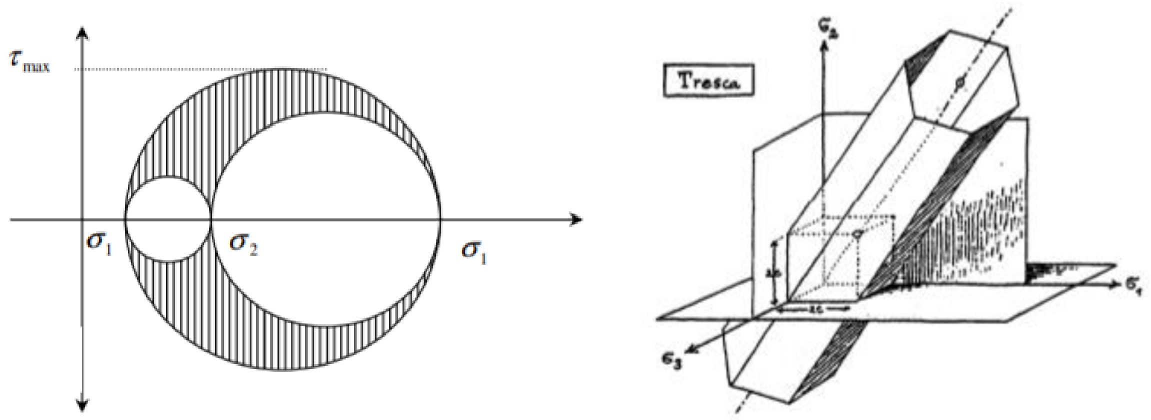

Figure 0-4 Tresca's Criterion

Tresca's hexagon fits perfectly in von Mises Circle.

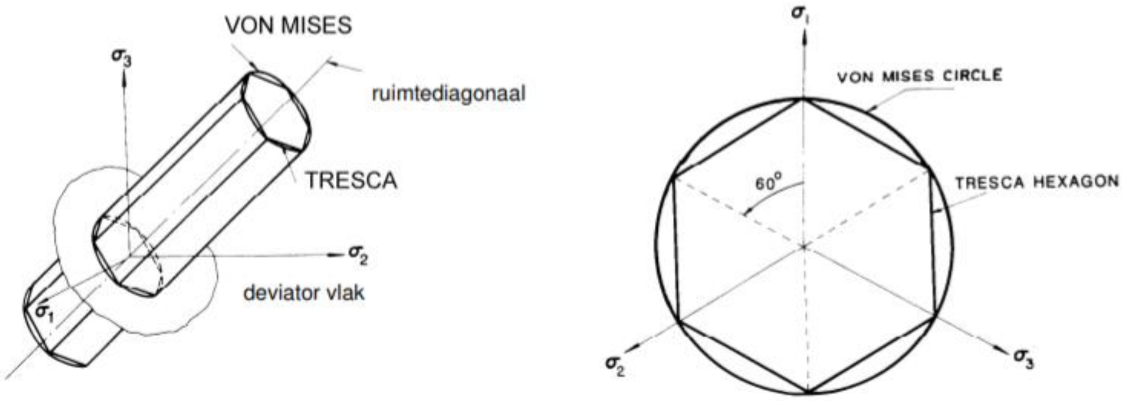

Figure 0-5 Von mises VS Tresca (left: 1-2-3 space & right: deviator space)

The failure models as described by Von Mises and Tresca are applicable for ductile materials. Because brittle materials and ductile materials fail in different ways, the same methods aren't applicable for both types of materials. For brittle materials, such as concrete, other failure models such as Mohr Coulomb is a better approach. These methods are however more complicated. Figure 0-6 Mohr-Coulomb Failure theoryshows the failure theory for Mohr Coulomb. As can be seen in this image, this method requires knowledge about the frictional and cohesive material properties.

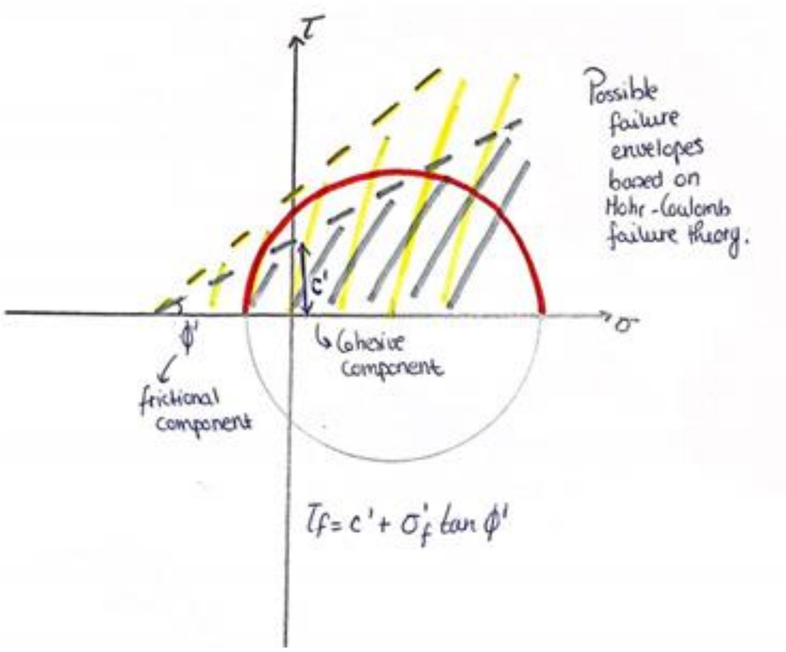

Figure 0-6 Mohr-Coulomb Failure theory

Appendix B: Cracks in Concrete

It is well known that the tensile strength of concrete is about ten times lower than its compressive strength. The reinforcement steel in concrete structures therefore has the function to bear the tensile forces. Loading a beam in bending will cause cracking. Cracking of a beam does not immediately mean failure. On the contrary, cracking of beams is a sign that the structure acts like we designed it to act. The tensile forces are transferred to the reinforcement.

Two main stages can be distinguished for the crack width. These stages have also been sketched in the figure below.

1. The first stage is indicated by number 2 in the graph: the crack formation stage. In this stage, the tensile force N is equal to the cracking force N_{cr} and the strain increases.
2. The second stage is indicated by number 3 in the graph: the stabilised cracking stage. In this stage, the strain and the tensile force N both increase and the crack width of the existing cracks formed in the previous stage increases. So, no the crack pattern is already developed and no new crack occurs.

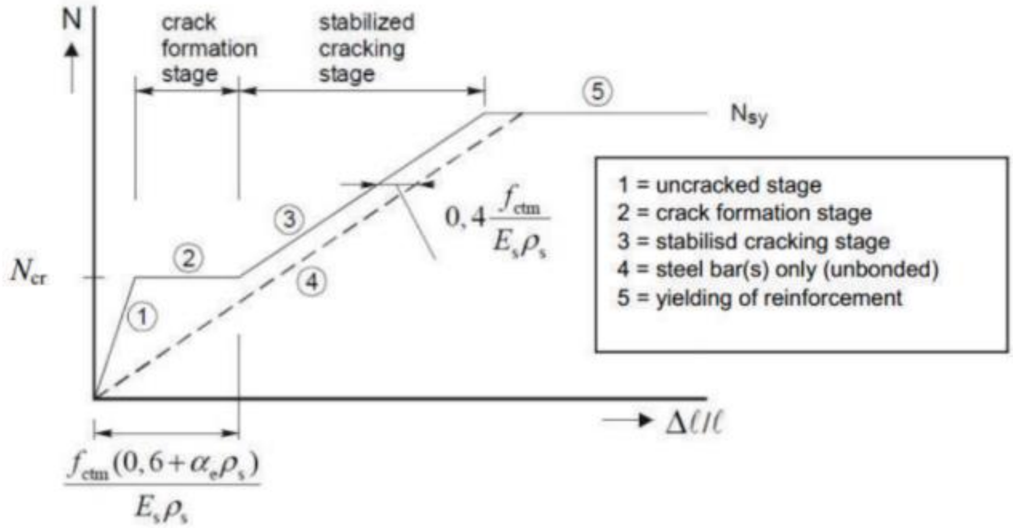

Figure 0-7 Force elongation diagram concrete

The result of cracks is that the compression zone of concrete decreases. A sufficient concrete cover is needed to protect the reinforcement against leakage due to cracks, especially for hydraulic structures. In the tropical weather, the humidity is 90%. The concrete cover should therefore be sufficient enough. This depends on the class of concrete that is used.

See Table 0-1 for maximum allowable crack width as described by the Eurocode 2. In the case of the Itaipu lock wall with reinforced concrete, the recommended maximum crack width is 0.3 mm.

Tabel 7.101N — Aanbevolen waarden voor w_{max} en van toepassing zijnde combinatieregels

Milieuklasse	Gewapende en voorgespannen elementen met voorspanning zonder aanhechting	Voorgespannen elementen met voorspanning met aanhechting
	Quasiblijvende belastingscombinatie	Frequente belastingscombinatie
X0, XC1	0,3 [a]	0,2
XC2, XC3, XC4	0,3	0,2 [b]
XD1, XD2, XD3, XS1, XS2, XS3		Decompressie

[a] Voor de milieuklassen X0 en XC1 heeft de scheurwijdte geen invloed op de duurzaamheid; deze grens is gesteld om een in het algemeen aanvaardbaar uiterlijk te verkrijgen. Bij afwezigheid van voorwaarden ten aanzien van het uiterlijk, mag deze beperking worden afgezwakt.

[b] Voor deze milieuklassen behoort, aanvullend, decompressie onder de quasiblijvende belastingscombinatie te zijn gecontroleerd.

Table 0-1 Eurocode Table 7.101N Maximum allowable crack width

Appendix C: Finite Element Approach

Finite element analysis is being used for different engineering applications but is mostly known for its applications in heat transfer and flow of liquids. This method is also a good solution for problems that become too complex to solve by hand, such as the flow of forces in structures with designs that deviate from the basic Euler-Bernoulli beam design. The FEM approach can be subdivided into a linear FEM (LFEM) approach or a non-linear FEM approach.

LFEA is often used in design. Stresses in an element can be mapped by performing a linear elastic static analysis. The use of material and thereby the design can then be based on these results.
The non-linear FEA is a more mature approach and reveals stress redistributions and capacity beyond elastic design stage. This approach is used for yielding of materials, cracks and instability problems.

FEM is used to solve complex problems, so for example for varying cross sections and therefore non-uniform stresses. The mechanical model will then exist of various sections/regions with a uniform cross section and the reality is approached less accurately. FEM composes the structure out of fine parts for which the force and displacement relationship is known, so also the stresses and strains, and the structure is then discretized. Then information about how the entire structure deforms is obtained. An finite element approach contains two steps: idealization in the mechanical model and discretization of space in FEM. The preprocessing and the postprocessing are done by the user.

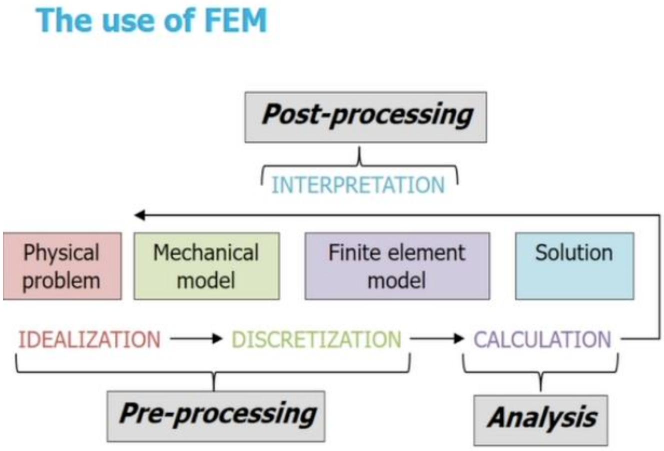

Figure 0-8 Use of FEM

It is possible to have either a contour plot or a vector plot as output. The advantage of the latter one is that it is also possible to see the trajectory of the stresses. Typically the displacements are continuous over an element boundary but the stress and strain are discontinuous.

There's a big range of FEM software used in the field of engineering. In Civil engineering, three commonly used software programs are: PLAXIS, DIANA and SCIA Engineer. PLAXIS is good tool to model soil-structure interaction and provide a FEM calculation for stresses and deformations. This software mainly focusses on the soil behavior and requires the user to understand the processes inside the soil during the different phases of construction. DIANA is a more multipurpose software with applications in the structural field as well as dynamics, heat flow or flow of fluids such as groundwater flow. Also the fluid structure interactions can be modeled with this software. Engineer is a more specialized software for the use in the structural field.

The finite element approach provides a general mechanical solution for complex problems and to know how a variable varies in its space. For a displacement based FEM, the primary unknown variables are the displacements (& rotations) and the relation between the displacements, rotations and the forces & moments is studied.

Every Finite Element is treated as a small piece of the structure and for this small piece the relation between displacements & forces and strains & stresses is known. This small piece is used to discretize the entire body and to find out the displacement field of the complex body.

For every element, the exact solution in only 2 parts is known: the nodes. Along the element, a simple variability of the displacement exists: the interpolation function of the displacement field. Every displacement along the element varies based on this function. For a quadratic interpolation more nodes are necessary.

In the nodes of the element, certain displacements are imposed and then the strength is calculated. Another quantity that describes the element are the integration points within the element. In the nodes the displacements are given and in the integration points the strains and stresses are calculated. Compatibility elements are needed to have a continuous displacement field.

The strain in the integration points is calculated in two steps:

- From displacements in the nodes to the integration points
- In the integration points: differentiate and find the strength

The process from the nodes to the integration points is called interpolation. The stresses in the integration point are calculated from the strain by using the constitutive law. So, the displacement and force inside the nodes are known and the stresses and strains inside the integration points are known. Forces in the integration points are calculated by integrating & extrapolating again from integration point to nodes.

The system has to be in equilibrium. This can be checked once the internal forces are calculated. All the elements are assembled and in every node the sum of the forces given by every element have to be in equilibrium with the external forces. If this is the case, the assumption of the displacement field was correct. In a non-linear situation, the software keeps looping for the equilibrium. If the user would need to guess a new displacement field, the program estimates a new element stiffness to guess the new displacement field.

Appendix D: Navigation Locks

Molenaar (2011) describes that the main function of navigation locks is to allow ship navigation from two sections of a waterway with different water levels. The functions of a lock are the following:

- Allow Ship navigation trough the lock (main, operational)
- Water retaining function (main)
- Water management function (main)
- Operating a filling and emptying system (operational)
- Allowing maintenance of the lock (operational)
- Role in the protection of the river/waterway

The design of a lock depends on different factors such as:

- CEMT ship class
- Hawser Forces
- Water level (indicating Top of Structure and Bottom of Structure)
- Water level difference
- Intensity of vessel traffic
- Type of filling and emptying system

In order to be able to fulfil these functions, the navigation lock consists of different elements. The main elements of a navigation lock are indicated in the image below:

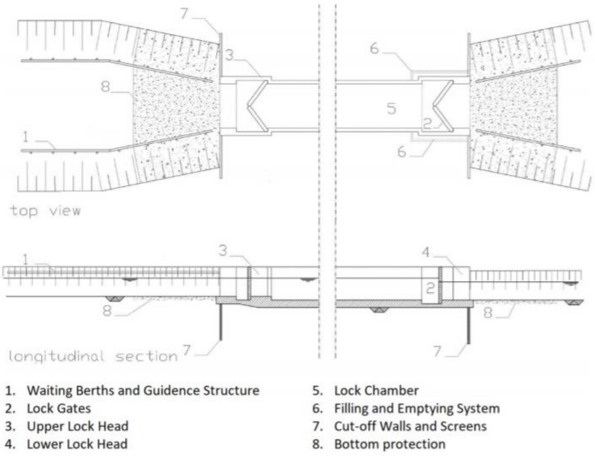

Figure 0-9 Elements Navigation Lock. (Olst,van B.,2019)

The schematization of the wall depends on how the wall is connected to the floor. There are different types of combinations and variations for the walls and floor of a lock chamber. The figure below gives an overview of the standard combinations and element variations.

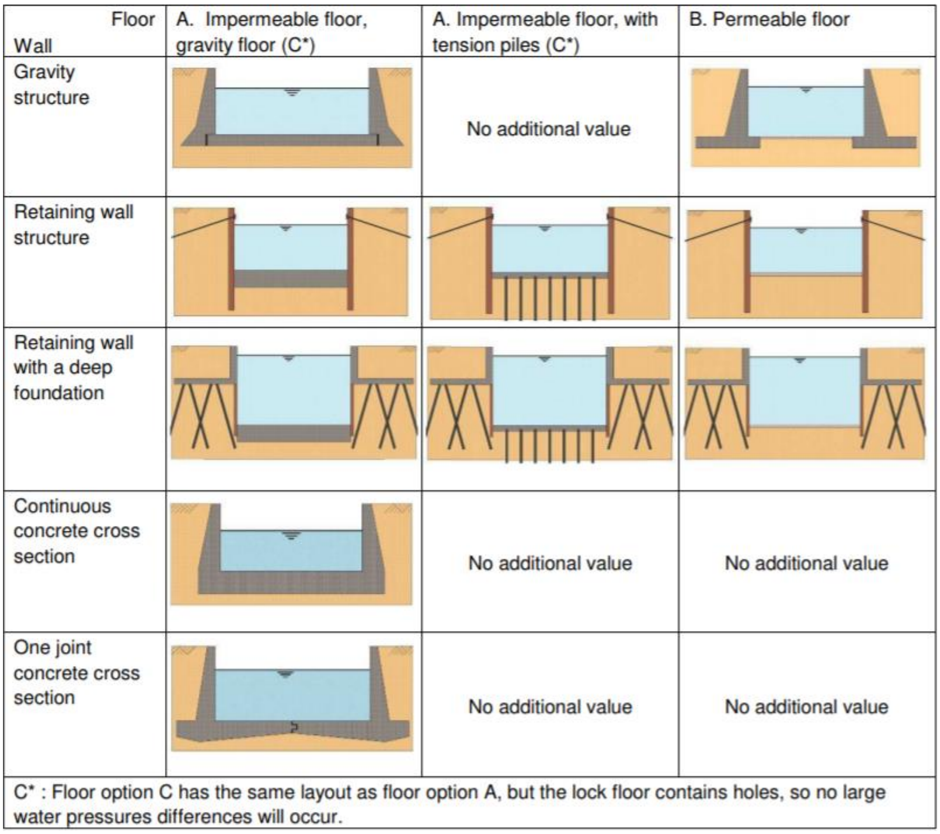

Floor / Wall	A. Impermeable floor, gravity floor (C*)	A. Impermeable floor, with tension piles (C*)	B. Permeable floor
Gravity structure		No additional value	
Retaining wall structure			
Retaining wall with a deep foundation			
Continuous concrete cross section		No additional value	No additional value
One joint concrete cross section		No additional value	No additional value
C* : Floor option C has the same layout as floor option A, but the lock floor contains holes, so no large water pressures differences will occur.			

Figure 0-10 Wall Floor Combination Lock Chamber. Source: W, Molenaar (2011)

The wall itself has its own set of functions. As can be seen in the image above, one of the functions of a lock wall is the retaining function. The wall has to retain the water inside the lock and the soil and groundwater outside the lock.

Typical loads acting on a lock wall having impact on the design, dimensions and stability of the wall are presented:

- ***Dead loads*** due to weight of structure and permanent equipment weight
- ***Horizontal earth pressures*** due to the self-weight and internal angle of friction of the soil and possible live loads next to the wall.
- ***Hydrostatic pressures (horizontal and vertical)*** from the water inside the lock chamber and the groundwater pressure on the soil side of the wall.
- ***Seismic loads*** due to earthquakes resulting in a dynamic horizontal soil pressure on the wall.

Appendix E: Complete Chapter: Verification Shear Resistance using a Finite Element Calculation

Disclaimer: This appendix contains a more detailed description of the finite element calculation and the achieved results. In chapter 6, these results are summarized.

The third method that is used to perform calculations regarding shear loading in the Itaipu lock walls is a finite element calculation using the software: 'DIANA FEA'. Both a linear and a non-linear model have been used in order to achieve the desired output. Both models are plane stress models instead of plane strain models. In the case of this lock wall, with a large length (out of plane direction), it would be more suitable to make use of a plane strain model. However, this raised some issues with the correct modelling of the reinforcement of the nonlinear model. Therefore, the choice has been made to use a plane stress model instead for both the linear and nonlinear models. The results of this decision is that the model will give zero stresses in the out of plane z direction while in real life this is not the case. However, for the 2D analysis in the x-y plane, this tradeoff does not affect the results.

First, the linear 2D model of the wall and the part of the floor that is attached to the wall is set up. The symmetry of the other half of the wall and floor is included in the model. The two geometry components of this model are the concrete part and an interface part. The interface represents the basalt subsoil and has a stiffness in vertical y direction (direction parallel to the self-weight/gravity) equal to the bedding constant of the basalt (50 MN/m^3). The bedding constant is a parameter which is determined by the Young's modulus of the material. In addition, the interface also has a shear stiffness in the horizontal x direction for which 1/100 of the stiffness in the y direction is taken as a rule of thumb, so 0.5 MN/m^3. The actual value of the shear stiffness is hard to precisely determine. The decision has therefore been made to model the stiffness in such a way that the stiffness is relatively low and it is assumed that the wall can shear off. This means that the friction is negligible compared to the large normal force originating from the self-weight of the wall.

Using a structural linear static analysis, the displacements and stresses in the wall & floor are calculated. Subsequently, the thickness of the wall is varied in this model and the results (displacements and stresses) will be displayed for different wall thicknesses. Based on the linear model, it can be concluded where the stresses are exceeded above a certain "failure" level.

In the nonlinear model, both concrete and reinforcement are modelled with non-linear material properties. The interface is the same as in the linear model. The first is the model of the current geometry of the wall and floor as designed / conceived by Witteveen+Bos. And the second model is includes the geometry with the thickness that is proposed as the optimal thickness where the wall still has sufficient shear capacity, derived from the results of the linear model. The added value of the non-linear model is to focus on the locations where it can be seen in the linear model that a certain limit value of stresses is exceeded. In the non-linear model, the structure can also be reinforced in such a way to assure a certain stress path.

The out of plane z direction is modelled to be 1m for both models. This means that the wall, floor and interface have a DIANA thickness[2] of 1m.

[2] This thickness differs from the use of the term thickness in this report. The thickness mentioned here is the dimension as defined by DIANA FEA, corresponding to the dimension 'width' (dimension out of plane; perpendicular to the thickness dimension used in this report). Note that this dimension will be referred to as DIANA thickness in the remainder of this report.

Linear Model

The current design of the Itaipu locks is translated into a 2D linear model.

Geometry

The model consists of one regular plane stress concrete element for the wall and the floor with the following material characteristics:

- Young's modulus: 30 MPa (C30/37)
- Poisson's ratio: 0.2
- Mass density: 2400 kg/m^3

The subsoil is modeled as a boundary interface with the following characteristics:

- Type: 2D line interface
- Normal stiffness modulus-y: 50 MN/m^3
- Normal stiffness modulus-x: 0.5 MN/m^3

The thickness for the wall+floor geometry and the interface is 1m.

Supports

The interface of the wall and floor are supported in both the x- and y-direction. And the floor is supported in only the x-direction to indicate the symmetry of the wall+floor.

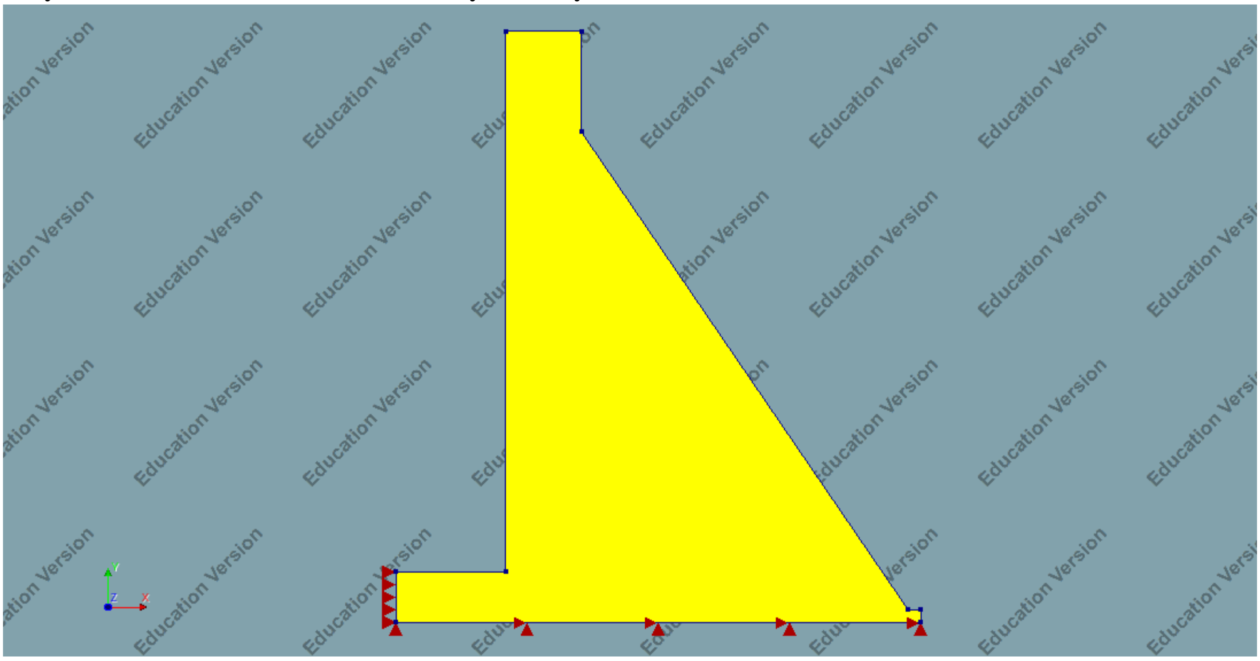

Figure 0-11 Supports

Loading

The loads consist of:

- Self-weight of the concrete
- Horizontal hydrostatic pressure on the wall (43m) and the vertical component of the hydrostatic pressure on the floor.

The analysis is performed with only 1 load combination where both loads act with a load factor of 1.0 simultaneously.

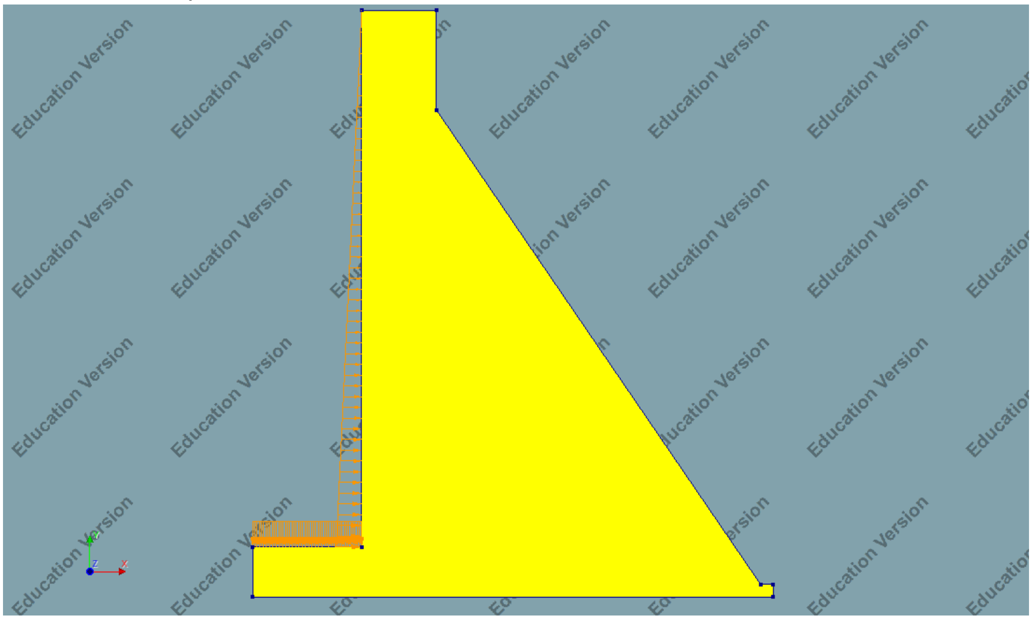

Figure 0-12 Loading

Mesh

A mesh is applied with an element size of 200mm over the entire shape of the wall+floor.

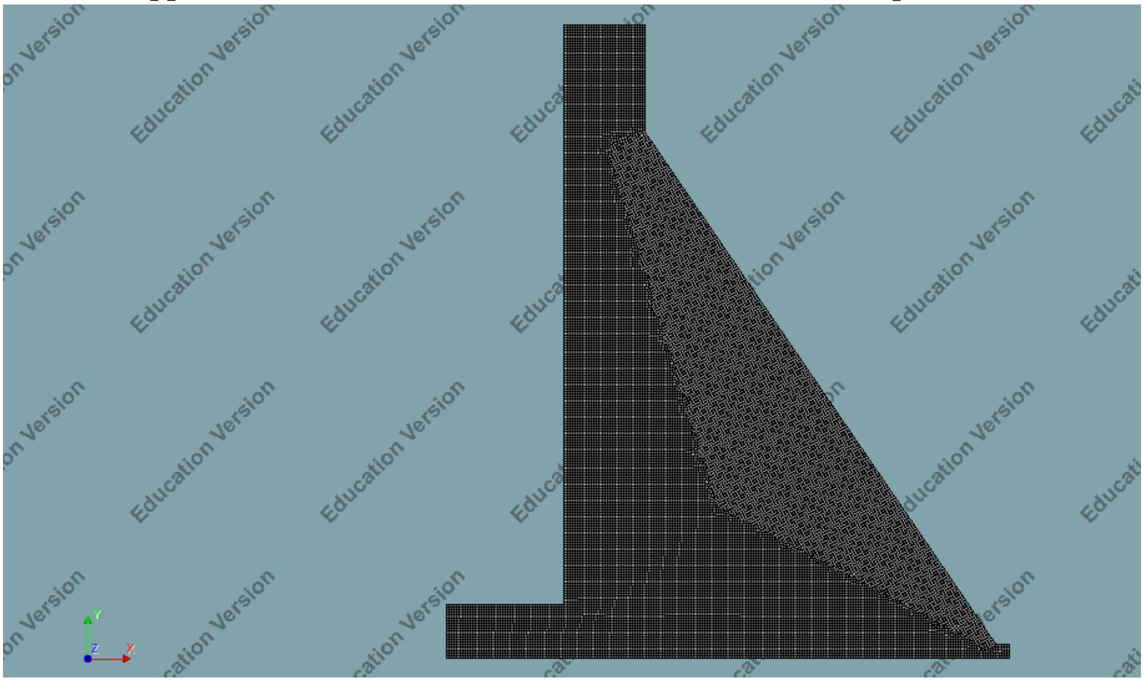

Figure 0-13 Mesh

Analysis

The type of analysis performed is a structural linear static analysis.

Results linear model original design

The results of the analysis are shown in contour plots. Note that for some of the contour plots, the maximum and minimum values are adjusted in order to prevent the plot being highly influenced by peak values. The actual maximum and minimum values can be seen in the description box in the top of each plot.

Displacements

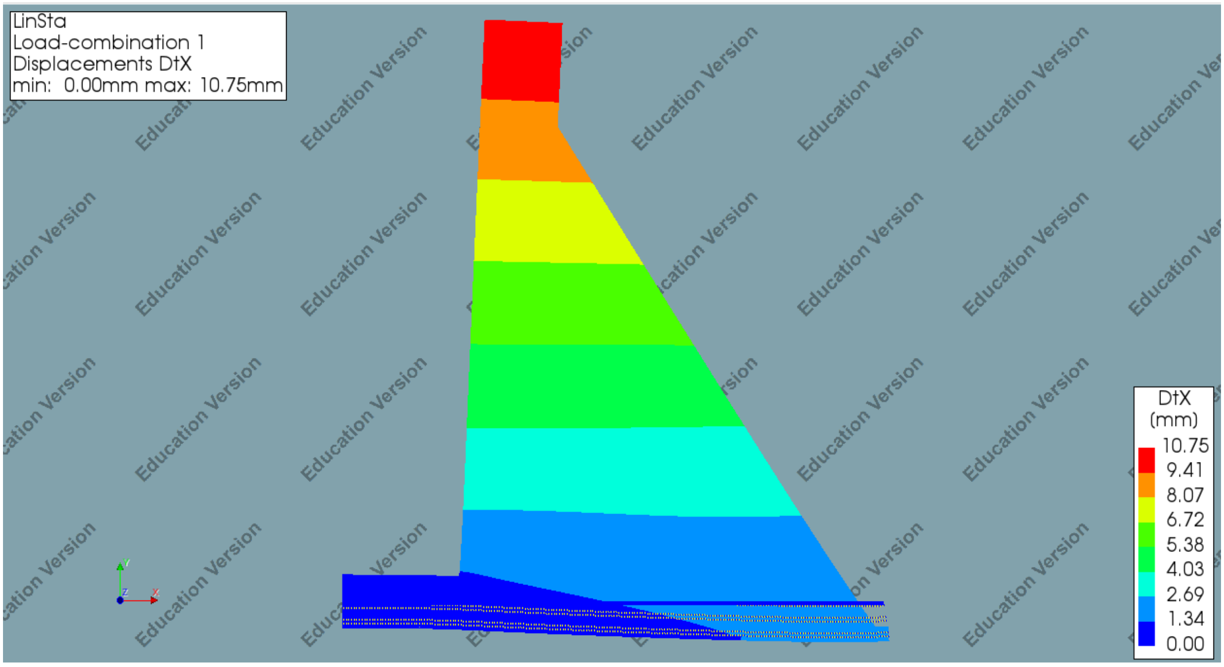

Figure 0-14 Displacement x-direction linear model original design

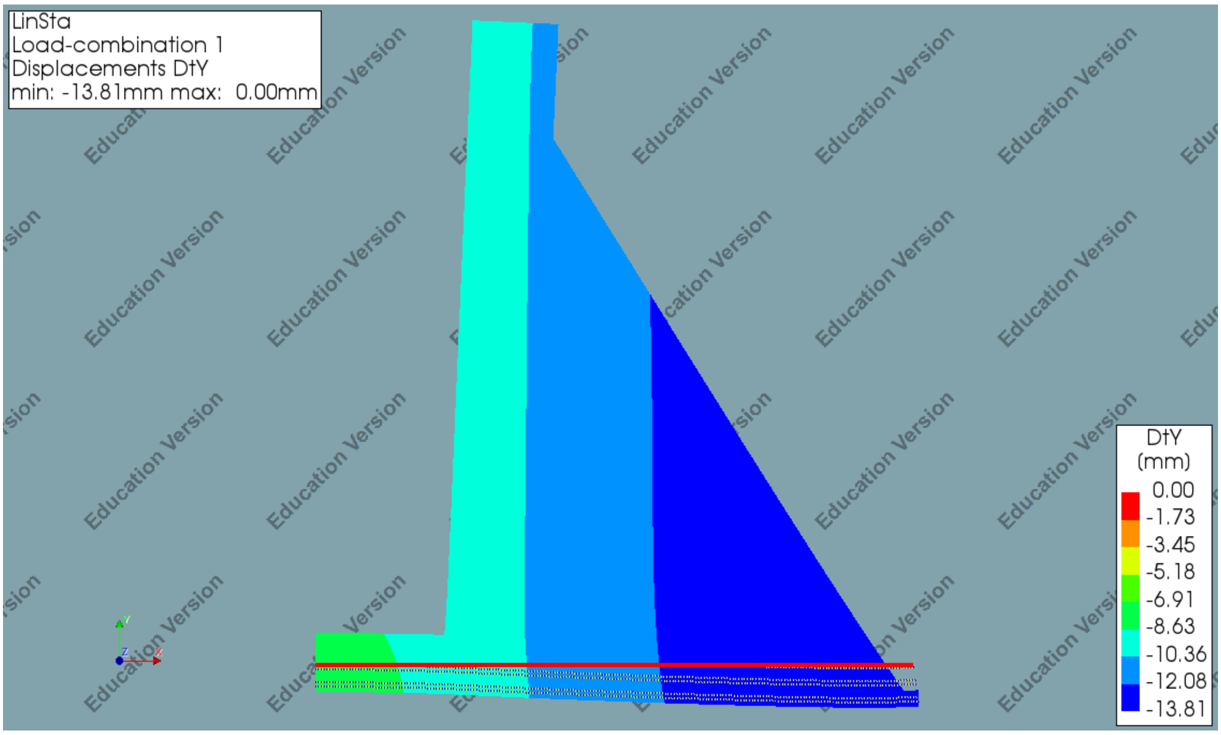

Figure 0-15 Displacement y-direction linear model original design

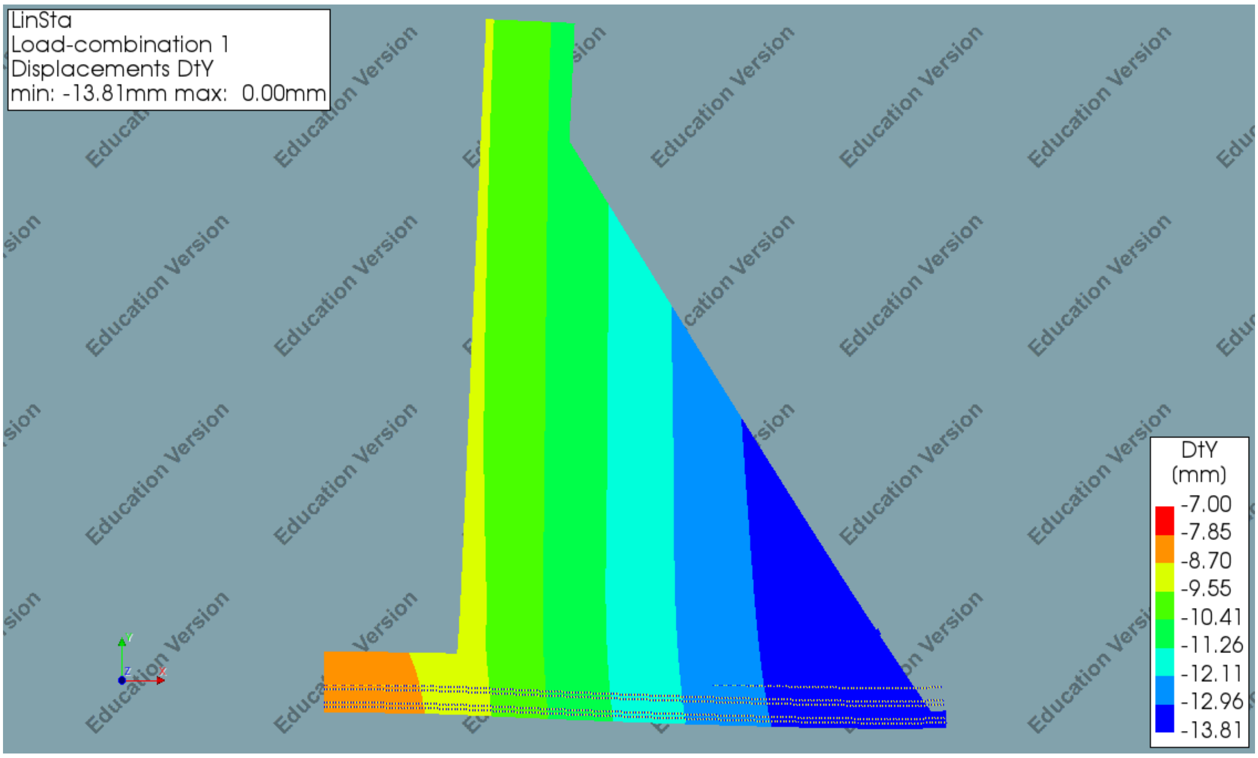

Figure 0-16 Adjusted view displacement y-direction linear model original design

Results Interface Relative Displacements

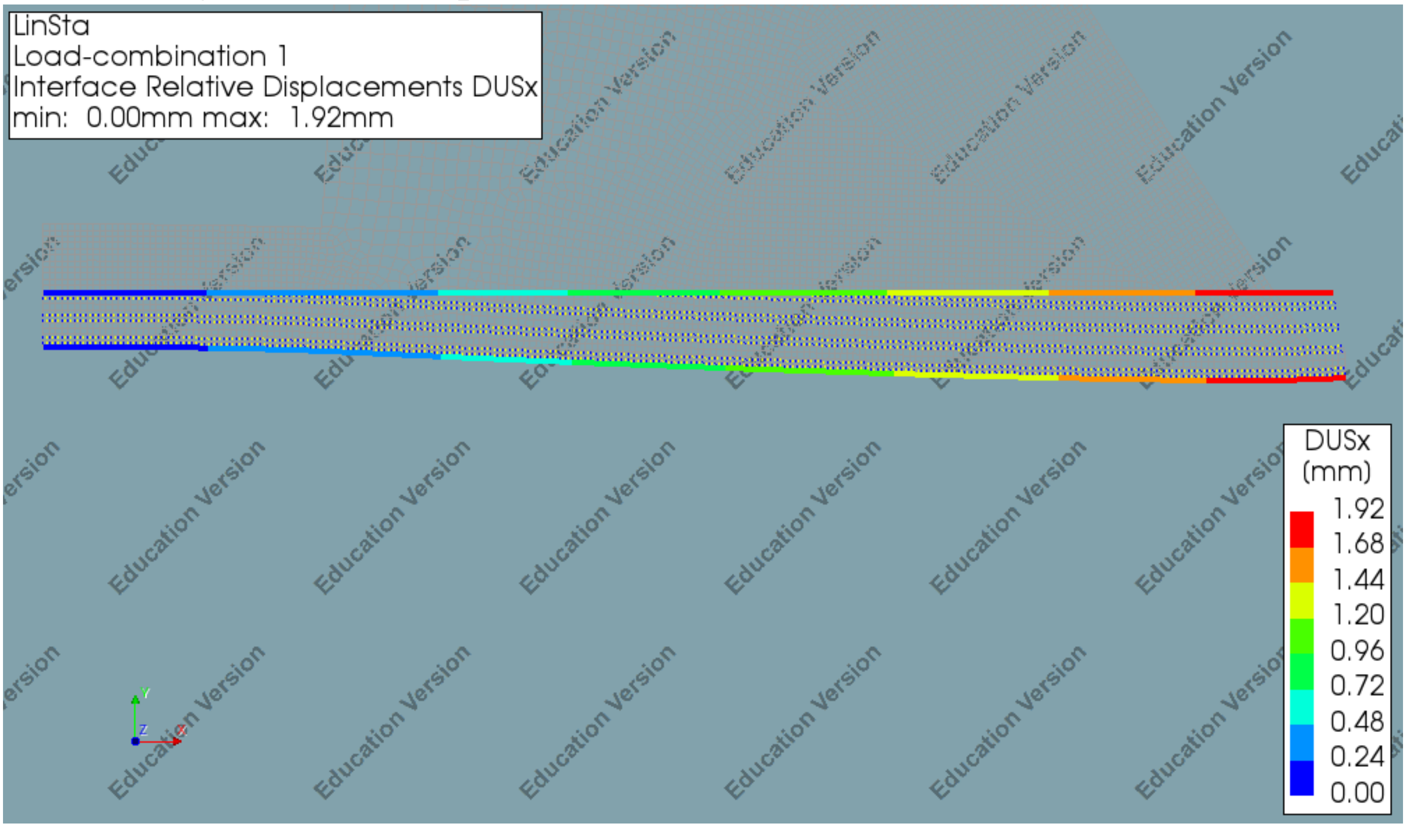

Figure 0-17 Interface relative displacements x-direction linear model original design

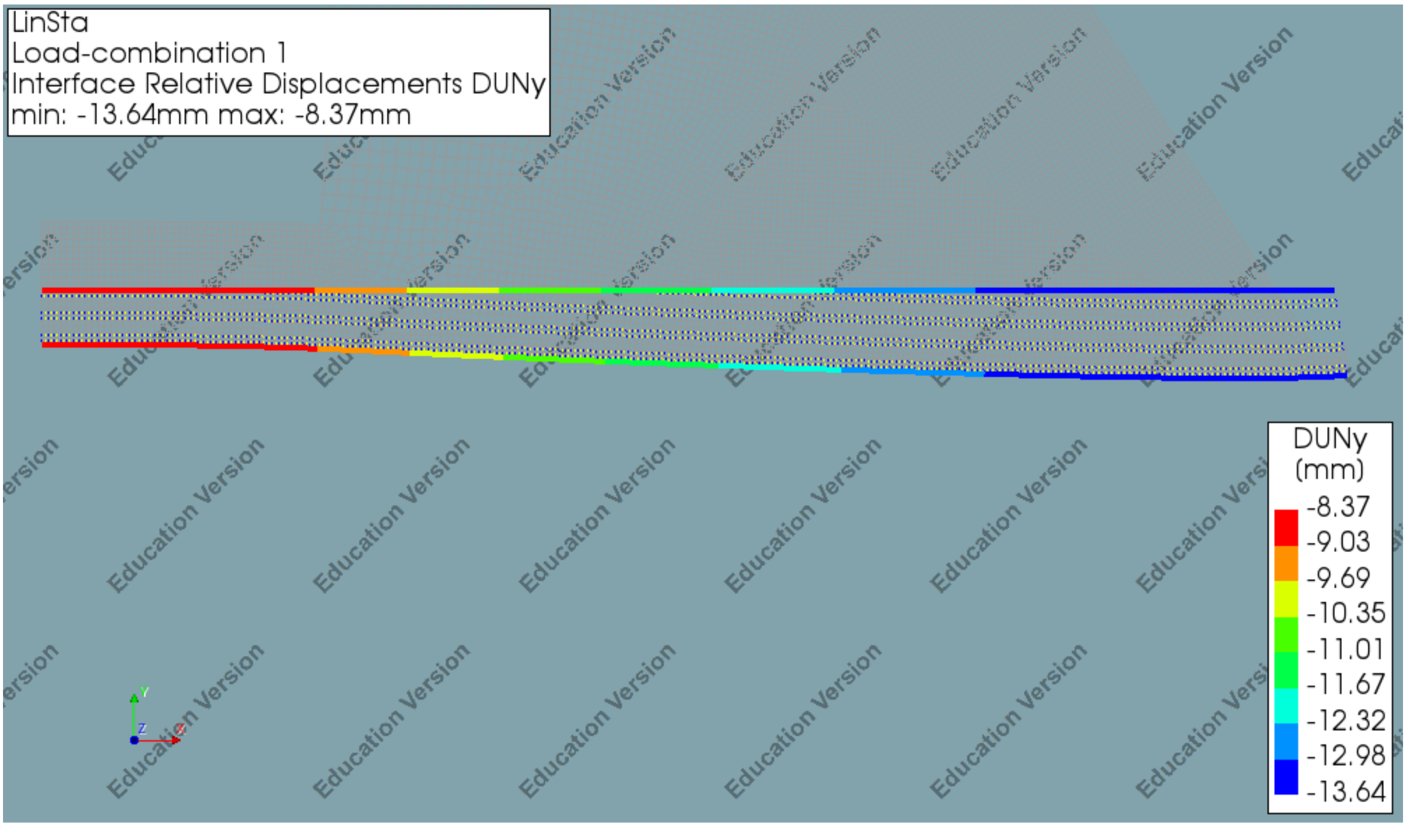

Figure 0-18 Interface relative displacements y-direction linear model original design

Results Stresses

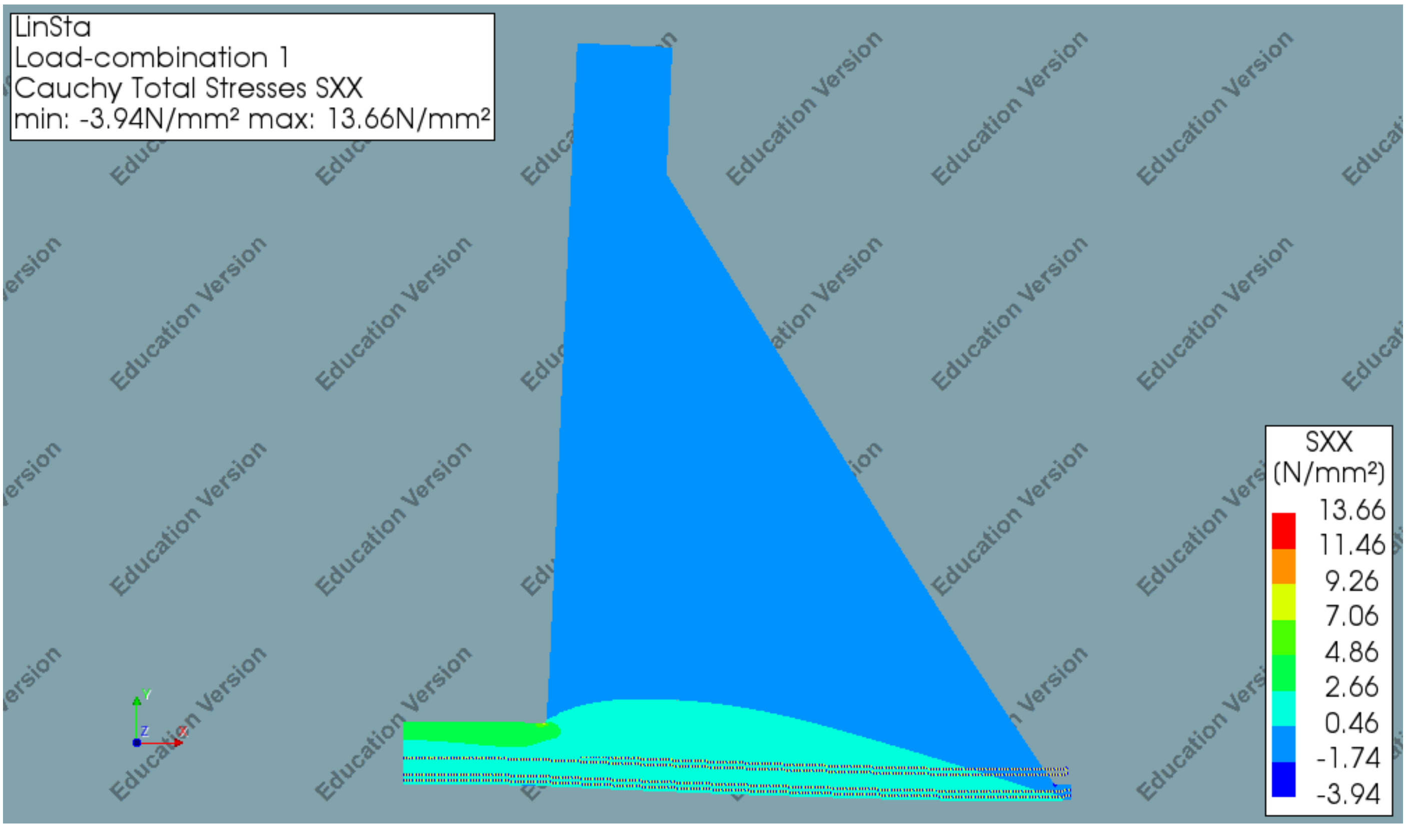

Figure 0-19 Cauchy total stresses SXX linear model original design

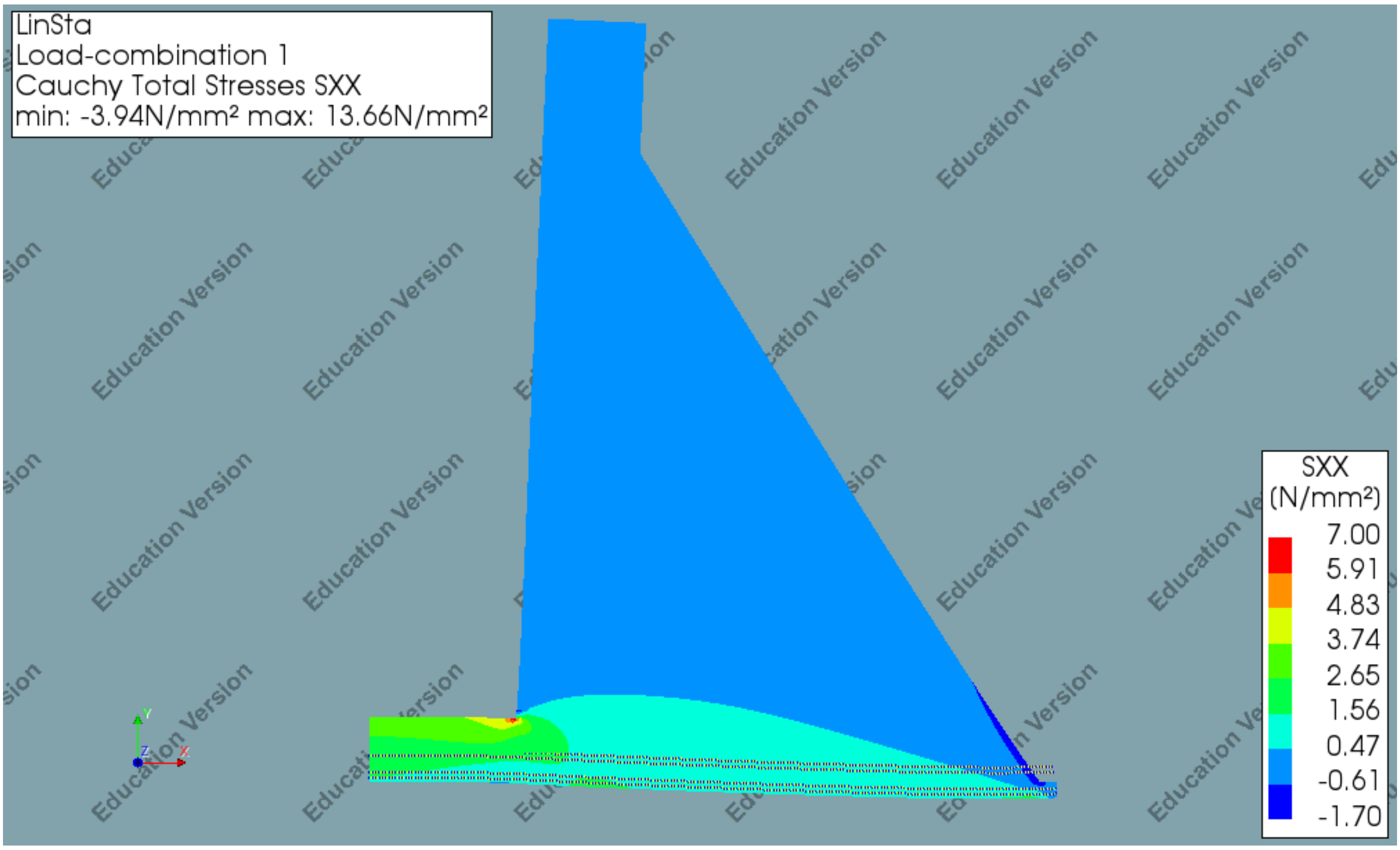

Figure 0-20 Adjusted view Cauchy total stresses SXX linear model original design

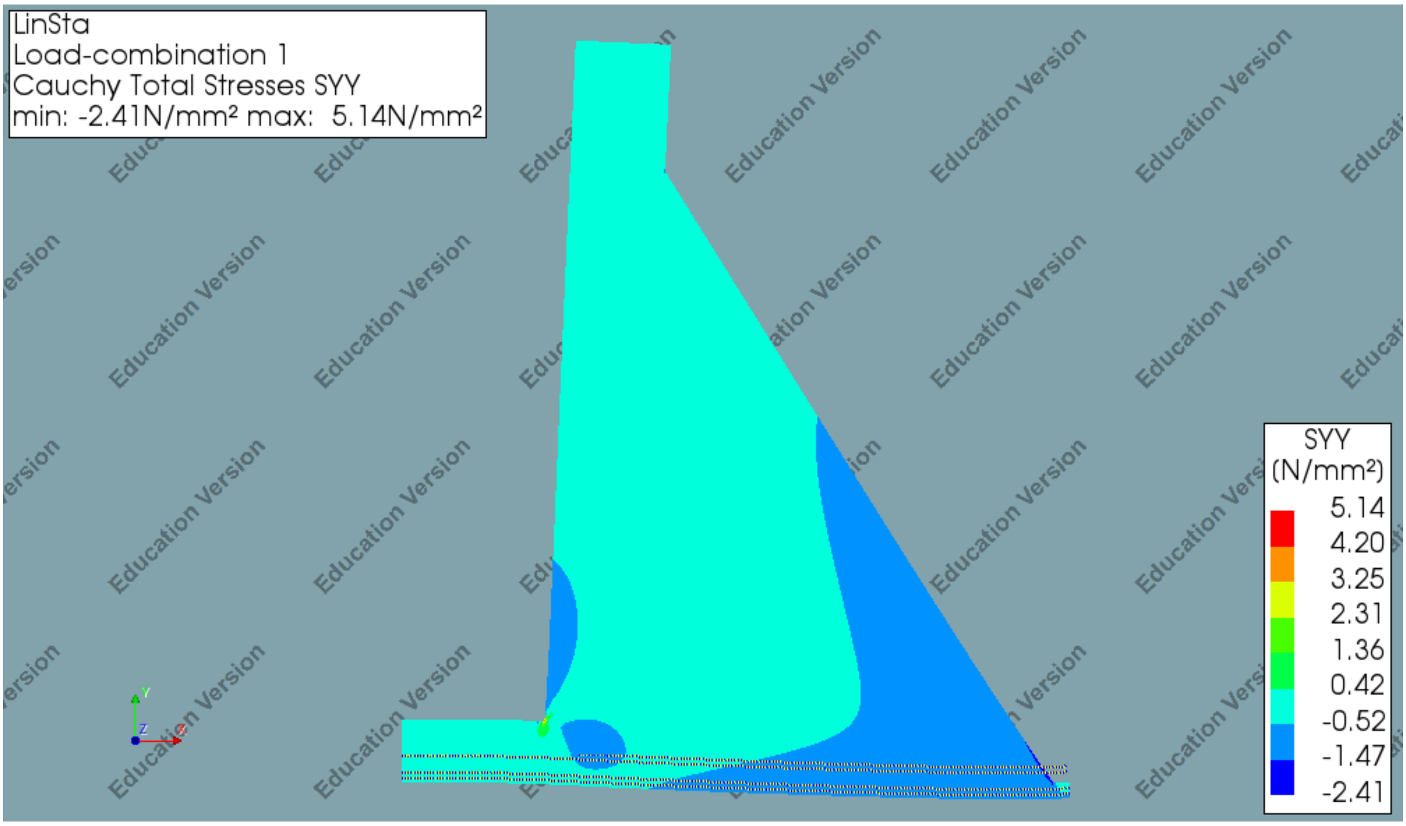

Figure 0-21 Cauchy total stresses SYY linear model original design

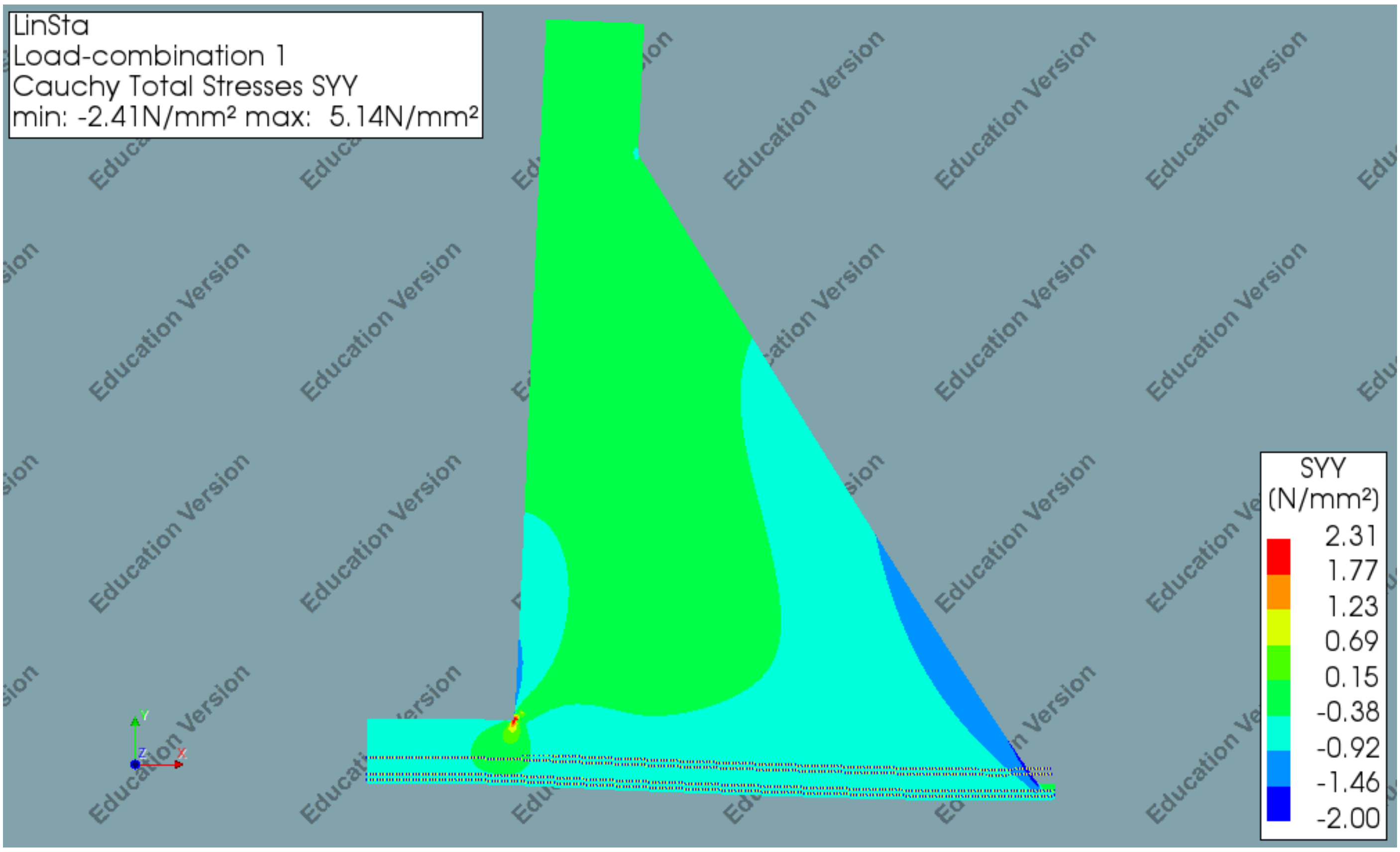

Figure 0-22 Adjusted view Cauchy total stresses SYY linear model original design

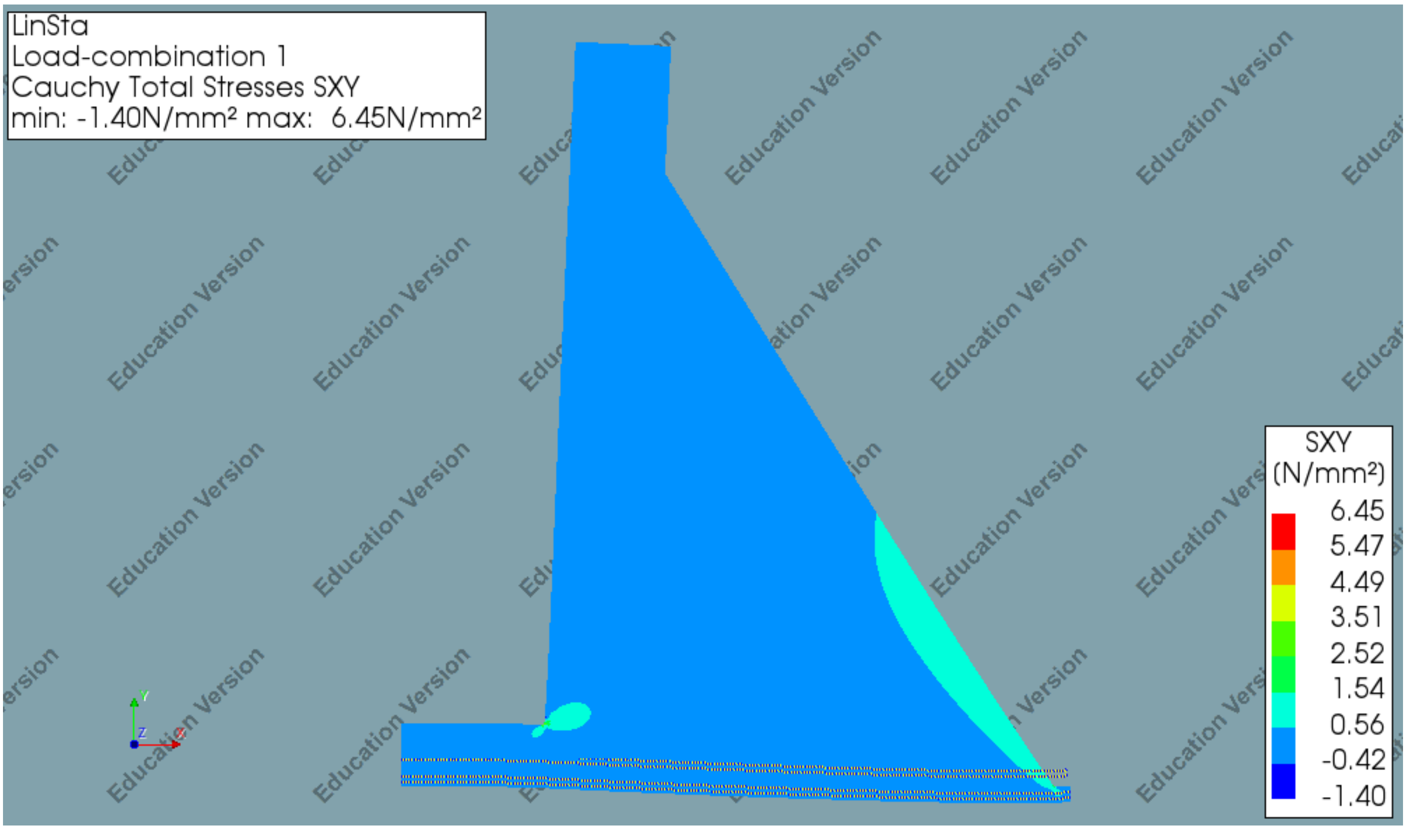

Figure 0-23 Cauchy total stresses SXY linear model original design

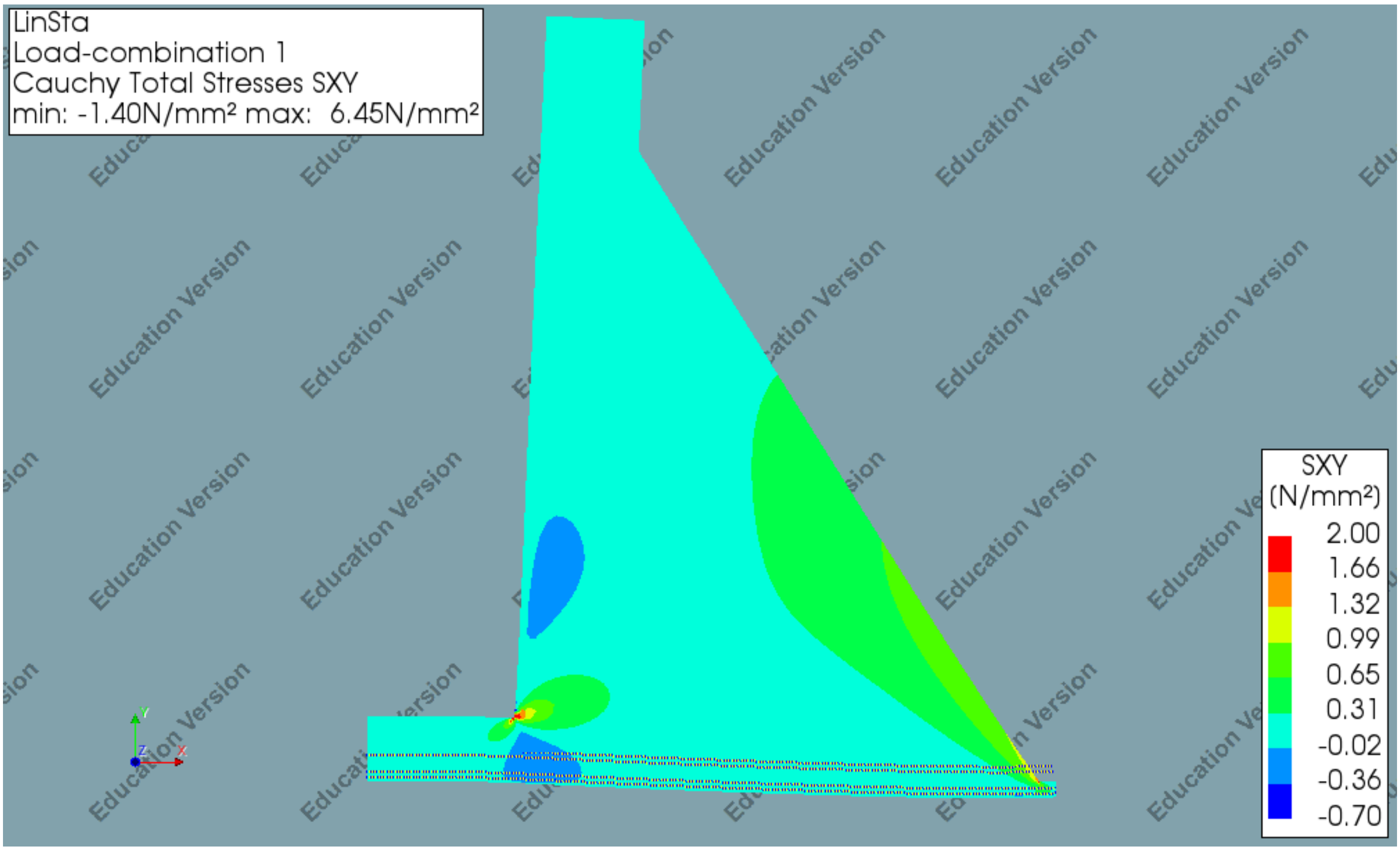

Figure 0-24 Adjusted view Cauchy total stresses SXY linear model original design

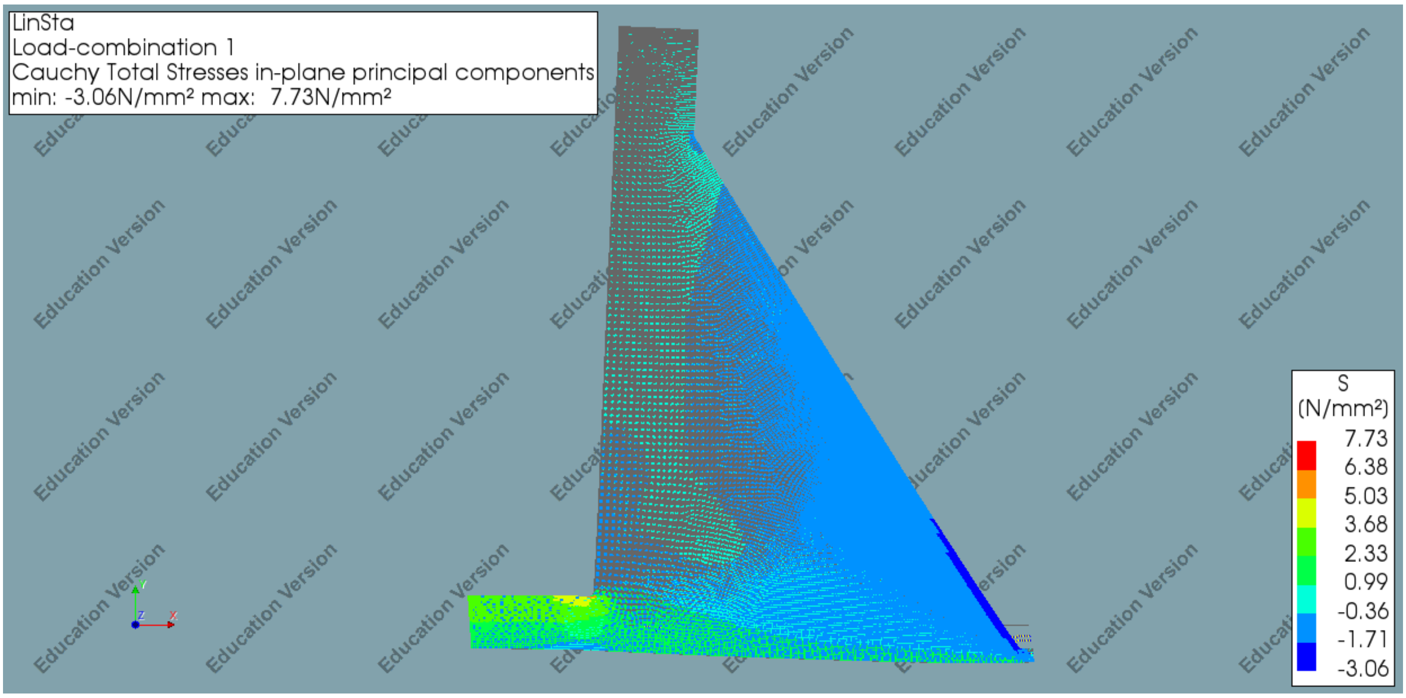

Figure 0-25 Principal stresses linear model original design

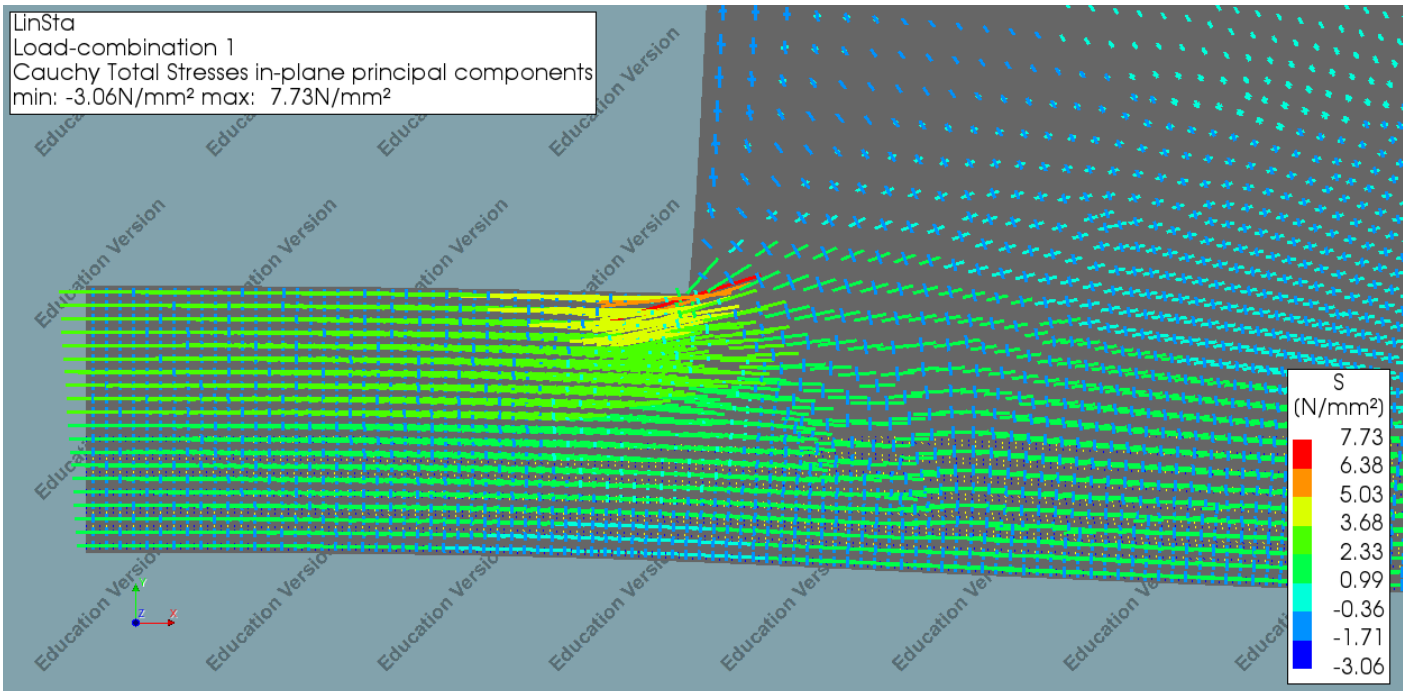

Figure 0-26 Zoom in on Principal stresses linear model original design

Decreasing wall thickness Linear Model

Results second alternative design: total wall thickness = 29m

Displacements

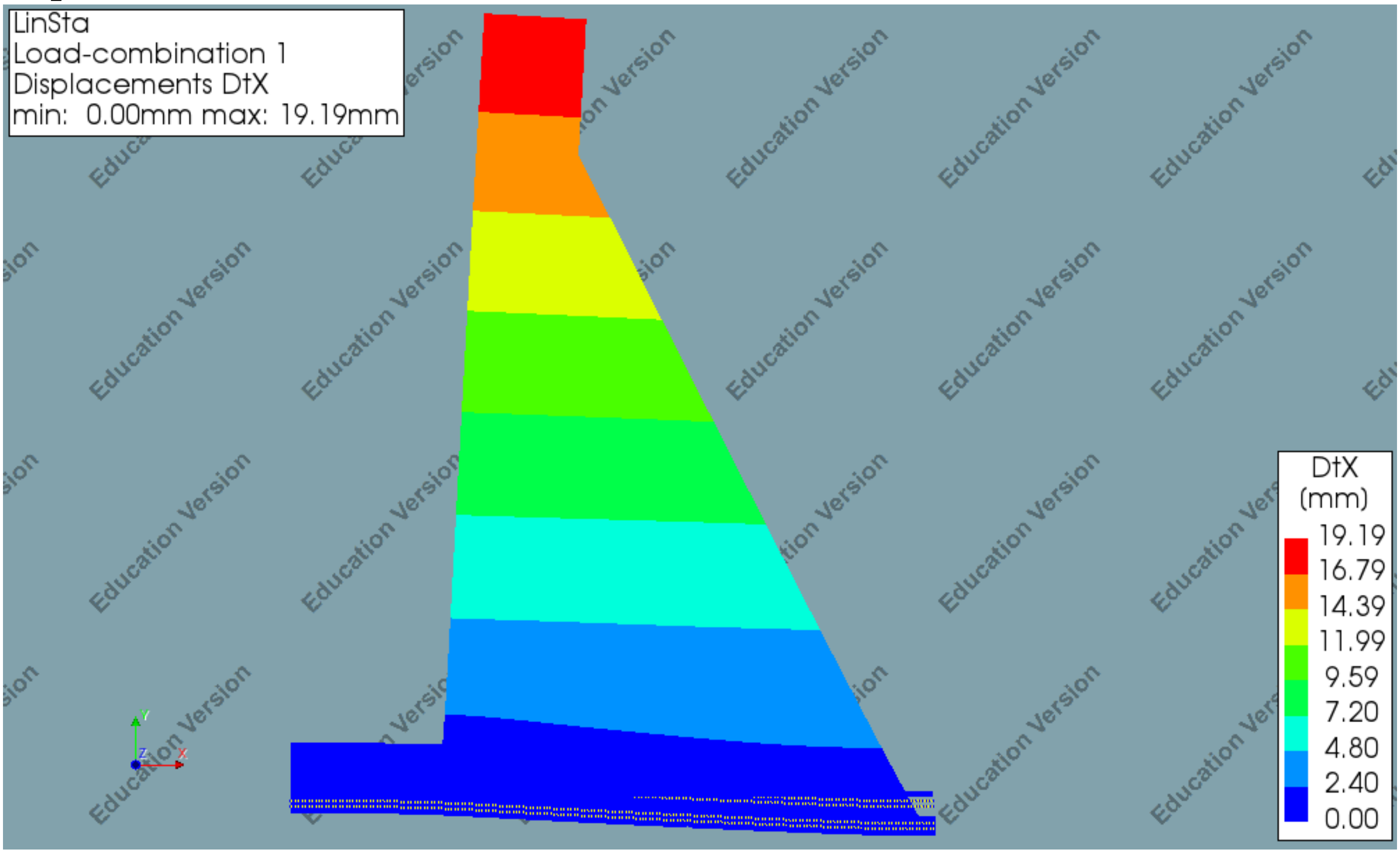

Figure 0-27 Displacements x-direction linear model second alternative design

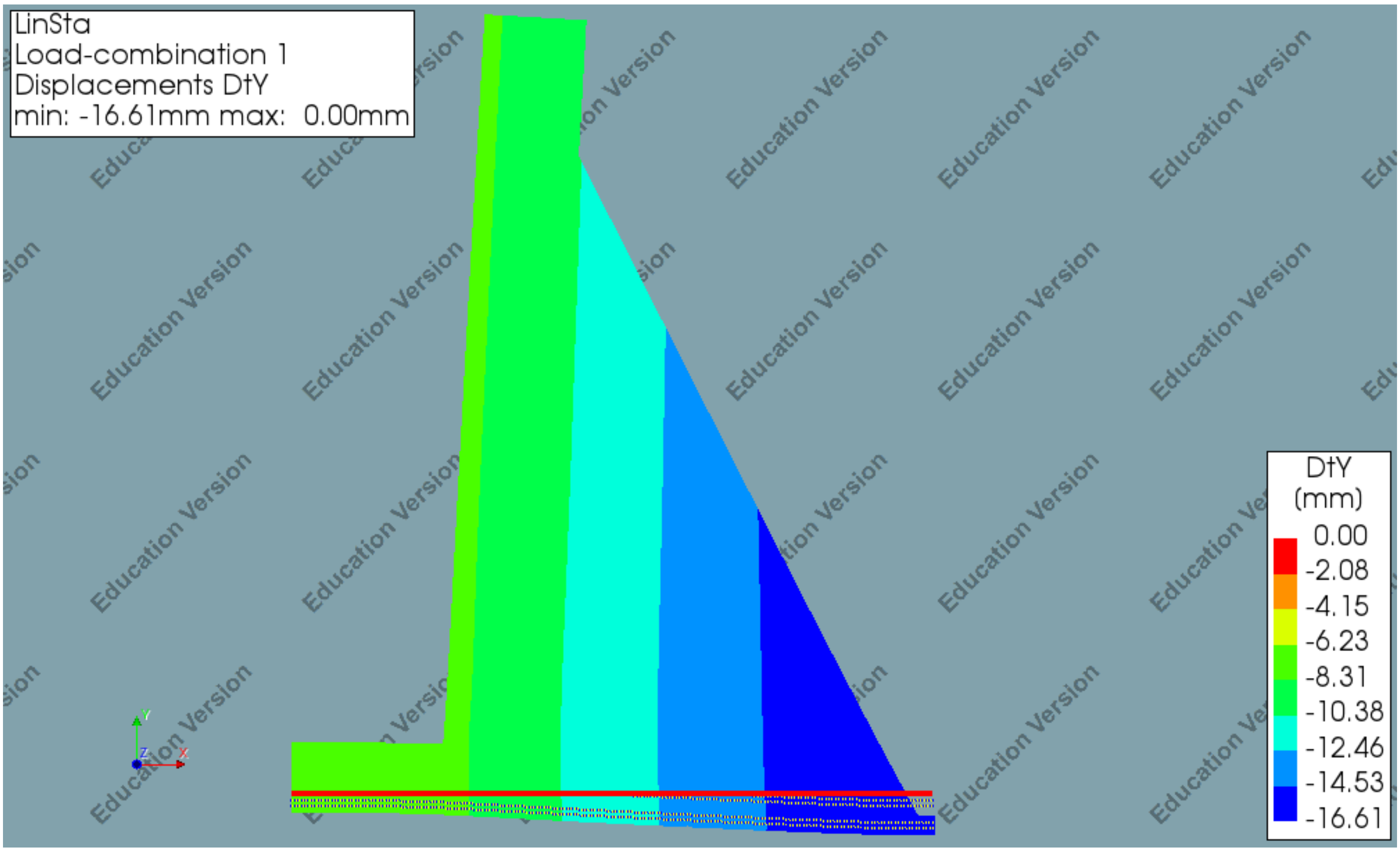

Figure 0-28 Displacements y-direction linear model second alternative design

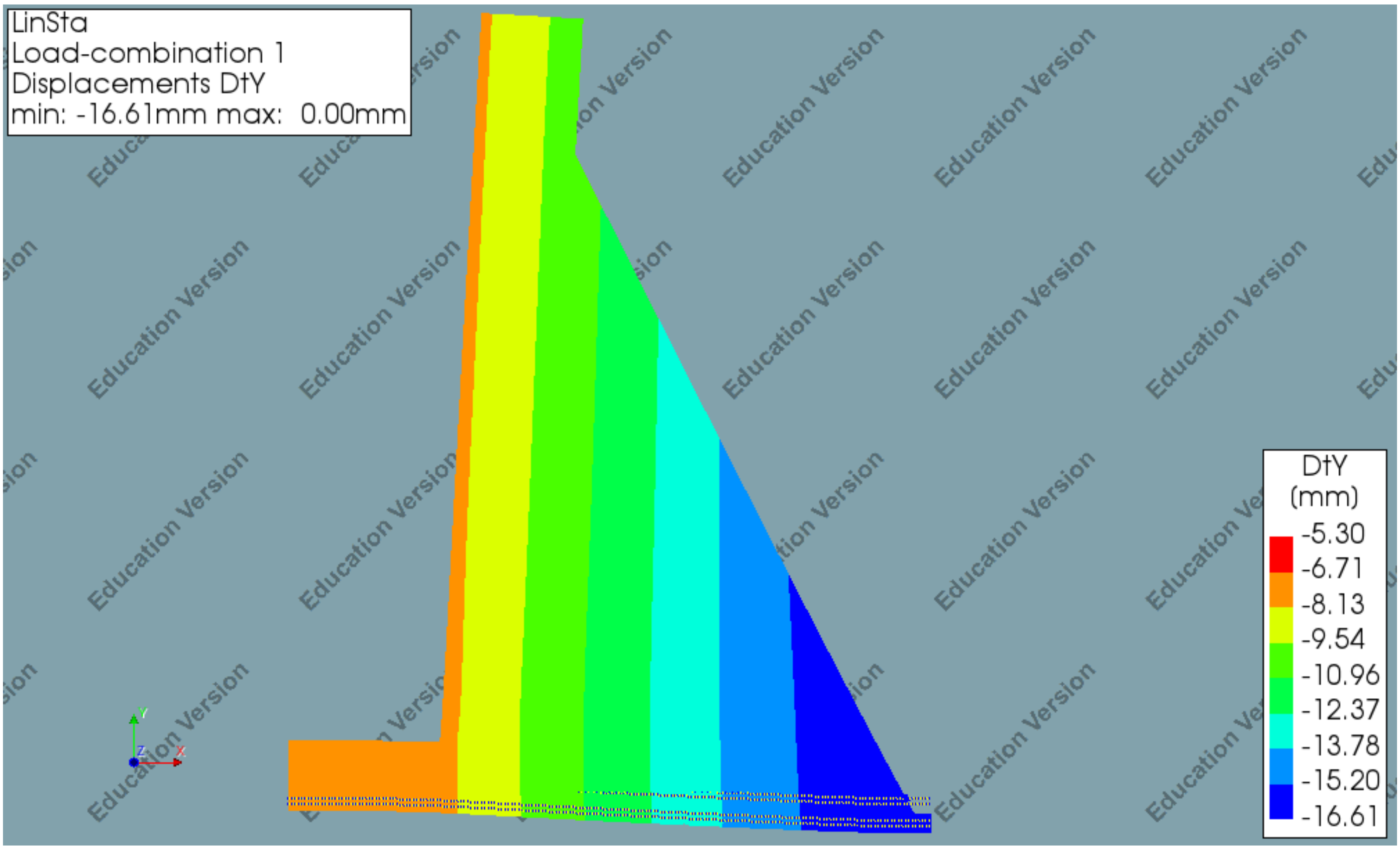

Figure 0-29 Adjusted view Displacements x-direction linear model second alternative design

Interface Relative Displacements

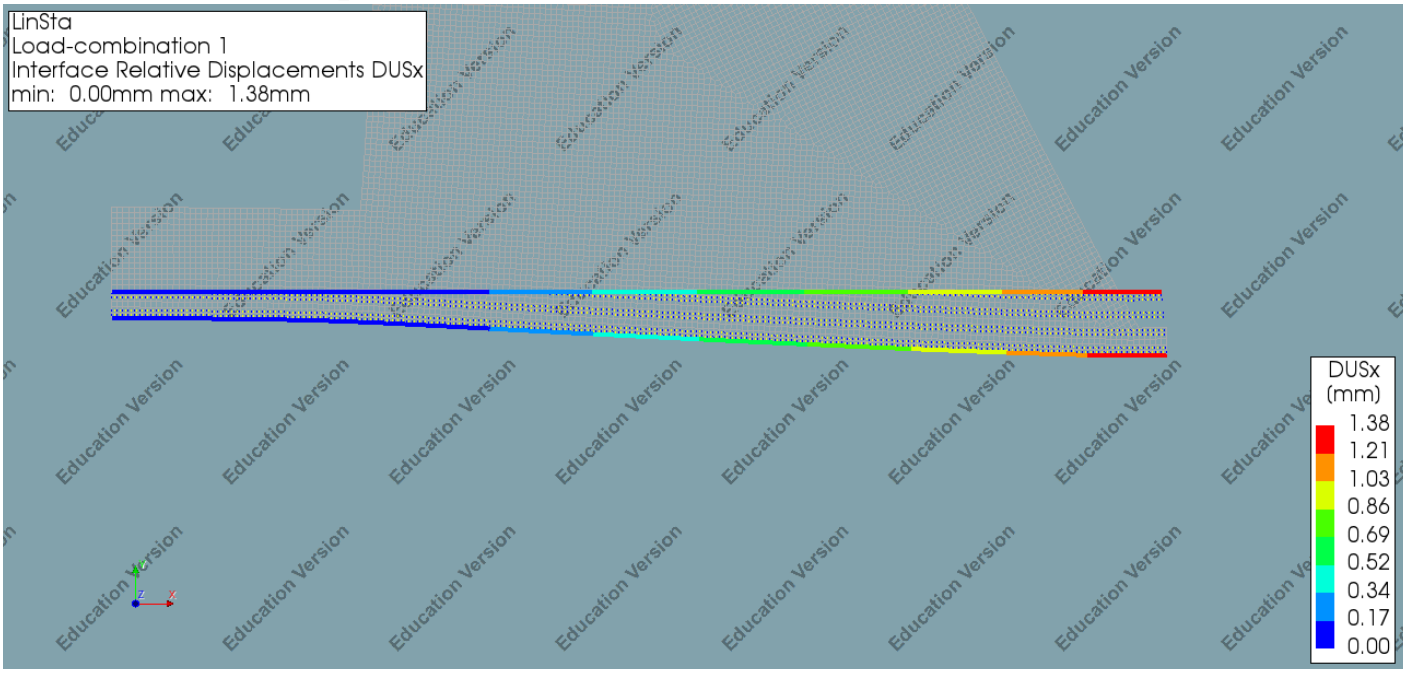

Figure 0-30 Interface relative displacements x-direction linear model second alternative design

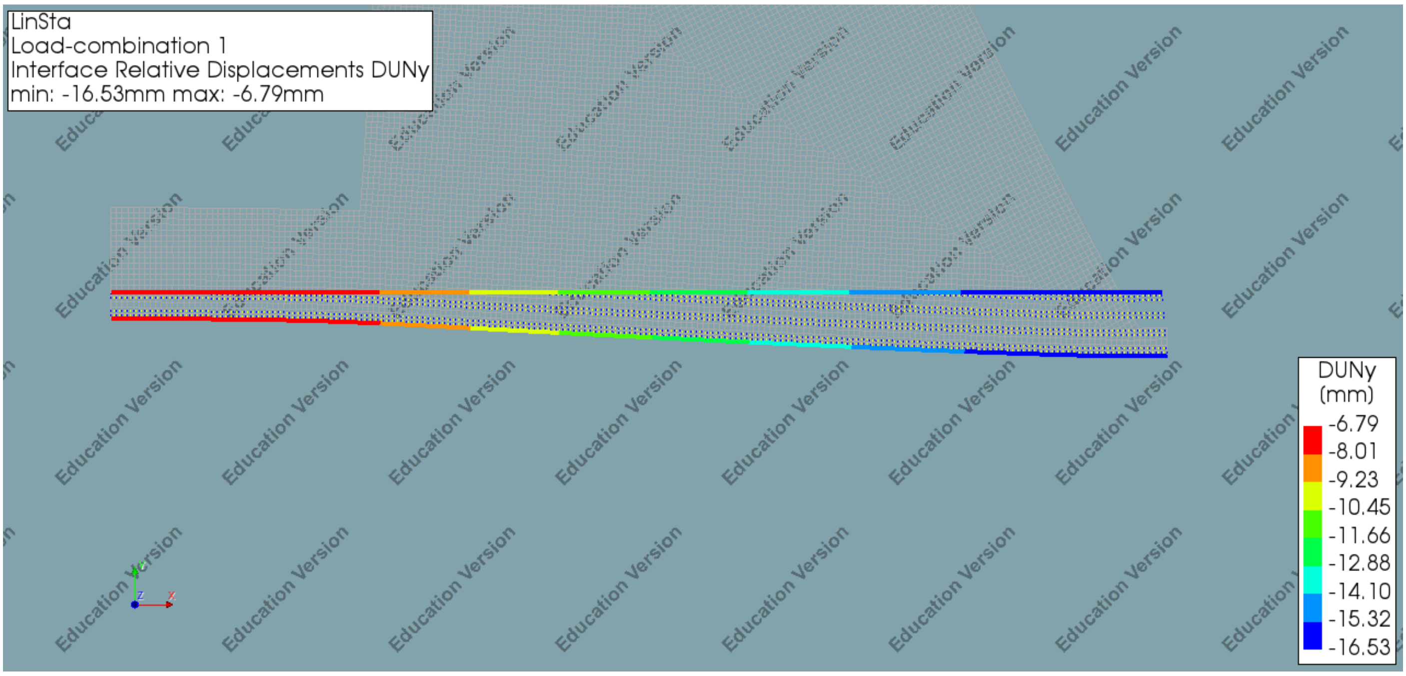

Figure 0-31 Interface relative displacements y-direction linear model second alternative design

Stresses

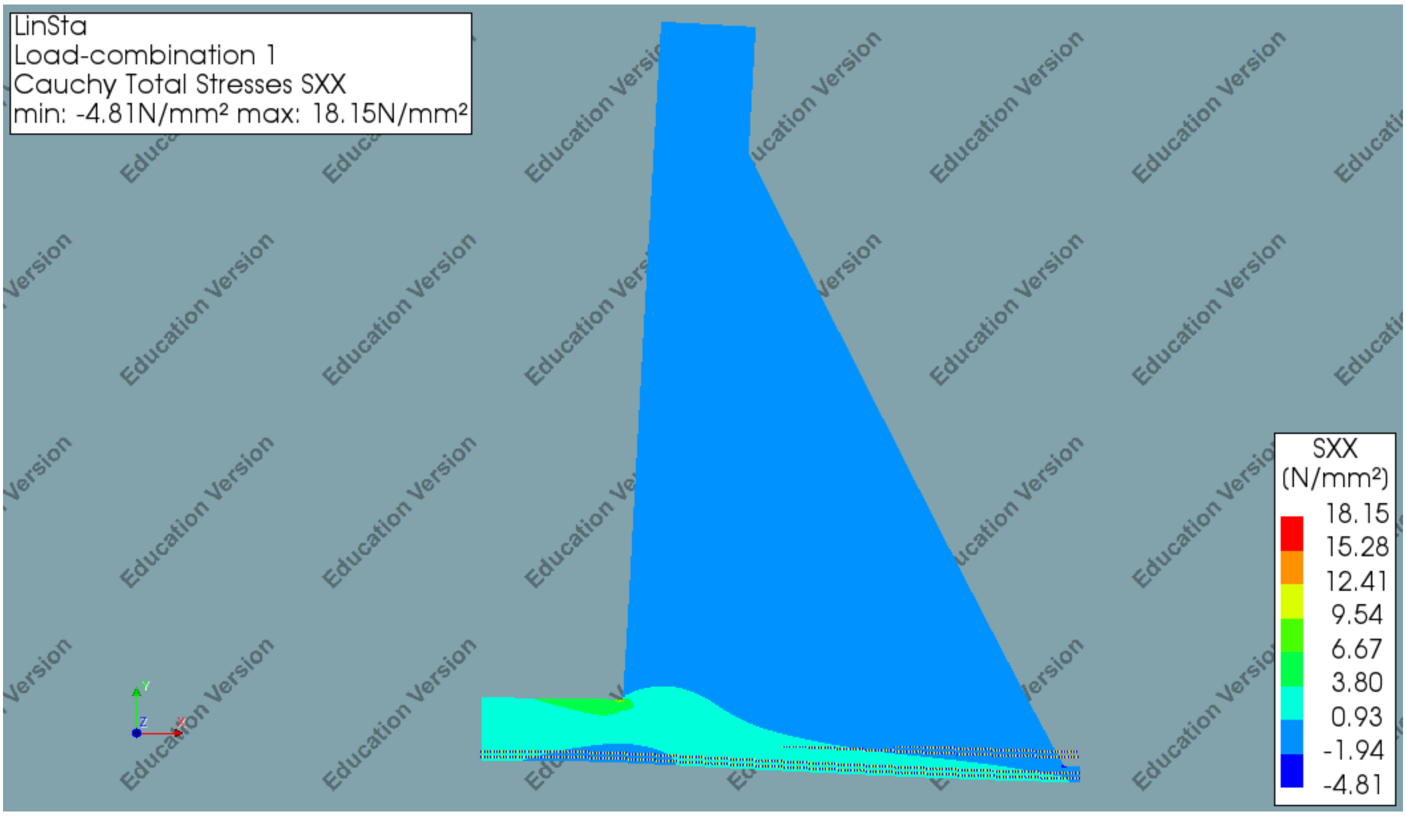

Figure 0-32 Cauchy total stresses SXX linear model second alternative design

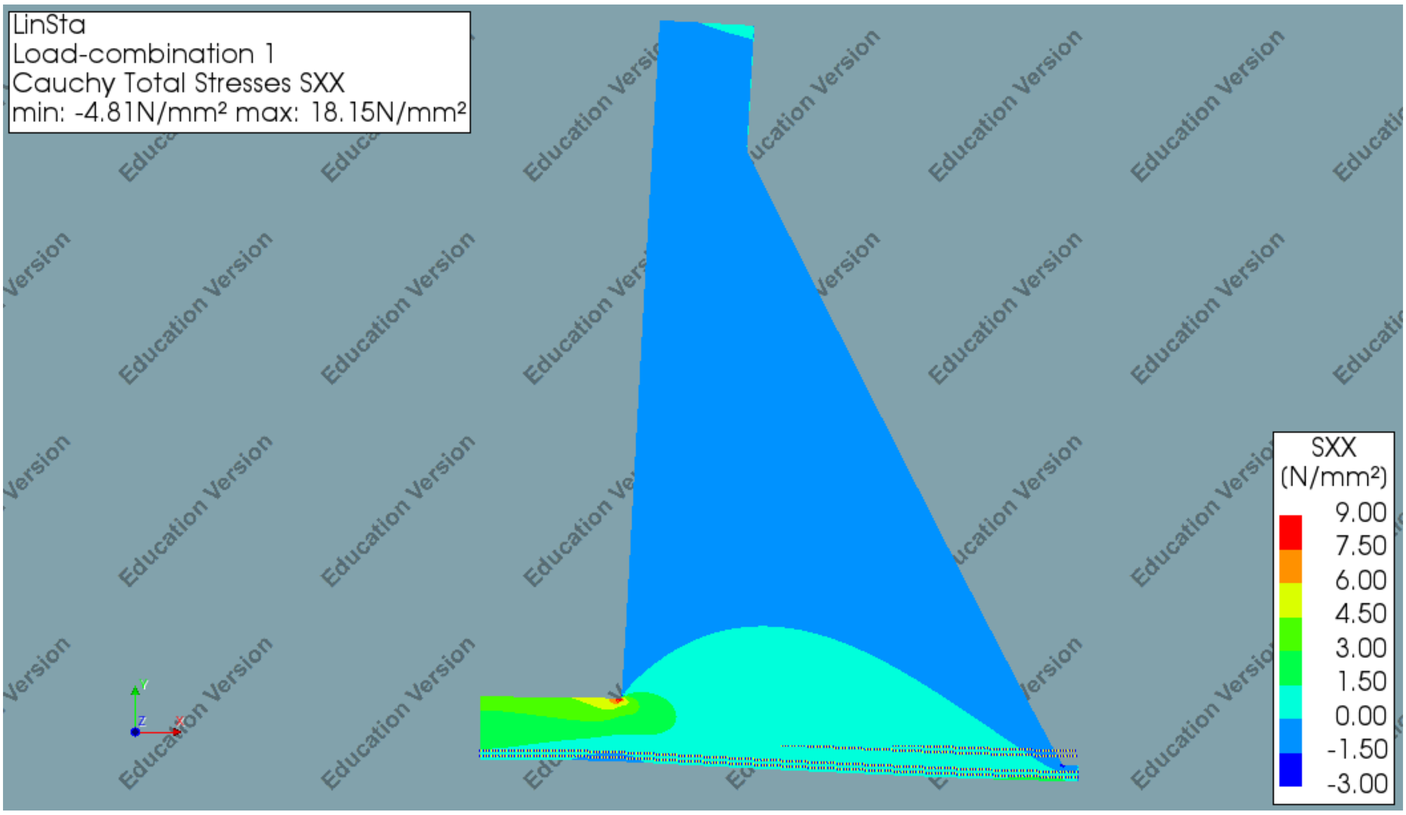

Figure 0-33 Adjusted view Cauchy total stresses SXX linear model second alternative design

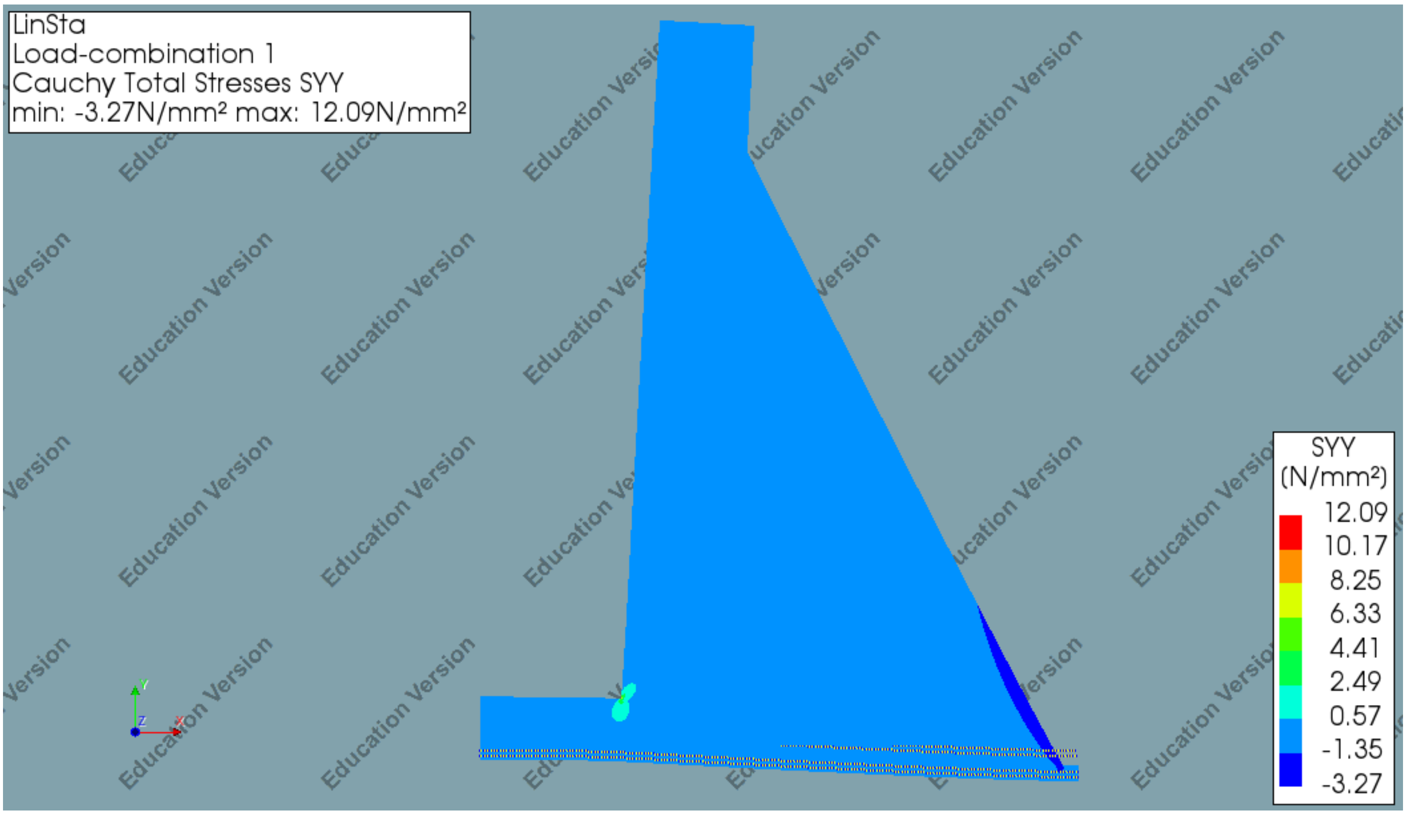

Figure 0-34 Cauchy total stresses SYY linear model second alternative design

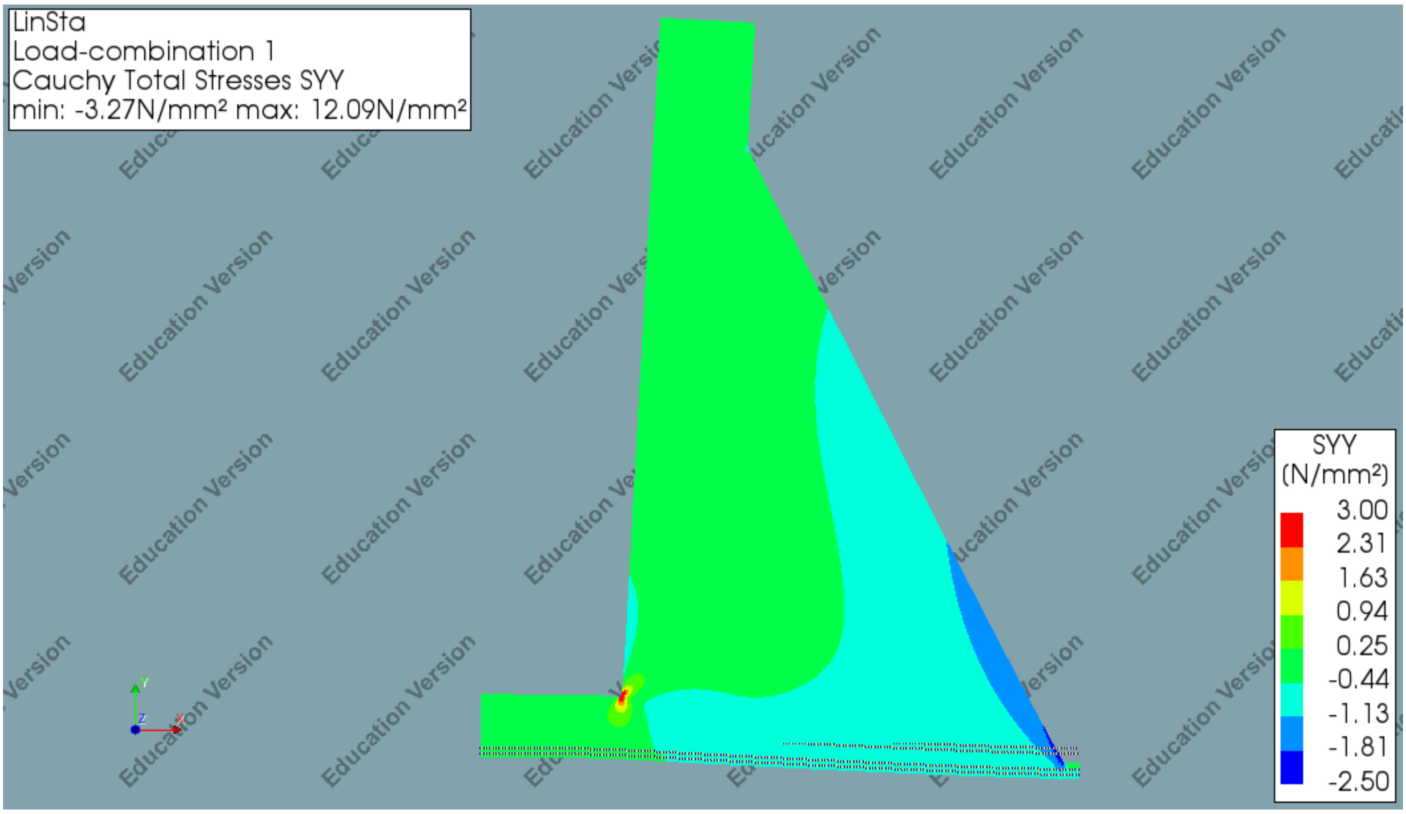

Figure 0-35 Adjusted view Cauchy total stresses SXX linear model second alternative design

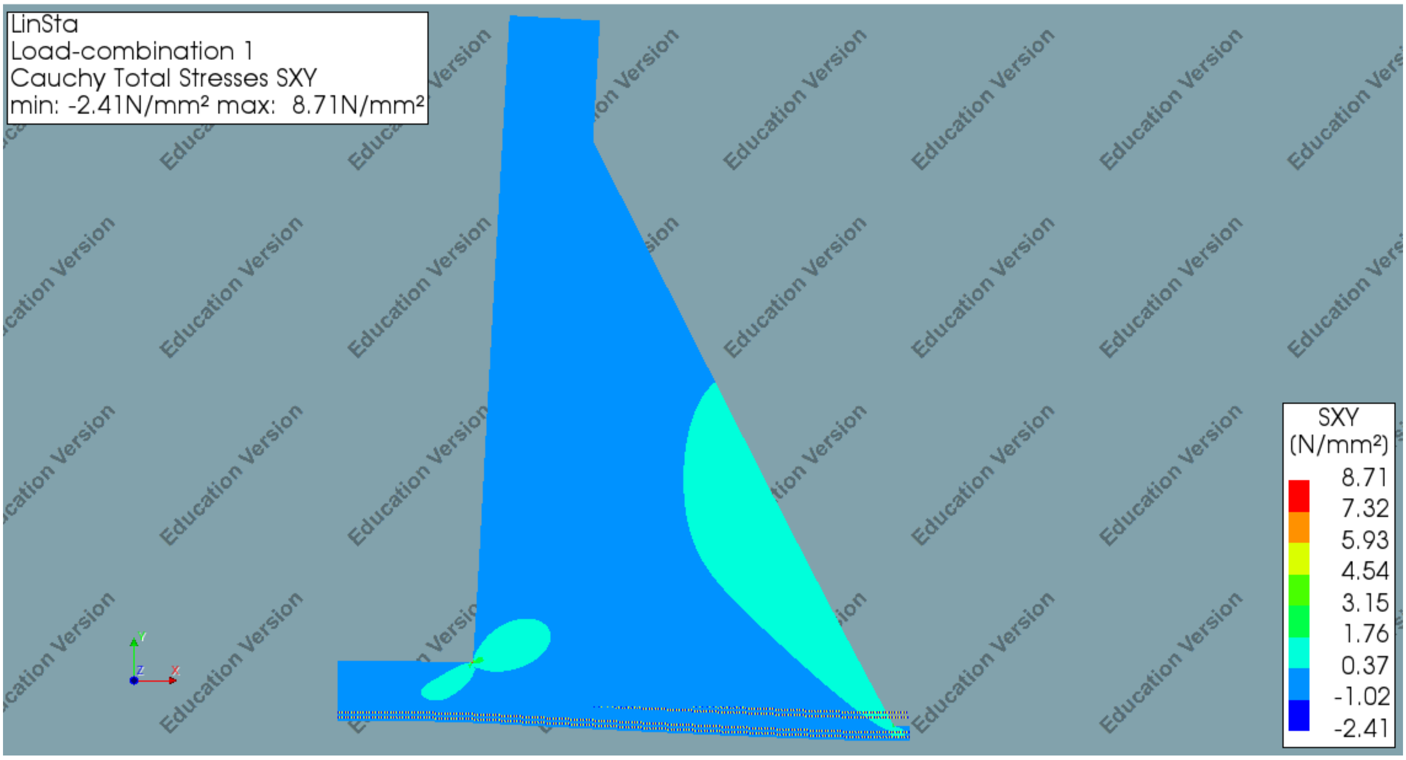

Figure 0-36 Cauchy total stresses SXY linear model second alternative design

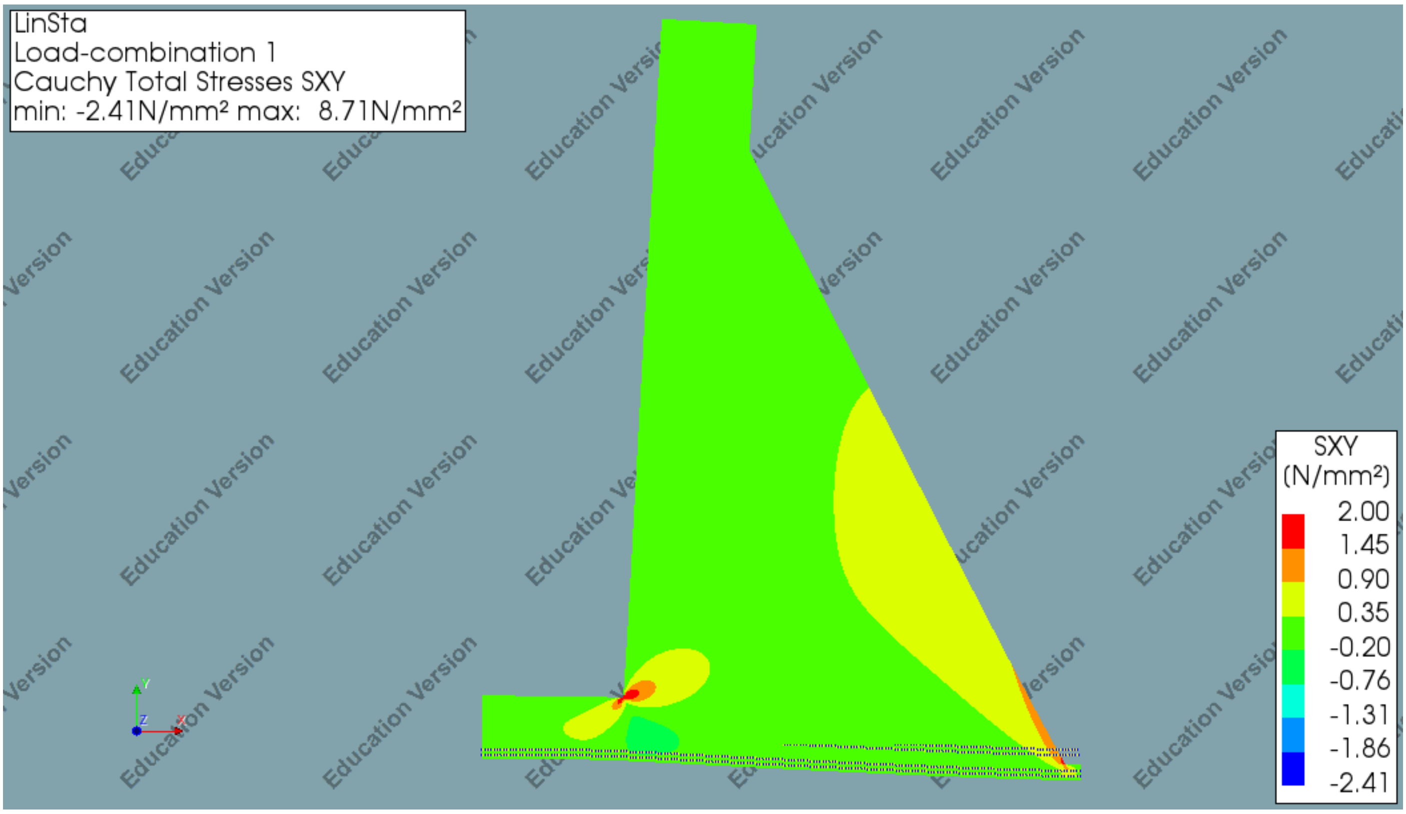

Figure 0-37 Adjusted view Cauchy total stresses SXY linear model second alternative design

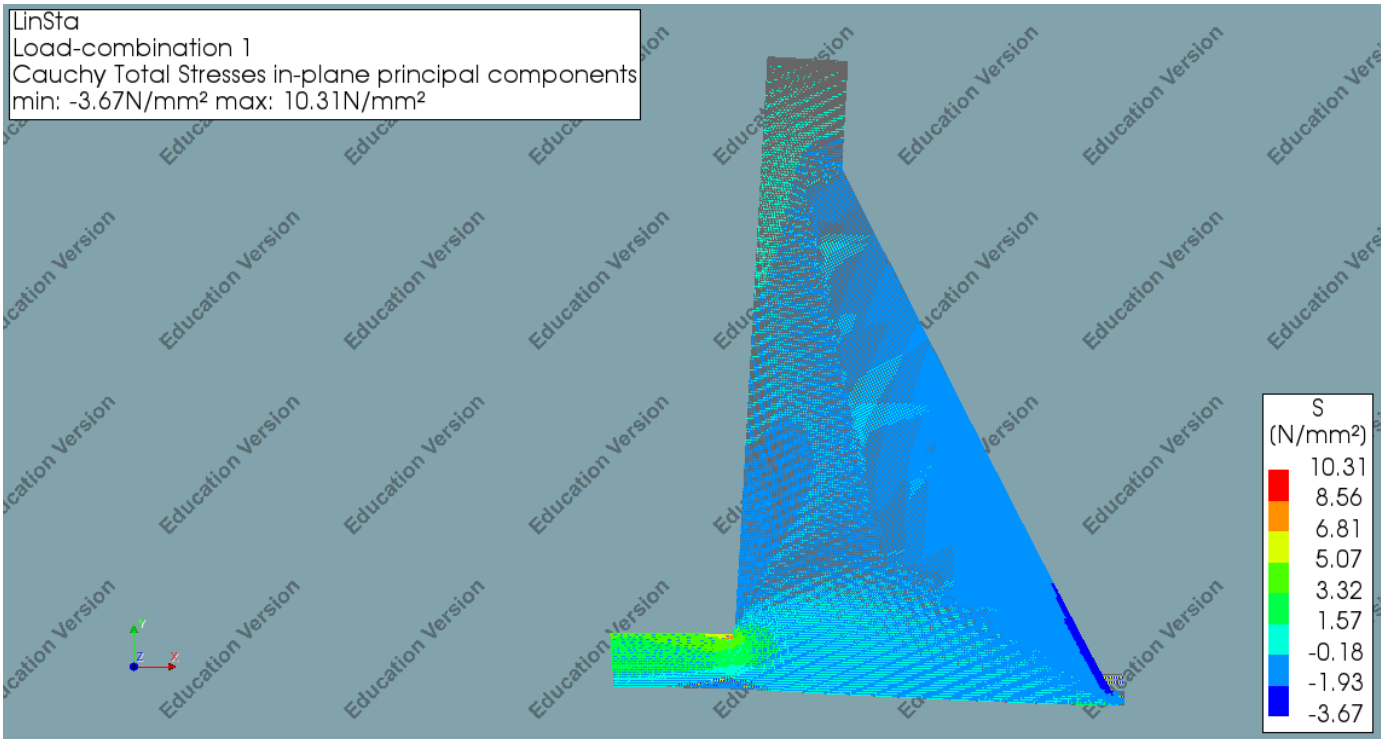

Figure 0-38 Principal stresses linear model second alternative design

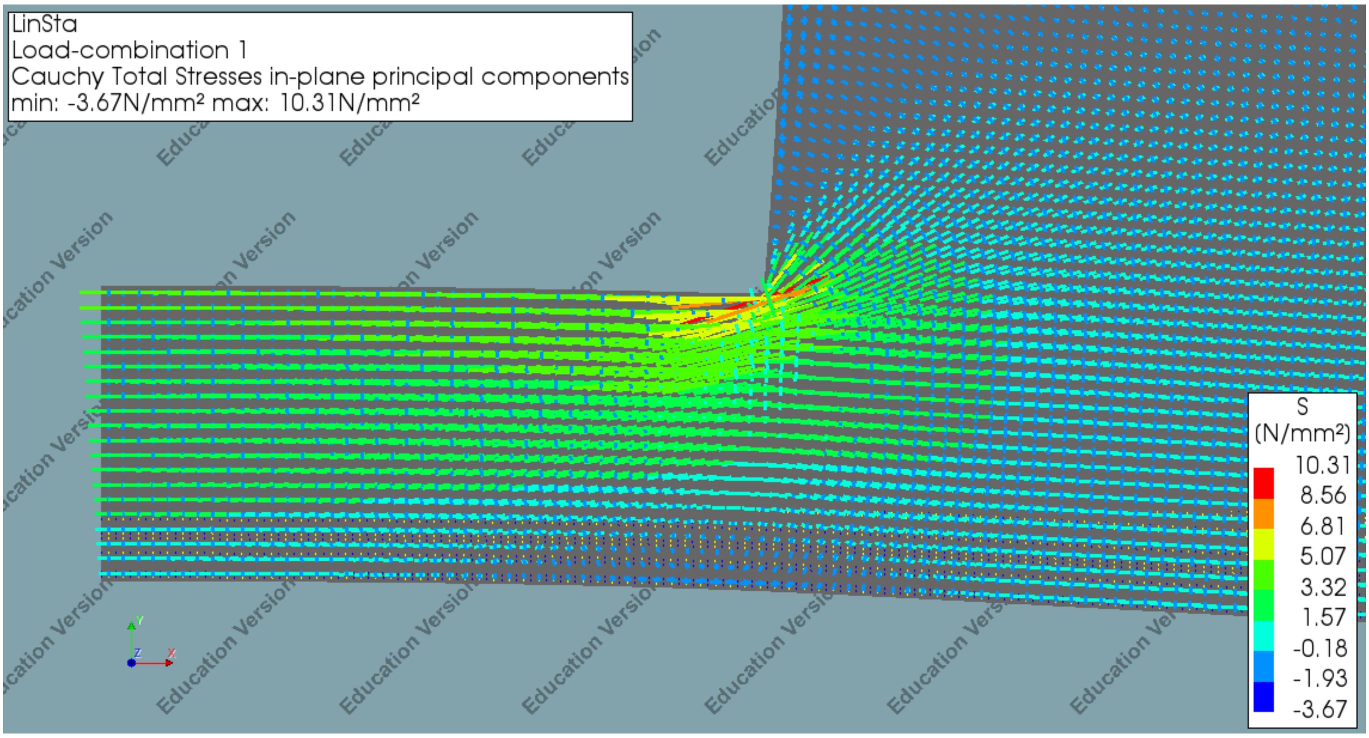

Figure 0-39 Zoom in on Principal stresses linear model second alternative design

Results first alternative design: total wall thickness = 17m.

Displacements

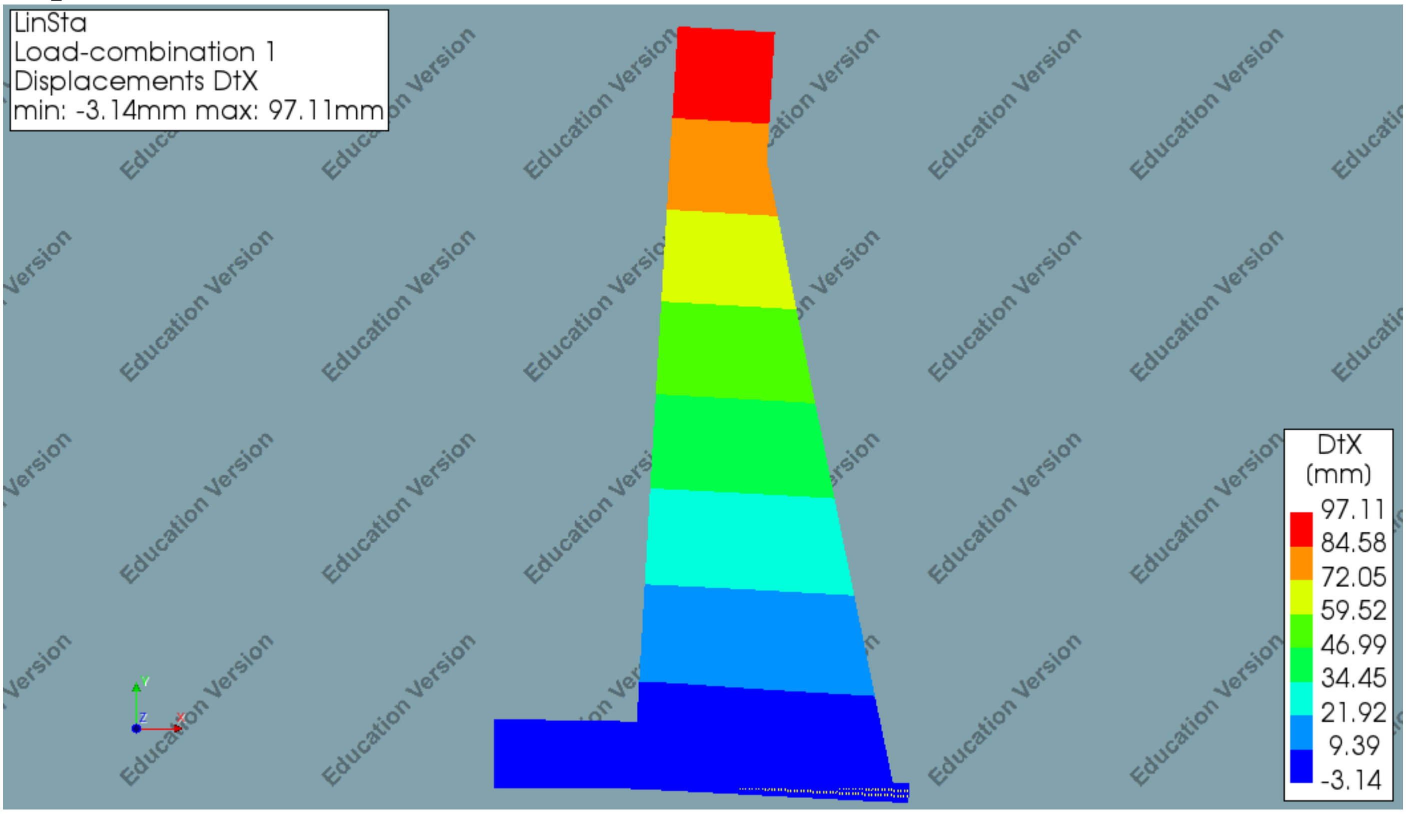

Figure 0-40 Displacements x-direction linear model first alternative design

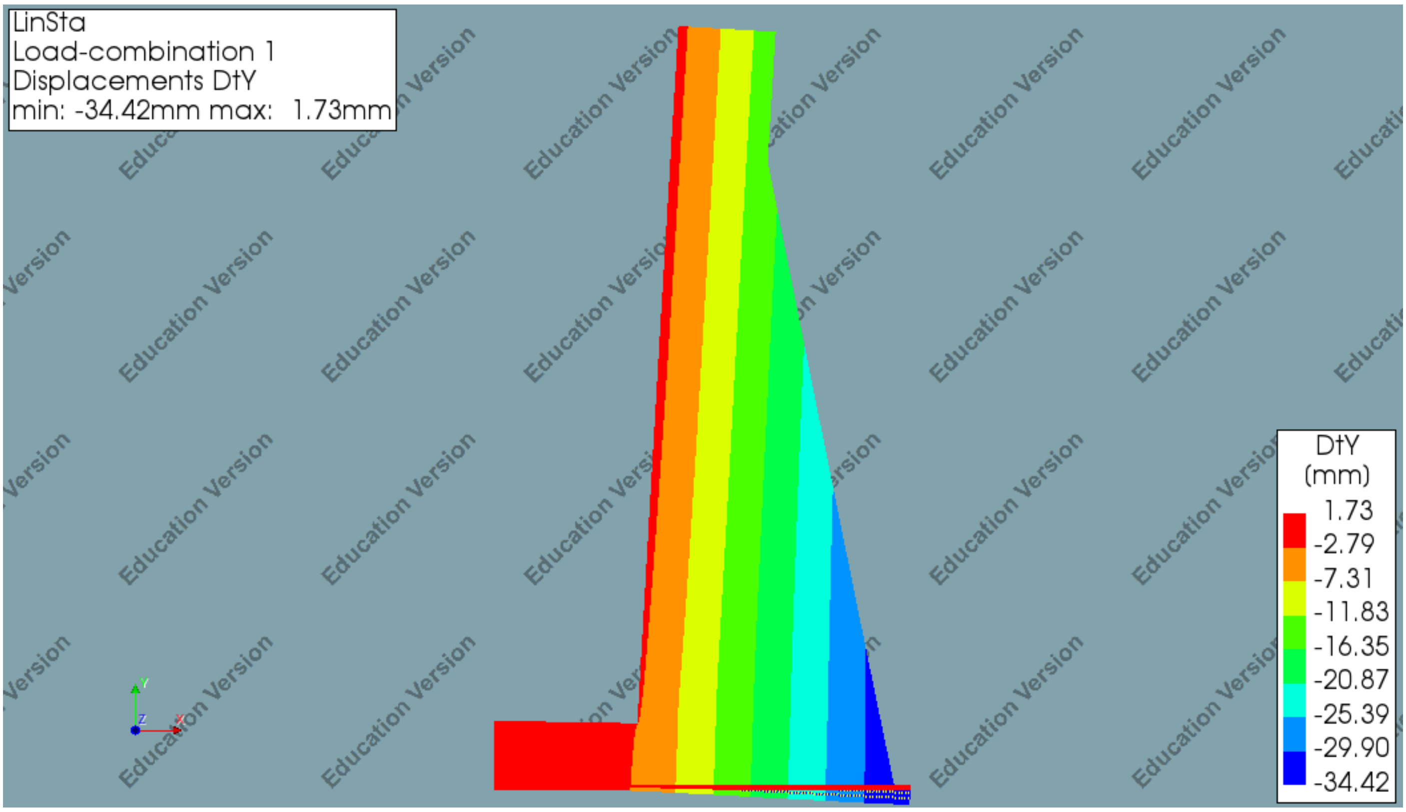

Figure 0-41 Displacements y-direction linear model first alternative design

Interface Relative Displacements

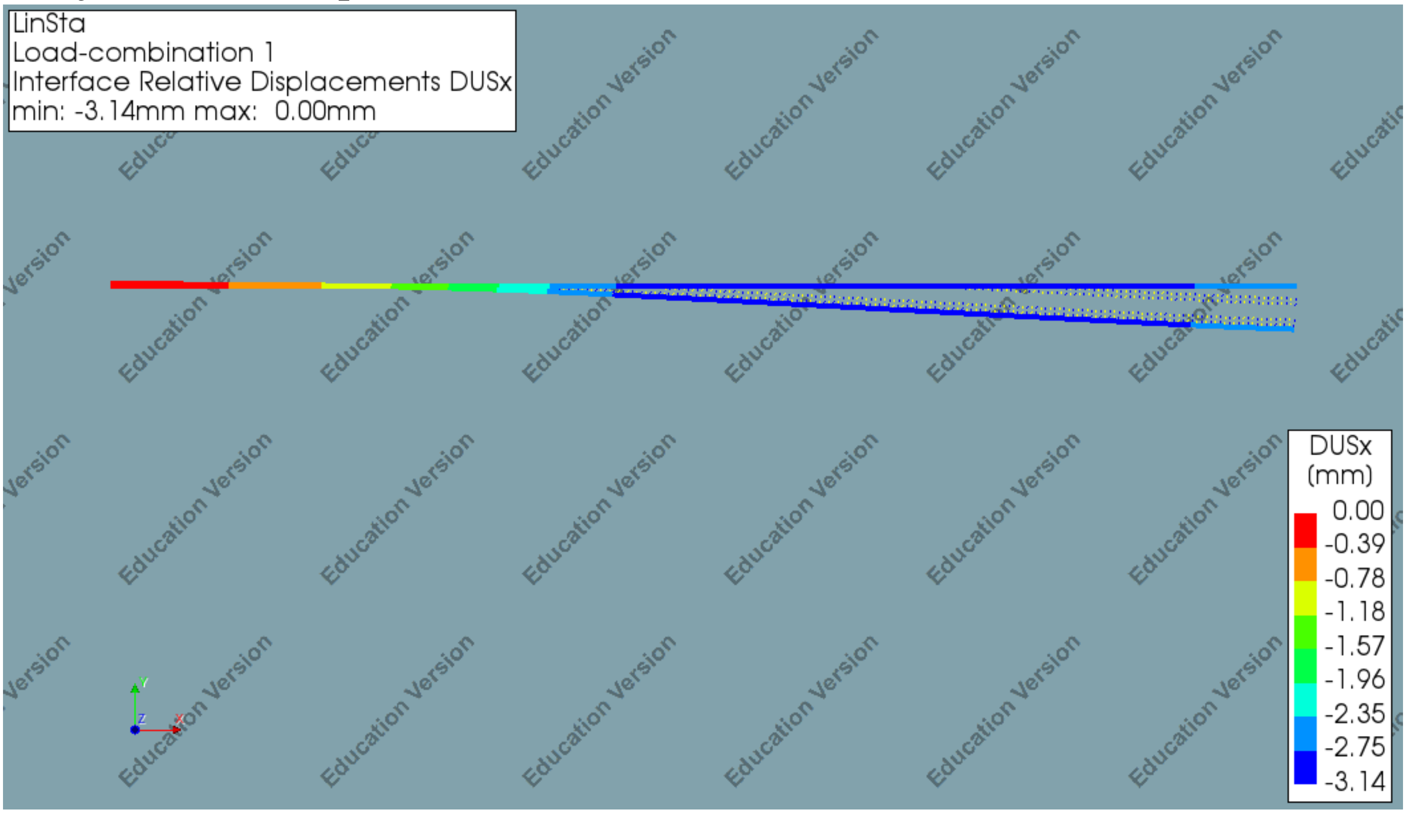

Figure 0-42 Interface relative displacements x-direction linear model first alternative design

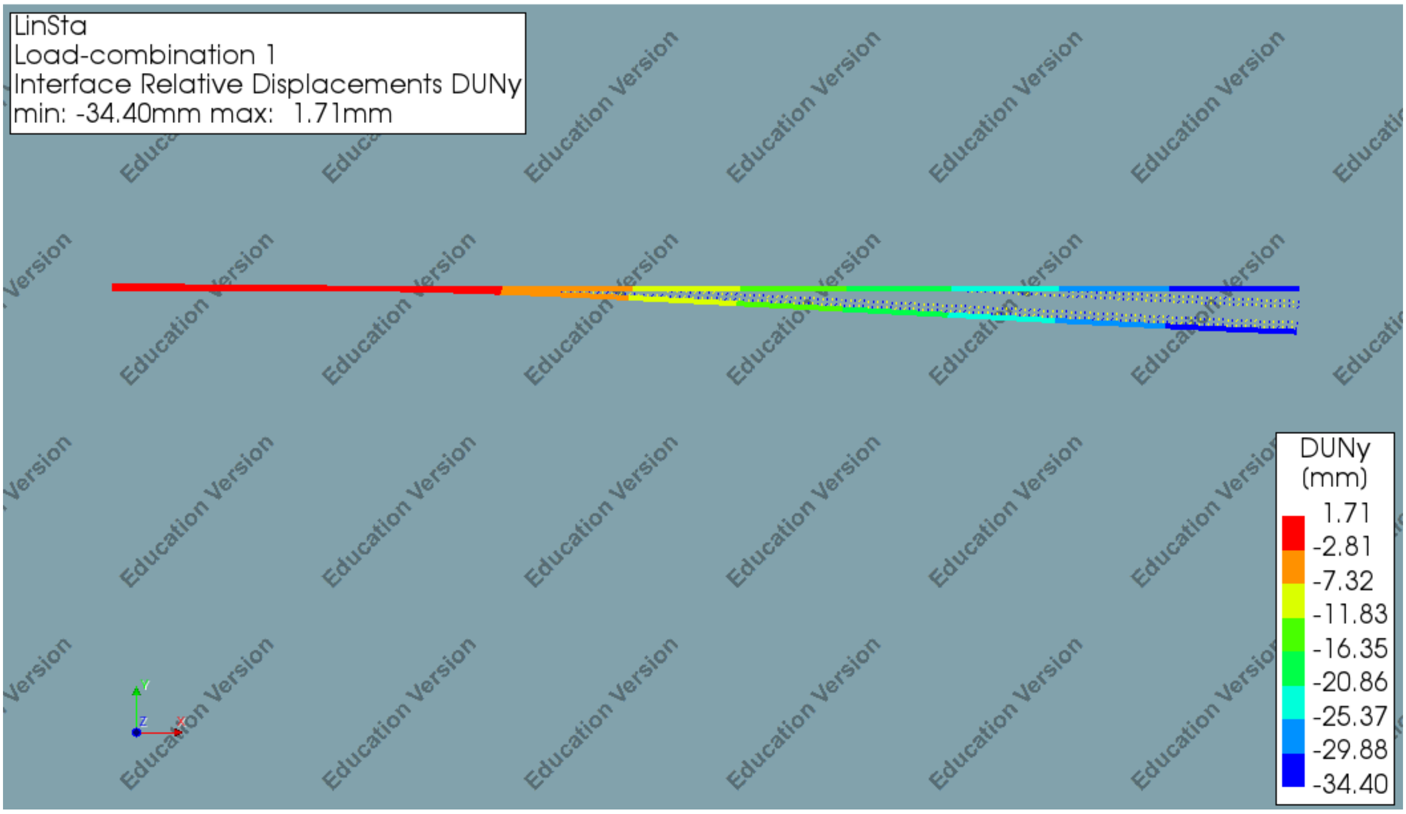

Figure 0-43 Interface relative displacements y-direction linear model first alternative design

Stresses

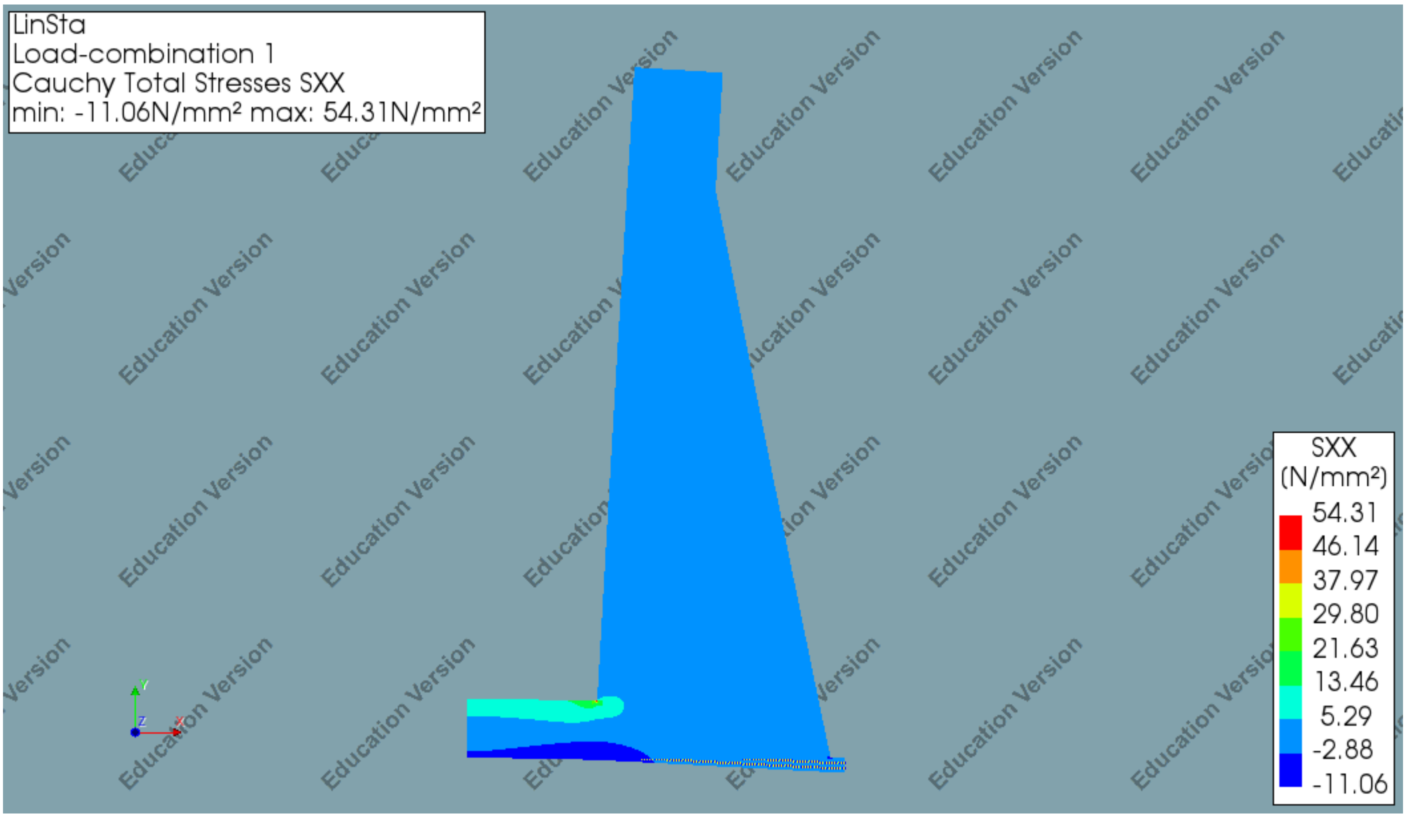

Figure 0-44 Cauchy total stresses SXX linear model first alternative design

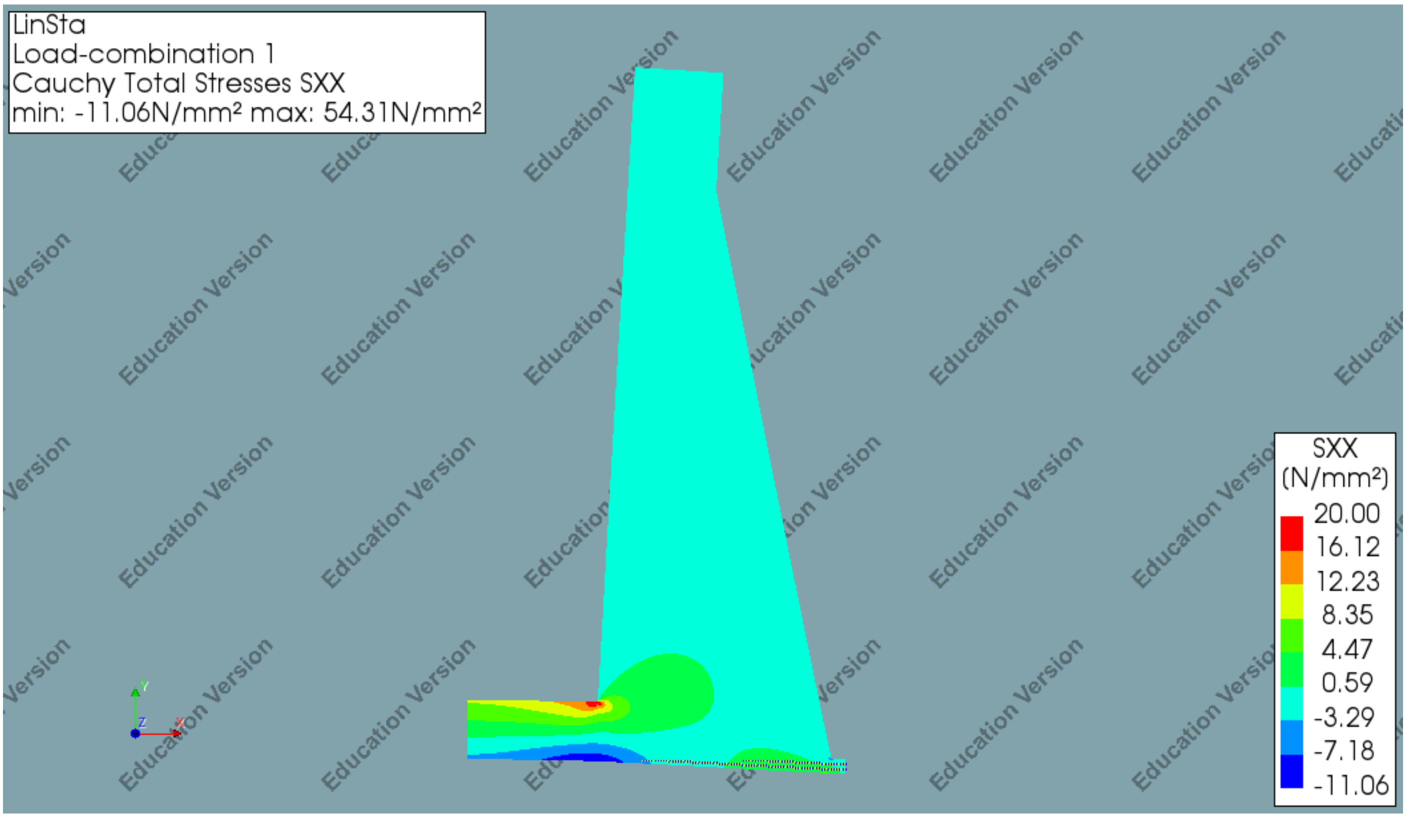

Figure 0-45 Adjusted view Cauchy total stresses SXX linear model first alternative design

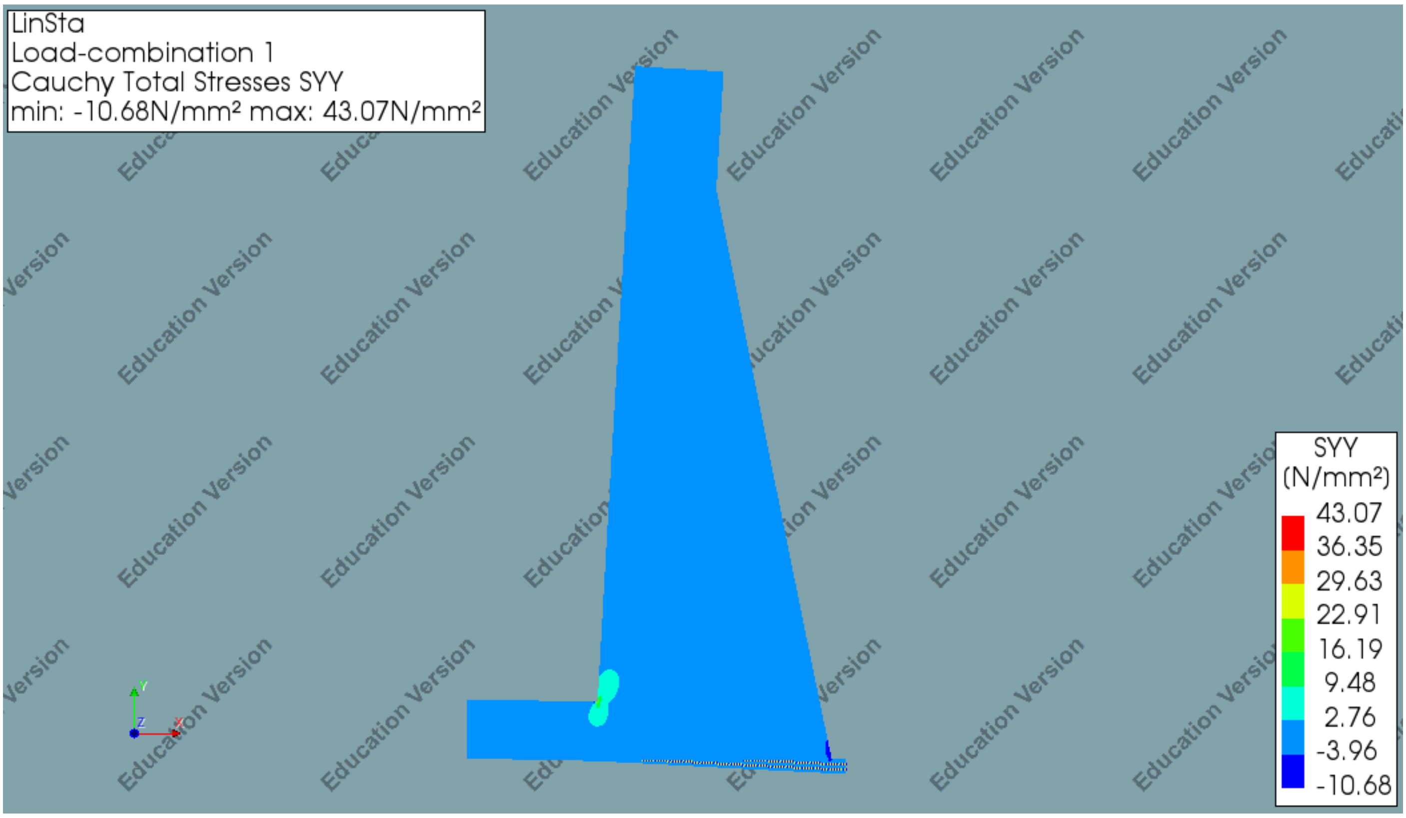

Figure 0-46 Cauchy total stresses SYY linear model first alternative design

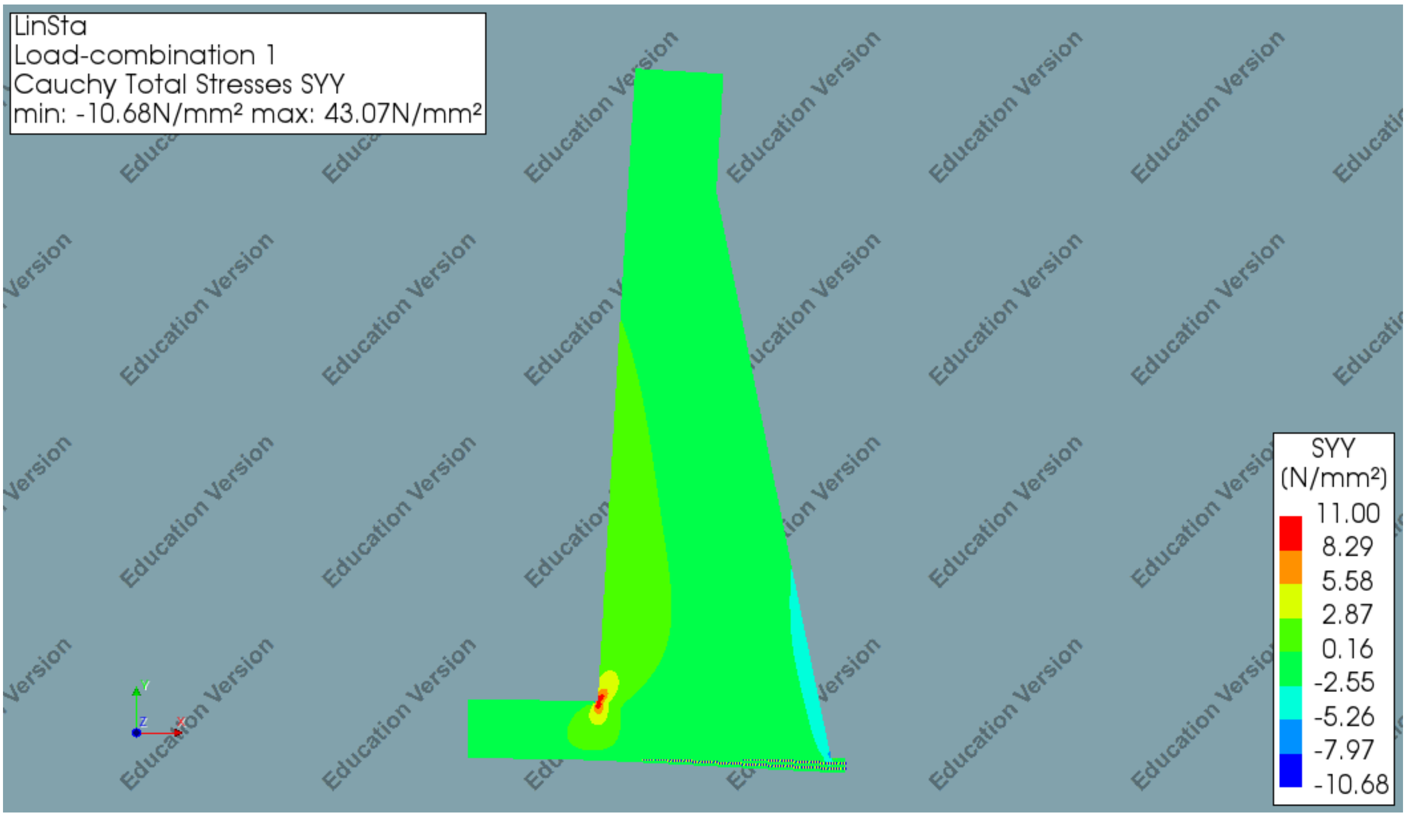

Figure 0-47 Adjusted view Cauchy total stresses SYY linear model first alternative design

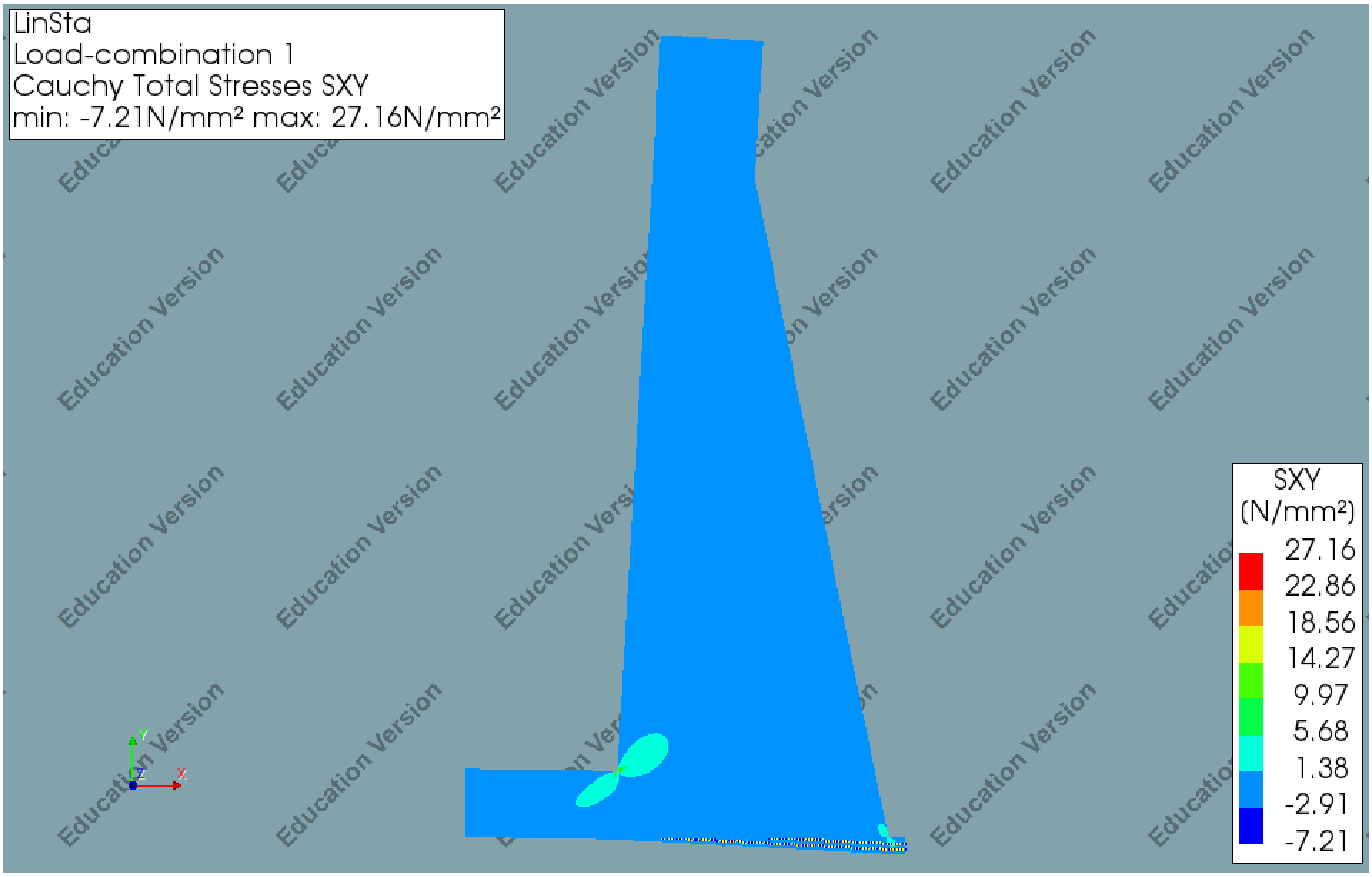

Figure 0-48 Cauchy total stresses SXY linear model first alternative design

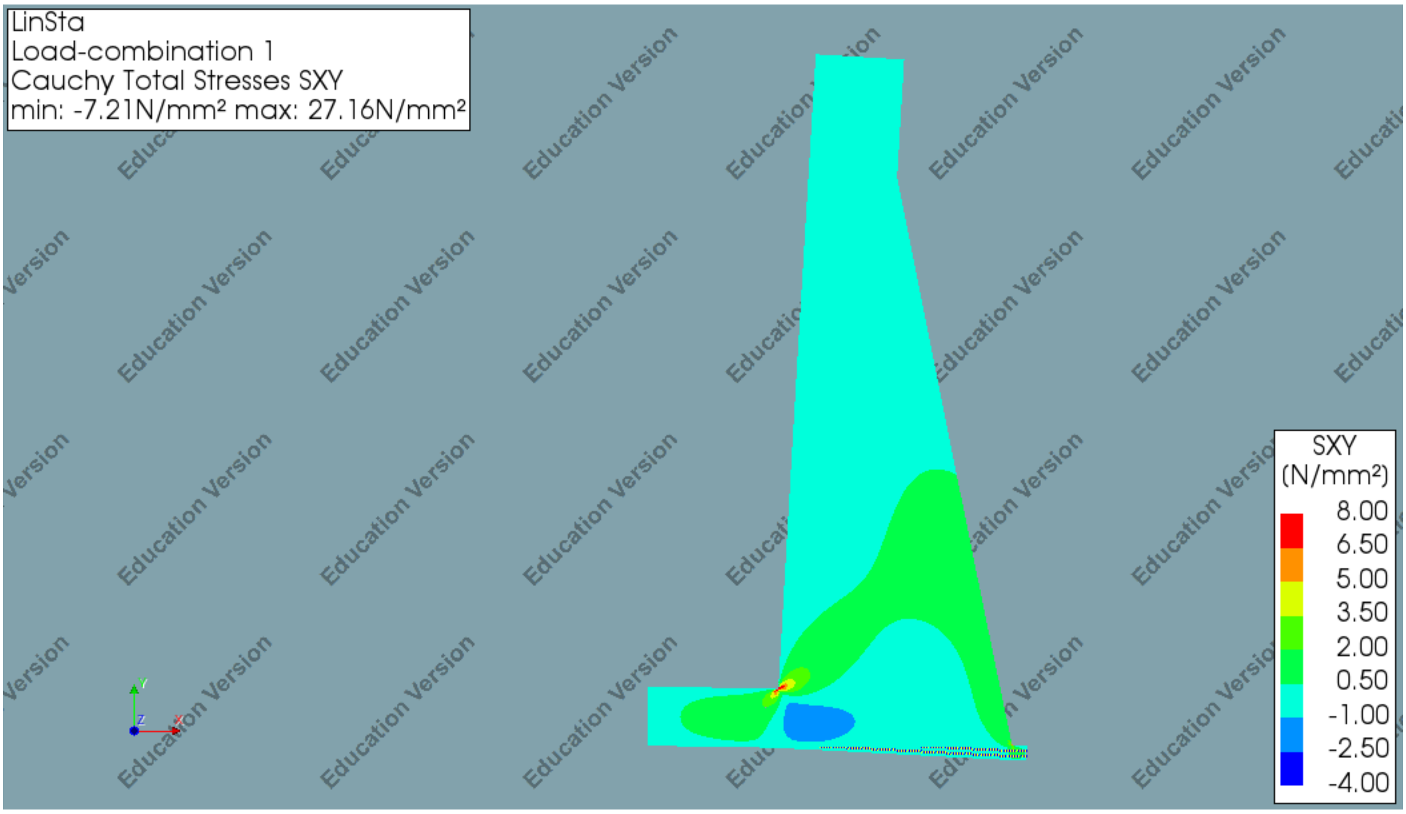

Figure 0-49 Adjusted view Cauchy total stresses SXY linear model first alternative design

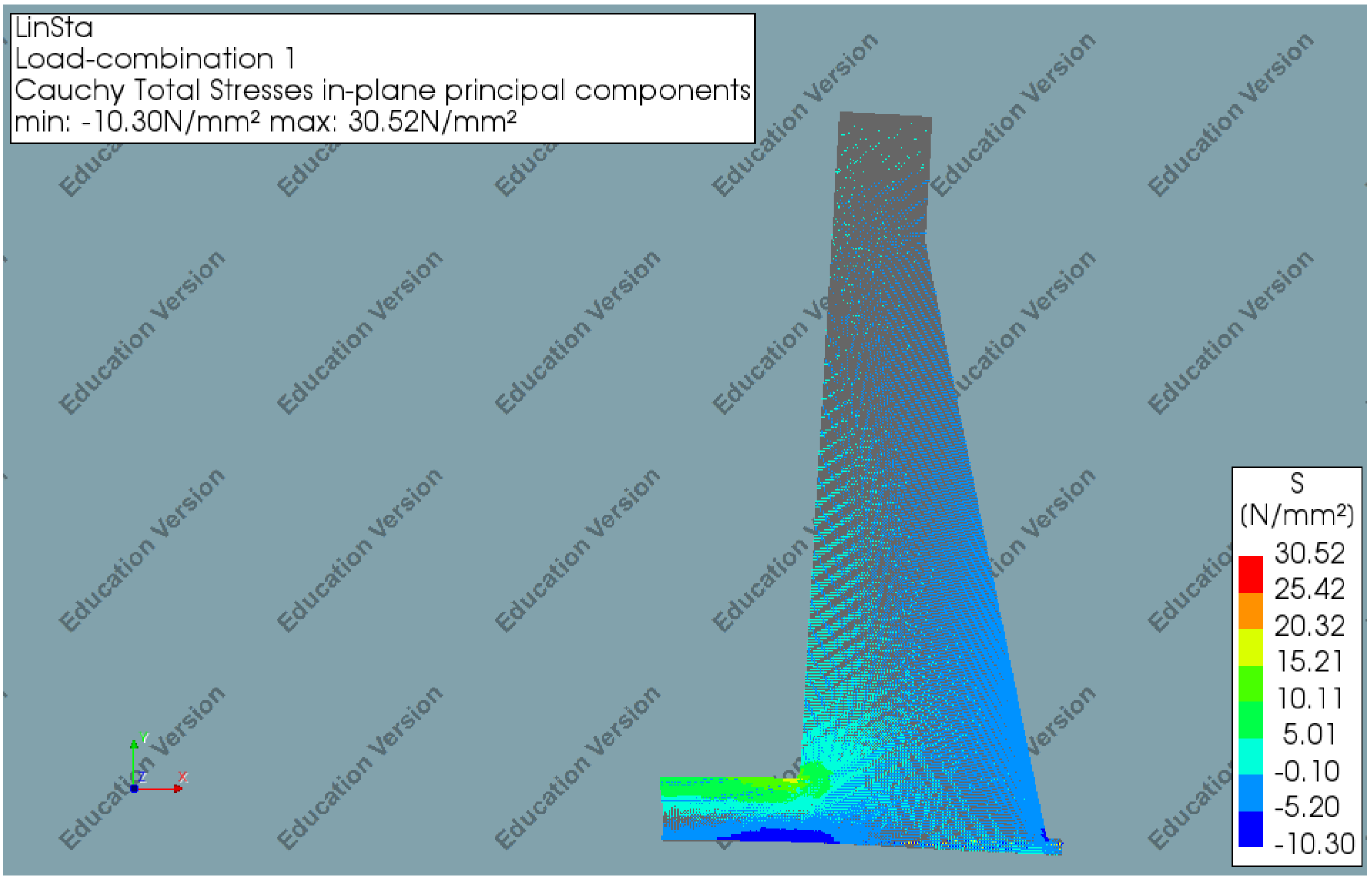

Figure 0-50 Principal stresses nonlinear model first alternative design

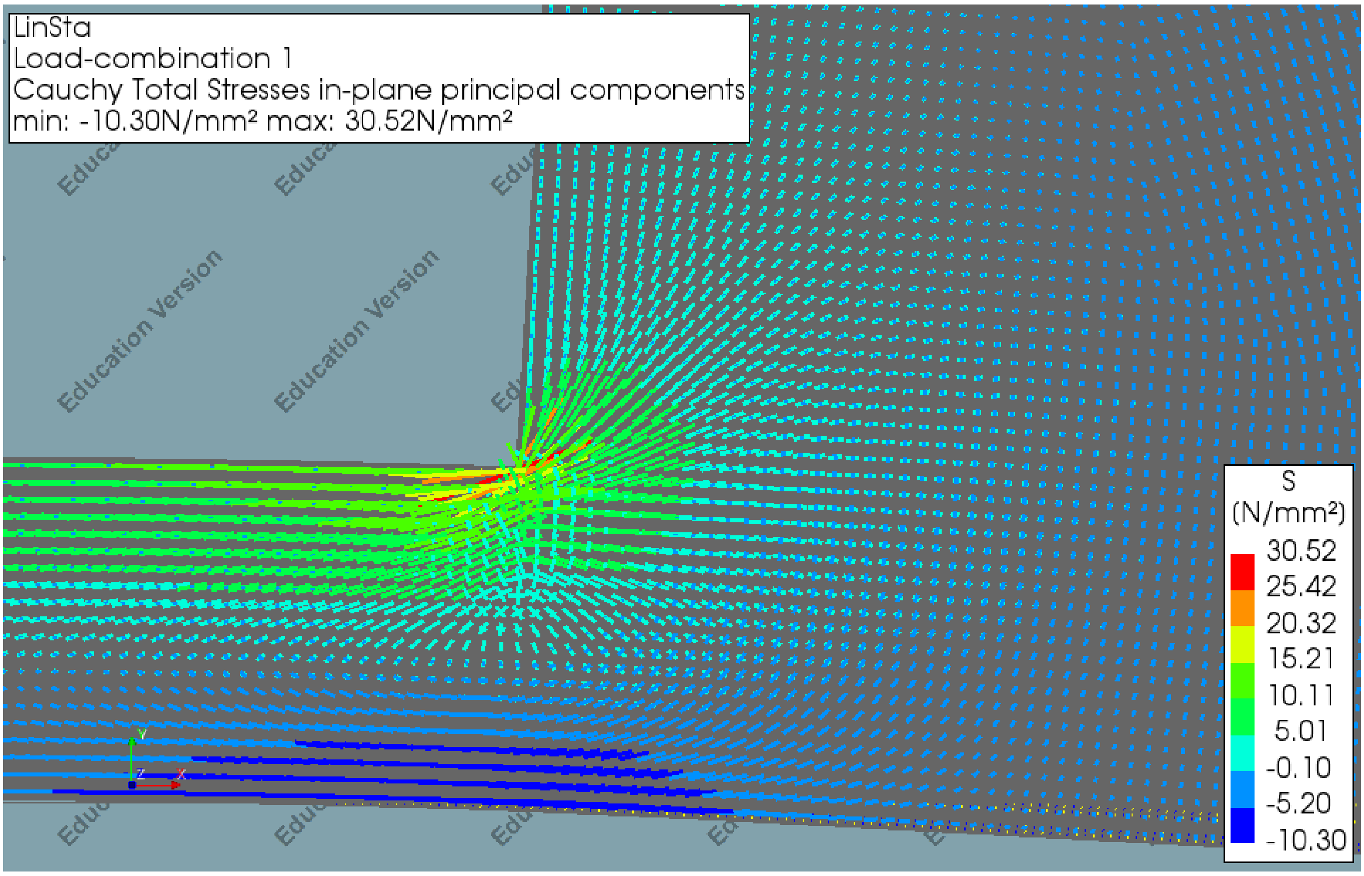

Figure 0-51 Zoom in on Principal stresses nonlinear model first alternative design

Nonlinear Model

The original W+B design of the Itaipu locks is also analyzed with a 2D nonlinear model.

Geometry

The model consists of one **regular plane stress concrete element** for the wall and the floor with the following material characteristics:

Linear material properties:

- Young's modulus: 30000 N/mm^2
- Poisson's ratio: 0.2
- Mass density: 2400 kg/m^3

Total Strain based crack model:

- Crack orientation: Fixed

Tensile behaviour:

- Tensile curve: Hordijk
- Tensile strength: 2.7 N/mm^2
- Mode-I tensile fracture energy: 0.144 N/mm
- Crack bandwidth specification: Govindjee
- Poisson's ratio reduction model: Damage based

Compressive beahviour:

- Compressive curve: Parabolic
- Compressive strength: 37 N/mm^2
- Compressive fracture energy: 35.975 N/mm
- No reduction due to lateral cracking
- Stress confinement model: Selby & Vecchio

Shear behaviour:

- Shear retention function: aggregate size based
- Mean aggregate size: 25mm

The model also includes the reinforcement of the floor. Resulting from the lack of high tensile stresses in the wall, as can be seen in the results of the linear analysis, the choice has been made not to reinforce the wall. In terms of project costs, minimal reinforcement is ideal. However, this decision is based purely on the results of the shear analysis. For other usability and/or durability requirements, the outer layer of the wall might still be reinforced. This specific reinforcement is not included in this calculation.

The **material properties** of all the **reinforcement bars** are the same and are modelled as follows:

Linear elasticity:

- Young's modulus: 200000 N/mm^2

Eurocode 2 EN1992-1-2:

- Yield stress: 435 N/mm^2
- Peak stress: 500 N/mm^2
- Strain at peak stress: 0.015
- Strain at start decay: 0.045
- Ultimate strain: 0.05
- Reinforcement class: hot rolled class N – Table 3.2a

The position of the reinforcement bars is indicated with the red color in the image below:

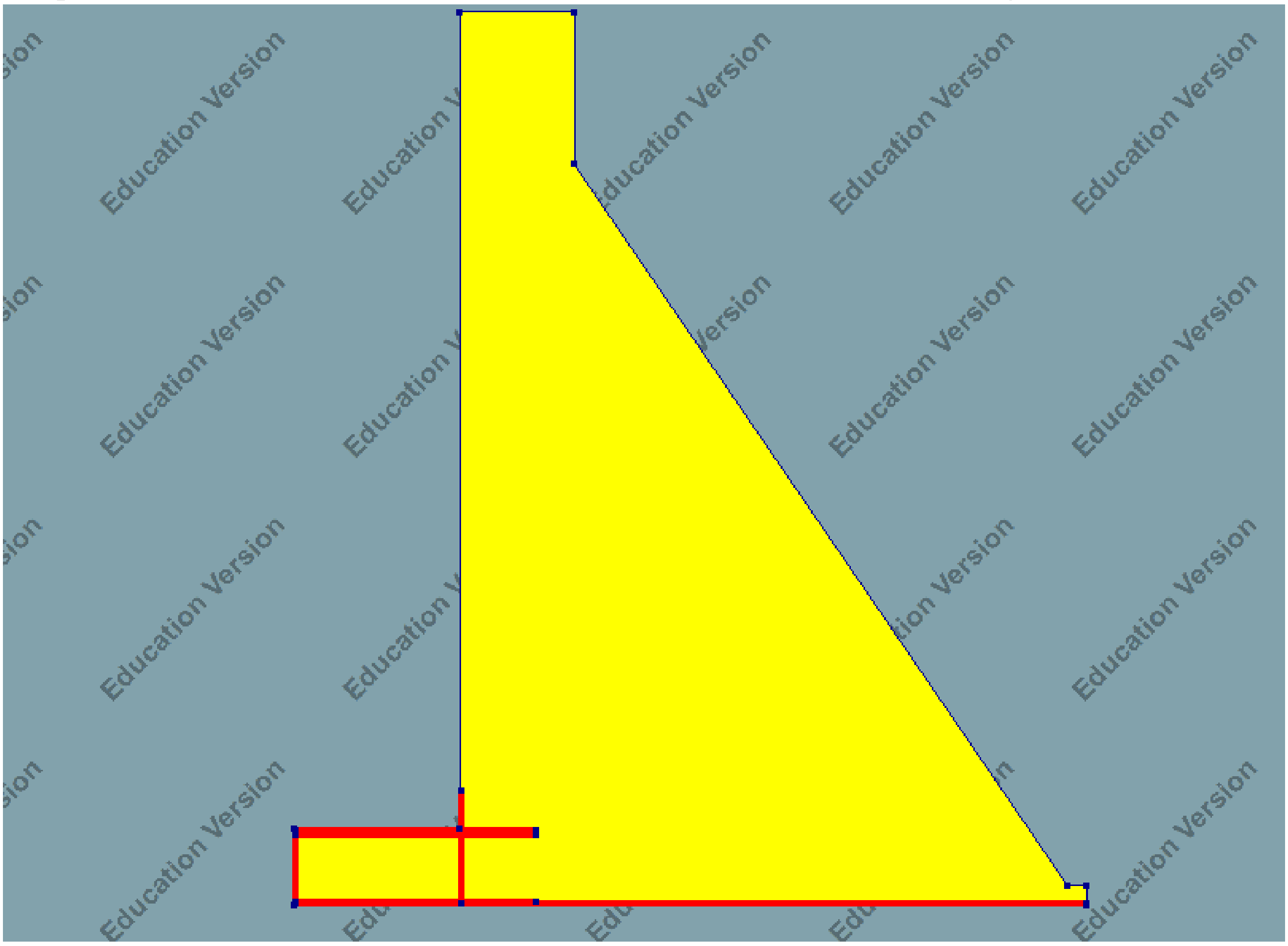

Figure 0-52 Reinforcement

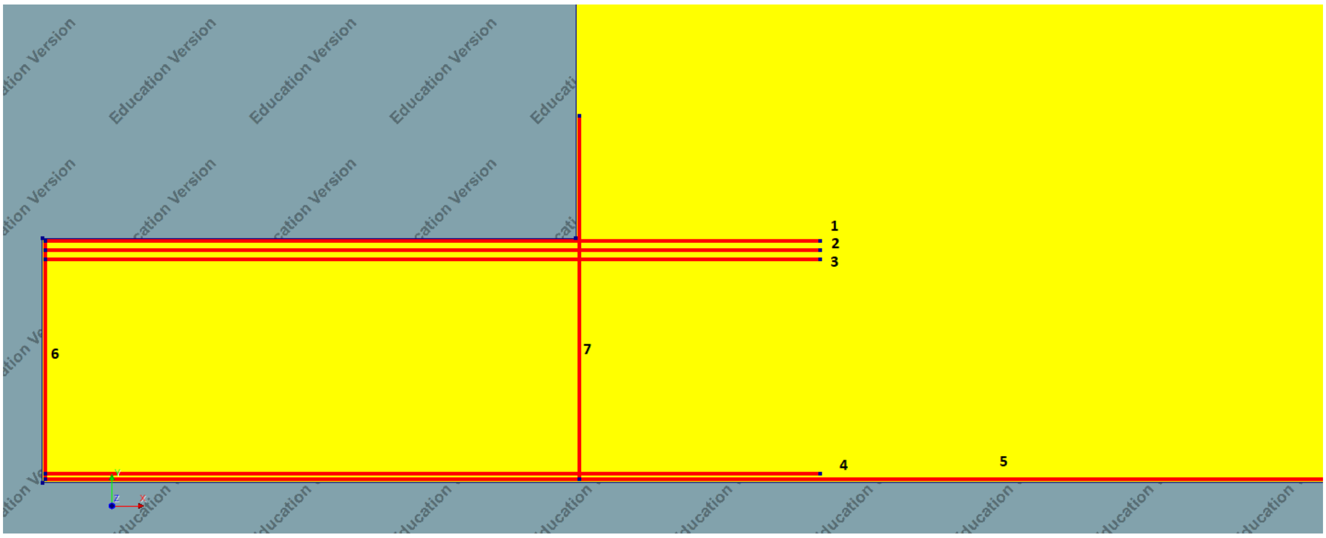

Figure 0-53 Reinforcement zoomed in

The reinforcement is modelled as imbedded bars and the total area per reinforcement is given. This means that the model doesn't include information about the amount of bars. The initial total area per reinforcement position is derived from the Strut and Tie model. Afterwards, this area was adjusted to meet the minimal crack width requirements as described by the Eurocode based on the results from the nonlinear model.

Reinforcement position	Total area (mm^2)
1	31253
2	31253
3	31253
4	31253
5	31253
6	31253
7	31253

Table 0-2 Total area of reinforcement

Supports

The supports, and mesh are similar to that of the linear model.

Loading and Analysis

The loads consist of:

- Self-weight of the concrete
- Horizontal hydrostatic pressure on the wall (43m) and the vertical component of the hydrostatic pressure on the floor.

The analysis performed is a structural nonlinear phased analysis with start steps. The first start step has a specified size of 1 and includes the load of only the self-weight. Afterwards, the load of both the vertical and horizontal water pressure is added to the structure with steps of 0.1 until the load factor of 1.0 is reached.

Results

The results of the final load step (load factor of 1.0 for both the water pressure and the self-weight) of the nonlinear analysis performed with DIANA FEA are included in this subchapter. The results of the analysis are shown in contour plots. Note that the maximum and minimum values are adjusted in order to prevent the plot being highly influenced by peak values. The actual maximum and minimum values can be seen in the description box in the top of each plot.

Displacements

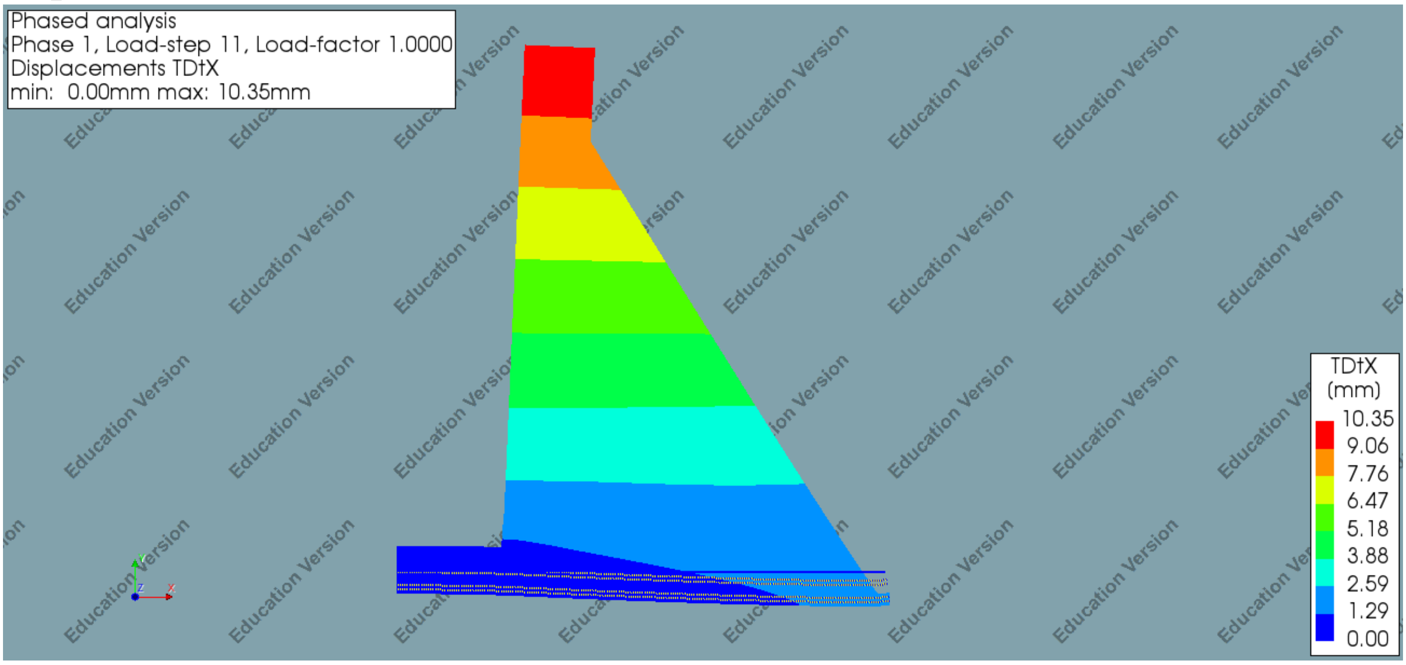

Figure 0-54 Displacement x-direction nonlinear model original design

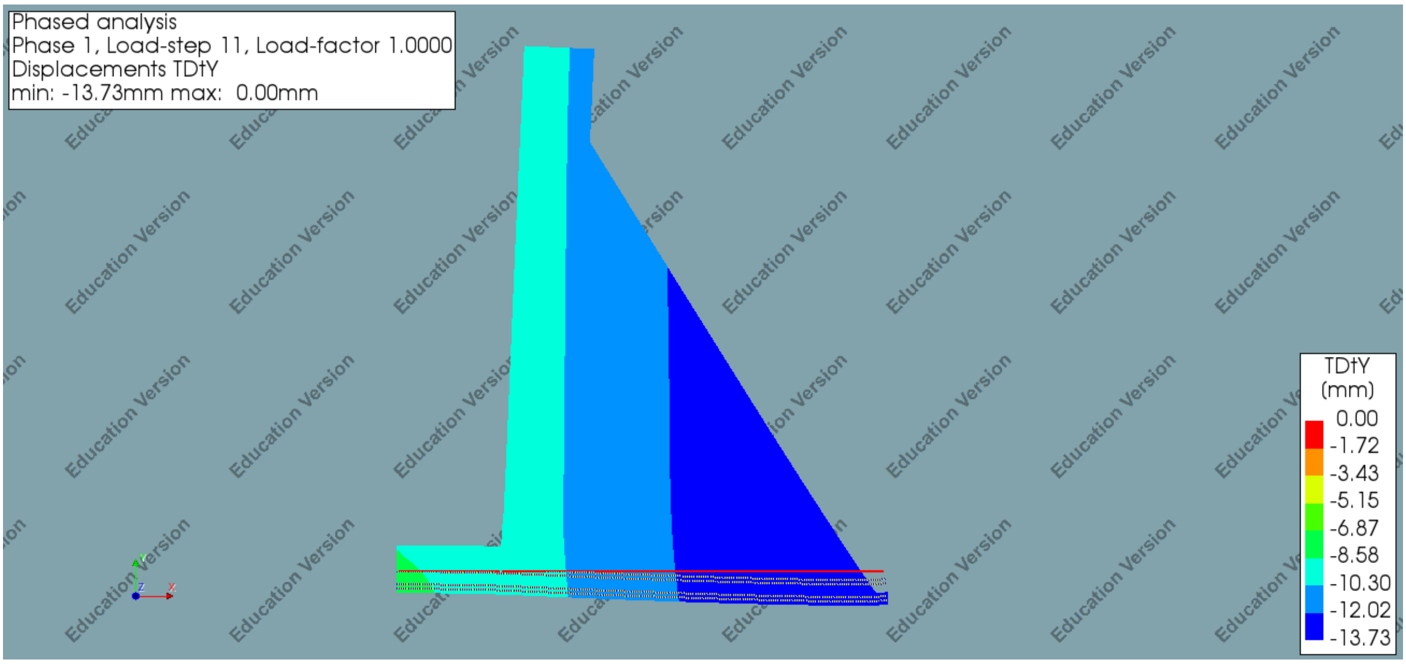

Figure 0-55 Displacement y-direction nonlinear model original design

Interface Relative Displacements

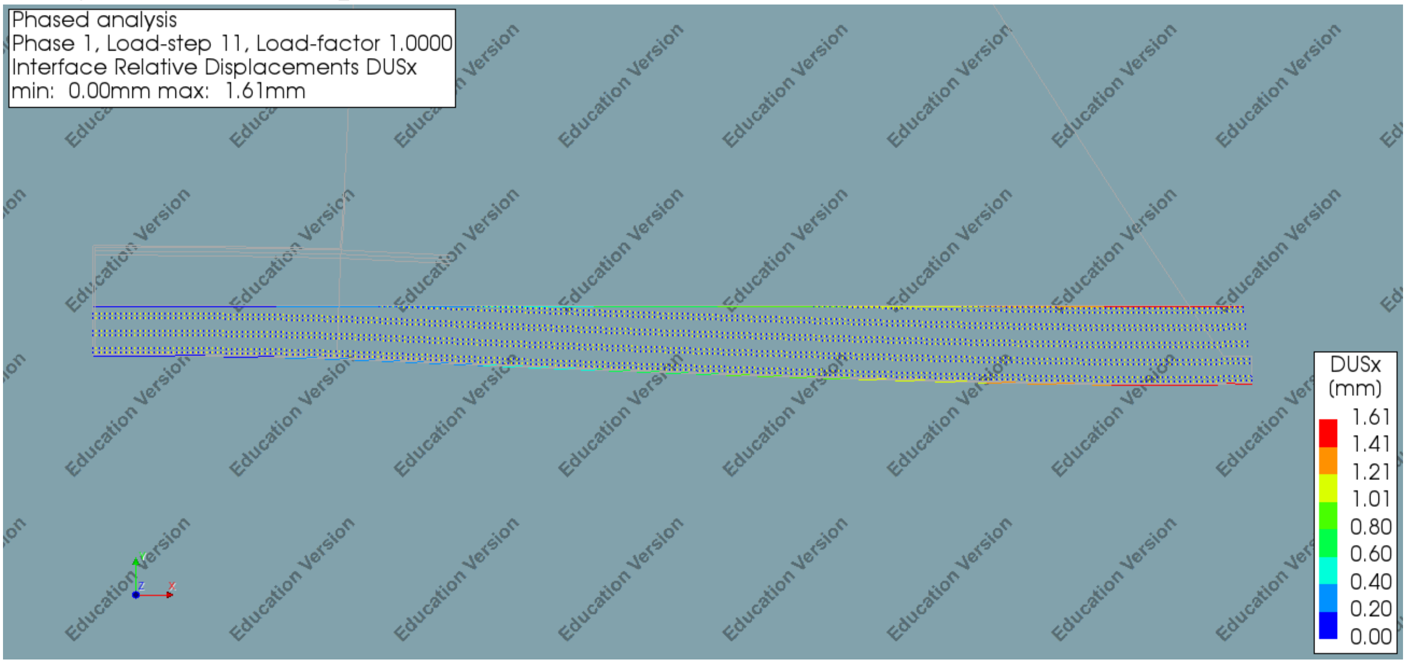

Figure 0-56 Interface relative displacements x-direction nonlinear model original design

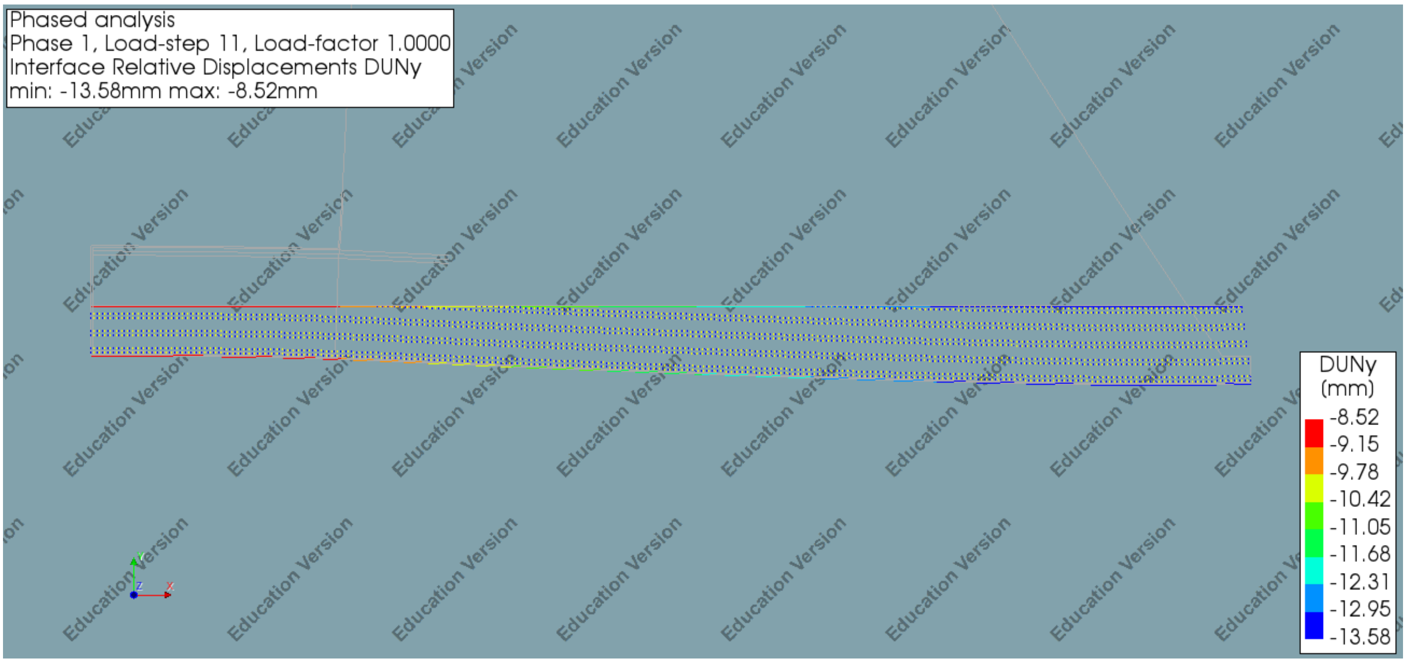

Figure 0-57 Interface relative displacements y-direction nonlinear model original design

Stresses

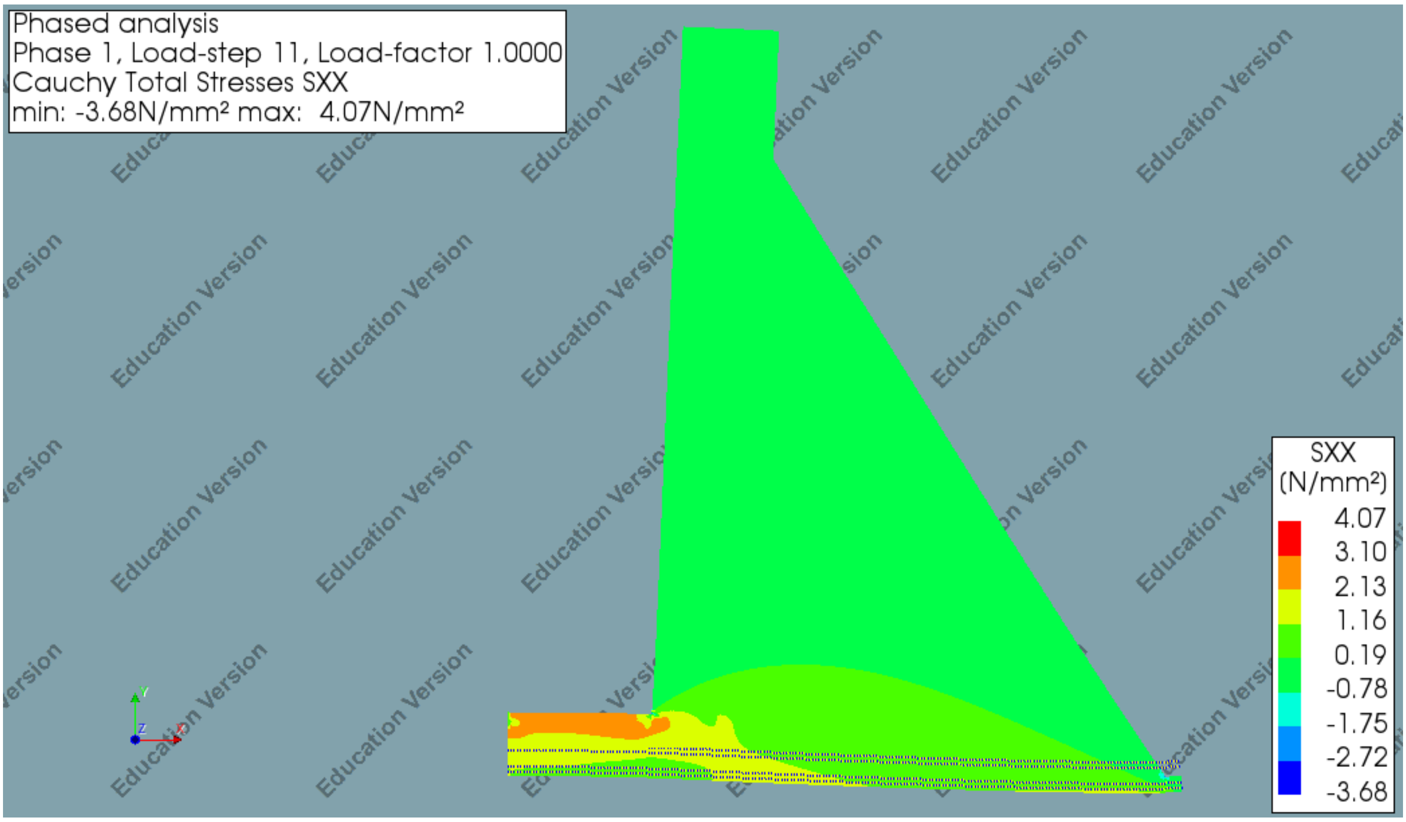

Figure 0-58 Cauchy total stresses SXX nonlinear model original design

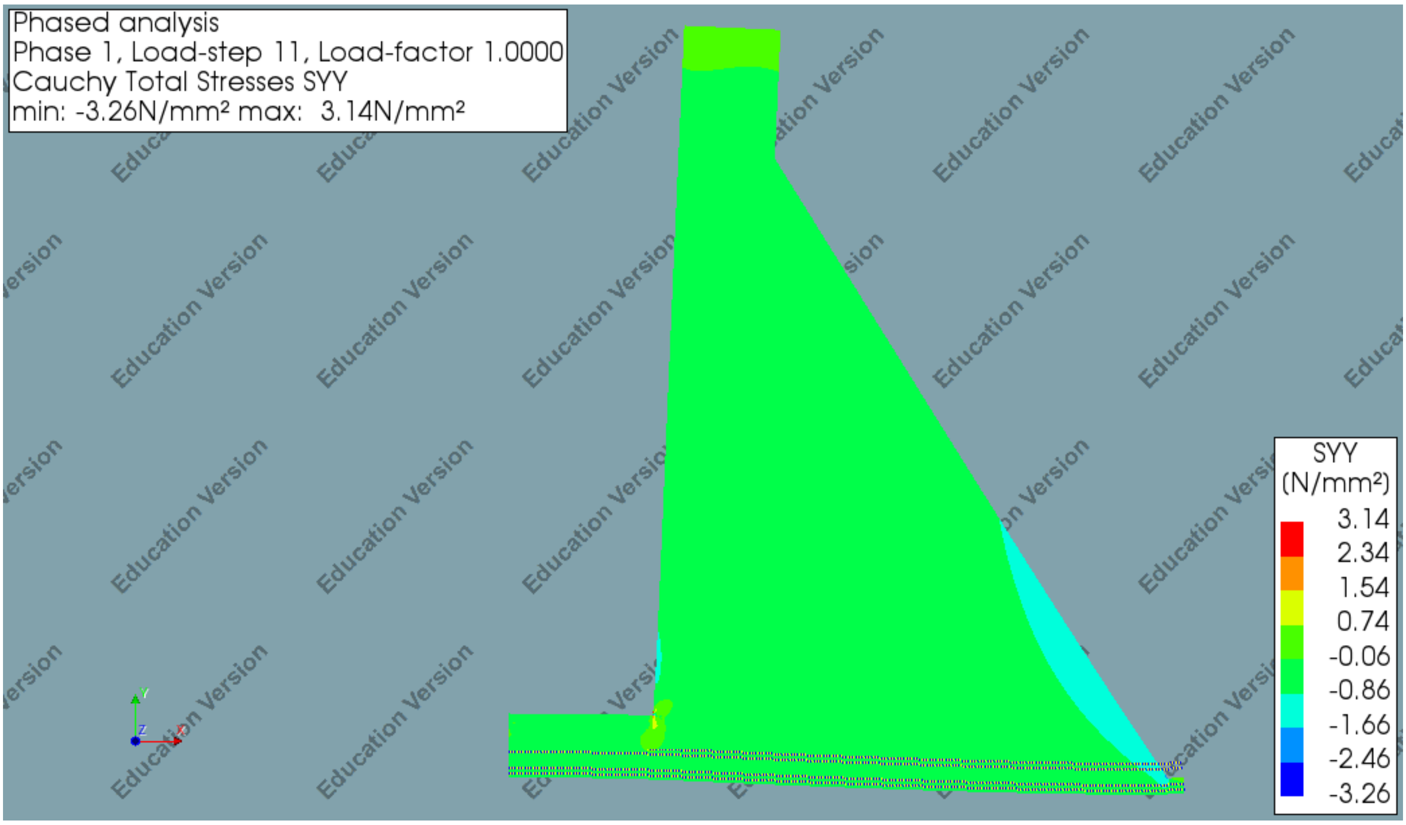

Figure 0-59 Cauchy total stresses SYY nonlinear model original design

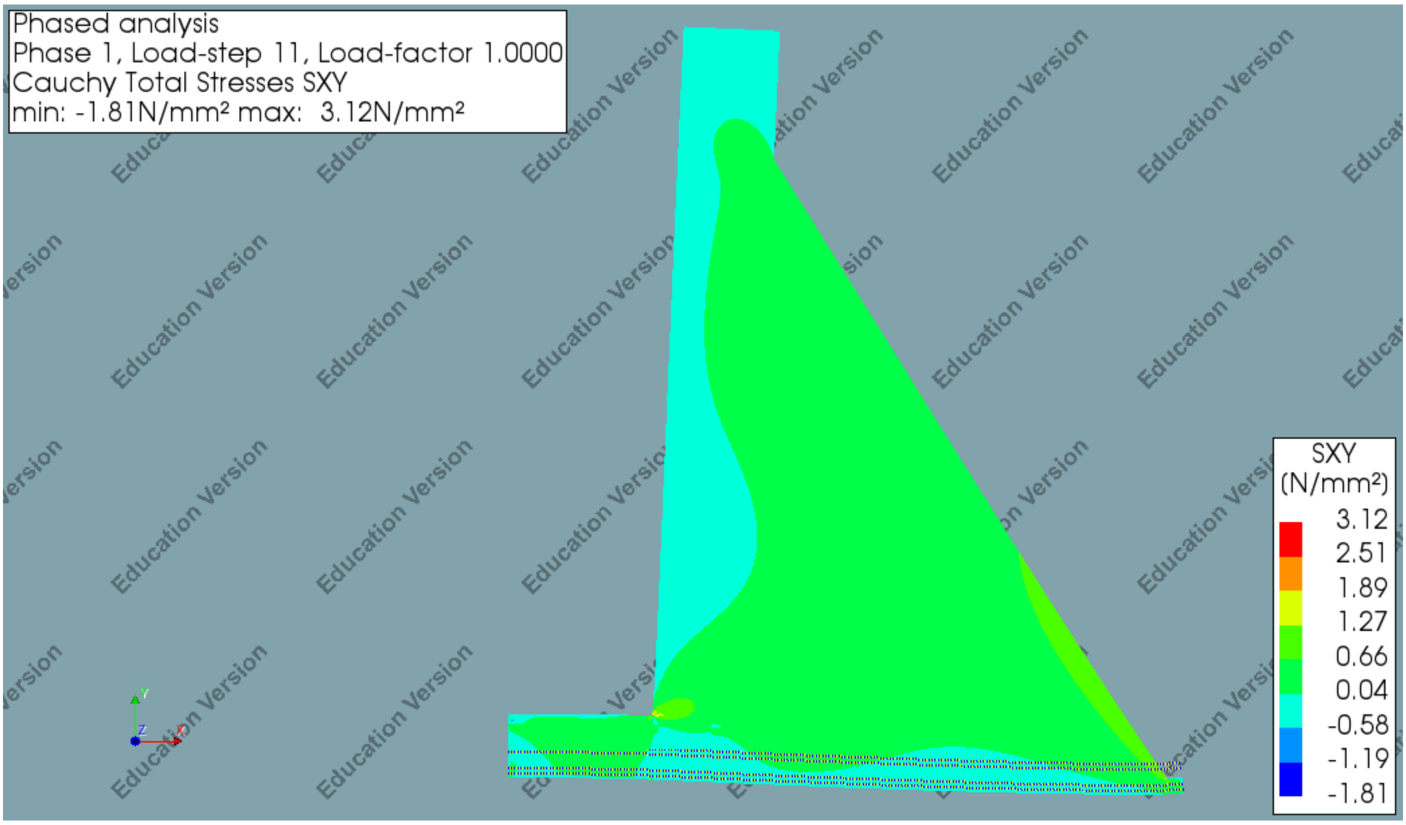

Figure 0-60 Cauchy total stresses SXY nonlinear model original design

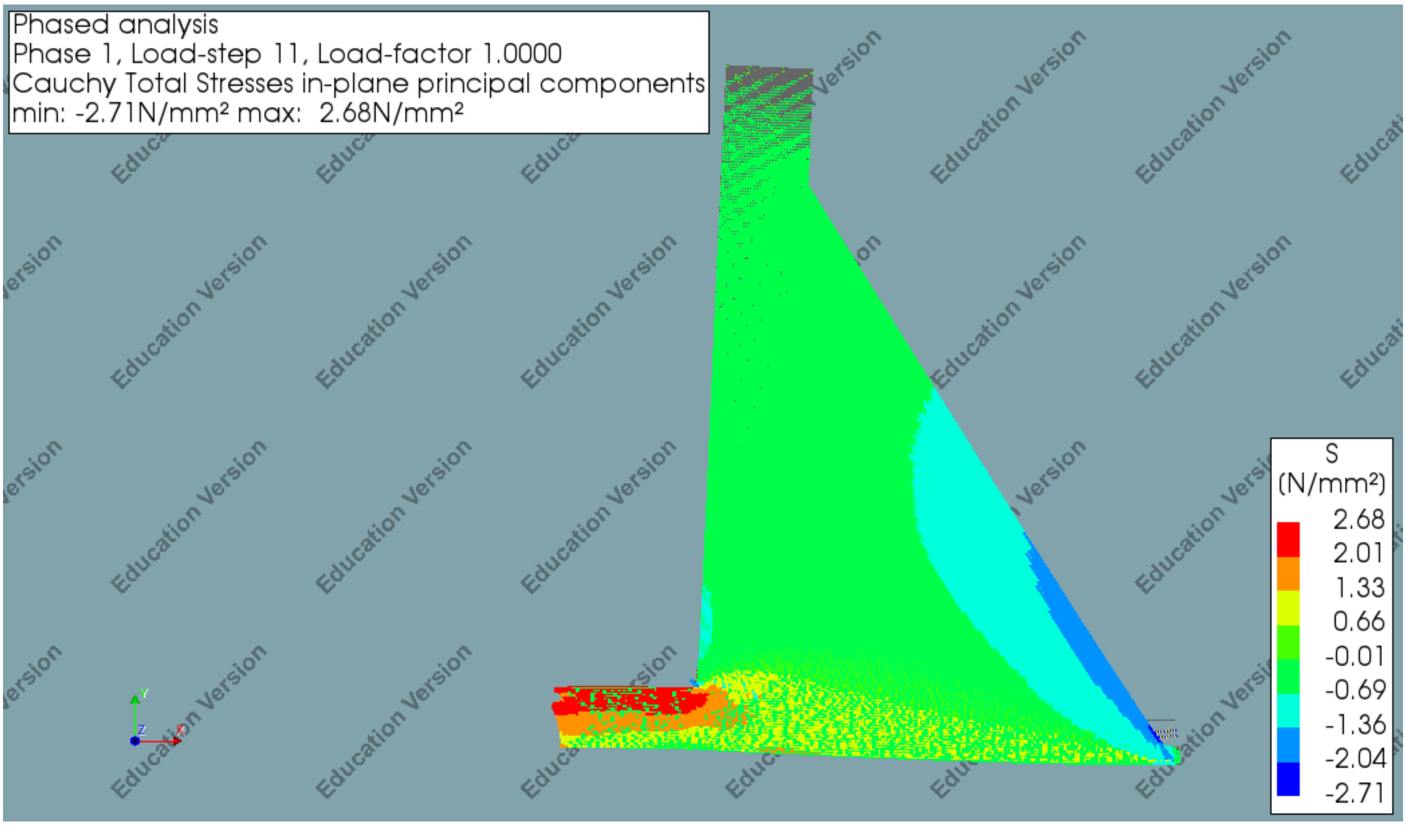

Figure 0-61 Principal stresses nonlinear model original design

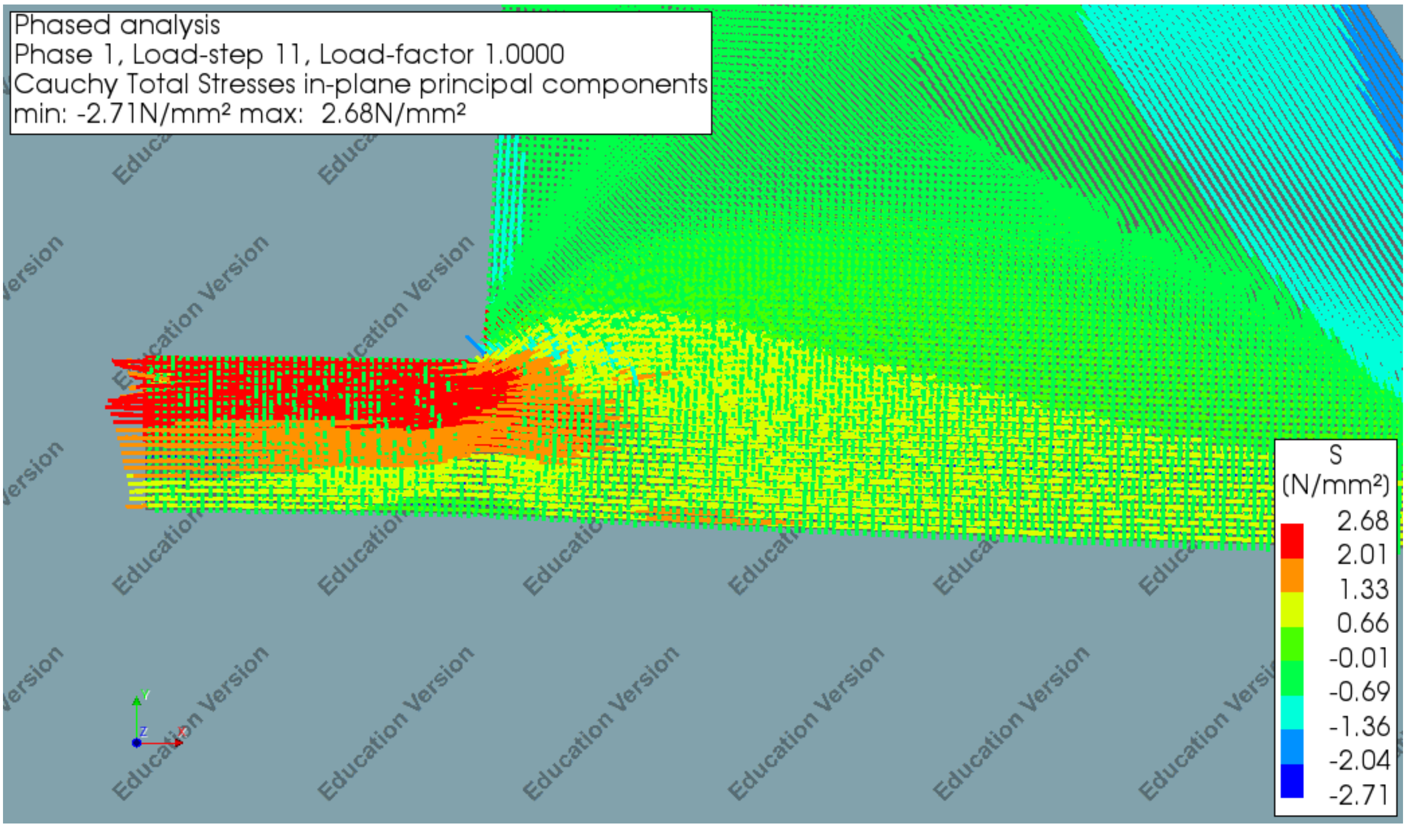

Figure 0-62 Zoom in on Principal stresses nonlinear model original design

Crack Widths

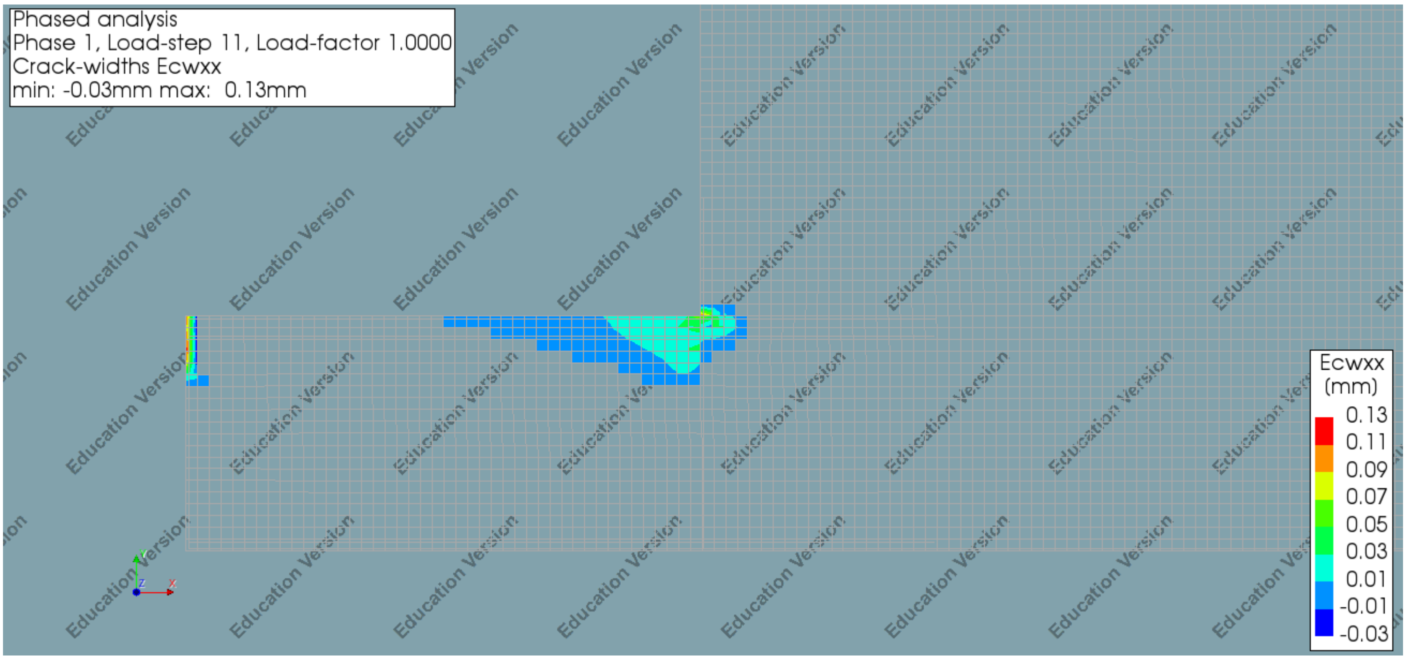

Figure 0-63 Crack widths nonlinear model original design

Appendix F Report Nonlinear Analysis DIANA

Outputfile written by Diana 10.3 (Latest update: 2019-09-11)

```
/DIANA/AP/PH40   01:48:06    0.02-CPU    0.03-IO     14-FA   BEGIN
PHASE 1 INITIALIZED
/DIANA/AP/PH40   01:48:07    0.09-CPU    0.12-IO     24-FA   PHASE
/DIANA/AP/NL41   01:48:07    0.00-CPU    0.06-IO     14-FA   BEGIN
   ELEM. STIFFNESS STORED.
   REINFO.STIFFNESS ADDED AND STORED
   RHS-VECTORS INITIALIZED: ML=    3 ND=  128096 SF.RHSIDE
   EXTER. LOAD INITIALIZED: ML=    3 ND=  128096 SF.EXTLOD
   CONST.DISP. INITIALIZED: ML=    3 ND=  128096 SF.DISCON
   ELEMENTLOAD TO RHS-VECT: NV=    3 SF.RHSIDE
   ELEMENTLOAD TO EXT.LOAD: NV=    3 SF.EXTLOD
   TOTAL MASS OF FE-MODEL FOR LOAD-CASE(  2): 0.20112D+04
   WEIGHT LOAD R.H.S.    : NV=    3 SF.RHSIDE
   WEIGHT LOAD EXTERNAL  : NV=    3 SF.EXTLOD

   SUM OF EXT.LOAD TO CALC: ML=    3 ND=  128096 SF.EXTLOD

SUM OF EXTERNAL LOADS:
=====================
LOADSET POSITION  TR  X      TR  Y      TR  Z      RO  X      RO  Y      RO  Z
    1         0.9245E+07 -0.3763E+07 0.0000E+00  0.0000E+00  0.0000E+00 -0.1794E+12
    2         0.0000E+00 -0.1973E+08 0.0000E+00  0.0000E+00  0.0000E+00 -0.3374E+12
    3         0.9245E+07 -0.2349E+08 0.0000E+00  0.0000E+00  0.0000E+00 -0.5168E+12
 ANALYSIS INCLUDES:

  PHYSICALLY NONLINEAR BEHAVIOR:
   PLASTICITY FIRST   NS=  25 TY= 1.000E-04
   TOTAL STRAIN-BASED CRACK MODEL

   ELEMENTLOAD TO RHS-VECT: MC=    3 SF.RESLOD

 STEP      1 INITIATED:
  LOAD INCREMENT:  START STEPS *   1.000E+00
   SPARSE: DIM=127217 NNZ(MAT)=2037469
   SOLVE: REDUCTION RES= 0.45E-09 (INIT. RES= 0.14E+06) NI=    1

 STEP      1 : DISPLACEMENT NORM =  2.823E+03       TOLERANCE =  1.000E-02
 STEP      1 : FORCE NORM        =  1.409E+06       TOLERANCE =  1.000E-02

 RELATIVE OUT OF BALANCE FORCE  =  4.106E-11       CHECK = TRUE

 STEP      1 TERMINATED, CONVERGENCE AFTER   0 ITERATIONS
  TOTAL LOAD FACTOR:  LOADING( 4) *   1.000E+00

  PLASTICITY LOGGING SUMMARY
  GROUP NAME       PLAST, PRV. PL, CRITIC, PLAST NEW, PRV.PL NEW, CRITIC NEW
  TOTAL MODEL          0       0       0        0         0         0
```

CRACKING LOGGING SUMMARY
GROUP NAME CRACK, OPEN, CLOSED, ACTIVE, INACTI, ARISES, RE-OPENS, CLOSES
TOTAL MODEL 0 0 0 0 0 0 0 0
CUMULATIVE REACTION: FORCE X FORCE Y
-0.26640D-05 -0.19730D+08

SEVERITY : WARNING
ERROR CODE: /DIANA/PO/WR42/1038
ERRORMSG.W: Specified output STRAIN CRKWDT GREEN LOCAL NODES is not available for any of the (selected) ELEMEN.
Loadcase is 1

SEVERITY : WARNING
ERROR CODE: /DIANA/PO/WR42/1038
ERRORMSG.W: Specified output STRAIN CRACK GREEN LOCAL INTPNT is not available for any of the (selected) ELEMEN.
Loadcase is 1

SEVERITY : WARNING
ERROR CODE: /DIANA/PO/WR42/1038
ERRORMSG.W: Specified output STRESS CRACK CAUCHY LOCAL INTPNT is not available for any of the (selected) ELEMEN.
Loadcase is 1

STEP 2 INITIATED:
LOAD INCREMENT: LOADING(1) * 1.000E-01
SPARSE: DIM=127217 NNZ(MAT)=2037469
SOLVE: REDUCTION RES= 0.68E-10 (INIT. RES= 0.69E+05) NI= 1

STEP 2 : DISPLACEMENT NORM = 2.168E+02 TOLERANCE = 1.000E-02
STEP 2 : FORCE NORM = 1.408E+06 TOLERANCE = 1.000E-02

RELATIVE OUT OF BALANCE FORCE = 3.108E-12 CHECK = TRUE

STEP 2 TERMINATED, CONVERGENCE AFTER 0 ITERATIONS
TOTAL LOAD FACTOR: LOADING(1) * 1.000E-01

PLASTICITY LOGGING SUMMARY
GROUP NAME PLAST, PRV. PL, CRITIC, PLAST NEW, PRV.PL NEW, CRITIC NEW
TOTAL MODEL 0 0 0 0 0 0
CRACKING LOGGING SUMMARY
GROUP NAME CRACK, OPEN, CLOSED, ACTIVE, INACTI, ARISES, RE-OPENS, CLOSES
TOTAL MODEL 0 0 0 0 0 0 0 0
CUMULATIVE REACTION: FORCE X FORCE Y
0.92450D+06 -0.20106D+08

SEVERITY : WARNING
ERROR CODE: /DIANA/PO/WR42/1038
ERRORMSG.W: Specified output STRAIN CRKWDT GREEN LOCAL NODES is not available for any of the (selected) ELEMEN.
Loadcase is 1

SEVERITY : WARNING

```
ERROR CODE: /DIANA/PO/WR42/1038
ERRORMSG.W: Specified output STRAIN CRACK GREEN LOCAL INTPNT is not available for any of the (selected) ELEMEN.
Loadcase is 1

SEVERITY  : WARNING
ERROR CODE: /DIANA/PO/WR42/1038
ERRORMSG.W: Specified output STRESS CRACK CAUCHY LOCAL INTPNT is not available for any of the (selected) ELEMEN.
Loadcase is 1


 STEP      3 INITIATED:
  LOAD INCREMENT:  LOADING( 1) *   1.000E-01
    SPARSE: DIM=127217 NNZ(MAT)=2037469
    SOLVE: REDUCTION RES= 0.67E-10 (INIT. RES= 0.69E+05) NI=    1

 STEP      3 : DISPLACEMENT NORM =  2.168E+02       TOLERANCE =  1.000E-02
 STEP      3 : FORCE NORM        =  1.431E+06       TOLERANCE =  1.000E-02

 RELATIVE OUT OF BALANCE FORCE  =  2.032E-03       CHECK = TRUE

 STEP      3 TERMINATED, CONVERGENCE AFTER   0 ITERATIONS
  TOTAL LOAD FACTOR:  LOADING( 1) *   2.000E-01

  PLASTICITY LOGGING SUMMARY
  GROUP NAME        PLAST, PRV. PL, CRITIC, PLAST NEW, PRV.PL NEW, CRITIC NEW
  TOTAL MODEL          0      0      0        0         0         0
  CRACKING LOGGING SUMMARY
  GROUP NAME             CRACK,    OPEN,   CLOSED,   ACTIVE,   INACTI,   ARISES, RE-OPENS,   CLOSES
  TOTAL MODEL               1        1        0        1        0        1        0        0
   CUMULATIVE REACTION:        FORCE X       FORCE Y
                   0.18460D+07    -0.20482D+08


 STEP      4 INITIATED:
  LOAD INCREMENT:  LOADING( 1) *   1.000E-01
    SPARSE: DIM=127217 NNZ(MAT)=2037469
    SOLVE: REDUCTION RES= 0.68E-10 (INIT. RES= 0.69E+05) NI=    1

 STEP      4 : DISPLACEMENT NORM =  2.168E+02       TOLERANCE =  1.000E-02
 STEP      4 : FORCE NORM        =  1.472E+06       TOLERANCE =  1.000E-02

 RELATIVE OUT OF BALANCE FORCE  =  2.727E-02       CHECK = FALSE

    SPARSE: DIM=127217 NNZ(MAT)=2037469
    SOLVE: REDUCTION RES= 0.11E-13 (INIT. RES= 0.40E+05) NI=    1

 RELATIVE DISPLACEMENT VARIATION =  9.254E-05       CHECK = TRUE
 RELATIVE OUT OF BALANCE FORCE  =  2.179E-02       CHECK = FALSE

 STEP      4 TERMINATED, CONVERGENCE AFTER   1 ITERATION
```

TOTAL LOAD FACTOR: LOADING(1) * 3.000E-01

PLASTICITY LOGGING SUMMARY
GROUP NAME PLAST, PRV. PL, CRITIC, PLAST NEW, PRV.PL NEW, CRITIC NEW
TOTAL MODEL 0 0 0 0 0 0
CRACKING LOGGING SUMMARY
GROUP NAME CRACK, OPEN, CLOSED, ACTIVE, INACTI, ARISES, RE-OPENS, CLOSES
TOTAL MODEL 2 2 0 2 0 1 0 0
CUMULATIVE REACTION: FORCE X FORCE Y
0.27373D+07 -0.20859D+08

STEP 5 INITIATED:
LOAD INCREMENT: LOADING(1) * 1.000E-01
SPARSE: DIM=127217 NNZ(MAT)=2037469
SOLVE: REDUCTION RES= 0.61E-10 (INIT. RES= 0.76E+05) NI= 1

STEP 5 : DISPLACEMENT NORM = 2.168E+02 TOLERANCE = 1.000E-02
STEP 5 : FORCE NORM = 1.525E+06 TOLERANCE = 1.000E-02

RELATIVE OUT OF BALANCE FORCE = 6.348E-02 CHECK = FALSE

SPARSE: DIM=127217 NNZ(MAT)=2037469
SOLVE: REDUCTION RES= 0.14E-13 (INIT. RES= 0.97E+05) NI= 1

RELATIVE DISPLACEMENT VARIATION = 2.756E-04 CHECK = TRUE
RELATIVE OUT OF BALANCE FORCE = 5.329E-02 CHECK = FALSE

STEP 5 TERMINATED, CONVERGENCE AFTER 1 ITERATION
TOTAL LOAD FACTOR: LOADING(1) * 4.000E-01

PLASTICITY LOGGING SUMMARY
GROUP NAME PLAST, PRV. PL, CRITIC, PLAST NEW, PRV.PL NEW, CRITIC NEW
TOTAL MODEL 0 0 0 0 0 0
CRACKING LOGGING SUMMARY
GROUP NAME CRACK, OPEN, CLOSED, ACTIVE, INACTI, ARISES, RE-OPENS, CLOSES
TOTAL MODEL 3 3 0 3 0 1 0 0
CUMULATIVE REACTION: FORCE X FORCE Y
0.35977D+07 -0.21235D+08

STEP 6 INITIATED:
LOAD INCREMENT: LOADING(1) * 1.000E-01
SPARSE: DIM=127217 NNZ(MAT)=2037469
SOLVE: REDUCTION RES= 0.44E-10 (INIT. RES= 0.11E+06) NI= 1

STEP 6 : DISPLACEMENT NORM = 2.168E+02 TOLERANCE = 1.000E-02
STEP 6 : FORCE NORM = 1.596E+06 TOLERANCE = 1.000E-02

RELATIVE OUT OF BALANCE FORCE = 9.402E-02 CHECK = FALSE

SPARSE: DIM=127217 NNZ(MAT)=2037469
SOLVE: REDUCTION RES= 0.16E-13 (INIT. RES= 0.15E+06) NI= 1

RELATIVE DISPLACEMENT VARIATION = 5.017E-04 CHECK = TRUE
RELATIVE OUT OF BALANCE FORCE = 7.520E-02 CHECK = FALSE

STEP 6 TERMINATED, CONVERGENCE AFTER 1 ITERATION
TOTAL LOAD FACTOR: LOADING(1) * 5.000E-01

PLASTICITY LOGGING SUMMARY
GROUP NAME PLAST, PRV. PL, CRITIC, PLAST NEW, PRV.PL NEW, CRITIC NEW
TOTAL MODEL 0 0 0 0 0 0
CRACKING LOGGING SUMMARY
GROUP NAME CRACK, OPEN, CLOSED, ACTIVE, INACTI, ARISES, RE-OPENS, CLOSES
TOTAL MODEL 4 4 0 4 0 1 0 0
CUMULATIVE REACTION: FORCE X FORCE Y
0.44644D+07 -0.21611D+08

STEP 7 INITIATED:
LOAD INCREMENT: LOADING(1) * 1.000E-01
SPARSE: DIM=127217 NNZ(MAT)=2037469
SOLVE: REDUCTION RES= 0.34E-10 (INIT. RES= 0.14E+06) NI= 1

STEP 7 : DISPLACEMENT NORM = 2.169E+02 TOLERANCE = 1.000E-02
STEP 7 : FORCE NORM = 1.682E+06 TOLERANCE = 1.000E-02

RELATIVE OUT OF BALANCE FORCE = 1.085E-01 CHECK = FALSE

SPARSE: DIM=127217 NNZ(MAT)=2037469
SOLVE: REDUCTION RES= 0.19E-13 (INIT. RES= 0.18E+06) NI= 1

RELATIVE DISPLACEMENT VARIATION = 7.304E-04 CHECK = TRUE
RELATIVE OUT OF BALANCE FORCE = 7.887E-02 CHECK = FALSE

STEP 7 TERMINATED, CONVERGENCE AFTER 1 ITERATION
TOTAL LOAD FACTOR: LOADING(1) * 6.000E-01

PLASTICITY LOGGING SUMMARY
GROUP NAME PLAST, PRV. PL, CRITIC, PLAST NEW, PRV.PL NEW, CRITIC NEW
TOTAL MODEL 0 0 0 0 0 0
CRACKING LOGGING SUMMARY
GROUP NAME CRACK, OPEN, CLOSED, ACTIVE, INACTI, ARISES, RE-OPENS, CLOSES
TOTAL MODEL 5 5 0 5 0 1 0 0
CUMULATIVE REACTION: FORCE X FORCE Y
0.53601D+07 -0.21987D+08

STEP 8 INITIATED:

```
 LOAD INCREMENT:  LOADING( 1) *   1.000E-01
   SPARSE: DIM=127217 NNZ(MAT)=2037469
   SOLVE: REDUCTION RES= 0.31E-10 (INIT. RES= 0.15E+06) NI=    1

STEP      8 : DISPLACEMENT NORM =  2.169E+02        TOLERANCE =  1.000E-02
STEP      8 : FORCE NORM        =  1.786E+06        TOLERANCE =  1.000E-02

RELATIVE OUT OF BALANCE FORCE   =  1.093E-01        CHECK = FALSE

   SPARSE: DIM=127217 NNZ(MAT)=2037469
   SOLVE: REDUCTION RES= 0.24E-13 (INIT. RES= 0.20E+06) NI=    1

RELATIVE DISPLACEMENT VARIATION =  9.658E-04        CHECK = TRUE
RELATIVE OUT OF BALANCE FORCE   =  7.919E-02        CHECK = FALSE

STEP      8 TERMINATED, CONVERGENCE AFTER   1 ITERATION
 TOTAL LOAD FACTOR:  LOADING( 1) *   7.000E-01

 PLASTICITY LOGGING SUMMARY
 GROUP NAME        PLAST, PRV. PL, CRITIC, PLAST NEW, PRV.PL NEW, CRITIC NEW
 TOTAL MODEL           0       0      0         0          0          0
 CRACKING LOGGING SUMMARY
 GROUP NAME             CRACK,    OPEN,   CLOSED,   ACTIVE,   INACTI,   ARISES, RE-OPENS,   CLOSES
 TOTAL MODEL                6        6        0        6        0        1        0        0
   CUMULATIVE REACTION:        FORCE X        FORCE Y
                       0.62739D+07    -0.22364D+08


STEP      9 INITIATED:
 LOAD INCREMENT:  LOADING( 1) *   1.000E-01
   SPARSE: DIM=127217 NNZ(MAT)=2037469
   SOLVE: REDUCTION RES= 0.29E-10 (INIT. RES= 0.16E+06) NI=    1

STEP      9 : DISPLACEMENT NORM =  2.170E+02        TOLERANCE =  1.000E-02
STEP      9 : FORCE NORM        =  1.925E+06        TOLERANCE =  1.000E-02

RELATIVE OUT OF BALANCE FORCE   =  1.624E-01        CHECK = FALSE

   SPARSE: DIM=127217 NNZ(MAT)=2037469
   SOLVE: REDUCTION RES= 0.67E-13 (INIT. RES= 0.31E+06) NI=    1

RELATIVE DISPLACEMENT VARIATION =  4.506E-03        CHECK = TRUE
RELATIVE OUT OF BALANCE FORCE   =  8.474E-02        CHECK = FALSE

STEP      9 TERMINATED, CONVERGENCE AFTER   1 ITERATION
 TOTAL LOAD FACTOR:  LOADING( 1) *   8.000E-01

 PLASTICITY LOGGING SUMMARY
 GROUP NAME        PLAST, PRV. PL, CRITIC, PLAST NEW, PRV.PL NEW, CRITIC NEW
 TOTAL MODEL           0       0      0         0          0          0
```

```
CRACKING LOGGING SUMMARY
GROUP NAME          CRACK,   OPEN,  CLOSED,  ACTIVE,  INACTI,  ARISES, RE-OPENS,  CLOSES
TOTAL MODEL            13      13      0      13      0      7      0      0
  CUMULATIVE REACTION:      FORCE X      FORCE Y
                 0.71949D+07   -0.22740D+08


STEP     10 INITIATED:
 LOAD INCREMENT:  LOADING( 1) *   1.000E-01
   SPARSE: DIM=127217 NNZ(MAT)=2037469
   SOLVE: REDUCTION RES= 0.26E-10 (INIT. RES= 0.18E+06) NI=    1

STEP     10 : DISPLACEMENT NORM =  2.176E+02       TOLERANCE =  1.000E-02
STEP     10 : FORCE NORM       =  2.081E+06       TOLERANCE =  1.000E-02

RELATIVE OUT OF BALANCE FORCE  =  1.964E-01       CHECK = FALSE

   SPARSE: DIM=127217 NNZ(MAT)=2037469
   SOLVE: REDUCTION RES= 0.16E-12 (INIT. RES= 0.41E+06) NI=    1

RELATIVE DISPLACEMENT VARIATION =  1.391E-02       CHECK = FALSE
RELATIVE OUT OF BALANCE FORCE  =  1.331E-01       CHECK = FALSE

   SPARSE: DIM=127217 NNZ(MAT)=2037469
   SOLVE: REDUCTION RES= 0.11E-12 (INIT. RES= 0.28E+06) NI=    1

RELATIVE DISPLACEMENT VARIATION =  6.613E-03       CHECK = TRUE
RELATIVE OUT OF BALANCE FORCE  =  1.150E-01       CHECK = FALSE

STEP     10 TERMINATED, CONVERGENCE AFTER   2 ITERATIONS
 TOTAL LOAD FACTOR:  LOADING( 1) *   9.000E-01

 PLASTICITY LOGGING SUMMARY
 GROUP NAME       PLAST, PRV. PL, CRITIC, PLAST NEW, PRV.PL NEW, CRITIC NEW
 TOTAL MODEL         0      0      0       0       0       0
 CRACKING LOGGING SUMMARY
 GROUP NAME          CRACK,   OPEN,  CLOSED,  ACTIVE,  INACTI,  ARISES, RE-OPENS,  CLOSES
 TOTAL MODEL            74      74      0      74      0      61      0      0
  CUMULATIVE REACTION:      FORCE X      FORCE Y
                 0.80550D+07   -0.23116D+08


STEP     11 INITIATED:
 LOAD INCREMENT:  LOADING( 1) *   1.000E-01
   SPARSE: DIM=127217 NNZ(MAT)=2037469
   SOLVE: REDUCTION RES= 0.19E-10 (INIT. RES= 0.25E+06) NI=    1

STEP     11 : DISPLACEMENT NORM =  2.194E+02       TOLERANCE =  1.000E-02
STEP     11 : FORCE NORM       =  2.252E+06       TOLERANCE =  1.000E-02
```

```
RELATIVE OUT OF BALANCE FORCE  =  2.224E-01        CHECK = FALSE

   SPARSE: DIM=127217 NNZ(MAT)=2037469
   SOLVE: REDUCTION RES= 0.37E-12 (INIT. RES= 0.50E+06) NI=    1

RELATIVE DISPLACEMENT VARIATION =  3.874E-02        CHECK = FALSE
RELATIVE OUT OF BALANCE FORCE  =  1.651E-01        CHECK = FALSE

   SPARSE: DIM=127217 NNZ(MAT)=2037469
   SOLVE: REDUCTION RES= 0.24E-12 (INIT. RES= 0.37E+06) NI=    1

RELATIVE DISPLACEMENT VARIATION =  1.871E-02        CHECK = FALSE
RELATIVE OUT OF BALANCE FORCE  =  1.508E-01        CHECK = FALSE

   SPARSE: DIM=127217 NNZ(MAT)=2037469
   SOLVE: REDUCTION RES= 0.15E-12 (INIT. RES= 0.34E+06) NI=    1

RELATIVE DISPLACEMENT VARIATION =  1.077E-02        CHECK = FALSE
RELATIVE OUT OF BALANCE FORCE  =  1.746E-01        CHECK = FALSE

   SPARSE: DIM=127217 NNZ(MAT)=2037469
   SOLVE: REDUCTION RES= 0.95E-13 (INIT. RES= 0.39E+06) NI=    1

RELATIVE DISPLACEMENT VARIATION =  7.776E-03        CHECK = TRUE
RELATIVE OUT OF BALANCE FORCE  =  1.673E-01        CHECK = FALSE

STEP     11 TERMINATED, CONVERGENCE AFTER   4 ITERATIONS
 TOTAL LOAD FACTOR:  LOADING( 1) *   1.000E+00

 PLASTICITY LOGGING SUMMARY
 GROUP NAME         PLAST, PRV. PL, CRITIC, PLAST NEW, PRV.PL NEW, CRITIC NEW
 TOTAL MODEL           0       0      0         0          0          0
 CRACKING LOGGING SUMMARY
 GROUP NAME             CRACK,    OPEN,   CLOSED,   ACTIVE,   INACTI,   ARISES, RE-OPENS,   CLOSES
 TOTAL MODEL              331      331       0      331       0      257        0        0
   CUMULATIVE REACTION:        FORCE X       FORCE Y
                         0.87221D+07    -0.23492D+08

/DIANA/DC/END    01:50:03   230.06-CPU   13.86-IO    77038-FA   STOP
```

Appendix G Load Case: Backfill soil

An alternative load case for the Itaipu lock wall has to be used when the soil next to the wall is backfilled after soil excavation and construction of the wall. This load situation has not been included in further calculations in this report. However, the load situation is still described in this appendix.

Groundwater

The groundwater table is located at level 159m. The pore pressure is calculated over the distance from this point to the toe of the wall at level 145m.

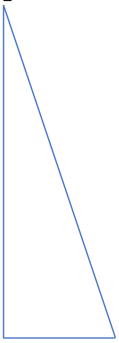

$$P = h*\rho*g = 14*1000*9{,}81 = 137\ kN/m^2$$

Soil pressure

The permanent soil pressure on the concrete structures is calculated on the basis of the following assumptions:

- Soil type: Clay
- Specific weight wet soil: 18 kN/m^3
- Specific weight groundwater: 10 kN/m^3
- Internal friction angle φ: 20°
- Ground level: 160 m
- Groundwater level: 159 m
- Bottom lock wall: 145 m

Vertical soil pressure

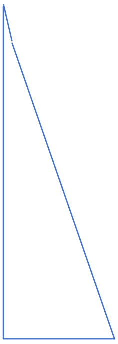

$$\sigma_v = (h*\gamma_{wet}) = (15*18) = 270\ kN/m^2$$

The vertical effective soil pressure at the toe of the wall then equals:

$\sigma_v' = \sigma_v - p = 270-(14*10) = 130\ kN/m^2$

Vertical force of soil on top of the wall

Due to the slope of the wall, there will also be a vertical force of the weight of the soil on top of the wall that will act on the wall. The area the soil on top of the wall, indicated by the orange triangle in the image below, is equal to 0,5*15*10,5=79m².

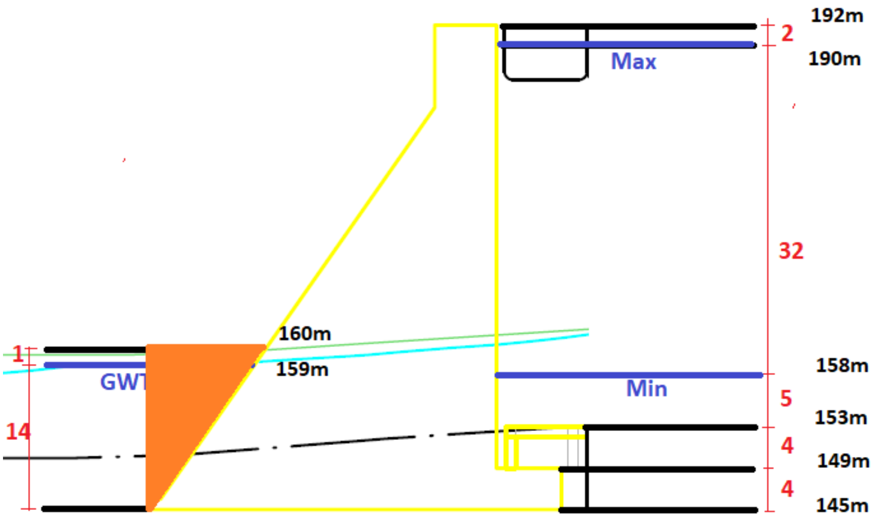

Figure 0-64 Boundary Conditions

The weight of the soil is equal to $79m^2 * 18\ kN/m^3 = 1422\ kN$. For simplicity reasons, the total area of the soil on top of the wall is assumed to be wet soil.

Horizontal soil pressure

The soil pressure will always have an active effect on the wall due to the shape. Therefore the active soil coefficient is used for a internal friction angle of 20 should be used. However, the conservative value of 0.7 is used instead, which comes closer to the neutral soil coefficient.

The horizontal soil pressure equals: $\sigma_h = \sigma_v{}' * K_a = 299*0.7 = 209\ kN/m^2$

The total horizontal pressure at the toe of the wall consists of the horizontal water pressure and the horizontal soil pressure and equals $137+209 = 346\ kN/m$

Loads

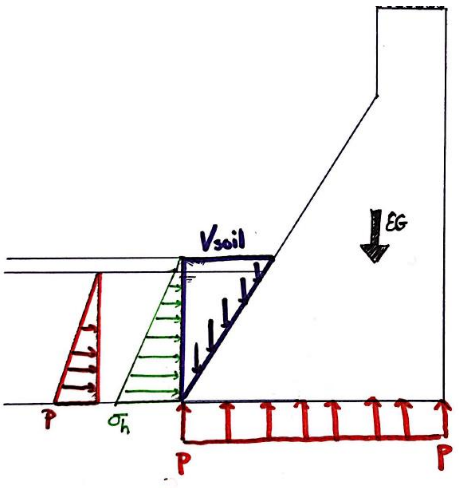

Figure 0-65 Loading Wall

	Unfavourable	Favourable

Self Weight Concrete (EG)	1,2	0,9
Horizontal Soil Pressure (σ_h)	1,2	0,9
Horizontal Ground Water Pressure (P)	1,2	0,9
Upward Ground water Pressure (P)	1,2	0.9
V_{soil}	1,2	0,9

Table 0-3 Partial Factors

Bibliography

A.K.Sengupta. (2005) Prestressed concrete structures. Module 5: Analysis and Design for Shear and Torsion. Indian Institute of Technology Madras.

ACI Committee 318 (2005) Building Code Requirements for Structural Concrete (ACI 318-05) and Commentary, American Concrete Institute, Farmington Hills, MI, USA

Alfrink, L. J. (2015). Geavanceerde staafwerkmodellen. Eindhoven University of Technology.

Bentz, E.C., F.J. Vecchio and Collins, M.P. (2005). The Simplified MCFT for Calculating the Shear Strength of Reinforced Concrete Elements Subjected to Shear," ACI Journal, 83(2): 219-231

Braam, C. R., Ing, H. C., & Walraven, J. C. (2019). Prestressed Concrete (No. 1). Faculty of Civil Engineering and Geosciences.

Braam, C. R., Lagendijk, P., Dees, W. C., Cement en Beton Centrum, & Cement en Beton Centrum. (2010). Constructieleer gewapend beton. Æneas.

Cotrim, I. J. R. (1994). Itaipu Hydroelectric Project: Engineering Features. Delft, Nederland: Itaipu Binacional.

Dutchwatersector. (2018, May 25). Witteveen+Bos to do feasibility study into bypass Itaipu dam, Brazil | Dutch Water Sector. Retrieved November 30, 2020, from https://www.dutchwatersector.com/news/witteveenbos-to-do-feasibility-study-into-bypass-itaipu-dam-brazil

El-Sayed, A. K., & Shuraim, A. B. (2015). Size effect on shear resistance of high strength concrete deep beams. Materials and Structures, 49(5), 1871–1882. https://doi.org/10.1617/s11527-015-0619-1

G. I. Zárate Garnica, "Analysis of shear transfer mechanisms in concrete members without shear reinforcement based on kinematic measurements," Delft university of technology, Delft, 2018.

Hamadi, Y. D., and Regan, P. E. (1980). "Behaviour in shear of beams with flexural cracks." Mag. Concr. Res., 32(111), 67–78

History.com Editors. (2020, September 29). Hoover Dam. Retrieved November 20, 2020, from https://www.history.com/topics/great-depression/hoover-dam

Lantsoght, E., Veen, C., Walraven, J., Boer, A. 2016.Case Study on Aggregate Interlock Capacity for the Shear Assessment of Cracked Reinforced-Concrete Bridge Cross Sections. Journal of Bridge Engineering. 21. 04016004. 10.1061/(ASCE)BE.1943-5592.0000847.

Miedema, S. (2001). Course Dredging Processes 1 Lecture Notes

Molenaar, W. F. (2011, March). Hydraulics Structures

Molenaar, W. F., & Voorendt, M. Z. (2016, February). Manual Hydraulic Structures. TU Delft, Department Hydraulic Engineering.

Naus D.J., Batson G.B., Lott J.L. (1974) Fracture Mechanics of Concrete. In: Bradt R.C., Hasselman D.P.H., Lange F.F. (eds) Fracture Mechanics of Ceramics. Springer, Boston, MA

NEN-EN 1992-1-1. (2012). [Eurocode 2: Ontwerp en berekening van betonconstructies - Deel 1-1: Algemene regels en regels voor gebouwen].

Olst van, B. (2019). Parametric design-tool to optimize preliminary design of navigation lock chambers.

Port of Amsterdam. (2020, December 1). Nieuwe zeesluis IJmuiden. Retrieved November 30, 2020, from https://www.portofamsterdam.com/nl/ontdek/nieuwe-zeesluis

Presvyri, S. (2019). Aggregate Interlock: Extending the aggregate interlock model to high strength concrete. TU Delft, 0. Retrieved from http://resolver.tudelft.nl/uuid:2fe5a685-7c00-488d-8841-29d5b659760c

Quach, Phillip T., P. T. (2016). Understanding and Safely Predicting the Shear Response of Large-scale Reinforced Concrete Structures. University of Toronto, TSpace, 0. Retrieved from http://hdl.handle.net/1807/73110

Raju Int. Journal of Engineering Research and Applications www.ijera.com ISSN : 2248-9622, Vol. 4, Issue 4 (Version 8), April 2014, pp.116-121

Roser, M. (2013, May 9). World Population Growth. Retrieved June 28, 2019, from https://ourworldindata.org/world-population-growth

Rozumek, D., & Macha, E. (2009). A survey of failure criteria and parameters in mixed-mode fatigue crack growth. Materials Science, 45(2), 190–210. https://doi.org/10.1007/s11003-009-9179-2

Sarkhosh, R., den Uijl , J. A., Braam, C. R., & Walraven, J. C. (2010). Shear Capacity of Concrete Beams without Shear Reinforcement under Sustained Loads. Delft University of Technology (TU-Delft) Faculty of Civil Engineering and Geosciences.

Sherwood, E., Bentz, E., Collins, M.P. 2006. Evaluation of Shear Design Methods for Large, Lightly-reinforced Concrete Beams. 10.1007/1-4020-4891-2_13.

Sherwood, E., Bentz, E., Collins, M.P., (2007). Effect of aggregate size on beam-shear strength of thick slabs. ACI Structural Journal. 104. 180-190.

Sherwood, E.,Bentz, E. (2008). Where is Shear Reinforcement Required? Review of Research Results and Design Procedures. (2008). ACI Structural Journal, 105(5), 0. https://doi.org/10.14359/19942

Shioya, T. (1989). Shear properties of large reinforces concrete member. Symposium Paper, 118(25), 259–280.

Taylor, H. P. J. (1974). The fundamental behavior of reinforced concrete beams in bending and shear, American Concrete Institute, Farmington Hills, MI, 285–303.

The Editors of Encyclopaedia Britannica. (2020). Three Gorges Dam | Facts, Construction, Benefits, & Problems. Retrieved November 30, 2020, from https://www.britannica.com/topic/Three-Gorges-Dam

Þórhallsson, E., Runar Birgisson, S., 2014. Shear strength of concrete beams without shear reinforcement.

TU Delft. (n.d.). De Oosterscheldekering. Retrieved November 30, 2020, from https://www.tudelft.nl/citg/over-faculteit/afdelingen/hydraulic-engineering/education/high-school-students-scholieren/field-of-activity-werkveld/de-oosterscheldekering/

Walraven, J, Lehwalter, N., 1989. "Het afschuifdraagvermogen van gedrongen liggers en korte consoles," Cement, vol. 4, pp. 27–34.

Walraven, J. C. (1988). Staafwerkmodellen als basis voor het detailleren van betonconstructies. Cement Online.

Walraven, J. C., & Bruggeling, A.S.G. (promotor). (1980). Aggregate interlock: A theoretical and experimental analysis. Aggregate Interlock: A Theoretical and Experimental Analysis, 196.

Yang, Y., Walraven, J., & Uijl, J. (2017). Shear Behavior of Reinforced Concrete Beams without Transverse Reinforcement Based on Critical Shear Displacement. Journal of Structural Engineering, 143(1), 04016146. https://doi.org/10.1061/(asce)st.1943-541x.0001608